THE DEVELOPMENT OF MICROSTRUCTURE DURING THE HYDRATION OF PORTLAND CEMENT

by

Karen Louise Scrivener, MA

A thesis submitted for the degree of Doctor of Philosophy in the University of London, and for the Diploma of Imperial College

Department of Metallurgy and Materials Science
Royal School of Mines
Imperial College of Science and Technology
University of London

July 1984

ABSTRACT

The hydration of commercial Portland cements and of synthetic Portland cement phases has been investigated, by electron optical methods and calorimetry.

Examination of fracture surfaces in the scanning electron microscope (SEM), of ion-thinned sections from bulk pastes by transmission electron microscopy (TEM) and by scanning transmission electron microscopy (STEM), of thin sections extracted from undried paste in the environmental cell of a high voltage (1MeV) electron microscope (HVEM) and of back scattered electron images from polished sections in the SEM have been combined to give a detailed picture of the development of morphology during cement hydration. The use of this combination of methods takes into account the effect of drying on microstructure and allows discussion of unrepresentative images produced by some methods.

The possible mechanisms by which the various phases hydrate and the way in which these are altered or modified in Portland cement itself are discussed.

The use of back scattered electron images of polished surfaces is presented as a method of quantifying the microstructure of a cement, and the potential of this technique for relating the microstructure to the mechanical properties and durability of cement is discussed.

ACKNOWLEDGEMENTS

I am grateful to Professor P. L. Pratt for his supervision, to Professor D. W. Pashley for the provision of research facilities, and to the Science and Engineering Research Council for financial support. I should also like to thank Dr P. W. Brown, Dr G. J. C. Frohnsdorff and Dr H. M. Jennings of the National Bureau of Standards, Washington, USA, for providing cements and synthetic phases used in this work and for enlightening discussions; Dr L. J. Parrott, Mr W. A. Gutteridge and Mr D. Killoh of the Cement and Concrete Association, Wexham Springs for providing synthetic phases, cement and clinker, and for carrying out QXDA and calorimetry; Blue Circle for providing cement; Mr L. Dutton for general technical assistance; Mr G. W. Briers and Mr J. Woodall for technical assistance in electron microscopy; Dr C. J. Gillham for writing the software for the calorimeter and for doing the image analysis; Mr J. Rossdale for printing the plates and Ms H. Stanley for typing this thesis.

Finally I would especially like to thank my husband, Mr K. Baldie, and my parents, Mr B. H. and Mrs S. Scrivener for all their help and encouragement.

CONTENTS

TABLES

LIST OF PLATES

FIGURES

GLOSSARY

In describing cement compounds a shortened notation is used in which the oxides are represented as:

$C = CaO$, $S = SiO_2$, $A = Al_2O_3$, $M = MgO$

$F = Fe_2O_3$, $\bar{S} = SO_3$, $H = H_2O$, $N = Na_2O$, $K = K_2O$.

Thus tricalcium silicate $3CaO.SiO_2 = C_3S$, tricalcium aluminate $3CaO.Al_2O_3 = C_3A$ and calcium hydroxide $Ca(OH)_2 = CH$, for example.

AFm phase	typically a tetracalcium monosulphoaluminate hydrate, usually with some substitution of Al by Fe.
AFt phase	typically ettringite, usually with some substitution of Al by Fe.
Alite	impure form of C_3S ($3CaO.SiO_2$) found in commercial Portland cement clinker.
Aluminate phase	$C_3A = 3CaO.Al_2O_3$.
Anhydrite	$C\bar{S} = CaSO_4$.
Belite	impure form of C_2S ($2CaO.SiO_2$) found in commercial Portland cement clinker.
BEI	back scattered electron image.
Cement clinker	nodular product from a cement manufacturing kiln.
Cement paste	mixture of cement powder with water.
Concrete	mixture of cement, sand and pebble aggregates.

C-S-H gel	calcium silicate hydrate, a colloidal and mainly amorphous gel with a rather variable composition, which is the major hydration product of Portland cement.
C/S ratio	molar ratio of CaO/SiO_2.
DTA	differential thermal analysis.
EDXA	energy dispersive X-ray analysis.
ettringite	$C_3A.3C\bar{S}.32H = 3CaO.Al_2O_3.3CaSO_4.32H_2O$.
ferrite phase	solid solution between C_2F and 'C_2A' of average composition $C_4AF = 4CaO.Al_2O_3.Fe_2O_3$.
free lime	$C = CaO$.
gypsum	$C\bar{S}.2H$ = calcium sulphate dihydrate $CaSO_4.2H_2O$.
hemihydrate	$C\bar{S}.\frac{1}{2}H$ = calcium sulphate hemihydrate $CaSO_4.\frac{1}{2}H_2O$.
HVEM	high voltage electron microscope/microscopy
interstitial phase	collective term for aluminate and ferrite phases which crystallise from the liquid phase when the clinker is cooled.
monosulphate	$C_3A.C\bar{S}.12H = 3CaO.Al_2O_3.CaSO_4.12H_2O$.
OPC	Ordinary portland cement.
QXDA	quantitative X-ray diffraction analysis.
SEM	scanning electron microscope/microscopy.
STEM	scanning transmission electron microscopy.
TEM	transmission electron microscope/microscopy.
TG	thermogravimetric analysis.
UPV	ultrasonic pulse velocity.
w/c ratio	ratio of mass of water to mass of cement in a cement paste.
w/s ratio	ratio of mass of water to mass of solid in a paste mixture.
XRD	X-ray diffraction.

Chapter One

INTRODUCTION

Portland cement, in the form of concrete, is the most extensively used material in the construction industry. Compared with steel, the other important construction material, cement is cheap and there are plentiful supplies of the raw materials needed for its manufacture. Yet, the mechanisms by which strength develops when cement is mixed with water and the factors affecting the durability of cement and concrete are poorly understood.

An understanding of the relationships between the microstructure and properties of metals has lead to great advances in their use. Control of microstructure has lead to the development of alloys which maximise the requirements of durability, toughness and cost in many different applications.

Thus, an understanding of the way in which the microstructure of cement develops during hydration would give a fundamental basis, from which the potential strength and durability of cement could be developed.

The present work is concerned with the microstructural development of cement hydrated at room temperature, without any admixtures, at realistic water to cement ratios around 0.5. A wide range of electron optical techniques and calorimetry have been used to study the hydration of cement. In addition, limited investigation has been made of the hydration of the constituent phases of cement.

The way in which cement is produced is described in Chapter 2, which also introduces some of the complexities of cement clinker compared to a simple mixture of its constituent phases.

Chapter 3 describes various techniques which have been used in the study of cement hydration and discusses their relative merits.

Chapter 4 deals with the hydration of the constituent phases of cement, while the hydration of cement itself is the subject of Chapter 5.

Chapter 6 presents an overview of the microstructural development of cement, discusses possible mechanisms of hydration, outlines areas for further work and summarises the conclusions of the present work.

Chapter Two

PRODUCTION AND CHARACTERISATION OF CEMENT

Portland cement is made by burning together a mixture of calcareous and argillaceous raw materials. The calcareous component (mainly calcium carbonate) is typically limestone or chalk, whilst the argillaceous component (mainly aluminium and iron silicates) may be clay or shale. Marls, which are a mixture of clay and chalk, are also used. Table 2.1 shows the chemical composition of some typical raw materials.

During manufacture the calcium carbonate is converted to CaO (lime) which then reacts with the aluminium ferrous silicates to give the compounds tricalcium silicate (Ca_3SiO_5 or C_3S), dicalcium silicate (Ca_2SiO_4 or C_2S), tricalcium aluminate ($Ca_3Al_2O_6$ or C_3A) and a calcium aluminoferrite solid solution (Fss) usually denoted by its average composition of $Ca_4Al_2Fe_2O_{10}$ or C_4AF. These four major compounds, together with minor impurities, constitute cement clinker which is then ground with gypsum to give cement.

2A Production of Clinker (Lea, 1970; Bye, 1983; Roy, 1981)

Commercially the burning of cement takes place in a rotary kiln; this is a long refractory lined cylinder, inclined at about 3° to the horizontal, which rotates on its axis. The fuel is burnt at one end of the kiln so producing a temperature gradient along its length (Fig 2.1). Two processes are used commercially for the production

Table 2.1 (from Lea, 1970)

Analyses of typical raw materials

	CHALK	CLAY	LIMESTONE	SHALE	MARL	TYPICAL RAW MIX
SiO_2	1.14	60.48	2.16	55.67	16.86	14.30
Al_2O_3	0.28	17.79	1.09	21.50	3.38	3.03
Fe_2O_3	0.14	6.77	0.54	9.00	1.11	1.11
CaO	54.68	1.61	52.72	0.89	42.58	44.38
MgO	0.48	3.10	0.68	2.81	0.62	0.59
S	0.01	-	0.03	0.30	-	-
SO_3	0.07	0.21	0.02	-	0.08	0.07
LOI	43.04	6.65	42.39	4.65	34.66	35.86
K_2O	0.04	2.61	0.26	4.56	0.66	0.52
Na_2O	0.09	0.74	0.11	0.82	0.12	0.13
	99.97	99.96	100.00	100.20	100.07	99.99
$CaCO_3$	97.6		94.1		76.0	79.3

of clinker. In the older 'wet' process the raw materials are mixed and crushed as a slurry with water. This allows close control of the raw mix, but the water must subsequently be evaporated, consuming energy and necessitating a long kiln (up to 200m). The total energy consumption for a wet process clinker is about 5500 kJ/Kg. In the dry process the raw materials are prepared as a blend of finely ground powders. The initial heating to about 800°C is then carried out on a preheater using the CO_2 evolved from the limestone and the hot combustion gases from the fuel as a source of heat. Thus, a shorter kiln can be used and the energy requirement can be reduced to as low as 3000 kJ/Kg. Recycling of the hot gases to improve the kiln efficiency may, however, give higher alkali levels in the final clinker, which may lead to adverse reaction with some aggregates.

As the material travels along the length of the kiln it passes through several zones of increasing temperature, in which particular physical and chemical processes predominate. Fig 2.2 shows the locations of these zones in different kiln systems and illustrates how the introduction of preheaters and precalciners reduces the kiln length.

Drying Zone - In the drying zone water evaporates from the slurry facilitated by chains slung across the kiln.

Preheating Zone - In the preheating zone the decomposition of the clay minerals occurs in the temperature range 350°-650°C.

Calcining Zone - In the calcining zone the decarbonation of calcite takes place in the temperature range 750°-1000°C.

In the 'dry' process there is no drying zone and preheating, and in some cases calcining take place before the charge enters the kiln.

Clinkering Zone - When decarbonation is complete the temperature of the material rises rapidly as it moves into the burning or clinkering

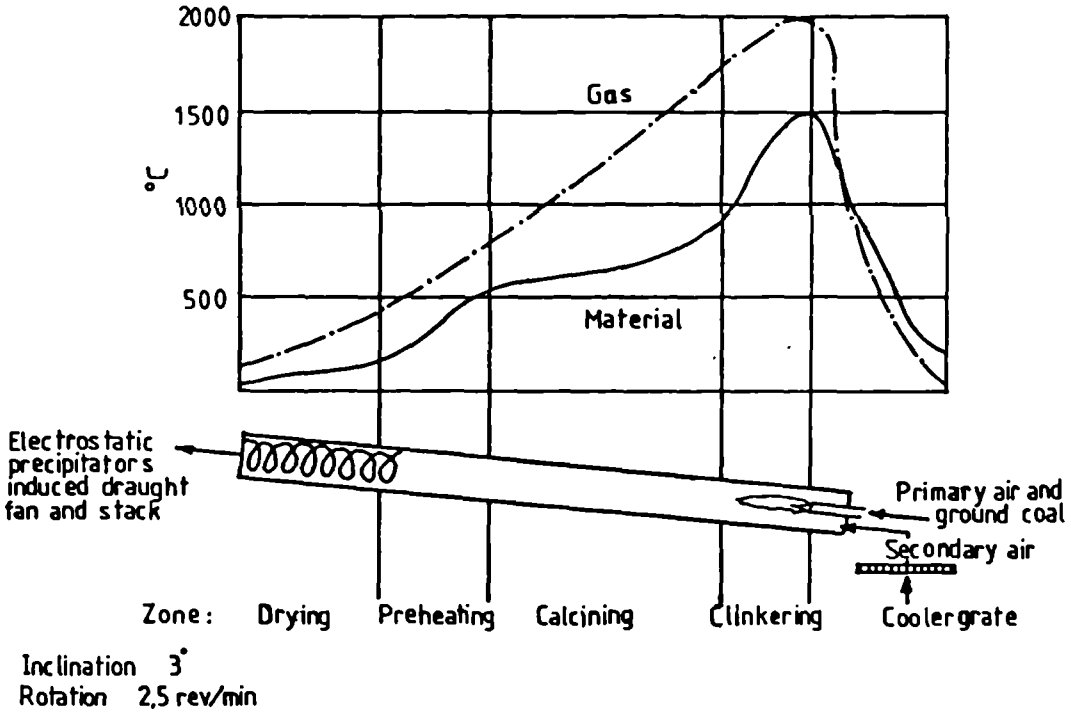

FIGURE 2.1 Zones in a wet process kiln with typical gas and material temperature profiles
from BYE 1983

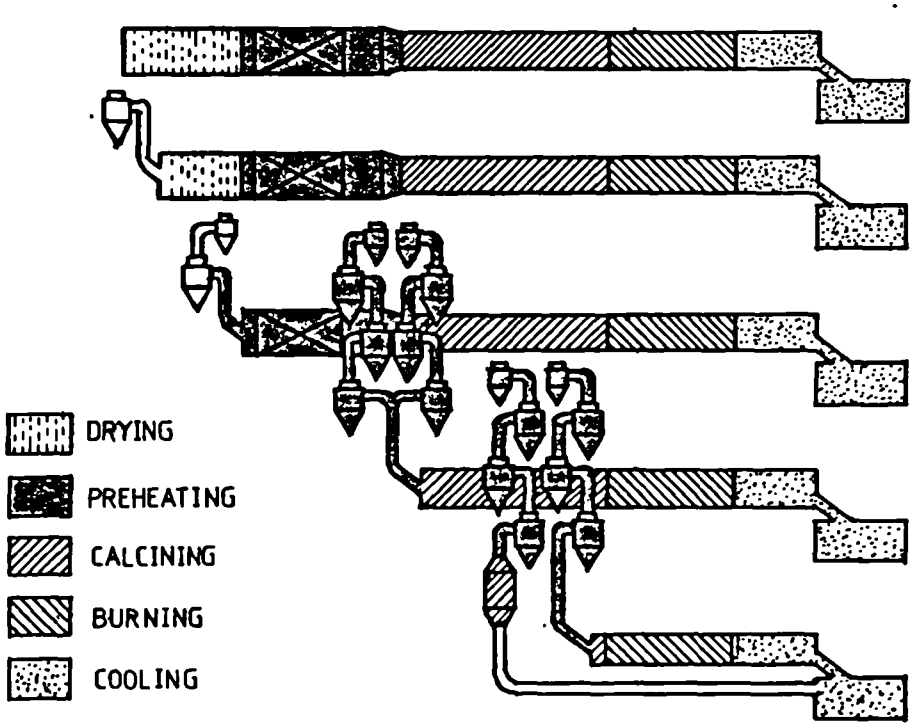

FIGURE 2.2 Location of zones for different kiln systems showing the decrease in physical size as development makes the manufacturing process more efficient
from ROY 1981

zone. During the 20-30 minutes spent in the hottest part of the kiln many complex reactions occur. All but the coarsest siliceous material is quickly converted to C_2S. Above 1170°C acidic melts form in silica-rich regions where interactions of lime, alumina and/or iron oxide can occur. The high surface tension of the melt produces capillary forces which cause rapid shrinkage and nodule formation. As the temperature increases above 1200°, C_3S starts to form by diffusion at the boundaries of the high and low lime regions and then, as the liquid phase forms, by crystallisation from the melt in which lime and C_2S have dissolved. The operation of these two mechanisms can lead to a bimodal distribution of the C_3S (or alite) particle size. The presence of liquid is essential if the reaction $C_2S + C \rightarrow C_3S$ is to proceed substantially during the time the clinker spends in the burning zone. The amount of melt phase formed is a function of the ratio of silica to the sum of alumina and iron oxide.

Cooling Zone - Finally, after passing the flame the material enters a short cooling zone in which the melt solidifies with the crystallisation of C_3A, C_4AF and dissolved silicates. Although the clinker enters a cooler on leaving the kiln, the microstructure of the clinker is primarily determined by the cooling which occurs before it reaches the kiln exit at about 1100°C.

The formation of the cement minerals within a kiln is shown in Fig 2.3.

2B Composition of clinker

If the raw materials react completely during clinkering to give only the four phases C_3S, C_2S, C_3A and C_4AF the relative proportions of these phases can be calculated from the oxide composition of the raw mix. Due to inhomogeneities in the raw mix, the presence of large

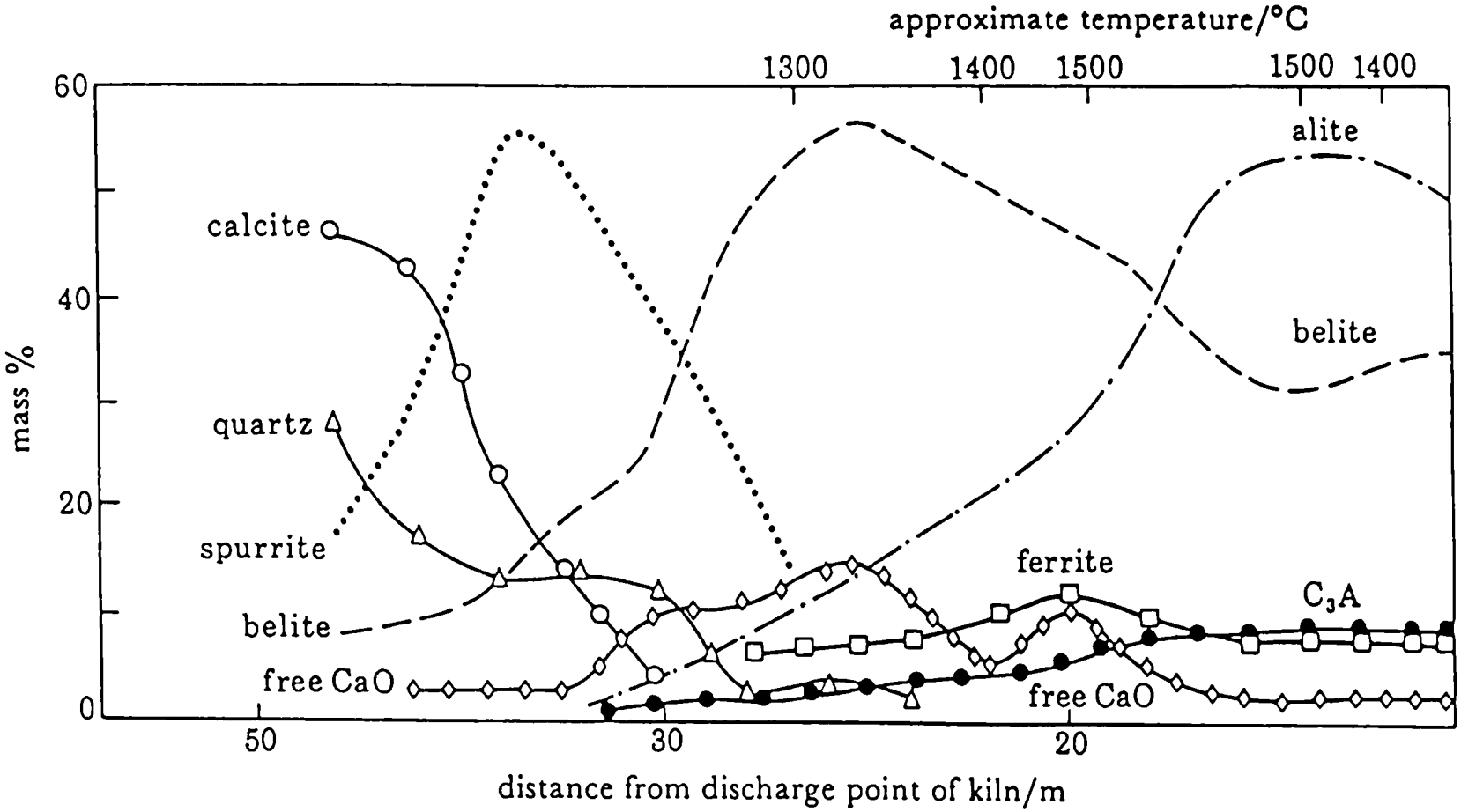

FIGURE 2.3 An example of the formation of the cement minerals within a kiln. (from Gutteridge & Pomeroy, 1983)

grains in the raw mix and the finite time spent in the burning zone, complete reaction never occurs in practice. If the free lime content of the clinker is determined the extent of the reaction

$$CaO + C_2S \longrightarrow C_3S$$

may be calculated and the potential phase composition calculated from the oxide analysis of the clinker or cement. The proportions of the phases are derived by means of the Bogue calculation (Bogue, 1929) as follows. First the amount of calcium oxide needed to form $CaSO_4$ with the SO_3 content and the free lime content are subtracted from the total lime content. It is then assumed that all the iron oxide is present as C_4AF. The C_4AF content is thus calculated and the amounts of lime and alumina combined in this phase are deducted from their totals. From the remaining alumina the C_3A content is calculated and the amount of combined lime again subtracted. Finally the amounts of C_3S and C_2S are derived from the remaining lime and silica (an example calculation is given in Appendix I).

The Bogue calculation, however, takes no account of any solid solution between the phases or of the presence of minor oxides. In practice the alumina/iron oxide ratio in the ferrite phase can vary from about 0.6 to 1.5 (Kristmann, 1978) in industrial clinkers. In addition, alumina and iron oxide may dissolve in the silicate phases and silica in the aluminate and ferrite phases. Minor oxides are also present in solid solution in the clinker phases, often replacing one of the major oxides. Magnesium oxide, for example, is usually present at a level of about 1% (often higher in the USA) and replaces calcium, especially in the interstitial phase. Table 2.2 shows the amounts of minor oxides typically found in solid solution in the major phases.

Table 2.2 Range of impurities found in portland cement clinkers (Ghose, 1980)

IMPURITY	ALITES, %	BELITES, %	INTERSTITIAL PHASES, %
Si			0.61-7.73
Al	0.34-2.96	0.28-1.69	6.19-16.46
Fe	0.02-1.85	0.02-1.16	0.30-21.07
Na	0.07-0.48	0.09-0.61	0.11-1.62
K	0.02-0.39	0.04-1.54	0-2.59
S	0-0.12	0-1.21	0-1.62
P	0.03-0.62	0.02-0.58	0-0.30
Mg	0.08-0.98	0.04-0.74	0.11-1.62
Mn	0-0.12	0-0.12	0-0.80
Cr	0-0.14	0-0.18	0-0.08
Ti	0.02-0.24	0.02-0.26	0.03-0.90
V	0-0.11	0-0.12	0-0.11

If for a particular cement the exact composition of each phase including all the minor elements were known it would be possible to calculate the phase composition from the oxide composition. It would not be possible, however, to carry out this procedure routinely.

The exact conditions of burning and cooling influence how the phase composition of the clinker departs from that predicted by the Bogue calculation. Although many modifications to the Bogue calculation based on knowledge of these influences have been proposed, none is particularly satisfactory due to the complex interactions which can occur.

Two other methods can be used to determine the proportions of the major phases: quantitative X-ray diffraction analysis (QXDA) and optical microscopy. QXDA (Struble, 1982; Berger et al, 1966) depends on measuring the relative intensities of the diffraction peaks of each phase from a clinker or cement of unknown composition and comparing these with the peak intensities from standards of each compound. If the crystallography and chemistry of each phase were constant and there was no overlap between the peaks this would be a relatively simple procedure. The presence of impurities in solid solution causes distortion in the crystal structure and may stabilise different polymorphs at room temperature, leading to alterations in the shapes, heights and positions of the diffraction peaks. In addition, many of the major diffraction peaks of the clinker minerals overlap with each other or with minor phases. Nevertheless fairly accurate analyses of the phase composition of cement can be made with QXDA, depending on the techniques used for calibration and analysis (Struble, 1982).

The method of QXDA developed by Gutteridge (1984), used in this work, gives a quantitative phase analysis of a cement to within 1%

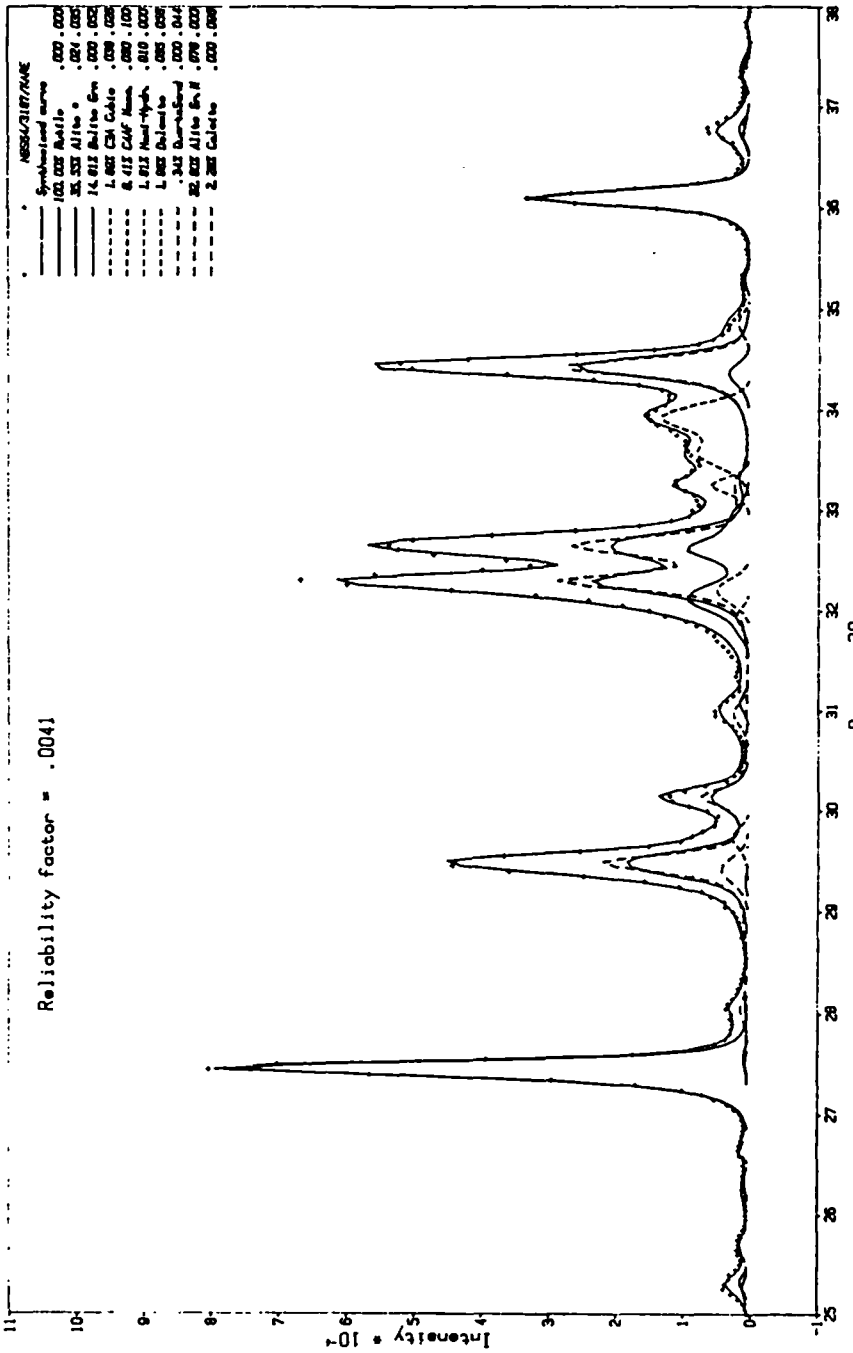

FIG. 2.4 QXDA for an O.P.C.

(absolute) for each phase. This analytical procedure uses the X-ray intensity data collected from a set of some thirty chemically synthesised cement minerals called primary standards. There are ten primary standards for alite, six for C_2S, four for C_3A and ten for the calcium alumino-ferrite solid solution with an F:A ratio varying from 33:67 to 67:33. A further nineteen primary standards are used to account for the minor phases. Two sub-samples are prepared from the cement by selective solvent extraction to remove the interstitial and silicate phases respectively; qualitative diffraction data from these samples is used to select appropriate primary standards. The quantitative X-ray intensity data for the whole cement, collected over the range 25°-38°, is then subjected to a least squares regression procedure with a combination of the primary standards chosen. The primary standard data can be broadened or shifted to enhance the fit, simulating a decrease in crystallite size and the effect of solid solution. This procedure is illustrated in Fig 2.4. Full experimental details of the sample preparation and analysis are given in Appendix II.

Accurate analyses can also be obtained by optical microscopy using a point counting method on polished and etched sections of clinker. Distinguishing finely divided phases can cause difficulties, but the main drawback is the small area which can be examined. However, if care is taken to prepare a representative sample (Hofmanner, 1975; Fundal) good agreement with the phase composition determined by QXDA can be achieved (Moore, 1964; Aldridge, 1982).

2C Microstructure of Clinker

Optical microscopy can also reveal much about the arrangement of phases within the clinker. Fig 2.5 shows an ideal clinker

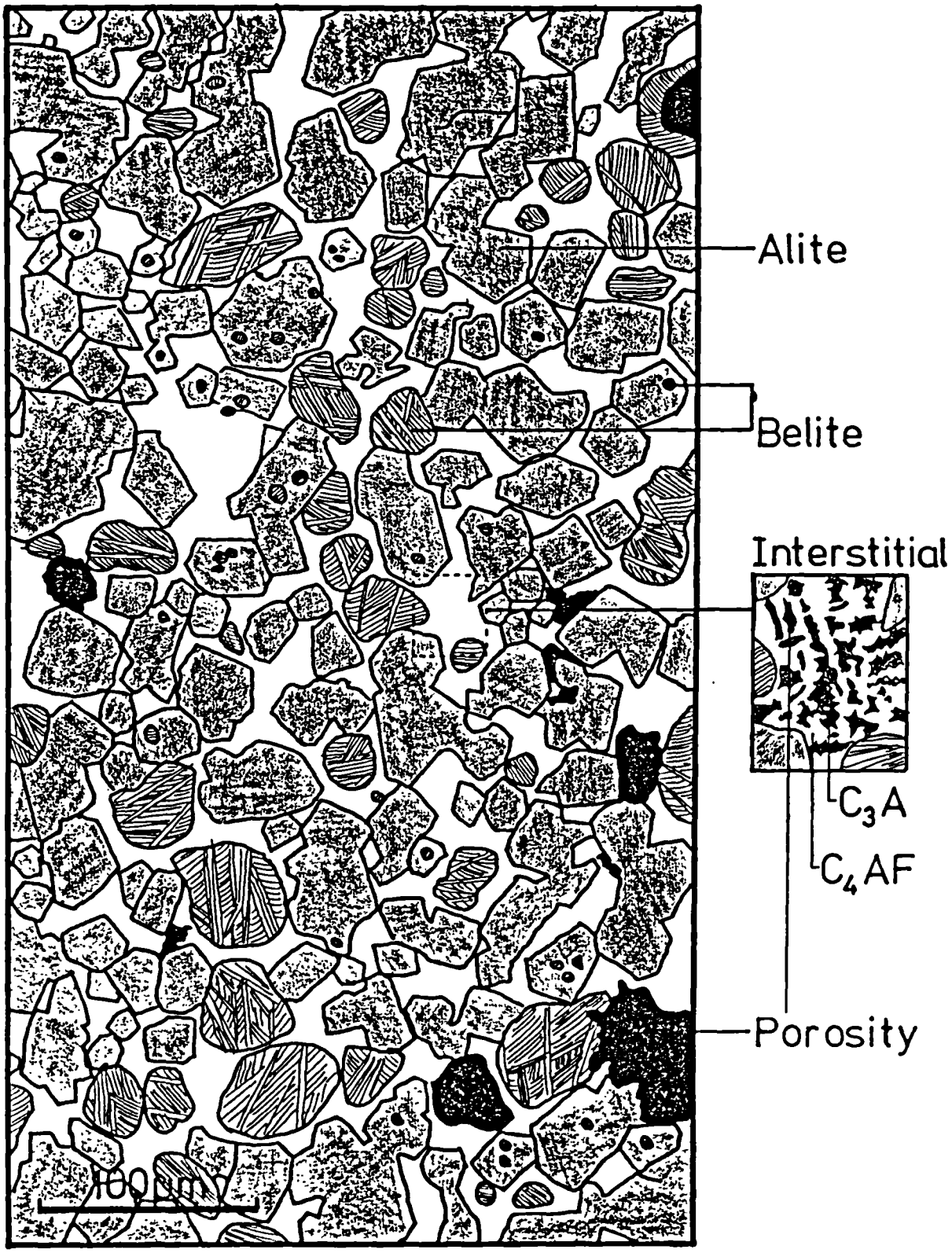

FIG. 2.5 Ideal clinker microstructure

microstructure (Hofmänner, 1975). This consists of grains of alite and belite in a matrix of the interstitial phases C_3A and C_4AF. The belite grains tend to be rounded and typically have a complex lamellar structure, or show polysynthetic twinning as a result of the α-α' or α'-β transformations (Groves, 1981, 1982; Ono et al, 1968). The alite grains tend to have a hexagonal section and frequently include small grains of belite. The interstitial phase is usually a finely divided mixture of intergrown aluminate and ferrite phases.

The size shape and distribution of the phases will vary in practice from this ideal picture according to the exact conditions of burning and cooling of the clinker and the physical and chemical characteristics of the raw mix (fineness, homogeneity and chemical composition).

For example, if a certain grain size is exceeded in the raw mix, the reactions can no longer take place completely within the burning zone and relict clusters of belite (from siliceous particles) or of free lime (from carbonate particles) may result in the clinker. Other microstructures which are found in commercial clinkers have been described by Hofmänner (1975) and Fundal.

2D Grinding of Cement Clinker (Bye, 1983)

The final step in the manufacture of portland cement is grinding the clinker. This is done in a large ball or tube mill which may be divided into two or three chambers containing size graded grinding media. Milling may be done on an open circuit with the cement passing directly to the silo or, as is more usual nowadays, an a closed circuit where the coarse material is returned for further grinding.

Gypsum is added to the clinker during grinding to control the setting of cement. The rapid hydration of the aluminate phase in the absence of gypsum causes premature stiffening of the cement with a loss of workability. The amount of gypsum added is determined experimentally by determining that addition which gives the maximum 28-day strength. Gypsum is more easily ground than clinker and so contributes disproportionately to the final surface area of the cement.

Due to the heat produced by the grinding process some dehydration of gypsum (calcium sulphate dihydrate) occurs. The product of dehydration is 'hemihydrate' which, despite its name, has a variable composition over the range $CaSO_4$ 0.01-0.63 H_2O; compositions at the lower end of this range are usually referred to as soluble anhydrite. If too much hemihydrate is present in the final cement this will rehydrate rapidly to gypsum when the cement is mixed with water causing false set. Too much undehydrated gypsum, however, can cause clumping during storage. To control the dehydration of gypsum the mill temperature is limited by supplying the mill with cool clinker, by cooling the recirculating air and in some cases by using an internal water spray.

The grindability of a clinker, the ease with which it can be ground, depends on its microstructure. The pore structure of the clinker has the major influence on the initial grinding, whilst the fracture properties of the individual phase dominate the later grinding. Petersen (1980) showed an almost linear relationship between the increase in the specific pore volume of the clinker and the decrease in power consumption to grind to a given fineness and discussed the effect of the clinker chemistry and burning conditions on the pore structure.

The fracture of the different phases is predominantly a function of their brittleness rather than their hardness. Hournain and Regourd (1980) found the relative brittleness of the major phases to be C_3S = 4.7, C_3A = 2.9 and C_2S and $C_4AF \sim 2$. C_3S often cracked during cooling further increasing its grindability. Beke and Opoczky (1969) ground separate samples of the four clinker phases and found C_3S to be most easily ground and β-C_2S least easily. C_3A and C_4AF showed intermediate behaviour, C_3A being close to C_3S and C_4AF close to C_2S. The grindability of the different phases determines how the relative amount of the phases varies with particle size and whether the cement grains are mono or polymineralic. QXDA of various size fractions by Gutteridge (1984) shows that belite tends to concentrate in the larger size fractions and alite in the smaller.

The fineness to which a cement is ground has a major effect on its hydration behaviour. Ordinary Portland cement is ground to a surface area in the range 300-350 m^2/Kg. The weight specific surface area (S_w) is usually determined by an air permeability method which depends on the relationship between S_w and the measured resistance to flow of a powder bed. Examples of such methods are the Lea and Nurse apparatus, the Rigden method and the Blaine method (Bye, 1983). The specific surface area of a cement determined from nitrogen adsorption measurements at 77K using the BET calculation procedure is much higher than that measured by air permeability, in the range 800-1000 m^2/Kg. Pores which are accessible from one end only are not measured in the permeability method because they do not contribute to flow, but are included in the total, surface area measured by the nitrogen adsorption method.

The particle size distribution of cement can be measured by several methods applicable to powders (Allen, 1981): sieving, sedimentation in a non-aqueous liquid, the Coulter counter, light

extinction and scattering methods. The vast majority of cement grains (~80%) lie in the size range 5-45 μm).

Chapter Three

TECHNIQUES FOR STUDYING THE HYDRATION OF CEMENT

Many methods have been used to study cement hydration. The overall rate of heat evolution can be followed by conduction calorimetry and this gives an indication of the overall rate of reaction. Most other techniques are concerned either with the solid or the liquid phase. The development of the hydrated phases and the depletion of the anhydrous phases has been studied by many techniques including quantitative X-ray diffraction analysis (QXDA), thermal analysis techniques (DTA / TG), and electron microscopical techniques. The separation of the liquid from the solid phase, however, may cause partial or complete dehydration of the hydrated phases and/or alterations in their morphology. The composition of the liquid phase may be analysed during hydration although, again, separation from the solid phase may be difficult without altering its composition. The advantages and disadvantages of the techniques most often used are discussed below.

3A Calorimetry

The conduction calorimeter measures the rate of heat evolution from hydrating cement. The calorimeter consists of the sample and a heat sink which is maintained at a constant temperature. Heat is conducted from the sample to the heat sink so hydration is effectively

isothermal. The small temperature difference between the hydrating cement and the heat sink is proportional to the rate of heat evolution of the cement; this is measured by a thermocouple. A conduction calorimeter was first made by Tian (1923) and a similar device was used by Carlson (1933) and by Lerch (1946) to study cement hydration. The calorimeter used in the present work was designed by Forrester (1970) (Appendix III) and is depicted in Fig 3.1. Fig 3.2 shows the typical rate of heat evolution for a cement which shows several maxima in the rate of heat evolution. The advantage of the calorimeter is that the hydration process can be followed at realistic water/cement ratios in situ without the need for drying or other specimen preparation which might produce artifacts. The disadvantage is that only the overall heat evolution can be measured which is the sum of the heat evolved by all the reactions occuring at any particular time. Indeed, if exothermic and endothermic reactions take place simultaneously the rate of heat output could be negligible even when the rate of reaction is high. To assign specific reactions to maxima in the rate of heat evolution other techniques must be used in conjunction with the calorimeter. The other problem in measuring the rate of heat evolution for cement hydration is the large amount of heat generated immediately on the addition of water (often referred to as pk 1). If this is to be measured by the calorimeter the water must be added to the cement inside the calorimeter, precluding adequate mixing. It has been found in the present work, however, that the degree of mixing critically affects the subsequent pattern of heat evolution.

3B QXDA

The use of QXDA to determine the relative proportions of the phases in unhydrated clinker or cement has already been described

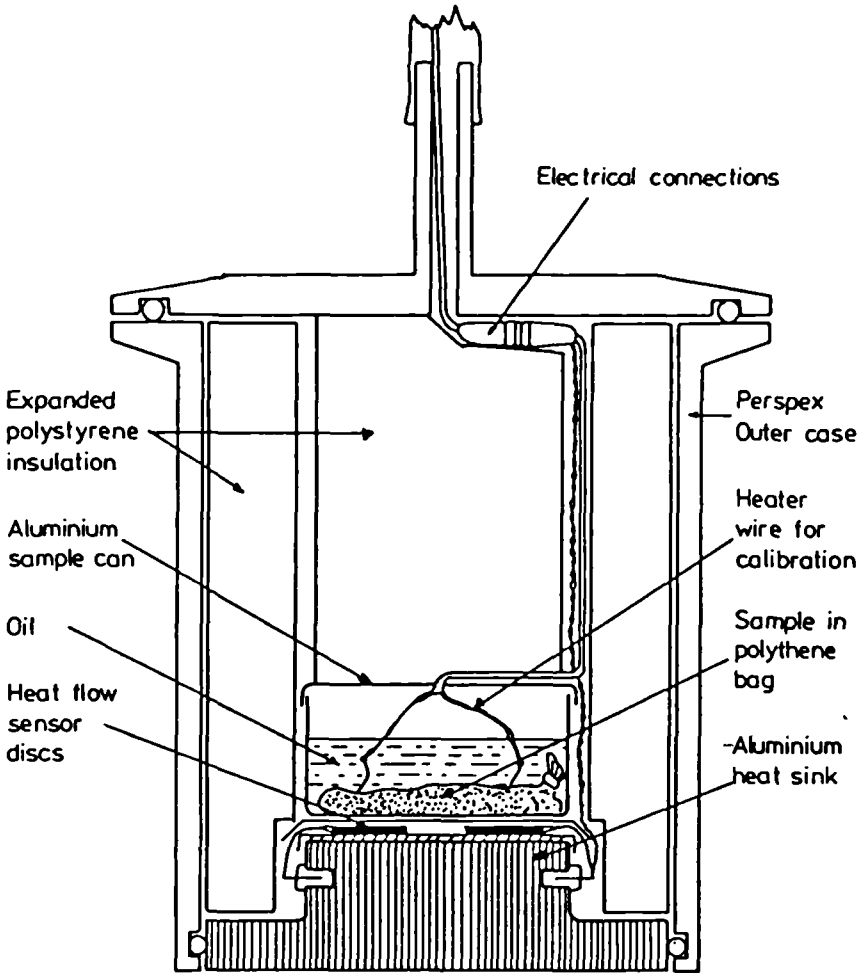

FIG. 3.1 Diagram of Calorimeter (from Forrester, 1970)

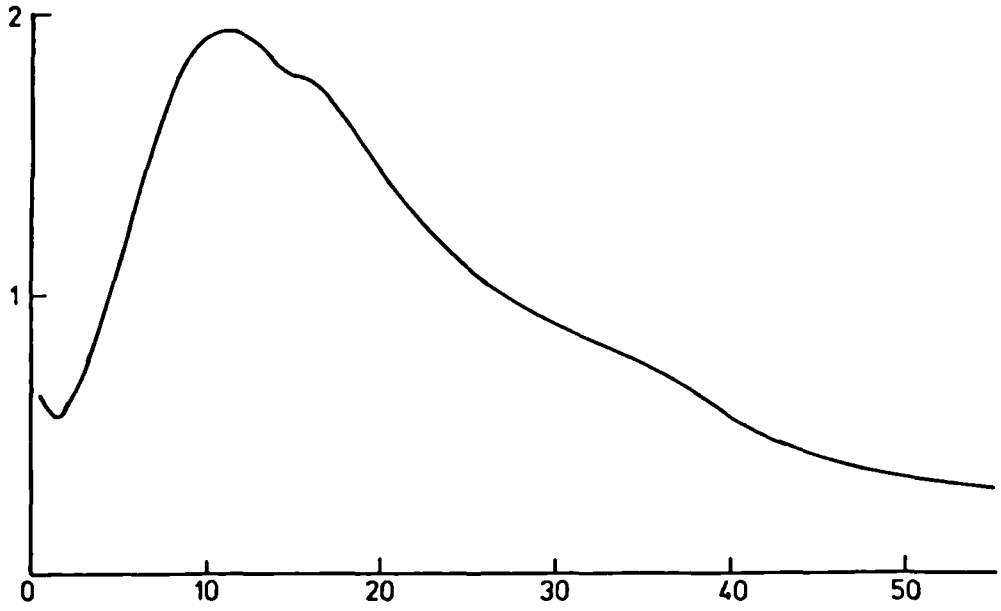

FIG. 3.2 Typical rate of heat evolution during the hydration of O.P.C. (from Pratt & Ghose, 1983)

(Chapter Two, Section C). This method may also be applied to hydrated cement. Several workers have used this technique to measure the quantities of the clinker minerals remaining unhydrated (e.g. Yamaguchi et al, 1960; Jons and Osbaeck, 1980, 1982; Gutteridge, 1984). Determination of the quantities of hydrated phases produced is, however, more difficult. Many of the hydration products are amorphous and so do not produce sharp diffraction peaks. Even the crystalline hydrated products show extensive solid solution and are often microcrystalline causing peak broadening and shifting. The diffraction peaks that can be identified tend to lie at a low angle where resolution is poorest and there are many overlaps between them. A study by several labs (Mather, 1976) showed that many of the hydrated phases (e.g. ettringite, calcium hydroxide, hydrogarnet, C-S-Hgel) could be identified by X-ray diffraction although only qualitatively. The results obtained showed some dependance on the sample preparation, some phases such as monosulphate, dehydrated if the sample was overdried and did not appear in the diffraction trace. It has, however, been possible to determine quantitatively the amount of calcium hydroxide in hydrated cement pastes (Gutteridge, 1984).

3C Thermal Methods

Thermal analysis methods depend on measuring the rate of heat evolution (DTA) or the dynamic weight loss (TG/DTG) from a sample as it is heated at a controlled rate.

Differential Thermal Analysis (DTA)

In DTA the temperature difference between the test sample and an inert reference material is measured against temperature. When a chemical change (such as the dehydration of a hydrate phase) occurs in the test sample, heat is taken in (endotherm) or given out (exotherm)

and so the temperature of the sample is lowered (endotherm) or raised (exotherm) relative to the reference material, both being supplied with heat at the same rate. This process produces a peak in the temperature difference curve measured by a thermocouple (Fig 3.3). The temperature at which the peak starts is characteristic of the reaction taking place, and the area of the peak is proportional to the amount of the reacting phase in the sample. The peak onset, however, is difficult to determine experimentally and the peak maximum is usually used for identification; this is a function of the sample (size, packing and composition), the equipment and experimental conditions (heating rate) as well as the reaction taking place.

In principle it should be possible to determine the quantities of various hydrated phases present at different hydration times using this method. Unfortunately, many of the phases produced during the hydration of cement dehydrate at very similar temperatures so their peaks overlap; many phases also lose water over a wide temperature range giving broad multiple peaks. In addition the presence of free or loosely bound water interferes with measurement of peaks at low temperatures, whilst rigorous drying partially or wholly dehydrates the phases giving rise to these peaks. Typical DTA curves from hydrated portland cement are shown on Fig 3.4. To determine the amounts of the different phases, calibrations must be run of pure phases or known mixtures, which presents the difficulty of synthesising phases identical to those found in cement itself. Despite these drawbacks DTA has been used extensively in the study of cement hydration (Ben-Dor, 1983). Kalousek (1976) presented the results of a study done on the same samples of hydrated cements and cement phases by several different labs; he showed great variability of the results from different instruments.

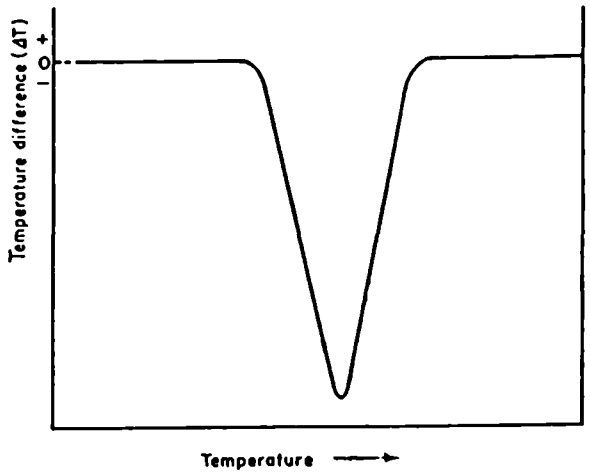

FIG. 3.3 Formalised Differential Thermal curve

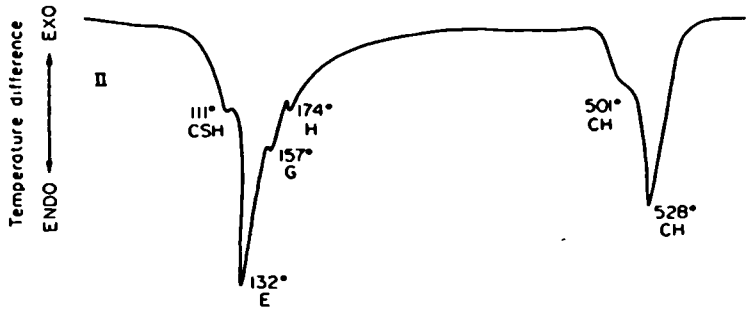

FIG. 3.4 Differential Thermal Analysis of O.P.C. Hydrated for 16hours. E-ettringite ; G-gypsum; H-hemihydrate; CH-calcium hydroxide ; CSH-calcium silicate hydrates from Bye, 1983

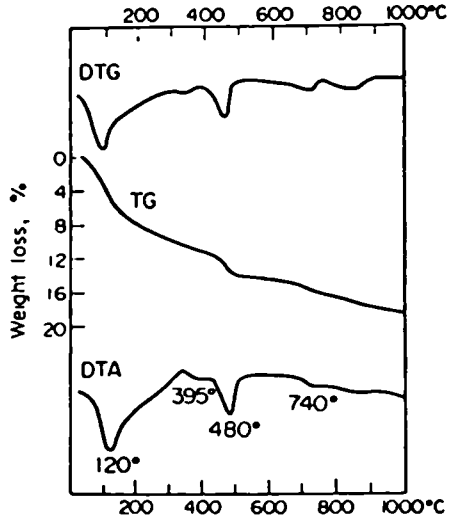

FIG. 3.5 Comparison of DTA, TG.& DTG of O.P.C. Hydrated for 28days. from Ben-Dor, 1983

Thermogravimetric analysis

Thermogravimetric analysis measures the weight loss of a sample against temperature for a constant heating rate. Weight loss occurs most rapidly at the dehydration temperatures of the hydrated phases, hence the reactions being followed are essentially the same as those by DTA, with the same problems. However, if the stoichiometry of the dehydration reaction is known, the amount of dehydrating material present can be calculated directly without depending on calibration curves. Fig 3.5 compares curves from DTA, TG and DTG (differentiated TG) for a portland cement.

TG can be used, however, to measure the total amount of water bound in all the hydrated phases and to measure the amount of calcium hydroxide (CH) present. The dehydration of calcium hydroxide does occur at a well defined temperature (425-550°C) giving a measurable step on the TG curve. Although measurements of the amount of CH made by TG agree well with those made by QXDA (Gutteridge, 1984) there are still several sources of error (Taylor, 1984).

3D Electron Microscopy

Electron optical techniques can provide a wide range of information, both qualitative and quantitative on the hydration of cement (Scrivener and Pratt, 1983). Fig 3.6 illustrates the main methods of imaging and analysis possible in transmission and/or scanning electron microscopes. Nevertheless, there are several problems in preparing cement for electron microscopy. Cement is non-conducting, and so must be coated with a conducting layer (i.e. gold or carbon); it is very brittle, making the preparation of electron transparent sections difficult; and it contains large amounts of water in its normal state, both as pore fluid and combined in hydration products.

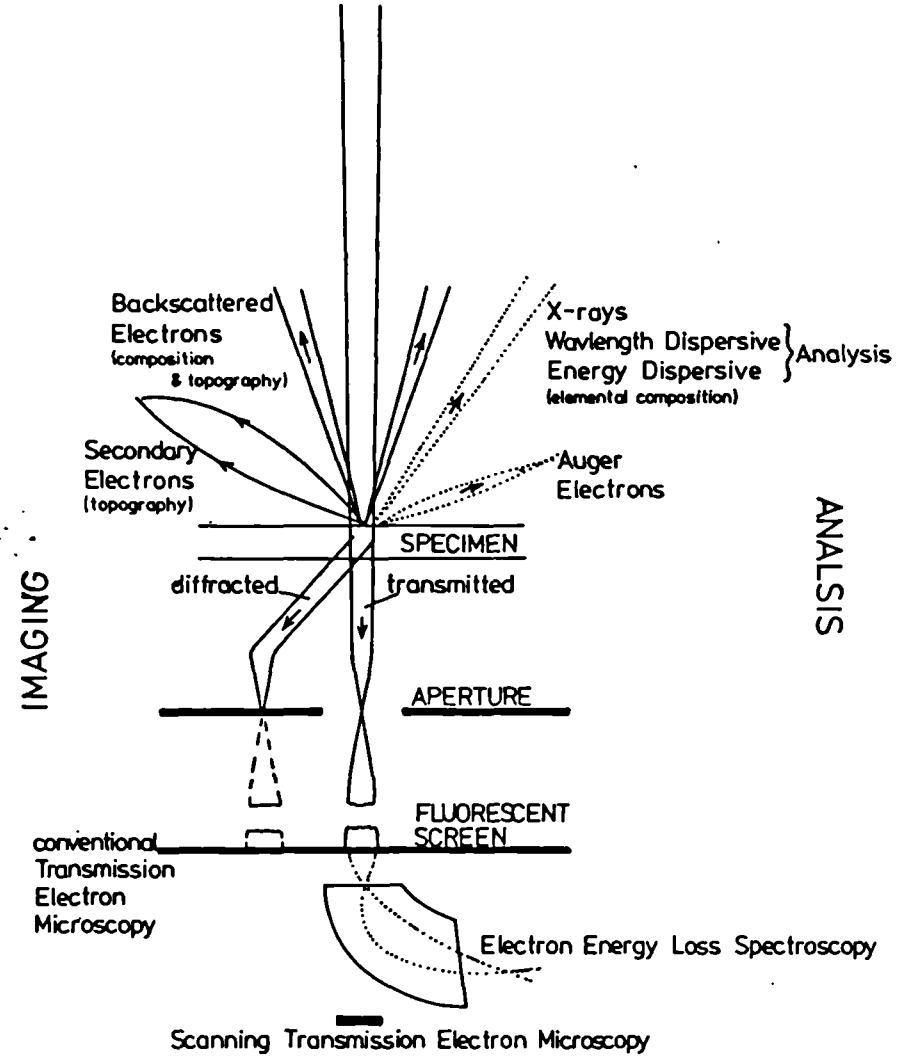

FIG. 3.6 Imaging and Analysis Techniques in the Electron Microscope

Early Transmission Electron Microscope (TEM) Studies

Early electron optical observations (such as reported by Grudemo, 1960, 1964, and by Copeland and Schultz, 1960, 1962) were made by grinding hydrated cement pastes. The resulting powder was then dispersed on carbon films and examined in the TEM. From these studies the crystal structure of those hydration products which were crystalline, such as calcium hydroxide, was identified by electron diffraction. Many hydration products, however, are amorphous and others dehydrate in the vacuum of the electron microscope. More recently this technique has been used to analyse the chemical composition of hydration products by EDXA in the AEM (Lachowski et al, 1980; Lachowski and Diamond, 1983a and b).

The usefulness of this technique is limited by the destructiveness of the sample preparation. Grinding of the cement paste destroys the spatial relationships between the hydration products and may alter their morphology, as may drying. In addition, in a suspension of ground cement heavier particles tend to sink more rapidly than lighter ones, so sampling may be unrepresentative.

Microscopy of dried fracture surfaces

Fracture surfaces of cement pastes provide a relatively simple means to observe the three dimensional arrangement of hydration products. Carbon replicas of fracture surfaces can be studied in the TEM but interpretation of these is difficult due to the small (perhaps unrepresentative) area visible and the heavily shadowed image. Since the development of the scanning electron microscope the direct observation of cement fracture surfaces (after coating with gold or carbon) has been possible. In the SEM low energy secondary electrons are generated by the incident beam fairly near the surface of the specimen, and are collected by a biased detector.

Their intensity increases as the inclination of the surface from the normal increases , thus a shadowless image of the surface is produced with fairly good resolution (Fig 3.7). This technique was first used to study the microstructure of hydrated cement paste by Chatterji and Jeffrey (1966). It has since been used by many authors, including Williamson (1972), Diamond (1976), Dalgleish et al (1982 a).

The microstructure observed, however, is that of cement paste which has been dried and exposed to the high vacuum of the electron microscope. Given the amorphous nature of the hydration products it is likely that some alteration in their morphology will occur during specimen preparation. Also, only fracture paths are revealed, so that weak areas of the structure predominate. In young pastes this is interparticular only showing the outer surface of the hydrated layer; in older pastes the fracture surface is dominated by areas of cleaved calcium hydroxide, which has grown to engulf the outer hydration products.

Many authors have reported chemical analyses of hydration products using EDXA on fracture surfaces. This is an extremely dubious technique. In cement paste the area from which characteristic X-rays are generated is greater than 2μm at 20kV, while on fracture surfaces the effective area sampled may be far larger due to the specimen geometry and its porosity. Most hydration products in portland cements are far smaller than this so the area from which X-rays are detected may include many other products as well as the one intended to be analysed.

Microscopy of 'wet' cement paste

The necessity of drying cement pastes for examination in the electron microscope can be avoided if the area around the specimen can be separated from the high vacuum in the microscope column.

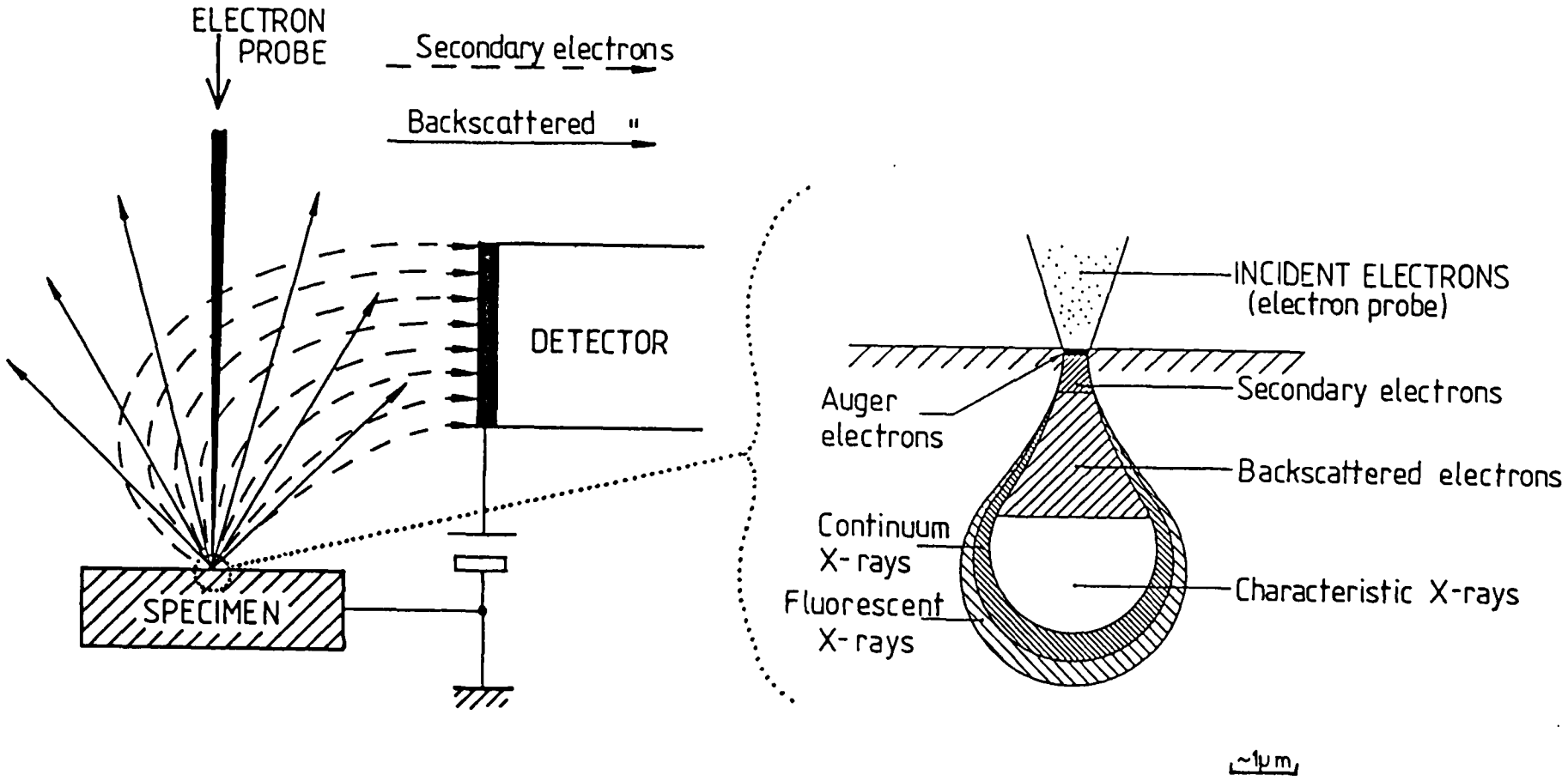

FIG. 3.7 Secondary Electron Imaging in the SEM to give a shadowless image (inset) depth of quantum generation

This is possible with the use of an environmental cell, the development of which has been reviewed by Flower (1973). In the AE1 EM7 1MeV high voltage electron microscope (HVEM) there is a comparatively large space (20mm deep and 50mm in diameter) between the objective pole pieces which permits the incorporation of an environmental cell around the specimen. Two designs of environmental cell have been used to study the hydration of cement in the AE1 EM7 microscope.

Double (1973) and co-workers (Double et al, 1978) have used a window type cell developed by Allinson (1970; Allinson et al, 1972, 1973). This cell is contained entirely within the specimen rod and can be removed without affecting the environment around the specimen, so the cement can be hydrated completely within the cell and examined at periodic intervals. The disadvantages of this design are the presence of physical windows and the high water/cement ratio required for the cement to remain transparent to the beam. Both these factors decrease the resolution of the microscope dramatically and the unrealistic water/cement ratio may also affect the hydration mechanism.

The cell used by Jennings and Pratt (1979a and 1980) and in the present work is a differentially pumped aperture type designed by Swann (1972, Swann and Tighe, 1972) shown in Fig 3.8. Thus although pressures can only be maintained up to 300τ the resolution is much improved over the window type as the electron beam only has to pass through 1.5mm of gas in addition to the specimen. The cell, however, is fixed inside the pole-piece and specimens must be prepared outside. Nevertheless, this has made it possible to study hydration at realistic water/cement ratios, as early as 10 minutes after mixing, with a minimum of drying before examination in the HVEM.

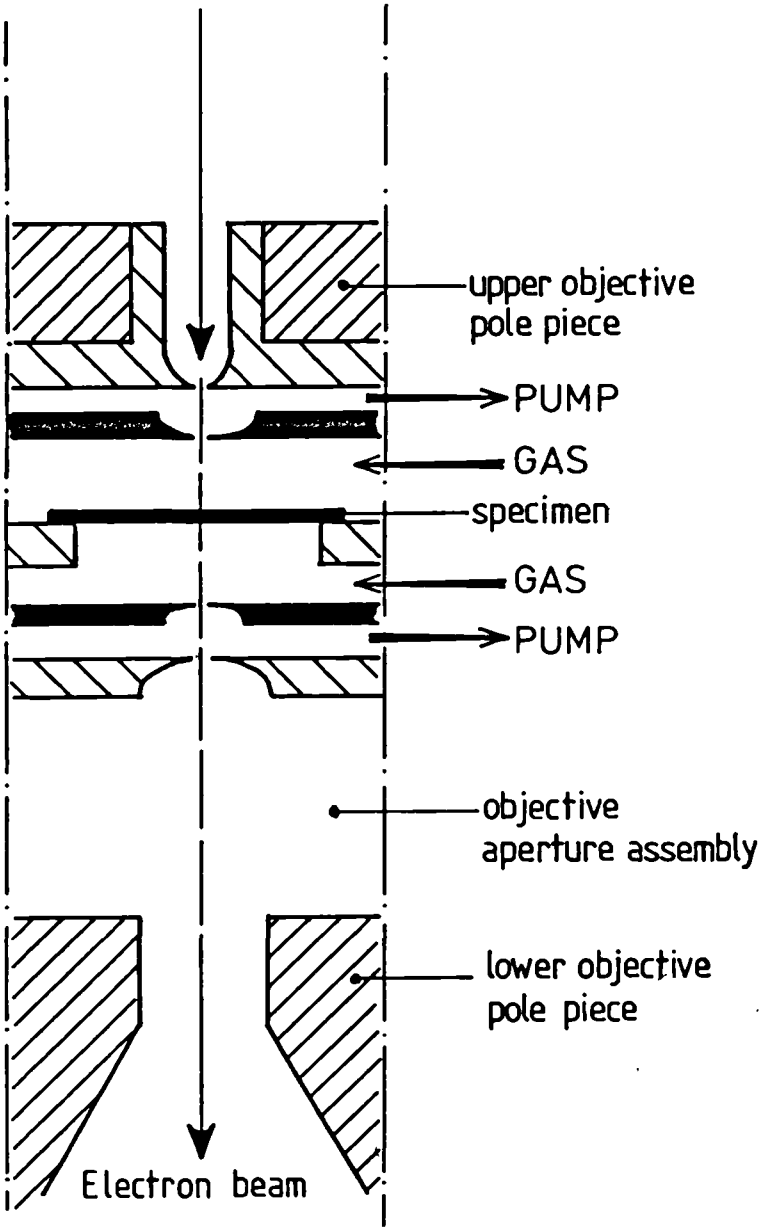

FIG. 3.8 Differentially Pumped Aperture Enviromental Cell in the HVEM

Despite the invaluable information gained on the morphology of hydration products in the 'wet' state using this method, it is still only the outer hydration surface of the particles that can be observed.

STEM of ion beam thinned foils

The preparation of electron transparent sections of cement allows the structure to be viewed in cross section. This has been done by Tiegs (1975), Javelas et al (1975) and Dalgleish et al (1980, 1981). As cement is very brittle the preparation of thin foils is very difficult and young pastes must first be impregnated with epoxy resin. The use of scanning transmission electron microscopy (STEM) minimises damage to the cement by the electron beam. Chemical analysis of the hydration products is also possible in thin foils using EDXA. The problem of beam spread is not present as the foil is very thin, but there may be distortions to the analysis by volatilisation of elements or contamination during thinning or in the electron beam.

With careful thinning at low angles fairly extensive electron transparent areas can be obtained, nevertheless a certain amount of selectivity is inevitable.

Scanning electron microscopy of polished cement surfaces

With polished cement sections large cross-sectional areas can be observed in the SEM. These do not, however, show good secondary electron contrast. The use of etches reveals some features of the microstructure such as the lamellae in belite grains (Fundal; Dalgleish et al, 1980) and some contrast between hydrated and unhydrated cement can be seen. Polished surfaces are used extensively for chemical analysis by EDXA (e.g. Stucke and Majumdar, 1976; Rayment and Majumdar, 1980; Taylor, 1984; Taylor and Newbury, 1984), as the

problems of specimen geometry, outlined earlier, are eliminated; the problem of beam spread, however, still remains.

Using a pair of back scattered electron detectors, images can be produced in which the intensity is dependant solely on the average atomic number of the scanned area, and is independant of small fluctuations in topography (Fig 3.9). Thus in polished unetched cement sections, the anhydrous material, massive calcium hydroxide, other hydration products and porosity can be distinguished (Scrivener and Pratt, 1983, 1984a). The contrast between the anhydrous grains and their surroundings is sufficient to allow quantitative image analysis of their total area and size distribution, so measuring directly the degree of hydration. If the contrast is enhanced sufficiently by the correct settings of microscope and photographic conditions the different clinker minerals may also be distinguished. In addition, the spatial distribution of massive calcium hydroxide may also be studied.

The form and distribution of the hydration products observable is comparable with, though of lower resolution than, that seen in the STEM of thin foils. However, backscattered electron images may be taken over a large cross sectional area, eliminating the selectivity of ion beam thinning used to prepare STEM specimens.

A combination of electron optical techniques reveals much about the development, size, shape, distribution and chemistry of the products produced during the hydration of cement. Care must, however, be taken to be aware of possible artifacts caused by a particular specimen preparation technique.

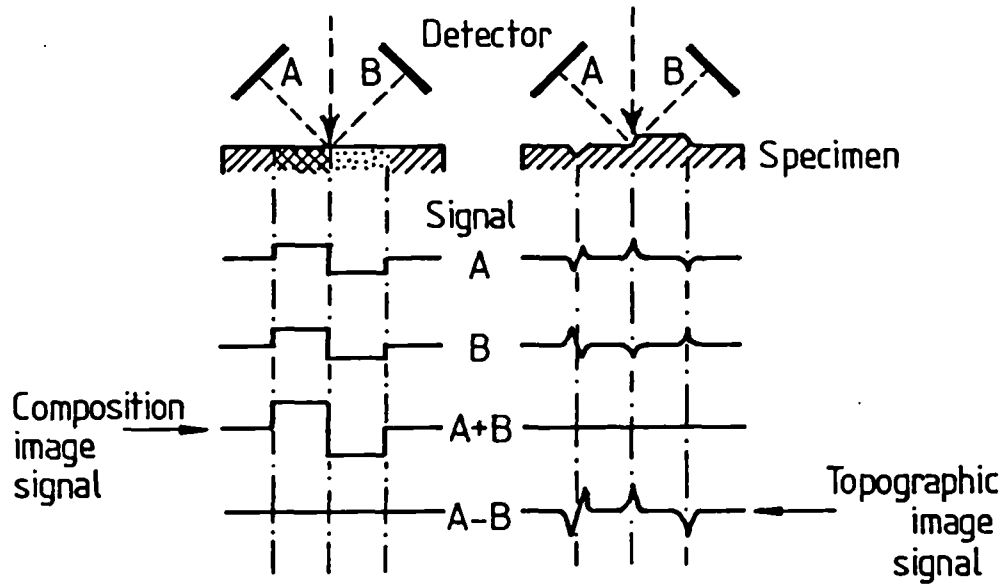

FIG. 3.9 Signal Processing for BEI in the JEOL JSM 35CF SEM

3E Solution Chemistry

The composition of the liquid phase in contact with the hydrating cement will have an important influence on, and be an important indication of, the reactions which take place during hydration, especially during the early stages of reaction. Separation and analysis of the liquid phase is, however, a difficult process at realistic water/cement ratios. After the cement has set and hardened great pressures are needed to extract the liquid from the capillaries of the paste; even before this stage the composition of the bulk liquid may not be the same as that at the surface of the hydrating grains and the composition may change during the extraction procedure. Also, contact of the extracted liquid with atmospheric CO_2 will lead to the precipitation of calcium carbonate, so altering the concentration of calcium ions in solution.

Calcium, sulphate and hydroxide ions are present at fairly high concentrations ($10^{-2} - 10^{-1}$ M), especially soon after the addition of water, and can be measured by titration. Other elements, however, such as silicon, aluminium and iron, are only present in very low concentrations ($\sim 10^{-6}$ M) which cannot be detected except by colormetric or atomic adsorption techniques which have only recently become generally available.

Analysis of the liquid phase has been used extensively in the study of the hydration of the pure clinker phases with water (Chapter Four), but less work has been done on the complex solutions produced on the hydration of cement. Early work was reported by Greene (1960), Kalousek et al (1943), Steinherz and Welchman (1958) and Hansen (1952) amongst others, for solutions formed soon after mixing of the cement with water. Lawrence (1966) studied the concentrations in solution up to 10-22 hrs by simple filtration, whilst Budnikov and Strelkov

(1966) used a pressure filter press (up to 2,000 psi) to extract the liquid phase from cement pastes up to 28 days. More recently Diamond and co-workers (Barneyback and Diamond, 1981, Diamond and Lopes Florez, 1981) have developed a press from a design of Longuet et al (1973) capable of exerting pressures up to 80,000 psi and extracting pore solutions from cement several months old. Solution phase analyses have also been reported by Thomas et al (1981) and by Rechenberg and Sprung (1983) (Ca^{2+}, SO_4^{2-} and OH^- only), both groups of workers using high water to cement ratios (>2) and only studying the first few hours of hydration.

Information on the total concentration of ions in solution can also be obtained by studying the electrical conduction of the paste. This technique has been used by Tamás (1982).

3F Other Methods

Porosity and surface area measurements

Of other methods for following the development of microstructure during the course of hydration, techniques which measure the porosity of the hydrating cement paste have probably received most attention. Information on the surface area and porosity of the hydrating paste indicate indirectly the structure and morphology of the products being formed. Mercury intrusion porosimetry (MIP), nitrogen adsorption using the BET equation, adsorption of water vapour and helium flow have been widely used, whilst results have been reported using solvent exchange (Parrott, 1983) small angle X-ray scattering (SAXS) (Winslow and Diamond, 1974), small angle neutron diffraction (SAND) (Pearson et al, 1982). Most methods give information on either pore size distribution or surface area but the second is often deduced from the first (or vice versa) by making assumptions about

contact angles or pore shapes. Since the pore sizes in cement range over 4 to 6 orders of magnitude several overlapping methods are needed to characterise the microstructure completely. Several of the methods give conflicting results which have been discussed by many authors (e.g. Ramachandran et al, 1981; Winslow, 1982). The interpretation of the absorption of water vapour is unclear due to the strong interaction of water with the hydrated structure. Of the other methods all measure the properties of dried paste except SAXS and SAND which are difficult to interpret and only yield information on pores at the lower end of the size range; and to a certain extent solvent replacement, which only gives the total pore volume.

Infrared absorption

This technique has been used by several authors in the study of cement paste (e.g. Kalousek and Roy, 1957; Takemoto et al, 1976; Bensted and Varma, 1974). Infrared absorption can yield information on the close environment of different atoms or groups of atoms and has been used to characterise the inter layer water and to investigate changes in the environment of the sulphate ion.

Silicate polymerisation

The extent to which the silicate ions polymerise in cement paste has been studied using Trimethlsilylation (reviewed by Taylor and Roy, 1980) and more recently by Nuclear Magnetic Resonance (NMR) studies (Rodgers et al, 1984).

Ultrasonic Pulse Velocity

Changes in UPV in hydrating cement reflect changes in its elastic properties and density. This technique has been used by Casson et al (1982) to study the setting and hardening of cement

paste and gives an indication of the changes taking place in the bonding between the cement grains, which can be related to changes in the microstructure.

Radiometric Emanation Method (REM)

Another novel technique that has been reported in the study of cement hydration (Balek and Dohnálek, 1983) is that of REM. The cement surface is impregnated with a radioactive isotope (Th-228 or Ra-224) and the rate of release of radon is measured against time after water has been added. Changes in this rate are indicative of changes occuring at the surface of the cement grains.

3G SUMMARY

Ideally several techniques are needed to characterise the hydration of portland cement. Calorimetry is useful in following the overall reaction and can be done 'in situ', but the reactions responsible for the heat evolution cannot be identified. The hydrated phases formed can be identified by QXDA and thermal analysis methods, but only in a qualitative manner (except perhaps for calcium hydroxide) and not always unambiguously. QXDA can also be used to measure the amounts of the anhydrous phases which have reacted.

The chemistry of the solution during hydration obviously has an important influence on the reactions taking place, but results of solution analysis are often difficult to interpret in the multi-component, multiphase system which comprises cement paste.

None of these methods, however, reveal anything about the size, shape and distribution of the hydration products.

Much more information about the development of microstructure can be gained by electron optical methods than by any other technique.

It is, however, most important that alterations to the structure, which may occur during specimen preparation, are taken into account. The appearance of the microstructure in the bulk paste can only be deduced from a combination of electron optical techniques, including examination of the cement in the undried state (i.e. in an environmental cell). Electron optical techniques can be used to study the chemistry of the hydrated phases, although, again, care must be exercised in interpretation of results. Using quantitative image analysis and backscattered electron imaging, measures of the extent of reaction can be made. Other techniques, used in conjunction with electron microscopy and calorimetry, can provide valuable, additional information.

Chapter Four

HYDRATION OF THE CONSTITUENT PHASES OF CEMENT

This chapter deals with the hydration of the phases which make up portland cement; C_3S or alite; β-C_2S or belite; the aluminate phase, C_3A, and the ferrite phase, C_4AF. In each section the literature on the hydration of one phase is reviewed followed by a description and discussion of the present work on the hydration of the same phase. The final section examines the previous work on physical mixtures of the phases and describes the present microstructural examination of the hydration of a C_3S:C_3A:$C\bar{S}$ mixture.

4A Hydration of Tricalcium Silicate

C_3S in its impure form as alite constitutes by far the largest part of portland cement and its hydration is primarily responsible for the strength development of cement. Consequently its hydration behaviour has received much attention and is often considered to be analogous to cement hydration. In order to avoid repeating previous work, little new work on the hydration of C_3S and alite is presented here.

4A.I Review of previous work

The literature on the hydration of C_3S has been extensively reviewed and discussed elsewhere (Taylor, 1979; Skalny and Young, 1980; Pratt and Jennings, 1981; Jennings, 1983; Pratt, 1982; Taylor et al, 1984). The summary presented here is not intended to be exhaustive and makes use of the report of Rilem committee 68-MMH Task Group 3 (Taylor et al, 1984) which summarises evidence regarding the mechanism of hydration of C_3S and alite at ordinary temperatures and discusses its interpretation.

4A.I.1 Structure and solid solution of C_3S

Pure C_3S exists as several polymorphic forms as a function of temperature. The various polymorphs have rhombohedral symmetry at high temperatures (> 1070°C), monoclinic symmetry between 1070°C and 980°C and are triclinic below 980°C (Regourd, 1979a). One rhombohedral, three monoclinic and three triclinic modifications are known; the transformations between them are displacive with small transition enthalpies and the high temperature modifications cannot be quenched to room temperature in the absence of impurities. The structures of all the polymorphs are very similar consisting of independant SiO_4 tetrahedra

linked by calcium ions. The calcium ions are octahedrally co-ordinated to three oxygen atoms which are not linked to Si^{4+}, and the structure contains three octahedral holes per formula unit, large enough to accommodate other atoms (Jeffery, 1952). The structure has also been described as alternating layers of C_2S and CaO which could explain the ready decomposition of C_3S into C_2S and CaO (Regourd, 1979a).

Many foreign ions, such as Al, Fe, Mg, Mn, Cr, Ti, K, Na and Zn may be incorporated into the C_3S crystal lattice at levels around 1% ; by substituting for Ca^{2+} or Si^{4+} or occupying interstitial holes. The interaction of these ions may stabilise monoclinic forms of C_3S at room temperature; indeed, most alites in portland cement show monoclinic symmetry (Maki and Chromy, 1978; Regourd, 1979a). Triclinic and rhombohedral forms of alite in cement have been reported (Berger et al, 1966; Regourd and Guinier, 1974), although recent work by Sinclair and Groves (1984 a and b) has shown that electron diffraction patterns from alites identified as rhombohedral by X-ray diffraction, can only be indexed on a triclinic lattice.

4A.I.2 Hydration of C_3S

Nature of products formed

The reaction of C_3S with water leads to the formation of calcium hydroxide (CH) and a calcium silicate hydrate (C-S-H) gel of indeterminate (and perhaps variable) composition. The amount of CH formed has been found to be about 1.3 mole per mole of C_3S, by QXDA, chemical extraction and thermal analysis methods (Taylor et al, 1984) and from an EPMA study on mature C_3S paste (Taylor and Newbury, 1984). This corresponds to an overall C/S ratio in the C-S-H of 1.7. Values between 1.5 and 2 have been found by EPMA and AEM, although taking considerations of beam spread, element excitation and specimen

preparation into account, the value of 1.7 is likely to be closest to the true value.

Calcium hydroxide crystallises as well formed hexagonal plates usually in the space originally occupied by water.

C-S-H gel has been reported as having several morphologies (Diamond, 1976; Jennings et al, 1981). The differences in morphology have been attributed to: time of formation, space available, mechanism of formation (through solution or topochemical), C/S ratio and degree of polymerisation. It is important, however, to take into account alterations to the morphology which may occur during specimen preparation.

Diamond (1976) classified these different morphologies as:

TYPE I - fibrous particles (needles or rolled sheets)

TYPE II - reticular network (interlocking or honeycomb structure)

TYPE III - equant grains (small, irregular grains ~ 0.3 μm in diameter)

TYPE IV - inner product (dimpled in appearance due to presence of pores or small grains about 0.1 μm in size).

This classification has been modified by Jennings et al (1981) as summarised in Table 4A.1.

The X-ray evidence shows that C-S-H has only short range order. From this evidence and by analogy with other basic salts, Taylor (1968) proposed a structure based on CaO sheets similar to those found in $Ca(OH)_2$, but with much of the OH replaced by oxygen atoms of randomly arranged silicate anions. Taylor (1979) considers this model may be too rigid to account for results of trimethylsilylation studies and later C-S-H morphologies (i.e. Diamond Type III) and proposes that sub-crystalline order may be confined to small fragments of Ca-O layers perhaps only some tens of Å large. A proposed schematic structure for C-S-H gel Type III is shown in Fig 4A.1 (Taylor, 1979).

Table 4A.1 - C-S-H morphologies from Jennings et al (1981)

Classification		Period Formed	Morphology and Habits
Early	Type E	First few hours Stages I and II	Thin flakes or foils which, when dried, become cigar-shaped tubes, 0.25 μm long, radiating from C_3S grains at all angles.
Middle	Type O	Between 2-24 hr Stages III and IV	Amorphous gel approximately 0.5 μm thick surrounding C_3S grains. Behaves as wet plastic material for first several days. Changes into other morphologies depending on space available.
	Type 1	Forms from type 0 during first few days	Slightly tapered needles, 0.75-1.0 μm long, radiating perpendicularly to C_3S grains, with aspect ratio of about 10. Formed from type 0 in open areas > 1 μm. Encouraged by drying and/or age.
	Type 1'	Can be formed from type 0 during first few days	Tapered fibres, 0.25-0.5 μm long, often branching. Formed from type 0 by pulling apart particles. Only seen on young fracture surfaces.
Late	Type 3	Forms from type 0 after several days	Partly crumpled foils which are interlocked. Formed as type 0 ages and/or dries in regions where original interparticles spacing < 1 μm
	Type 4	After first 24 hours	Dense gelatinous inner product

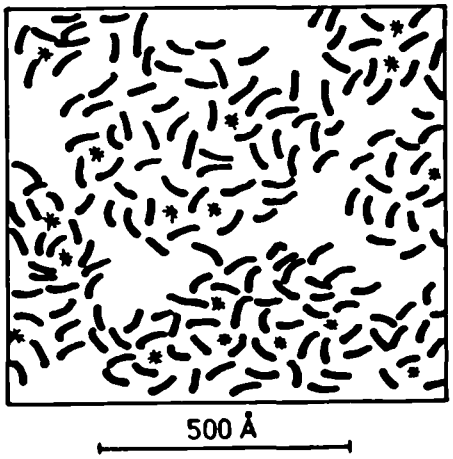

—Ca-O sheets with attached anions including Si_2O_7

* typical spaces contain CaH_2O anions, including compact polysilicate anions

FIG. 4A.1
Suggested structure for Type III C-S-H (schematic)
(from Taylor, 1979)

Form of hydration reaction

The hydration reaction is usually considered in several time periods or stages corresponding to different regions of the rate of heat evolution against time curve (Fig 4A.2) (Kondo and Ueda, 1968; Pratt and Jennings, 1981): Stage I, the pre-induction period, characterised by an initial maximum in the rate of heat evolution and a rapid rise in the concentration of species in solution; Stage II, the induction period, during which the rate of heat evolution is low; Stage III, the acceleratory period in which the rate of heat evolution rises again, large quantities of hydration products are formed and the amount of unhydrated C_3S drops significantly; Stage IV, the deceleratory period, during which the rate of reaction decreases continuously.

Hydration mechanisms

Many hypotheses have been advanced to explain this pattern of reaction. During the acceleratory period it is widely believed that the rate of reaction is controlled by a chemical or phase boundary process, such as the dissolution of C_3S or the nucleation and growth of C-S-H, although the details of the rate controlling reaction are unclear. In the deceleratory period the reaction is thought to become controlled by diffusion through a product layer, although lack of space for formation of the products (Powers and Brownyard, 1948) or the decreasing surface area of C_3S (Knudsen, 1980, 1982) may also be important factors. Much controversy, however, exists over the causes of the induction period and its termination.

The majority of proposed theories conjecture the formation, and subsequent disruption, of an inhibitive layer around the C_3S grains.

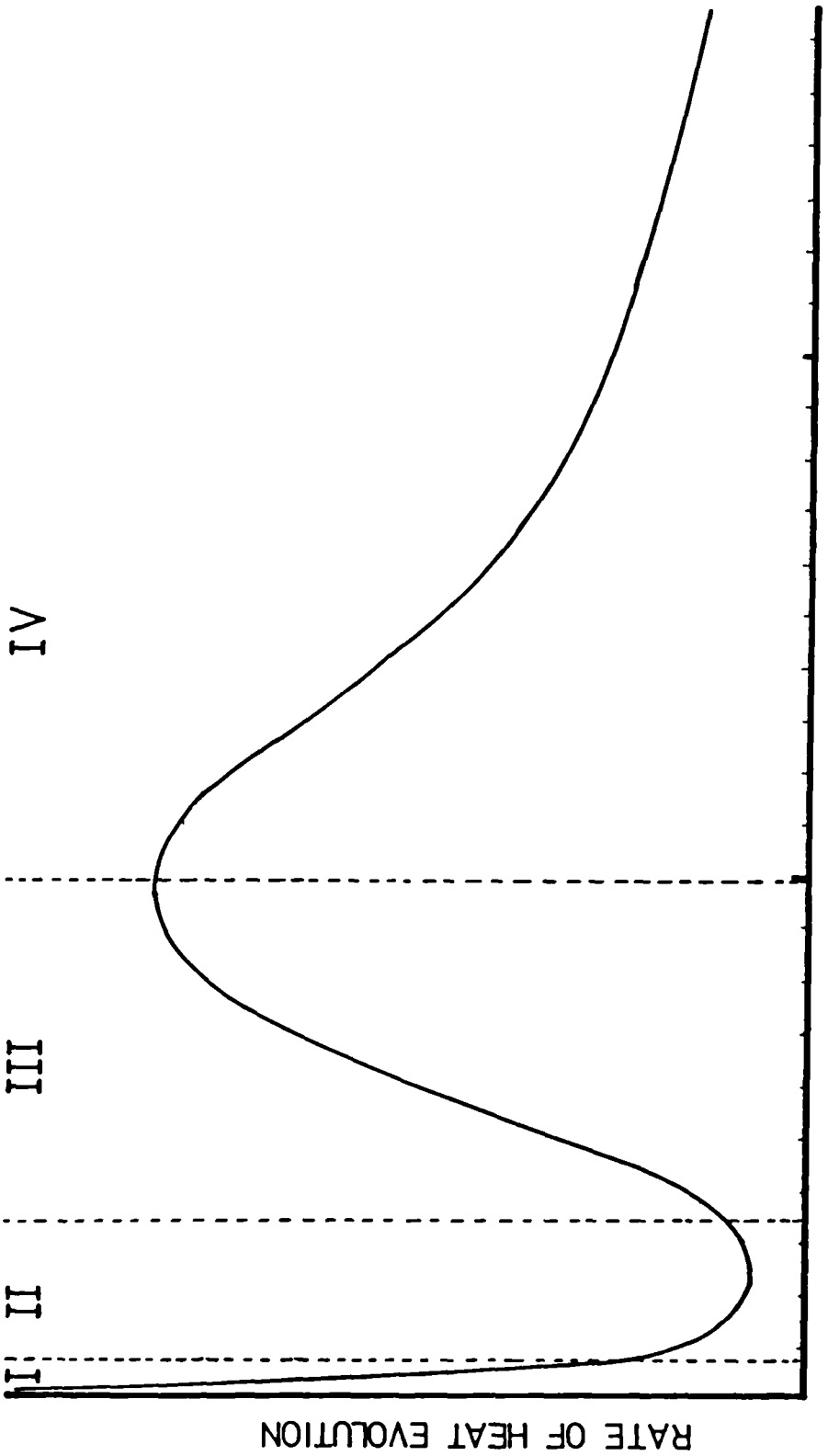

FIG. 4A.2 Schematic representation of the different stages of hydration for C_3S.

Young, Skalny and co-workers (Tadros et al, 1976; Skalny and Young, 1980; Young et al, 1977) have proposed that the incongruent dissolution of C_3S leaves a Si-rich layer on the surface of the grains onto which Ca^{2+} ions absorb. The electrical double layer so formed impedes the passage of ions into solution. At the end of the induction period the precipitation of calcium hydroxide occurs which then acts as a sink for calcium ions, weakening the double layer and allowing renewed hydration of the C_3S. This theory is supported by the near coincidence of the maximum calcium ion concentration and the end of the induction period and by evidence of a positive zeta-potential on the C_3S grains during the induction period, consistent with chemisorption of calcium ions (Tadros et al, 1976; Suzuki et al, 1981).

Alternatively it has been proposed (Stein and Stevels, 1964; de Jong et al, 1967, 1968; Kondo and Daimon, 1969) that a layer of hydrate is formed over the surface which has a low permeability and so restricts further hydration. This primary hydrate subsequently undergoes conversion to a second hydrate which is more permeable and so the rate of reaction increases. There is no conclusive evidence, however, for the existence of a continuous hydrate layer of low permeability.

It has also been suggested that, for C_3S hydrating in cement, this barrier layer is a continuous semi-permeable membrane which is subsequently disrupted by osmotic pressure (Powers, 1961; Double et al, 1978; Birchall et al, 1978; Double, 1983). From proposed structures of C-S-H it seems unlikely that a layer of C-S-H could be permeable to water and impermeable to calcium and silicate ions and so act as an osmotic membrane.

The termination of the induction period has been widely attributed to the eventual nucleation of one of the hydration products: either calcium hydroxide, as described earlier, or C-S-H.

Fierens and Verhaegen (1976a, b, c) maintain that the nucleation of C-S-H occurs preferentially on defects at the grain surfaces and that these nuclei must attain a critical size before rapid growth, at the end of the induction period, can occur. Theories involving the delayed nucleation of C-S-H, without the first hydrate acting as a barrier layer, have also been proposed by Sierra (1974), Odler and Dörr (1979) and Barret et al (1980a, b).

Theories that postulate the delayed nucleation of C-S-H, including those in which the first hydrate acts as a barrier layer, are supported by the results of seeding experiments. Odler and Dörr (1979) found that the induction period was shortened when prehydrated C_3S containing CH and C-S-H was added to the initial mix, whilst the addition of CH alone was ineffective. These results were also found by Brown (1984b).

When the growth of CH is poisoned by organic admixtures (Young, 1972; Thomas and Birchall, 1983) the induction period can be prolonged indefinitely, suggesting that nucleation of CH is indeed the critical factor in ending the induction period. The same admixtures have, however, been shown to poison the growth of C-S-H as well (Birchall and Thomas, 1984). This indicates that the nuclei of CH and C-S-H may be similar and it is possible that extensive nucleation and growth of CH and C-S-H cannot take place independently of one another in C_3S pastes.

As pointed out by Taylor et al (1984) all the principal hypotheses agree in supposing that any nuclei of CH formed before the end of the induction period are poisoned by silicate and do not grow until a fairly high level of supersaturation has been reached.

Phase equilibrium approach

Recently Brown et al (1984) found that the concentrations of lime and silica in solution during the early hydration of C_3S fell on a curve, as did solution compositions reported by other workers, both from hydrating C_3S and from mixtures of soluble lime and silica in which C-S-H precipitated (Fig 4A.3). Indeed, Jennings (1984) has found that all solution compositions in contact with C-S-H, reported in the literature, fall on one of two curves (reasons for the existence of two curves being unclear). This evidence suggests that the CaO-SiO-H_2O phase equilibrium diagram might be relevant to the hydration of C_3S, the solution being in equilibrium with C-S-H during the induction period. A schematic version of this phase diagram (grossly distorted as regards scale) is shown in Fig 4A.4 (Taylor et al, 1984). Brown et al (1984) found that the initial dissolution of C_3S was congruent as reported by Barret et al (1980a), but rapidly becomes saturated with respect to C-S-H with a C/S ratio less than 3. The precipitation of this hydrate leads to a drop in the silicate concentration in solution. Brown et al (1984) assumed a solid solution range for C-S-H with C/S varying from 1 to 1.7, but this is not required thermodynamically to explain the range of calcium and silicate ions found in solution. In addition, using this approach, it is not necessary to assume that the growth of CH is poisoned by silicate ions as the solution is not saturated with respect to calcium hydroxide until the point A is reached (Figs 4A.3, 4A.4).

Bailey and Hampson (1982) calculated the activities (as opposed to concentrations) of calcium and hydroxide ions in solution by taking into account the interaction of the ions and any complex ions that would be likely to be formed. They found, on the basis of the ionic activity product of calcium hydroxide, that high degrees

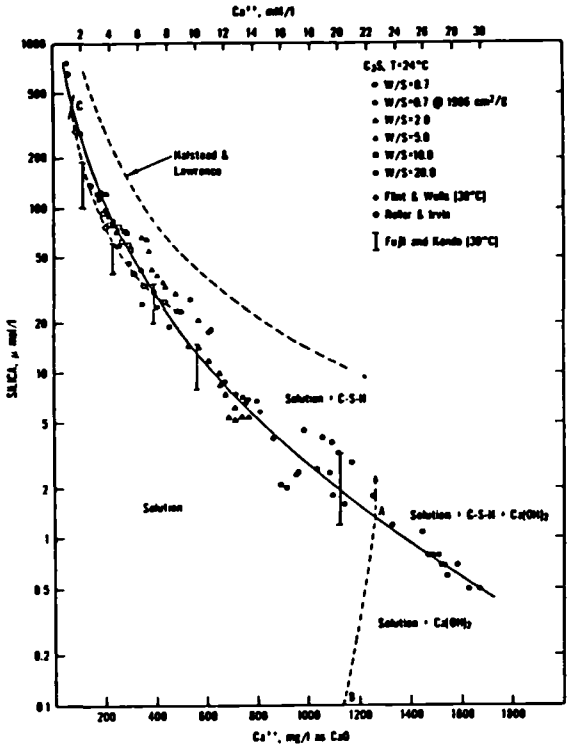

FIG. 4A.3
Solubility curve
for C-S-H

from Brown et al, 1984

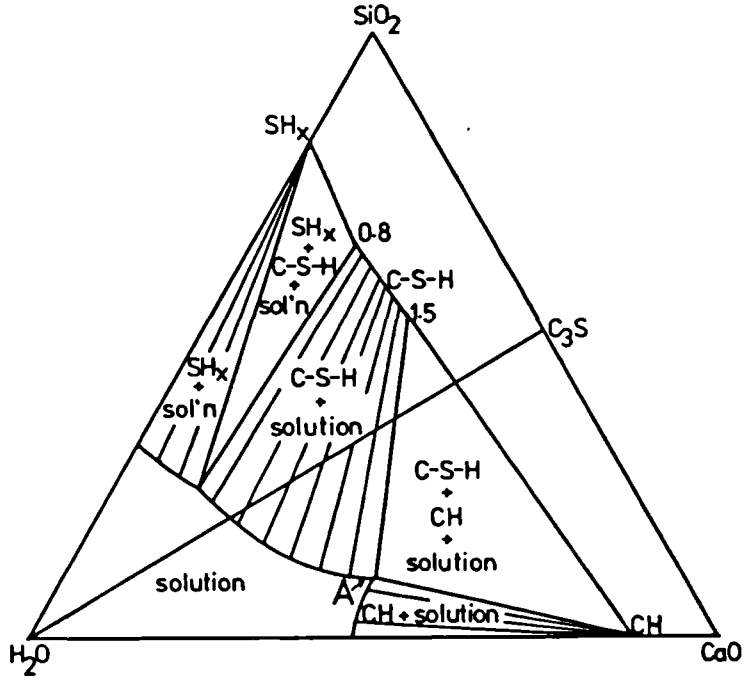

FIG. 4A.4 Schematic $CaO-SiO_2-H_2O$ phase diagram
NOT TO SCALE from Taylor et al, 1984

of supersaturation with respect to calcium hydroxide were not achieved during the hydration of C_3S and cement. This evidence further supports a phase equilibrium approach.

Development of microstructure during the early hydration of C_3S

Kantro et al (1962) reported a 1000 fold increase in the surface area of hydrating C_3S during the first 20 minutes after the addition of water and interpreted this as the formation of C-S-H as thin sheets typically 30-40 Å thick and extending as much as a micron in the other two dimensions. Any product of this nature might be expected to undergo drastic changes on drying and subsequent preparation for electron microscopy. As discussed in Chapter 3D, possible alterations in the microstructure and the representativeness of the area observed must be borne in mind when interpreting electron optical observations of hydrated C_3S pastes.

Despite the destructive nature of the preparation techniques used, early observations on ground and dispersed C_3S and cement (e.g. Grudemo, 1960, 1964; Copeland and Schultz, 1960, 1962) reported foils and fibres of C-S-H in addition to a structureless gel.

Ménétrier et al (1979) studied pellets of C_3S dipped in water and observed uneven attack of the surface after 5 minutes. After 15 minutes a 'honeycomb' product was observed, formed by layers peeling off the surface; this product continued to develop during the following 2 hours. Fujii and Kondo (1974) reported the appearance of a flaky product on the surface of C_3S after twenty minutes hydration; whilst Ings et al (1983) observed a hydrate layer on C_3S single crystals after only 5 minutes hydration. Foils and needles were also seen on the surface of C_3S grains by Stewart and Bailey (1983) after 30 minutes hydration. All these observations were made on dried microstructures.

Using an environmental cell in the HVEM, Jennings et al (1981) observed flakes and exfoliating thin sheets on the C_3S surface after 30 minutes in an undried sample. These flakes curled and crumpled to produce tapered needles, if the specimen was allowed to dry out.

Small particles of calcium hydroxide were observed during the induction period by Ménétrier et al (1979) and by Ings et al (1983), although these could have been artifacts of drying.

At the end of the induction period a rapid increase in the amount of C-S-H and CH takes place. On fracture surfaces the C-S-H is generally observed as needles or fibres (Diamond Type I), whilst Jennings et al (1981) observed a gel like product which transformed to other morphologies on drying as outlined in Table 4A.1.

Distribution of products in the later microstructure

Williamson (1972) reported the appearance of pseudomorphs of the original grains on the fracture surfaces of a C_3S paste hydrated for 2 years. There was a distinct difference in morphology between the product that had been formed in the originally water filled space, 'outer' product, and that which formed as pseudomorphs, 'inner' product. The same distinction is made in Diamond's classification, where types I, II and III are 'outer' product and type IV 'inner' product and similarly in the classification of Jennings et al (Table 4A.1). Taylor and Newbury (1984) found no such distinction between inner and outer product in a 22-year old C_3S paste, and no compositional differences between the C-S-H in different regions, except that calcium hydroxide was found largely or completely in the outer hydrate. However, ion beam thinned sections prepared by Dalgleish (Jennings et al, 1981) show that distinctions between the morphologies of 'inner' and 'outer' hydrate can only be seen in transmission and are not visible on fracture surfaces, or in secondary electron images

of polished or thinned sections. Barret et al (1980b) have suggested that C-S-H is always formed by a 'through solution' mechanism, albeit the distance between the C_3S grain surface and the point at which C-S-H is precipitated being very small. With C_3S, however, there does not appear to be any separation between the anhydrous grain and the surrounding hydrated layer, in contrast to the situation observed in cement pastes (Chapters 5 and 6).

Even after 22 years (Taylor and Newbury, 1984) calcium hydroxide is still found in massive regions which were probably originally water filled space.

Effect of polymorphism and impurities on the hydration of C_3S

The effect of polymorphism on hydration is difficult to study independently from the effect of the solute ions introduced to stabilise different polymorphs at room temperature. Mascolo et al (1973), Nurse et al (1966) and Števula and Petrovič (1981) have all studied the effect of polymorphism on the hydration of C_3S and conclude that the chemical effect of the stabilising solute was far greater than polymorphic effects. Thompson et al (1975), studying the reactivity of MgO stabilised alites, found that the early heats of hydration were similar for the monoclinic and triclinic polymorphs containing the maximum amount of MgO in solid solution. It was also found that both decreasing the amount of MgO in solid solution from the maximum and increasing it from zero resulted in a marked decrease in reactivity. Harada et al (1978) found the order of reactivities at early ages of hydration to be: monoclinic < triclinic < rhombohedral, but any differences diminished with increasing degrees of hydration. These authors also reported variations in the C-S-H morphology between the different polymorphs as was reported by Stewart and Bailey (1983).

Valenti et al (1978) studied the rate of hydration of synthetic alites, bearing Al, Fe or Mg in concentrations of about 1%, over 24 hours. The degree of hydration was found to be lower than that of pure C_3S, especially in the case of Al and Fe bearing alites. Scanning electron micrographs of the Fe bearing alite hydrated for 24 hours show slight separation of the hydrated shell from the unhydrated core, similar to that seen in cements (Chapter 5). In contrast Kaushunskii and Timashev (1978) found Al-bearing alites to be more reactive than pure C_3S, although reactivity does not increase linearly with concentration. They suggest that the reactivity of alite surface is increased by the alteration in the electron band levels in the C_3S produced by substitution of Al^{3+} for Si^{4+}.

It is apparent that the reactivities of C_3S and alites may vary with the type and concentration of species in solid solution.

4A.II Present Work

4A.II.1 Materials and Techniques Used

The alite used in the present work was supplied by Dr L. Parrott of the Cement and Concrete Association (C&CA). The quantity available (3g) limited the number of specimens that could be prepared. The chemical analysis of the alite is given in Table 4A.2. The rate of heat evolution for this material at $^{w}/s = 0.5$, determined by Mr D. Killoh from C&CA, is shown in Fig 4A.5.

A piece of alite hydrated for 6 months ($^{w}/s = 0.5$) was also supplied by Dr Parrott, from which a fracture surface was prepared.

Preparation of specimens for examination in the environmental cell of the HVEM (AE1 EM7)

A small amount of alite was placed into a specially made plastic bag (Fig 4A.6). These bags were made from thin gauge polythene food bags (e.g. 'Snappies'); the edges were fused together using a soldering iron with a piece of paper between the soldering iron and the plastic. A measured amount of water (to give $^{w}/s = 0.5$) was then added to the alite with a pipette. Holding the top of the bag closed, to minimise CO_2 contamination, the paste was mixed between the fingers for about 2 minutes.

Beforehand, a carbon film was evaporated onto an optical microscope slide, and floated off onto the surface of a trough of water. 3mm copper 200 mesh electron microscope grids, previously placed on mesh boats at the bottom of the trough, were then lifted up underneath the carbon film. These microscope grids carrying carbon support films were then carefully buried in the paste using fine tweezers. After the required hydration time the bags were cut open, the microscope grids extracted and placed immediately in the environmental cell.

Table 4A.2 Properties of alite

	Wt %
SiO_2	25.45
CaO	71.74
Al_2O_3	1.20
MgO	1.25
Fe_2O_3	0.10
LOI	0.39

Density 3190 kg/m³

Specific surface area 365 m²/kg

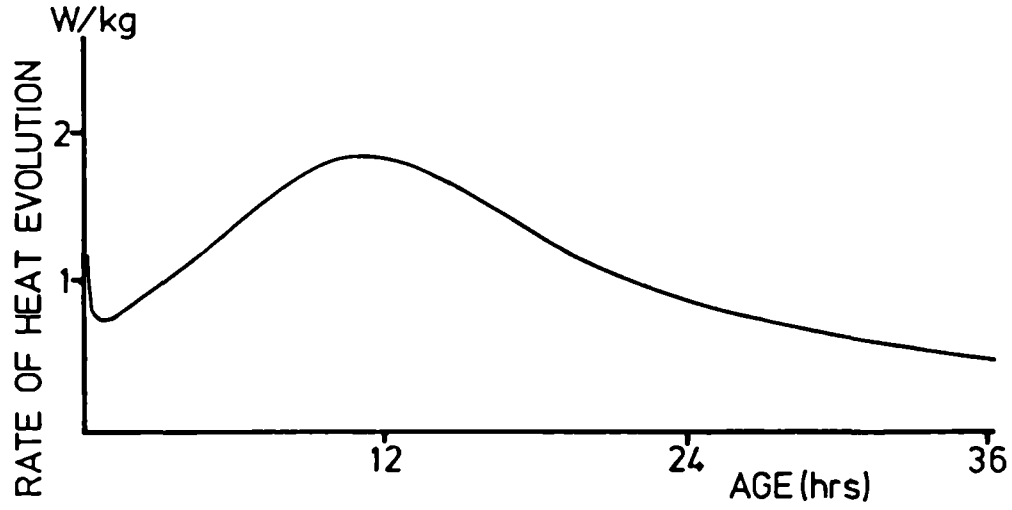

FIG 4A.5 Rate of Heat Evolution during the Hydration of Alite

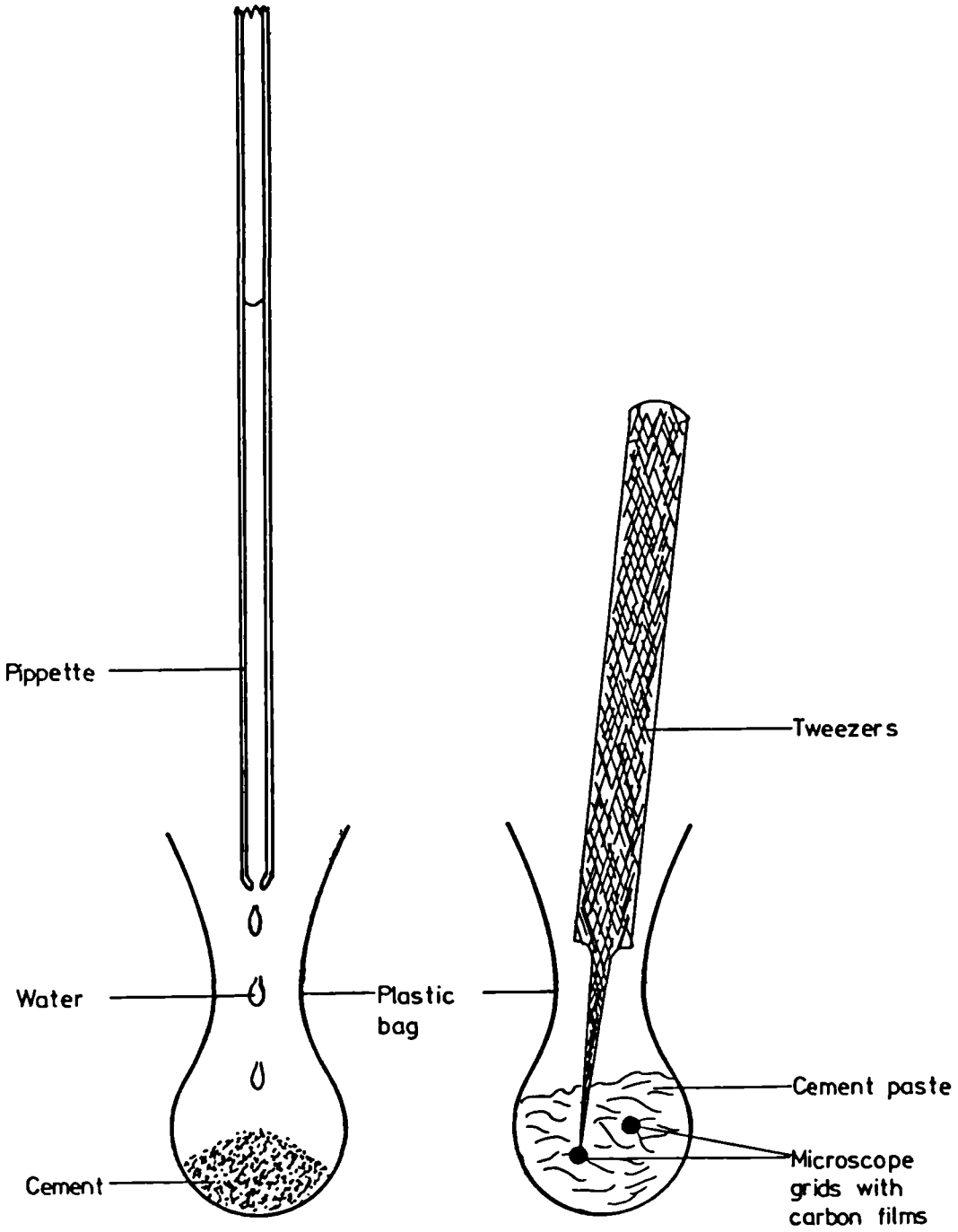

FIG. 4A.6 Specimen preparation for the HVEM (actual size)

The cell and microscope used are described in Chapter 3D.

This method of sample preparation was developed to minimise the contamination of the hydrating paste by CO_2 or by any glassware. The amount of water available for hydration, however, is limited to that added initially, as the samples are not cured in saturated limewater. It is possible that slow evaporation of water will occur which may retard (or stop) later hydration.

The same specimen preparation method was used for all the phases and cement examined in the environmental cell.

4A.II.2 E.M. Observations of Alite Hydration

HVEM observations of undried, hydrated alite in the environmental cell

Examples of the undried microstructure of the alite hydrated for various times are shown in Plate 4A.1.

Plate 4A.1(a) shows the surface of an alite grain 1½ hours after the addition of water. The surface is covered by crumpled foils of product extending about 0.5-0.7 μm into the solution. If exposed to the electron beam for too long or the supply of water saturated nitrogen to the cell is stopped these foils collapse onto the surface of the grain or crumple to form fibres. The foils are very thin (< 50 Å), so the fraction of alite which has reacted may be very low (<1%) despite their number. Some sheets appear to have a hexagonal habit, suggesting their structure could be close to that of calcium hydroxide.

After hydration for 1 day (plate 4A.1(b) more filmy product can be seen covering the grains. It is difficult to estimate the depth of the product layer as electrons are only transmitted where the specimen is thin enough; Fig 4A.7 illustrates this problem. Thus although the outer region of the product appears to have a similar

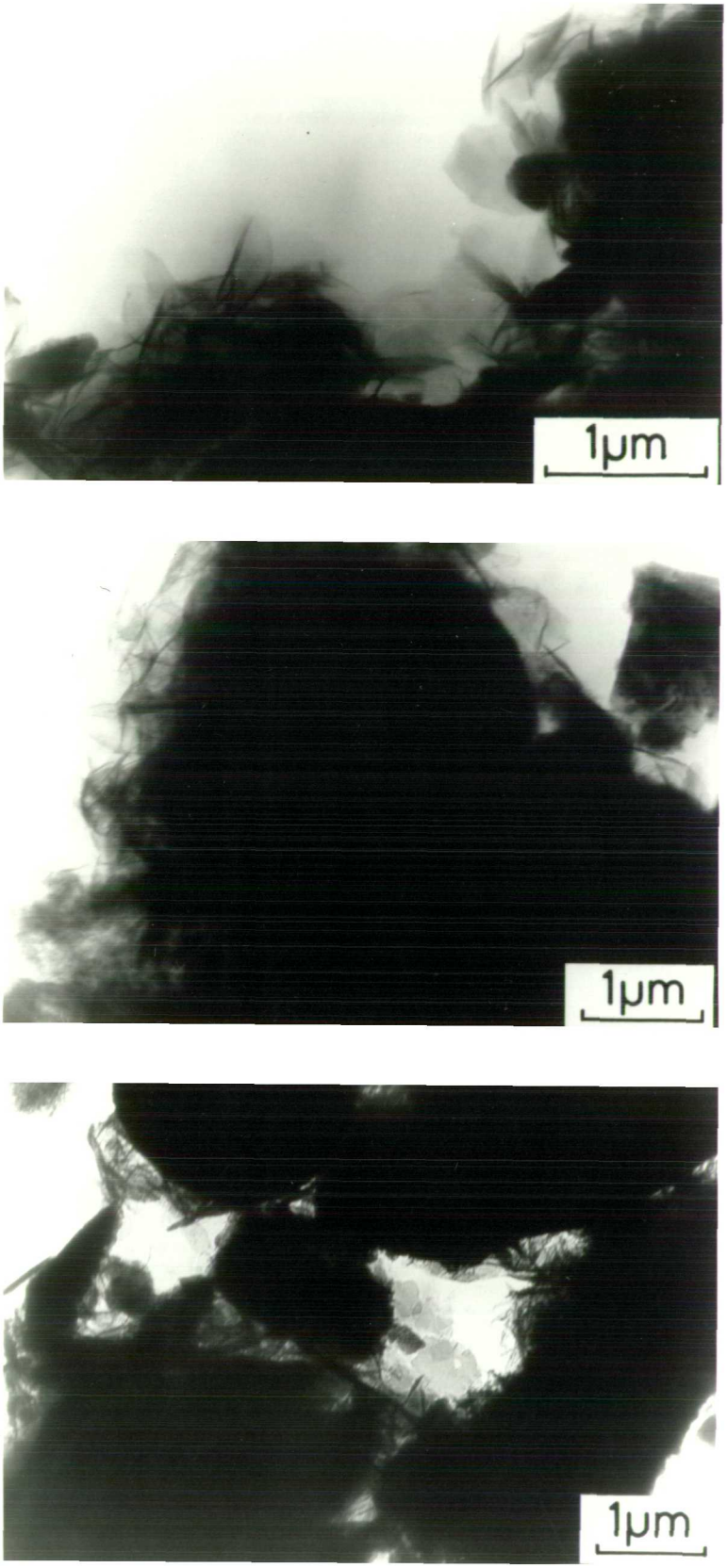

Plate 4A.1 Hydration of Alite in the HVEM

(a) 1½ hours
(b) 1 day
(c) 3 days

morphology to that seen at 1½ hours, the nature of any underlying product cannot be deduced. In the region at the bottom left of the micrograph, away from the edge of the product, well defined foils cannot be identified and the product appears to have a more 'gel' like structure; several crumpled foils on top of each other might, however, produce similar contrast in the image. Where the specimen is thin enough similar, more homogeneous, product can be seen bridging gaps between particles. Whilst, as explained, the morphology of these regions could be 'gel' or crumpled foils, it is highly unlikely to be interlocking fibrils (as suggested by Bailey and Stewart, 1984) as these are not seen in the thin regions where the morphology is unambiguous, in the 'wet' state. Fibrils are produced, if the specimen is allowed to dry in the microscope. The particle in the top right corner of the micrograph shows diffraction bend contour fringes, indicating its crystalline nature. This is probably a particle of calcium hydroxide.

Plate 4A.1(c) shows an area of the microstructure after 3 days hydration. The specimen was not cured under water and there was no sign of free water at this stage. In fairly open areas such as just to the right of the centre of the micrograph the C-S-H has a distinctly fibrular morphology. This is probably as much a function of the dryness of the specimen as of age. In areas surrounded by grains, however, the C-S-H is denser and more homogeneous as described previously. (Slight astigmatism in the micrograph, which has been much enlarged, is responsible for the NE-SW streaking). Thin plates, probably of calcium hydroxide, have precipitated on the carbon support film and are probably atypical of calcium hydroxide in the bulk microstructure; large particles of calcium hydroxide (similar to that described in plate 4A.1(b) were observed elsewhere in this specimen.

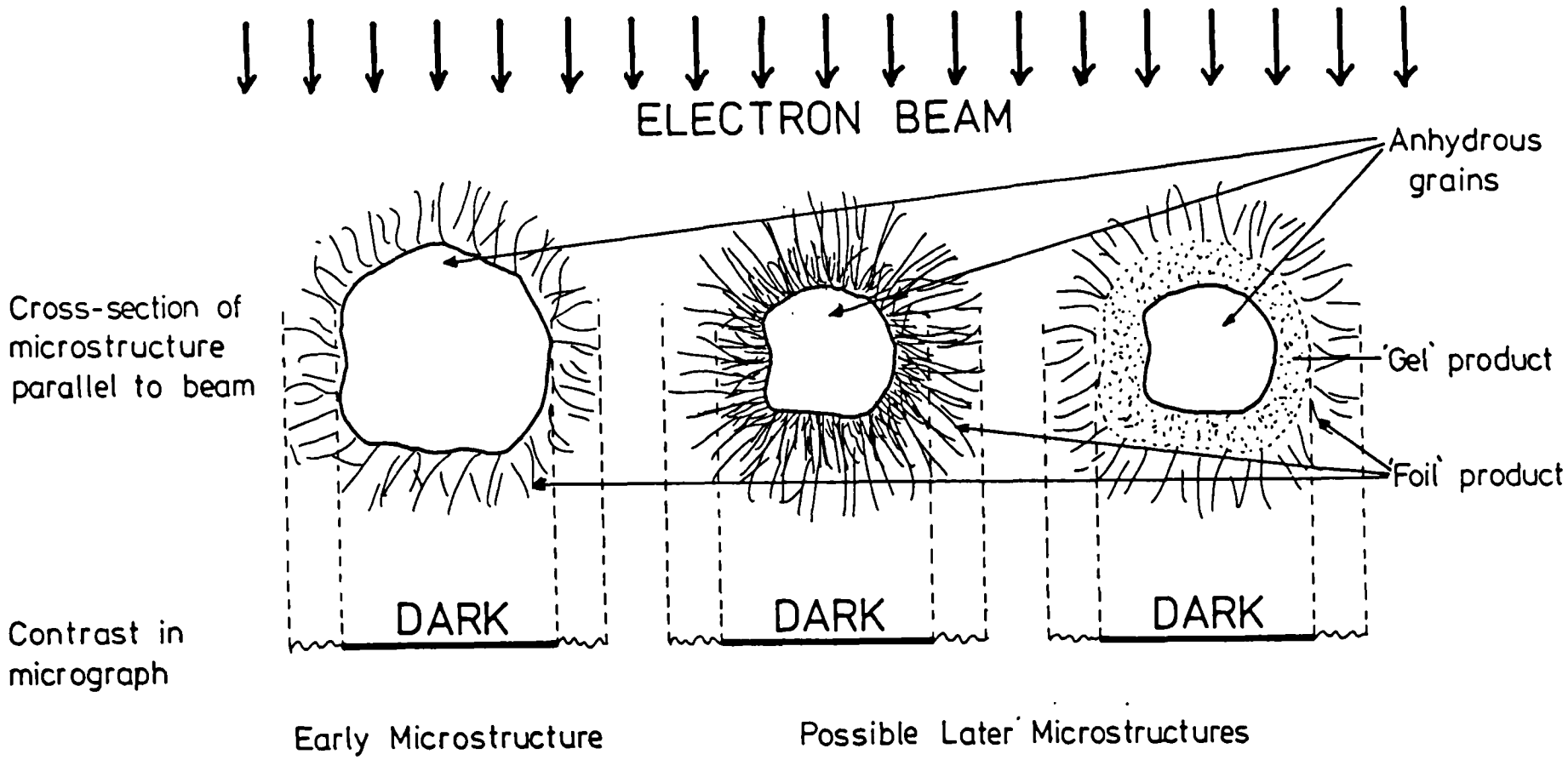

FIG. 4A.7 An Example of the Difficulty in Interpreting Images Taken in the HVEM

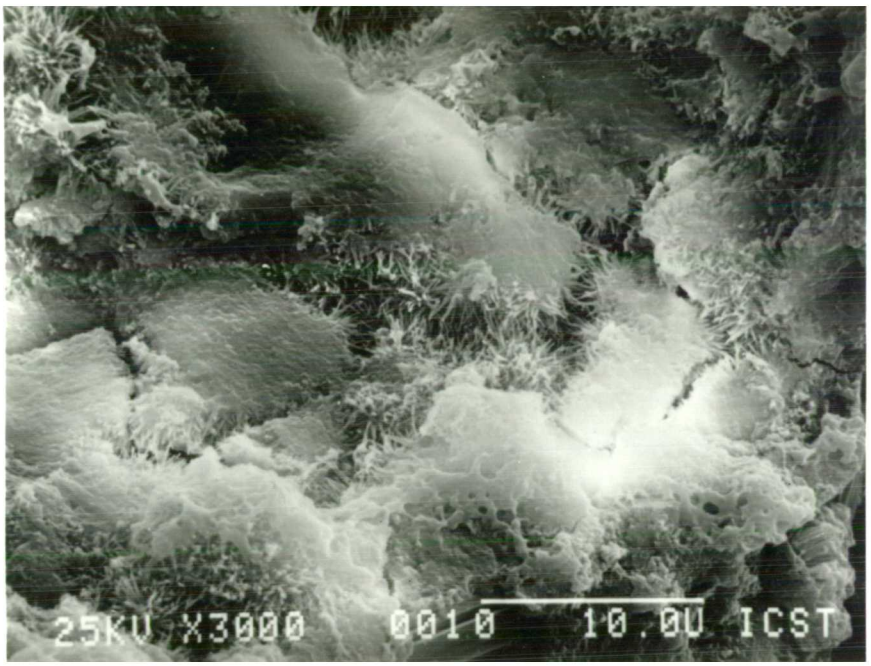

Plate 4A.2 Fracture Surface of 6 month Alite Paste

SEM of 6 month fracture surface

An area of the fracture surface of the 6 month paste sample is shown in plate 4A.2. In the pore space C-S-H with a pronounced fibrillar morphology can be seen, the length of the fibrils being about 1-2 μm. The more dense areas appear relatively homogeneous, there being no sign of any anhydrous material or distinct 'inner' and 'outer' product. This homogeneity, however, might be deceptive as illustrated in the SEM and STEM micrographs of ion thinned C_3S paste taken by Dalgliesh (Jennings et al, 1981). Areas of calcium hydroxide cleavage can be seen at the right edge and bottom of the micrograph.

4A.II.3 Discussion

In the present work C-S-H produced during the hydration of alite was observed to have a foil-like morphology which tended to become fibrillar on drying and/or ageing. A substantial amount of product could be observed after 1½ hours hydration, around the end of the induction period as indicated by conduction calorimetry (Fig 4A.5).

This exfoliating foil morphology of the early hydrate does not seem to be consistent with a low permeability barrier layer which inhibits the dissolution of C_3S during the induction period. However, only the outer surface of the hydrating grains can be observed, so any barrier layer may be underneath the observed product.

The morphology of the C-S-H appears very similar after 1½ hours to that seen after 1 day which is at variance with hypotheses postulating a first hydrate which transforms to a second hydrate at the end of the induction period. It may be that this transformation has already occurred after 1½ hours in this alite, but the morphology of the C-S-H observed is similar to that observed at

earlier times by Jennings et al (1981) and Ménétrier et al (1979) allowing for differences in specimen preparation.

Following the phase equilibrium approach, it is not necessary that the C-S-H, precipitated initially, forms a barrier layer around the C_3S. As long as the precipitation of C-S-H from the saturated solution is always rapid the solution will remain in equilibrium with the product. It is, however, necessary to explain the reduction in the rate of C_3S dissolution which occurs soon after mixing as indicated by the drop in the rate of heat evolution, the changes taking place in the composition of the solution, and the slow development of product during the induction period. Although the initial dissolution of C_3S appears to be congruent (Barret et al, 1980, Brown et al, 1984) there is no evidence that it remains so, as the composition of the solution changes. Skalny and Young (1980) quoted evidence indicating that congruent dissolution is only transient in suspensions with a high solids content (Andreeva and Keshelava, 1976) and presumably this would also be the case in pastes. Jennings (1983) points out that the solubility of silica is very sensitive to the pH and to any traces of alumina in solution and suggests that a disturbed surface layer rich in silicates may form on the C_3S grains, inhibiting dissolution. A disturbed surface layer might also adsorb calcium ions as suggested by Tadros et al (1960) which would also inhibit the dissolution of C_3S.

If the C_3S continues to dissolve slowly with immediate precipitation of C-S-H (with $C/S < 3$) the composition of the solution follows the solubility curve of C-S-H (Figs 4A.3 and 4A.4), becoming enriched in calcium and depleted in silica until it is saturated with respect to calcium hydroxide as well as C-S-H (point A in Fig 4A.3 and 4A.4). At this point both phases should start to precipitate simultaneously. In practice it is likely that the solution will become slightly

supersaturated with respect to calcium hydroxide as observed by Brown et al (1984) (solution compositions beyond point A in Fig 4A.3). When calcium hydroxide starts to precipitate the flux of ions in solution changes and this may allow rapid dissolution of C_3S to occur again, possibly through the weakening of an electrical double layer as proposed by Tadros et al (1976). If this sequence of events were in fact correct there would be no need to postulate the formation of two types of C-S-H which interconvert. The C-S-H formed during the induction period and the acceleratory period could be the same, its rate of formation being affected by the dissolution of C_3S. The shortening of the induction period by the introduction of more lattice defects (Fierens and Verhaegen, 1976a, b, c; Odler and Schüppstuhl, 1981) could be explained by the higher inherent solubility of C_3S mitigating the inhibitive effects of a distorted surface or electrical double layer. The effect of inorganic admixtures could also be explained by their influence on the activities of calcium and silicate ions in solution and thus on the composition of the liquid saturated with respect to both CH and C-S-H (point A).

Further study of the very early hydration of C_3S and alite in the environmental cell might be able to distinguish between these mechanisms of a C-S-H barrier layer which transforms to a second hydrate at the end of the induction period and continues formation of a single C-S-H at different rates.

4B Hydration of Dicalcium Silicate

Dicalcium silicate (C_2S) constitutes about a fifth of portland cement. It hydrates more slowly than C_3S and so does not make a significant contribution to early strength development. It may, however, be important in contributing strength at later ages, in controlling the early heat evolution of cement paste and in the durability of cement and concrete.

4B.I Review of previous work

4B.I.1 Structure and solid solution of C_2S

Dicalcium silicate exists in several polymorphic forms all consisting of independent SiO_4 tetrahedra connected by calcium atoms (Lea, 1970). In the absence of impurities only the γ form is stable at room temperature, but five high temperature polymorphs: α, α_L', α_H', α_M' and β have been characterised, and all of these can be stabilised at room temperature (Ghosh, 1983; Midgley, 1974).

In portland cement the vast majority of dicalcium silicate, or belite as the impure form is known, is present in the β form; although the α or α' forms may be found, depending on the minor elements present and the cooling conditions of the clinker. The β-γ transformation involves a large volume increase leading to dusting, which can cause problems in clinker production. The α-α' and α'-β transformations often produce complex lamellar or twinning structures in the belite grains in clinker (Groves, 1982; Ono et al, 1968).

Many oxides form solid solutions with C_2S up to several percent including: Al_2O_3, Fe_2O_3, MgO, MnO, Na_2O, K_2O, BaO, B_2O_5, P_2O_5, V_2O_5, SO_3 and Cr_2O_3. These often influence the stability of the different polymorphs.

The stabilisation of the various polymorphs has been reviewed by Ghosh (1983, Ghosh et al, 1979), but the factors determining which polymorph is stable at room temperature are not fully understood. Pressure and rate of nucleation are believed to affect the stabilisation of C_2S polymorphs; whilst replacement of SiO_4 by smaller ions of higher negative charge is thought to be effective in stabilising β-C_2S. Substituting ions which lead to an extension of an axis are held to favour the α-form (Ghosh, 1983).

4B.I.2 Hydration of C_2S

Effect of polymorphism and solid solution on reactivity of C_2S

γ-C_2S is almost non reactive although Bensted (1978) has reported the very slow reaction (~20% in 5 years) of this polymorph containing Fe_2O_3, to give C-S-H and calcium hydroxide. This low reactivity has been attributed : to the regular co-ordination of its calcium ions with oxygen atoms in the olivine type ($MgSiO_4$) orthorhombic structure; to the absence of holes of atomic dimensions; and to its supposed 'through solution' mechanism (Skalny and Young, 1980).

Whilst hydrating more slowly than C_3S, β, α, and α'-C_2S all show appreciable reactivity. The relative reactivity of these polymorphs appears to vary with the type and concentration of the stabilising oxide and the method by which they are synthesised. The hydration of the different polymorphs has been reviewed by Ghosh et al (1979) and by Skalny and Young (1980). In most cases the sequence of reactivity found was $\alpha > \alpha' > \beta$ (Suzuki et al, 1978, 1980; Bikbau, 1974; Gutt and Osborne, 1970; Jelenic et al, 1978; Ono et al, 1968; Boikova, 1980), although the α and α' polymorphs could only be stabilised by higher additions of impurity which could have affected

their relative reactivity. An exception was found in the case of P_2O_5 polymorphs (Welch and Gutt, 1960) where the β modification was more reactive, but the reactivity of P_2O_5 stabilised β-C_2S was found to decrease with increasing concentration of stabiliser (Fierens and Tirlocq,1983) and again the α and α' forms required higher P_2O_5 additions. As in the case of C_3S it is difficult to separate the effects of polymorphism from those of solid solution.

The effect of different impurities on β-C_2S has been studied by Nurse (1952), Pritts and Daugherty (1976) and by Fierens and Tirlocq (1983). The reactivity was found to vary with the type and concentration of impurity used. Pritts and Daugherty (1976) found that reproducible results could only be obtained after repeated firings of the preparations; those fired only once were more reactive and this was attributed to heterogeneous distribution of stabiliser or to differences in crystallite size.

Hydration of β-C_2S

As with C_3S, the hydration of β-C_2S produces calcium hydroxide and C-S-H gel, although much less CH is formed. If it is assumed that the C/S ratio for C-S-H in hydrated β-C_2S is the same as that in hydrated C_3S (i.e. 1.7), only 0.3 moles of CH per mole of β-C_2S will be formed. The smaller amount of CH formed is reflected in the higher porosity of hydrated β-C_2S pastes as compared to C_3S pastes with the same $^{w}/_{s}$ ratio (Berger et al, 1979)

The general pattern of reaction of β-C_2S follows the same sequence as that of C_3S; an initial rapid rate of heat evolution being followed by an induction period, an accelerating period and a period of deceleration. The induction period is generally longer than that for C_3S with the onset of the acceleratory period occurring after 5-7 hours by calorimetry (Fierens and Tirlocq, 1983; Maycock et al, 1974).

The length of the induction period was determined to be 100 hours by Odler and Schüppstuhl (1982) using X-ray diffraction (XRD) and 80 hours by Fujii and Kondo (1979) from the maximum in the concentration of calcium in solution. Although these differences are probably due to differences in preparation of the β-C_2S used, different methods for detecting the end of the induction period are not necessarily analogous.

In the study of Fierens and Tirlocq (1983) the maximum calcium ion concentration and the beginning of the rapid increase in the rate of heat evolution were nearly coincident for most belites studied. In the case of β-C_2S doped with 3% vanadium, however, the nucleation of C-S-H seemed to have a relative chronological freedom with regard to calcium hydroxide precipitation. In this sample the calcium ion concentration continued to rise slowly even after the rate of heat evolution increased, although this increase was small compared to the other samples. In other work by Odler and Schüppstuhl (1981) the induction period of C_3S (after storage for one year) was found to be 6 hours by XRD but only 3 hours by calorimetry. The lower maximum in the rate of heat evolution for β-C_2S (compared with C_3S) suggests that the amount of material reacting in the acceleratory period may be small and may not be easily detected by XRD. In addition, the transition from phase boundary controlled reaction kinetics to diffusion controlled kinetics, which would be expected to occur when the surface of the reactant is covered by a significant layer of product, does not occur until after 1 month in β-C_2S (Fierens and Tirlocq, 1983). This suggests that areas of the surface remain free of product for some considerable time so early localised reaction might only consume a small fraction of the anhydrous material.

Development of microstructure during the hydration of β-C_2S

Most studies on the microstructure of hydrated C_2S have reported the appearance of the C-S-H to be generally similar to that seen in C_2S, although sometimes having a different distribution. All authors report the hydration of C_2S as being slower than C_3S.

Benstead and Varma (1974) found that C-S-H formed from β-C_2S was similar to that from C_3S by infrared absorption and Berger et al (1979) found similar polysilicate vs. time curves for hydrated β-C_2S and C_3S pastes. Kurczyk and Schwiete (1960) found identical electron diffraction patterns from the poorly crystalline C-S-H formed during the hydration of β-C_2S and C_3S. Williamson (1972) examined fracture surfaces of β-C_2S and C_3S up to a year old. The hydration of β-C_2S was slower but the C-S-H formed appeared similar to that in C_3S pastes albeit with a greater tendency to adopt a needle like or fibrillar morphology. Similar conclusions were reached by Ciach and Swenson (1971) and by Young and Tong (1977).

Lawrence et al (1974) prepared thin films with the composition of C_2S by vapour deposition and studied their hydration. They observed foils and fibres at various ages with similar morphologies to C-S-H in hydrated C_3S. The films were, however, amorphous which would be expected to increase their reactivity (Roy et al, 1978).

Ménétrier et al (1980) studied the hydration of compressed pellets of β-C_2S powder from 15 seconds to 1 day. After 1 minute preferential dissolution of the pellets at the grain boundaries had occurred, but no uniform coating could be seen on the surface. The C-S-H produced formed unevenly and did not cover the entire surface even after 24 hours hydration. Nevertheless the appearance of the hydration products was similar to those seen in the hydration of C_3S.

Groves (1981) immersed thinned sections of clinker in water and observed the hydration in the HVEM. He reported an uneven gel coating on the belite in clinker after 30 minutes, with the interlamellar regions (formed during $\alpha \longrightarrow \alpha' \longrightarrow \beta$ transformation) having suffered preferential attack.

Fujii and Kondo (1979) studied hydrated samples of β-C_2S in the SEM. After a few days they reported the occurence of isolated regions of C-S-H on the surface of the β-C_2S grains as crusts, needles or flakes. At later ages they reported a thin layer of hydrate beneath the initial product with well developed 'crystals' of C-S-H growing densely beneath this hydrate layer into the grain.

These two types of hydration have also been reported by Funk (1960). He concluded that β-C_2S could hydrate 'through solution' to give foil-like or platy C-S-H and could also hydrate directly to give well oriented needle shaped 'crystals' of C-S-H producing peaks in X-ray diffraction patterns.

In both the above cases the later 'in situ' mechanism seemed to be favoured by hydration in purified water.

4B.II Present Work

4B.II.1 Materials and techniques used

The sample of belite studied was obtained from Dr Parrott of the Cement and Concrete Association and was synthesised at Brunel University. Its oxide analysis is given in Table 4B.1 and the calorimetry curve obtained by Mr Killoh is shown in Fig 4B.1. QXDA of the sample suggested that there could be as much as 1% alite present (Gutteridge, private communication) although this is within the error of the QXDA method.

The samples were prepared for examination in the environmental cell as described for alite (4A.II.1).

4B.II.2 Observations of the hydration of belite

After 6 hours hydration there was little sign of any reaction of the belite sample. Occasionally small amounts of filmy product could be seen (plate 4B.1) in small areas between particles rather than on exposed surfaces. After 1 day several clumps of filmy product could be seen 'sprouting' from the surface of the grains whilst most of the surface remained unreacted (plates 4B.2 and 4B.3). This filmy product was very susceptible to beam damage. The small, denser particle amongst the foils in plate 4B.3 could be calcium hydroxide. It was initially thought that these reactive areas might correspond to areas of alite which QXDA suggested might be present. However, striations could be seen on several of the smaller (thinner) grains, probably due to twinning of the belite during the α'-β transition, and the areas where product had formed corresponded to the changes in crystal orientation. A rather poor example of this is shown in plate 4B.2. Unfortunately, it was not possible to record a better example as beam damage was so rapid.

Table 4B.1 Properties of belite

	Mass %
CaO	66.72
SiO_2	32.55
MgO	0.01
LOI	0.38
Free lime	0.47
Density (kg/m^3)	3235
Specific surface	360

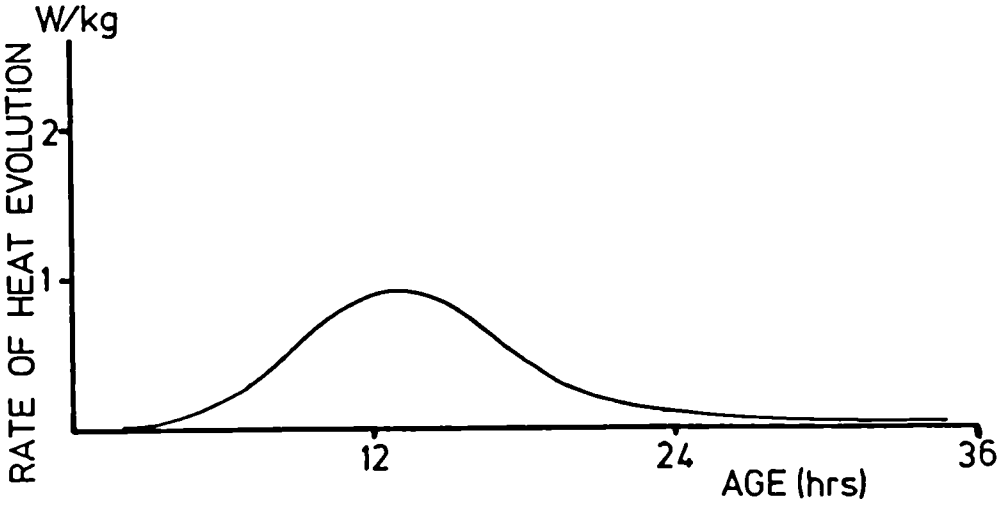

FIG 4B.1 Rate of Heat Evolution during the Hydration of Belite

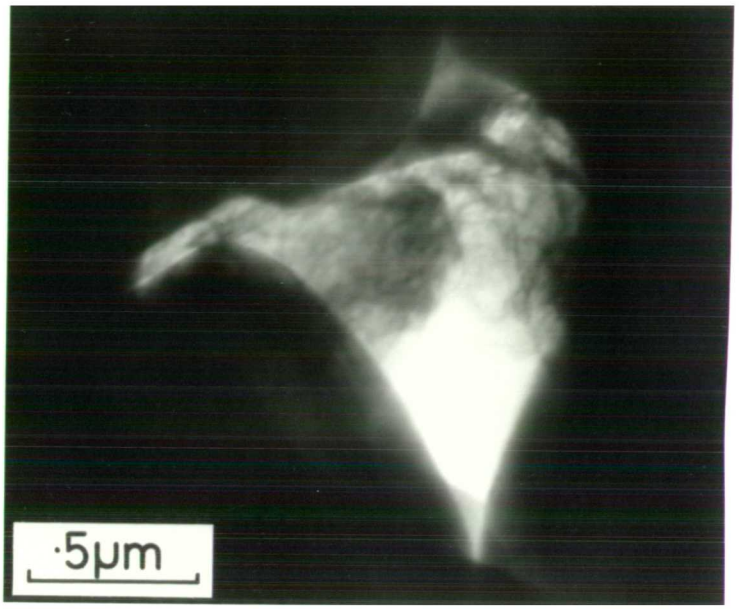

Plate 4B.1 Belite in the HVEM after 4 hours Hydration

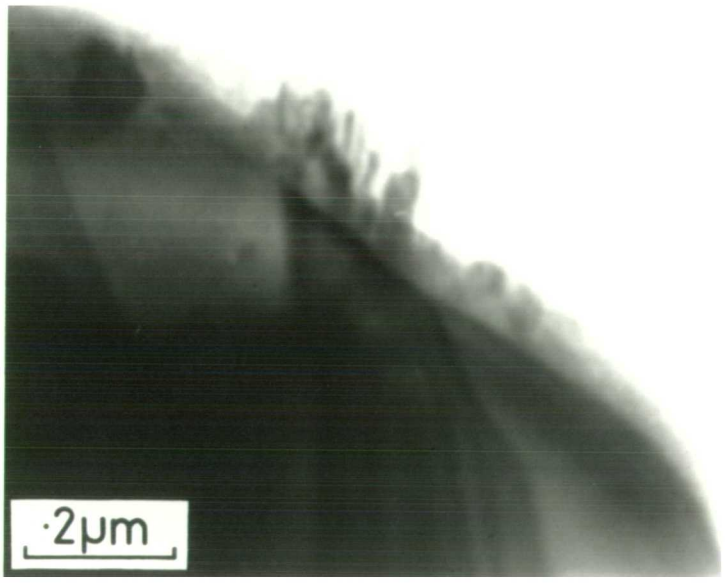

Plate 4B.2 Belite in the HVEM after 1 day Hydration

Plates 4B.3 and plate 4B.4 show how the morphology of these C-S-H 'clumps' changed between 1 day and 8 days hydration. After 1 day the C-S-H is 'filmy' or 'veil' like whilst it appears more fibrillar in morphology after 8 days. A similar change in the morphology of C-S-H was observed during the hydration of alite (4A.II.2), C_3S (Jennings et al, 1981) and cement (plate 5.15, Chapter 5C.2.)

At later ages various morphologies were observed. Initial examination of the sample hydrated for 22 days showed a continuous colloidal like product (plate 4B.5); this was probably calcium hydroxide precipitated on exposure to air, as reported by Grudemo (1960). This product disappeared on exposure to the beam (plate 4B.6(a) and (b)), which also caused changes in the appearance of the grain surface. This behaviour might be explained if the surface of the grain had hydrated topochemically to a depth of about 0.5 μm, the heat of the beam causing bubbling owing to the presence of water. Such 'in situ' hydration has been reported by Funk (1960) and by Fujii and Kondo (1979).

When the same sample was examined in the SEM after drying, the typical, spikey, dried C-S-H morphology was observed all over the grain surfaces (plate 4B.7). As both the 'wet' and dried morphologies were widespread throughout each examination of the specimen, it would seem that the gel like product observed in the HVEM transformed to the spikey C-S-H on drying. A similar transformation of gel to spikey product has been reported in alite pastes by Jennings et al (1981).

After 47 days hydration areas of C-S-H were observed in the HVEM which were stable to the electron beam and to drying in the microscope (plate 4B.8). This denser product appeared amorphous and could be imagined to be composed of rounded gel particles or

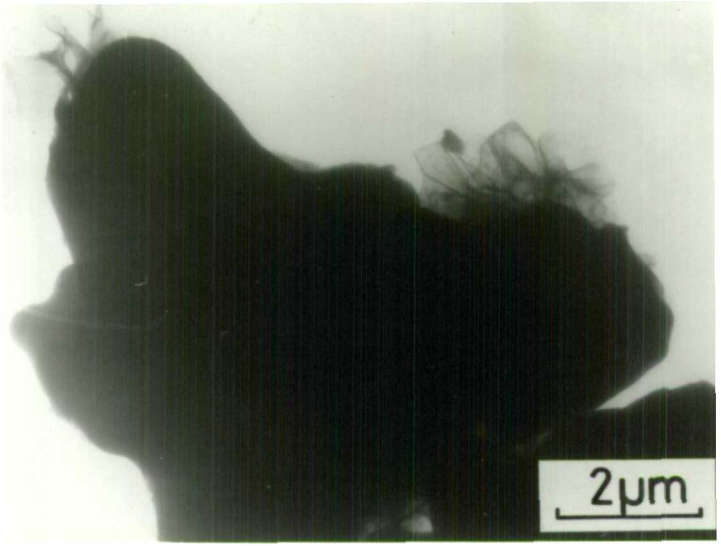

Plate 4B.3
Belite in the HVEM Hydrated for 1 day

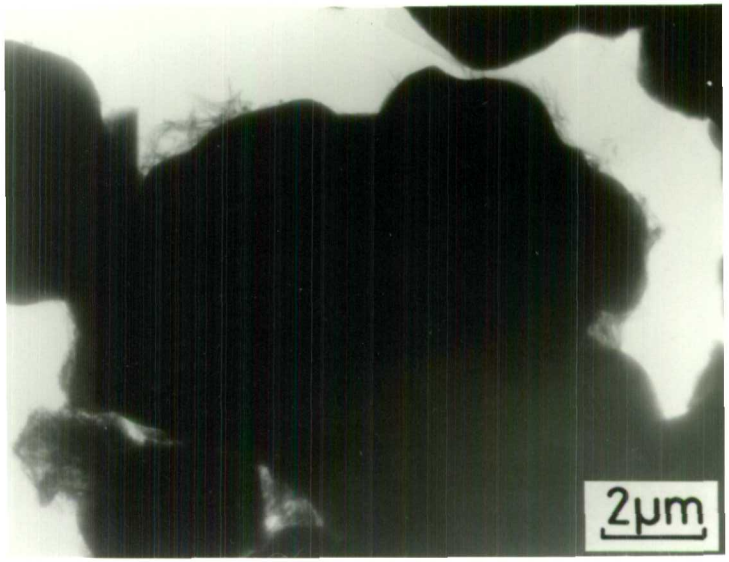

Plate 4B.4
Belite in the HVEM Hydrated for 8 days

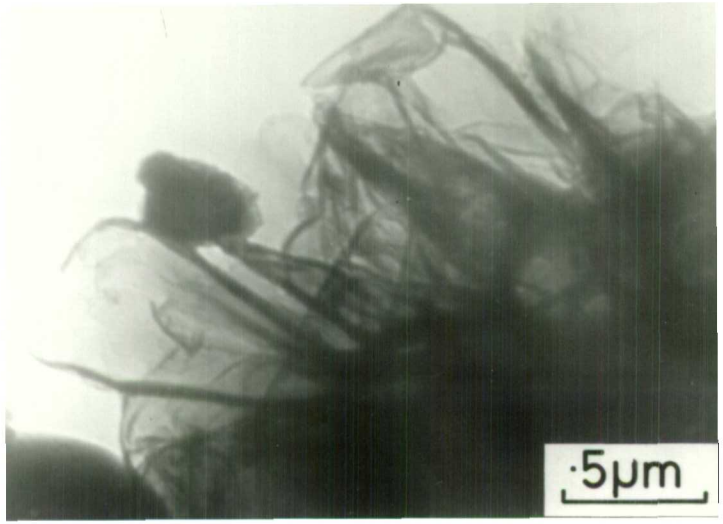

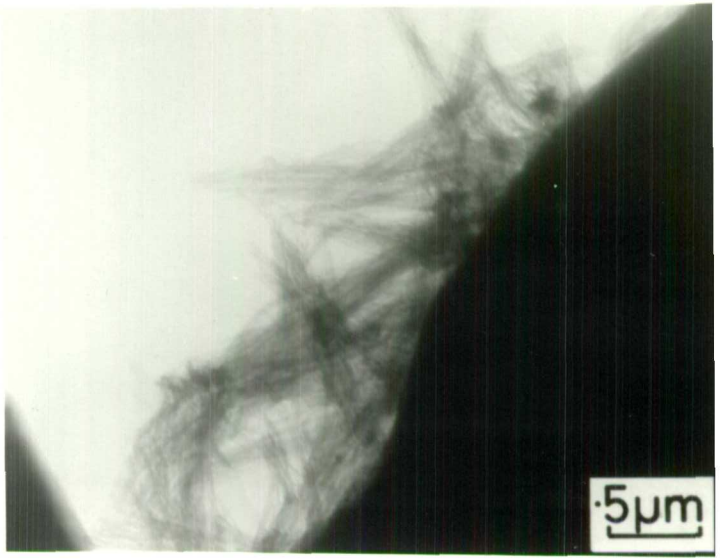

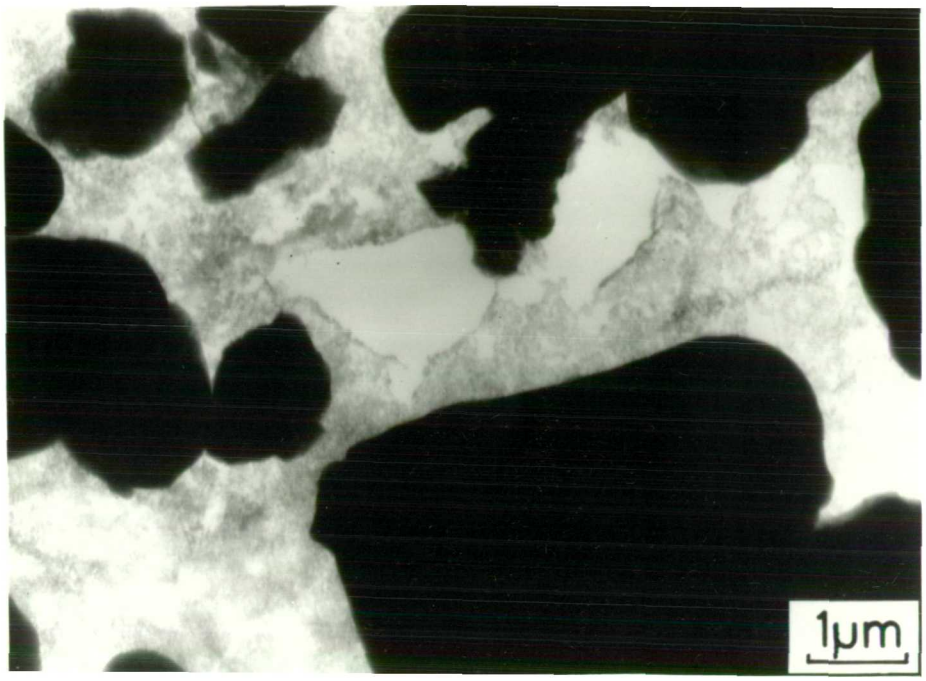

Plate 4B.5 22 Day Hydrated Belite in the HVEM

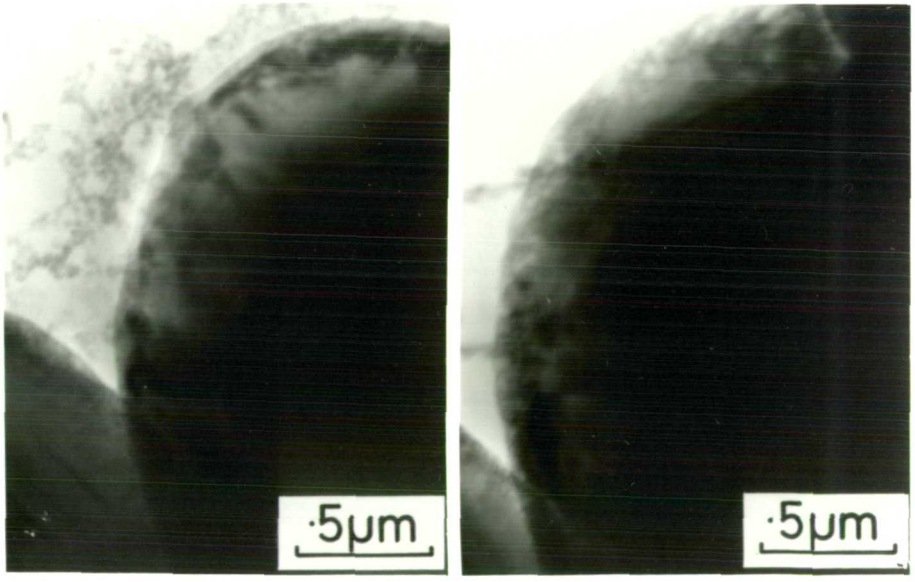

Plate 4B.6 Detail of above, (a) Before & (b) After Beam Damage

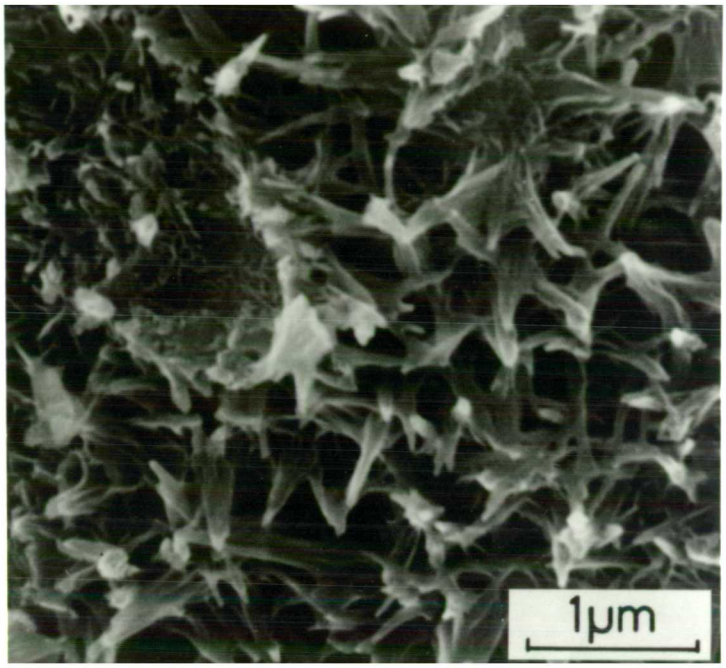

Plate 4B.7 Belite Hydrated for 22 days,
Dried Fracture Surface in the SEM

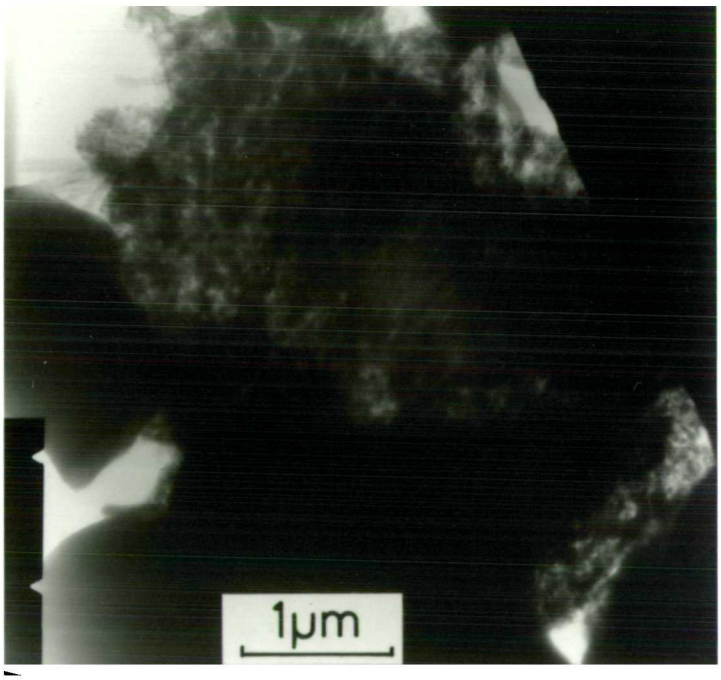

Plate 4B.8 Belite Hydrated for 47 days in the HVEM

possibly of crumpled, densely intergrown foils. This type of product was only seen in small regions enclosed by several belite grains.

4B.II.3 Discussion

The present work confirms the low reactivity of belite as compared to alite. The C-S-H produced during the reaction of belite appears similar in morphology to that formed in alite. The initial product is foil-like and transforms on ageing or drying to a fibrillar, needle-like morphology in areas where space is available.

The belite reacted unevenly as reported by several other workers (Ménétrier et al, 1980; Groves et al, 1981; Fujii and Kondo, 1979). Local differences in the reactivity of the belite seem to correspond to changes in crystal orientation produced by twinning. Groves also reported preferential reaction of belite in interlamellar regions, although this was in a sample of thin clinker where the other phases present may affect the hydration.

The areas of the belite surface not associated with the foil-like C-S-H do not appear to have any gel coating or barrier layer on them even in the 'wet' state.

There seems to be some evidence for topochemical reaction of belite as previously reported (Funk, 1960, Fujii and Kondo, 1979). This was only seen in one sample, however, and could be an artifact. More work would be needed to confirm this observation.

4C Hydration of Tricalcium Aluminate

4C.I Review of previous work

Tricalcium aluminate (C_3A) constitutes about 6% (by QXDA) of ordinary portland cements. The proportion of C_3A in cements has decreased over the past thirty or forty years as the C_3S content has increased. Due to extensive solid solution of aluminium in the ferrite phase and in the alite phase, the Bogue calculation tends to overestimate the amount of C_3A in cements. If insufficient gypsum is added to the clinker, the rapid hydration of the aluminate phase causes rapid loss of workability, known as flash set.

4C.I.1 Structure and solid solution of C_3A

Pure C_3A is cubic and shows no polymorphic transformations. However, the substitution of alkalies, Na and K, for calcium gives rise to five different polymorphic forms: two cubic, two orthorhombic, and one monoclinic (Boikova et al, 1977; Regourd, 1979a and b; Ghosh, 1981). In commercial clinker C_3A can be cubic or orthorhombic, but is rarely monoclinic (Regourd, 1979b); the polymorphism being a function of the raw material used, the combustion reaction, and the cooling process.

Fe, Mg, Si, Ti, Na and K can all enter into solid solution with C_3A. The limits of these solid solutions are variously given as between 2 and 10% (Regourd and Guinier, 1974; Tarte, 1968; Varma et al, 1981; Lea, 1970).

4C.I.2 Hydration of C_3A

The reaction of C_3A with pure water leads, eventually, to the formation of the cubic hydrate C_3AH_6. At temperatures below about 40°C, however, the first crystalline hydration products are usually

the metastable hexagonal hydrates C_2AH_8 and C_4AH_{19} (Breval, 1976). The transformation of the hexagonal calcium aluminate hydrates to the cubic phase may occur in a matter of minutes, hours or days, depending upon such factors as temperature, water to solids ratio, grain size and the presence or absence of CO_2.

$$2C_3A + 27H \longrightarrow C_2AH_8 + C_4AH_{19} \longrightarrow 2C_3AH_6 + 15H$$

In the presence of sufficient lime C_2AH_8 does not form and the C_4AH_{19} is stabilised at room temperature.

$$C_3A + CH + 12H \longrightarrow C_4AH_{19}$$

This reaction causes flash set in cements hydrated without added gypsum (Bensted , 1981).

Investigations of the $CaO-Al_2O_3-H_2O$ system by Jones and Roberts (1962) and by D'Ans and Eick (1953a) showed that amorphous hydrated alumina (AH_3) gel exists as a persistant, metastable phase in this system up to quite high lime concentrations (~ 0.4) g/l. Their findings are shown in Fig 4C.1.

Breval (1976) reports the formation of a gel phase on the surface of the C_3A grains within the first few minutes of hydration and suggests that the crystalline hydrates form by transformation of this phase as well as through solution.

Marinho and Glasser (1984) studied the dissolution of C_3A (and its Na solid solutions) in the region of undersaturation. They found an excess of calcium in solution suggesting that an aluminate rich phase precipitates close to the surface of the C_3A.

Two calcium alumino sulphate hydrates exist in the system $CaO-Al_2O_3-CaSO_4-H_2O$ (Eitel, 1957). The 'high sulphate', $C_3A(C\bar{S})_3 32H$, has the same composition as the natural mineral ettringite and has a

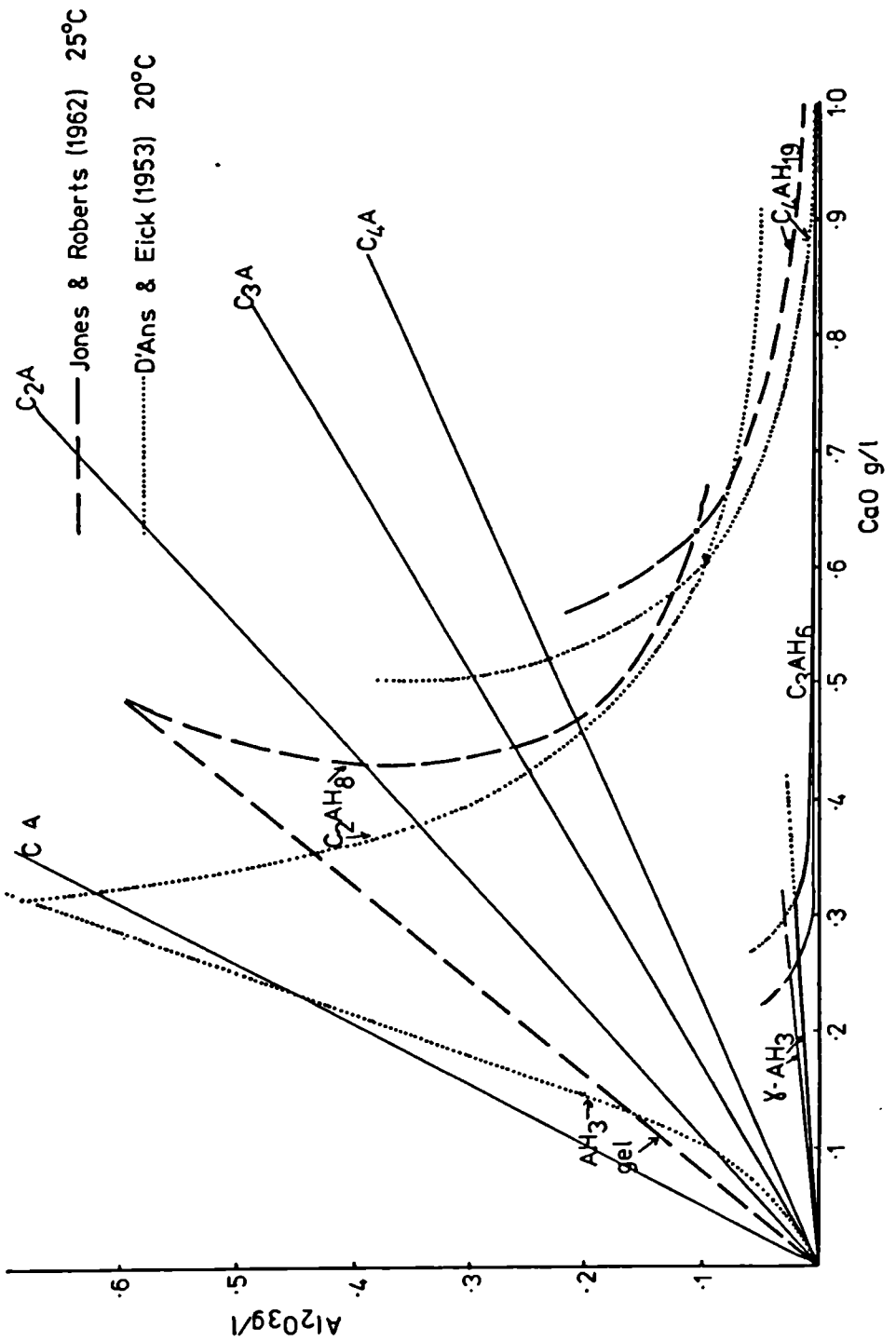

FIG. 4C.1 Solubility Curves in the System $CaO-Al_2O_3-H_2O$

characteristic morphology of fine, hexagonal needles. The 'low sulphate' or 'monosulphate', $C_3AC\bar{S}12H$ crystallises in hexagonal plates (often aggregated to form star shaped spherulites) and is isomorphous with the aluminate hydrate C_4AH_{13} (which can be written C_3ACHH_{12}), with which it forms a series of solid solutions (Eitel, 1957).

It was found by Jones (1939, 1944) and later by D'Ans and Eick (1953b) that ettringite is the only stable calcium alumino sulphate hydrate, the 'monosulphate' being only metastable at room temperature. The decomposition of ettringite to C_3AH_6 with increasing lime is, however, extremely sluggish and the high concentrations of calcium hydroxide found in portland cement pastes may favour the unstable crystallisation of monosulphate if, at the same time, the concentration of sulphate in solution is low. These workers also found that the stable phase, alumina hydrate, AH_3, seldom crystallised in this system appearing as a 'flocculant hydrogel' (Jones, 1939) or an 'aged cryptocrystalline' phase (D'Ans and Eick, 1953a and b). This amorphous hydrous alumina gel was the first phase precipitated from solutions where the calcium to aluminium ratio was less than 3. Jones (1939) noted changes of the appearance of the AH_3 gel with increasing lime in solution and suggested that it is not a pure phase, but can incorporate both Ca^{2+} and SO_4^{2-}.

Study of the rate of heat evolution during the hydration of C_3A with calcium sulphate shows a period of rapid reaction followed by a region in which the rate of heat evolution decreases continuously. After some time a second peak in the rate of heat evolution is observed corresponding to the formation of monosulphate (as determined by X-ray diffraction) (Stein, 1963; Brown, 1984a). Stein also found the concentration of sulphate in solution to be zero just before the

second peak. The time at which the second peak occurs varies considerably according to the amount of calcium sulphate present; whether it is added as gypsum or hemihydrate; the amount of lime present and the surface area of the C_3A. Collepardi et al (1978, 1979) reported the occurence of the second peak at around 5 hours when 20% gypsum was added and around 40 hours with 40% gypsum. Brown (1984a) added sufficient gypsum for all the C_3A to react to form monosulphate (~70 wt % gypsum addition) and did not observe a second peak until 8 days after the addition of water. The presence of lime further retards the reaction of C_3A + ettringite to monosulphate (Collepardi et al, 1978; Brown, 1984a). Some of the results reported by Collepardi et al (1978, 1979) are shown in Fig 4C.2.

It can be seen that the initial heat peak is much smaller for C_3A hydrated with gypsum than for C_3A hydrated without gypsum. Different products are being formed in the two cases, however, and the relative heights cannot be compared.

The cause of the decreasing reaction rate and the delay before ettringite is converted to monosulphate has been the cause of much controversy. The retardation of the reaction has variously been attributed to:

a) an initial hydrolysed layer (Feldmann and Ramachamdran, 1966; Skalny and Tadros, 1977);

b) the formation of an amorphous layer at the reacting interface (Corstanje et al, 1973, 1974; Holten and Stein, 1977; Stein, 1980);

c) the formation of a coating of ettringite crystals around the C_3A grains (Schweite et al, 1966; Collepardi et al, 1978, 1979).

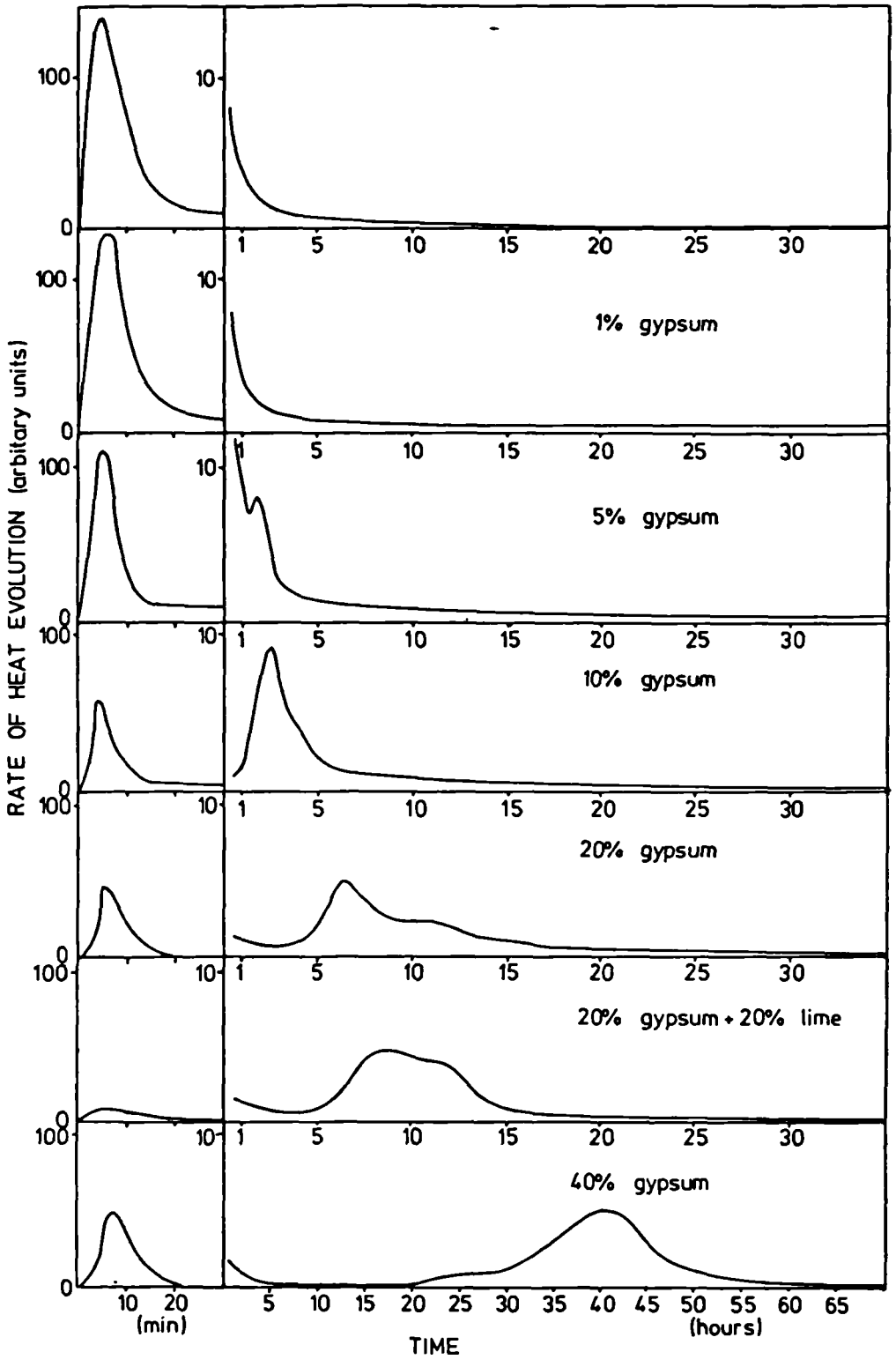

FIG. 4C.2 Influence of Gypsum, and Gypsum + Lime on the Rate of Heat Evolution during the Hydration of C_3A (from Collepardi et al 1978, 1979)

Feldman and Ramachandran (1966) studied the hydration of C_3A alone and with additions of 0.25, 2.5, 10% and 20% gypsum. They measured the extent of the reaction by the total area of peaks found by DTA and by length changes. As the products produced at these very different levels of sulphate addition will be different and hence the peaks seen in DTA will be different it is difficult to draw any conclusions from their results. They concluded however, that the formation of ettringite has no direct effect upon the reaction rate and that the reactivity of C_3A was reduced by sorption of $(SO_4)^{2-}$ ions on active surface sites. They also observed that gypsum reduces the rate of conversion of the hexagonal aluminate hydrates to the cubic C_3AH_6; this too was attributed to the sorption of $(SO_4)^{2-}$ ions on the hexagonal hydrates. From the work of Jones (1939, 1944), Breval (1976) and Collepardi et al (1978) it would seem far more likely that the presence of sulphate ions modifies any amorphous layer formed on the surface of the grains and stabilises the hexagonal hydrates by solid solution, both of which could be expected to reduce the rate of reaction of the C_3A.

Skalny and Tadros (1977) have developed the theory of Feldmann and Ramachandran (1966). They propose that the initial dissolution of C_3A is incongruent, leaving an aluminate rich layer on which calcium ions adsorb, producing positively charged particles. This process decreases the number of active dissolution sites. Sulphate ions adsorb on the positively charged particles, leading to further reduction in the number of dissolution sites. Skalny and Tadros (1977) support this view with observations of the dissolution and electrokinetic behaviour of C_3A in acid and neutral media, in contrast to the alkaline conditions found in cement hydration. This interpretation of their results has been questioned by Chatterji

(1980) who suggests that precipitation of amorphous AH_3 occurs and is responsible for the induction period observed.

Collepardi et al (1978, 1979) found that a reduction in the rate of reaction of C_3A, as measured by the rate of heat evolution, only occurred when calcium sulphate was present so that ettringite was formed. Sodium sulphate had no effect on the reaction rate. This led them to conclude that ettringite was responsible for the reduction in the rate of reaction. Alternatively, the presence or absence of calcium ions might affect the permeability of any amorphous layer surrounding the grains and so affect the rate of reaction.

Schwiete et al (1966) studied the hydration of C_3A with gypsum ($\sim$ 1:1 mole ratio) and a small amount of lime, with $^{w}/s$ = 5. TEM investigations of the dried and dispersed solid phase showed small ettringite needles ($\sim$ 0.25 μm long) on the C_3A surface after 30 seconds hydration. These grew to cover the surface after 5 minutes. This coating of ettringite needles, which were considered to form topochemically, was concluded to be the cause of the reduction in the rate of reaction.

Like Schwiete et al (1966), Mehta (1969, 1976) also observed short ettringite needles after 30 seconds hydration in C_3A and gypsum pastes which were dried and examined in the SEM. In this case, however, the ettringite was observed not only on the surface of the C_3A but throughout the paste. Hence the formation of ettringite by a through solution mechanism was suggested.

It would seem improbable that the well crystallised ettringite observed by electron microscopy provides a barrier of sufficient permeability to significantly reduce the migration of ions to and from the reaction C_3A surface. The samples must, however, be dried before examination so the products seen are not necessarily those present in the reacting paste. Any amorphous phase would be especially

susceptible to alteration during specimen preparation. In addition fracture surfaces only reveal the outer hydration surface and other phases may be present beneath the ettringite layers.

Chatterji (1980) advocates the theory proposed by Gupta et al (1973) that thin plates of C_4AH_{19} form close to the C_3A surface and act as a barrier to ion transport. There is evidence for the formation of small amounts of C_4AH_{19} (Gupta et al, 1973, Schwiete et al, 1966, Collepardi et al, 1978, 1979). In the hydration of C_3A without sulphate, however, the formation of C_4AH_{19} does not retard the hydration reaction to the same extent as is seen in the hydration of C_3A with sulphate.

Holten and Stein (1977) suggest that,whilst not completely screening the C_3A, the formation of ettringite will lead to a depletion of $(SO_4)^{2-}$ near the C_3A surface. This allows amorphous AH_3 to form in the surface region and retard the hydration. Considering the colloid chemistry of the calcium aluminate hydrates, Stein (1980) suggests that the amorphous layer is more properly described as a disturbed surface layer formed by preferential extraction of Ca^{2+} from the C_3A and its replacement by H^+.

This theory has the advantage of requiring the formation of ettringite, as found by Collepardi et al (1978, 1979) without supposing that the incoherent ettringite observed by Schwiete et al (1966), Mehta (1969, 1976) and others, reduces ion transport sufficiently to bring about the observed reduction in the rate of reaction. It is also consistent with the findings of Jones (1944) and of D'Ans and Eick (1953) that amorphous AH_3 exists as a metastable phase over a wide range of concentrations. It is also possible that a layer of C_4AH_{19} exists between the AH_3 and the C_4AH_{19}.

Stein (1963) and recently Brown and La Croix (1984) have shown that the kinetics of the decreasing rate of reaction are consistent

with diffusion control through a hydrate layer. A study of the reaction kinetics, however, does not reveal the nature of the hydrate layer.

Direct evidence for an amorphous layer is difficult to obtain; especially when crystalline hydrates are also formed around the C_3A grains. Drying the hydrating paste for electron optical observation would be expected to drastically alter any amorphous product.

Influence of alkalies on hydration of C_3A

The presence of Na_2O in solid solution with C_3A has been reported to decrease its reactivity (Spierings and Stein, 1976b; Boikova et al, 1977). This has been attributed to the formation of a less reactive structure as Na^+ ions fill holes in the lattice (Regourd, 1979a). However, the release of Na^+ into solution has a complex effect on the solubilities of calcium and aluminium and on the stabilities of the various hydrates (Spierings and Stein, 1976; Shin and Glasser, 1983; Marinho and Glasser, 1984). The most pronounced effect of Na^+ in solution is to increase the solubility of aluminium and decrease that of lime; Spierings and Stein (1976) attribute the retardation of C_3A hydration, in the presence of sodium, to the presence of amorphous lime on the surface of the grains. The time of conversion of the hexagonal hydrates to C_3AH_6 was found by Spierings and Stein (1976) to be affected by the concentration of Na^+ in solution; the retardation of the conversion was a maximum at about 0.5M NaOH occuring more quickly at lower and higher concentrations. The influence of sodium on the hydration of C_3A also appears to depend on whether the sodium is present in solid solution in the C_3A or is present in the mixing solution (Spierings and Stein, 1976; Shin and Glasser, 1983).

Little work has been reported on the effect of alkalies on the hydration of C_3A with sulphate present. Jones (1944a and b) investigated the quinary systems $CaO-Al_2O_3-CaSO_4-K_2O-H_2O$ and $CaO-Al_2O_3-CaSO_4-Na_2O-H_2O$ at concentrations of 1% KOH or NaOH in solution. He found that the solubility of alumina markedly increased in both cases, which would be expected to affect the stability of any amorphous AH_3 layer on the C_3A grains. Shin and Glasser (1983) found that the addition of gypsum to C_3A solid solutions containing sodium decreased the solubility of aluminium.

The way in which alkalies affect the hydration of C_3A both with and without sulphate is very complex and as yet unclear.

4C.II Present work

4C.II.1 Materials and techniques used

The hydration of three samples of C_3A was investigated using the environmental cell in the HVEM (Chapter 3D). Two samples, denoted AI and AII, one cubic and one orthorhombic, were $C_{3-x}N_xA$ solid solutions supplied by Dr F. P. Glasser of Aberdeen University. (For preparation details see Cervantes Lee and Glasser, 1979). The third sample, denoted NBS, was supplied by Dr P. W. Brown of the National Bureau of Standards, Washington, USA. Table 4C.1 gives characterisation data for these samples.

The hydration of AI and AII was observed both with and without gypsum up to 2 hours. The sample NBS was hydrated with hemihydrate or gypsum for times from 10 minutes to 4 days. Details of all preparations are given in Table 4C.2. All preparations were mixed with water to give a water to solids ratio of 0.5 throughout. Specimens were prepared for examination in the environmental cell as described for alite (4A.II.1).

Table 4C.1 Details of C_3A used

Sample	Symmetry	Composition	Surface area (cm^2/g)
AI	Cubic	C_3A+0.38%Na_2O	1200
AII	Orthorhombic	C_3A+4.5%Na_2O	940
NBS	Cubic	C_3A	3300

Table 4C.2 Specimens prepared for HVEM

Sample	Sulphate addition wt %	Hydration times
AI	-	10 min, 30 min, 2 hrs
AII	-	10 min, 30 min, 2 hrs
AI	Gypsum 30%	10 min, 30 min, 2 hrs
AII	Gypsum 30%	10 min, 30 min, 2 hrs
NBS	Gypsum 50%	10 min, 1 hr
NBS	Hemihydrate 50%	10 min, 30 min, 1 day, 4 days

Notes

1 C_3A + 53% $C\bar{S}\frac{1}{2}H$ allows complete reaction to form monosulphate $C_3AC\bar{S}12H$

2 In commercial OPCs (C_3A + C_4AF): $C\bar{S}2H$ 0.3-0.5

4C.II.2 E.M. observations on the hydration of C_3A alone and with sulphate

Hydration of C_3A alone (effect of Na)

The microstructure of the hydrated low sodium, cubic C_3A is shown in plate 4C.1. After 10 minutes there is a layer of filmy amorphous product surrounding the grains (plate 4C.1(a). This product covers the surface unevenly, exfoliating in places. This amorphous product is essentially unchanged after 30 minutes (plate 4C.1(b)) apart from the appearance of small particles within it, which could be nuclei of calcium aluminate hydrates or possibly of calcium hydroxide precipitating as the sample dries. After 2 hours (plate 4C.1(c)) there are many well formed crystals present. The profile of the thick dark crystals are consistent with their being icositetrahedra of C_3AH_6 (as seen by Breval, 1976); the thin hexagonal plates are probably C_2AH_8 or C_4AH_{19}.

Initially the hydration of the high sodium, orthorhombic C_3A (AII) (plate 4C.2) appears similar to that of the low sodium C_3A. An amorphous layer can be seen surrounding the grains after 10 minutes (plate 4C.2(a)). A few very thin hexagonal plates can be seen after 30 minutes (plate 4C.2(b)) and more after 2 hours (plate 4C.2(c)), here forming at the edge of the amorphous layer. Unlike the low sodium C_3A, however, there is no evidence of the C_3AH_6 hydrate.

Hydration of C_3A with gypsum (effects of Na)

Plate 4C.3 shows the early hydration of the low sodium, cubic C_3A, AI. After 10 minutes (plate 4C.3(a)) the surface is covered with an amorphous looking layer about 0.5 μm. This layer covers the surface much more evenly than in the case of C_3A hydrated without

Plate 4C.1
Hydration of low sodium C_3A(AI)

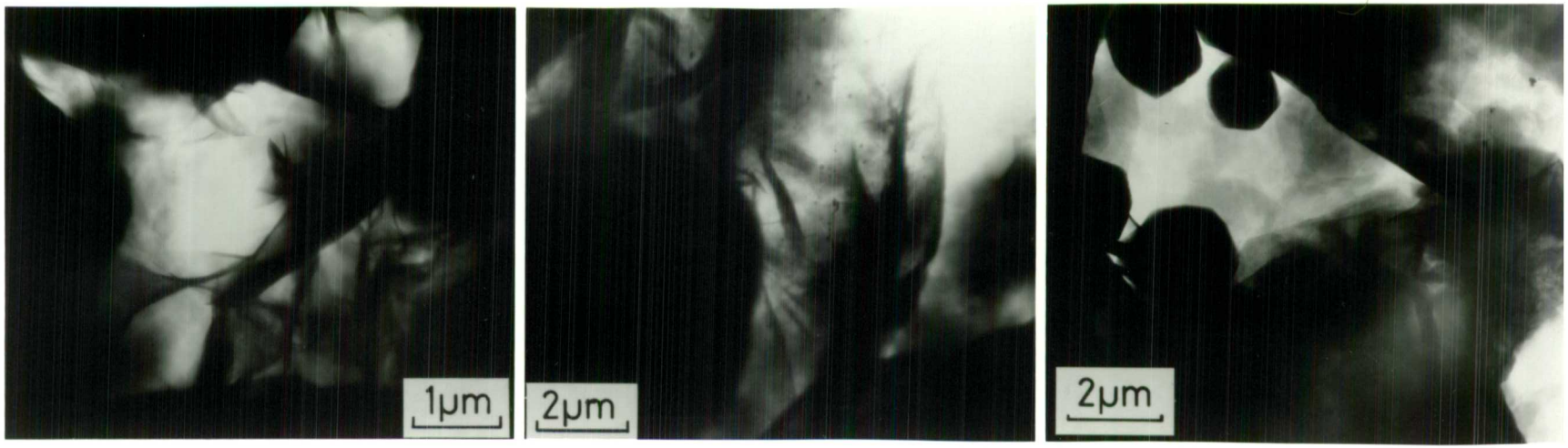

(a) 10 minutes (b) 30 minutes (c) 120 minutes

Plate 4C.2
Hydration of high sodium C_3A(AII)

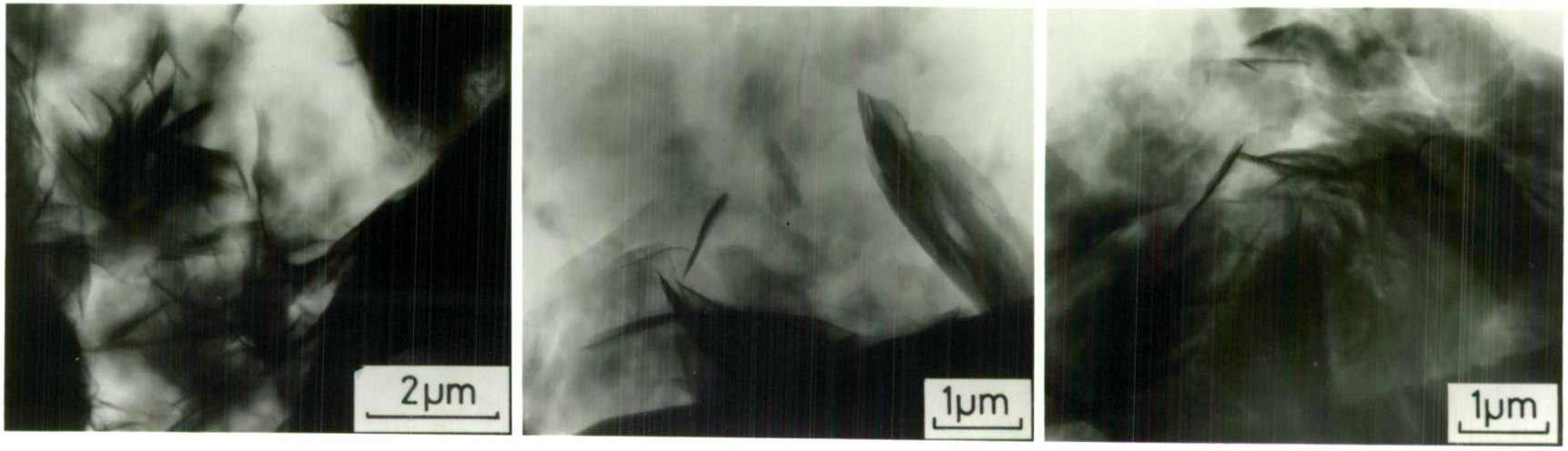

sulphate and appears denser and less permeable. There is a definite boundary between the amorphous layer and the underlying grain suggesting that the layer forms by precipitation from solution rather than by a topochemical mechanism. The structure observable in the underlying grain arises from product on top of the grain (c.f. Fig 4A.7). At the edge of this layer rods can be seen which are very susceptible to damage by the electron beam, there is also a suggestion of a thin, platy, hexagonal phase amongst the rods. Many more rods have formed after 30 minutes (plate 4C.3(b)) and obscure the surface of the grain, but there is still a lot of filmy product in evidence. After 2 hours (plate 4C.3(c) the rods are larger, more definitely faceted and are more stable to the beam, suggesting a higher degree of crystallinity. Little amorphous product could be seen but the surfaces of the grains were obscured by a dense mass of rods. After 2 hours the rods have a similar morphology to that reported for ettringite and rods seen earlier are probably poorly crystallised ettringite or AFt phase.

In the high sodium, orthorhombic C_3A hydrated with gypsum (plate 4C.4) an amorphous layer again appears to form within the first 10 minutes (plate 4C.4(a)). The grain surface, however, is obscured by a dense mass of tangled, irregular rods which tend to bubble up under the electron beam. After 30 minutes (plate 4C.3(b)) the amount of product has increased. The rods in open space have a more definite, discrete morphology, consistent with a higher degree of crystallinity, but amorphous looking areas can still be seen close to the surface of the grains. After 2 hours (plate 4C.3(c)) a dense mass of rods have formed obscuring the grain surface. As with the low sodium C_3A the rods formed have the morphology of ettringite. There appears to be more product formed in the high

Plate 4C.3
Hydration of low sodium C_3A(AI) with gypsum

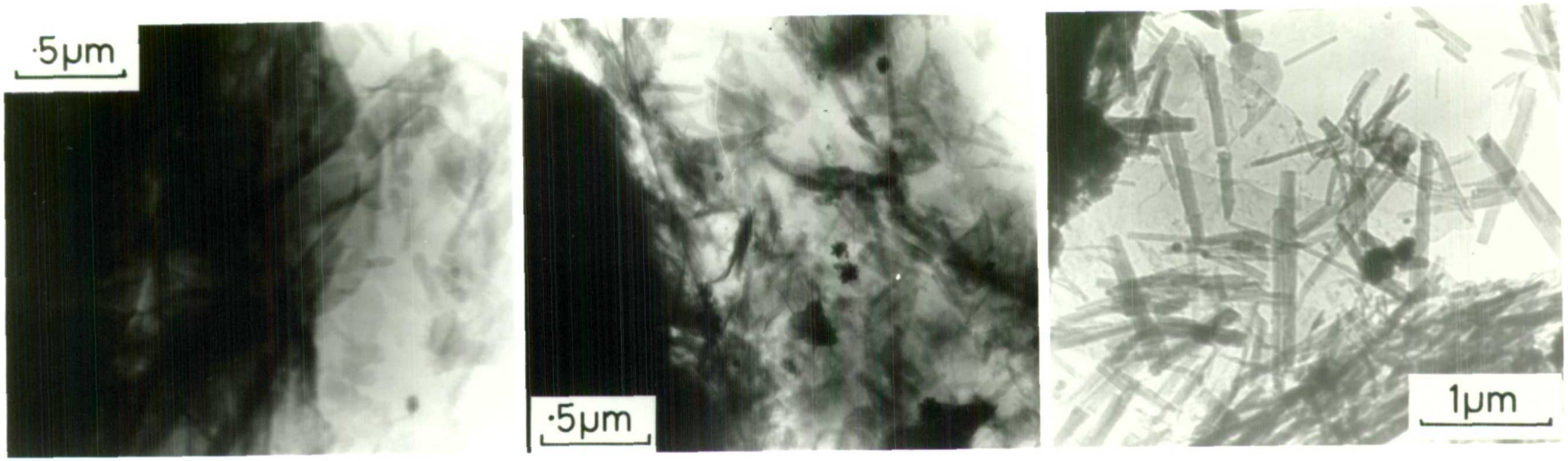

(a) 10 minutes (b) 30 minutes (c) 120 minutes

Plate 4C.4
Hydration of high sodium C_3A(AII) with gypsum

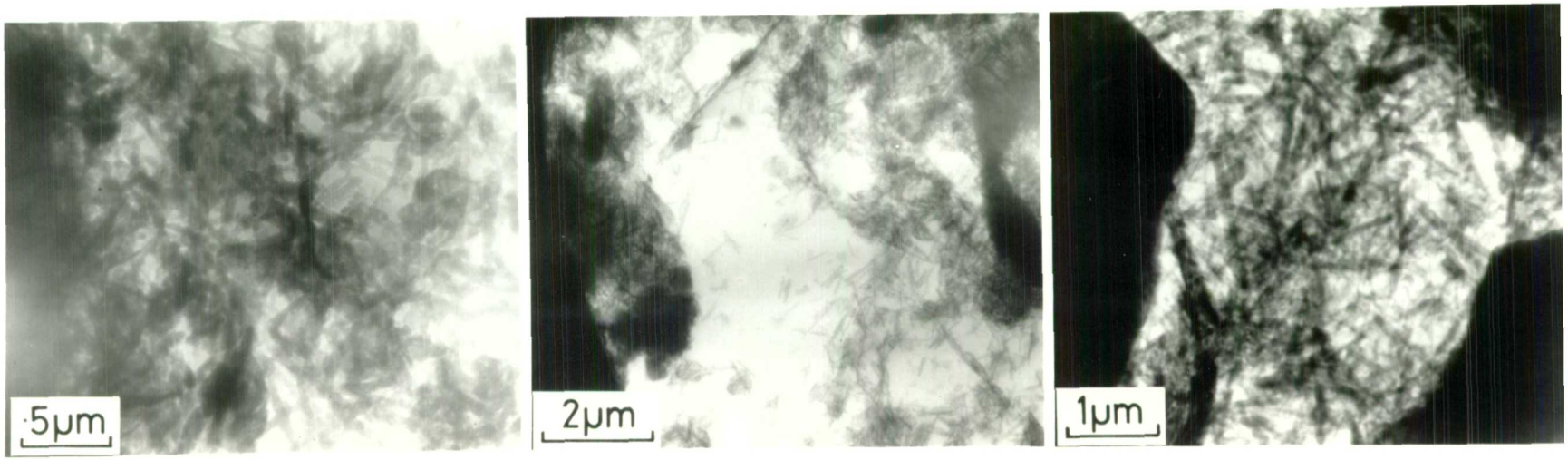

sodium C_3A but the selectivity of the sample preparation technique could be misleading. The morphology of the rods in the two cases are similar.

Effect of drying on C_3A and gypsum pastes

Plate 4C.5 shows the microstructure of the sample NBS hydrated for 10 minutes: in the 'wet' cell (plate 4C.5(a)); dried in STEM (plate 4C.5(b)) and in SEM (plate 4C.5(c)). Before the sample is dried (plate 4C.5(a)) the surface of the C_3A is covered with a filmy amorphous product with a few, poorly crystallised rods at the edges of this layer and in solution. After drying in a desiccator (plates 4C.5(b) and (c)) there are many more rods present, which are larger and more crystalline. The removal of the free water has caused the amorphous layer to contract back onto the surface of the grains.

Hydration of C_3A with hemihydrate

The microstructures of pastes of C_3A (NBS) plus hemihydrate hydrated for various times are shown in plate 4C.6. After 5 minutes (plate 4C.6(a)) the microstructure is dominated by crystals of gypsum from the rehydration of the hemihydrate. Amongst these large crystals many small rods can be seen with an ettringite type morphology, but much shorter and more squat than those seen in C_3A plus gypsum pastes (plates 4C.3(a), 4C.4(a)). These rods are not well faceted and bubble up quickly under the electron beam, indicating a low degree of crystallinity. After 30 minutes the number of rods and their apparent crystallinity has increased (plate 4C.6(b)), covering the surface of the C_3A grains in a dense mass. After hydration for 1 day the microstructure is much the same as after 30 minutes. The rods now have a well faceted hexagonal habit although in some areas a dense tangled mass of product can be seen which has a less discrete

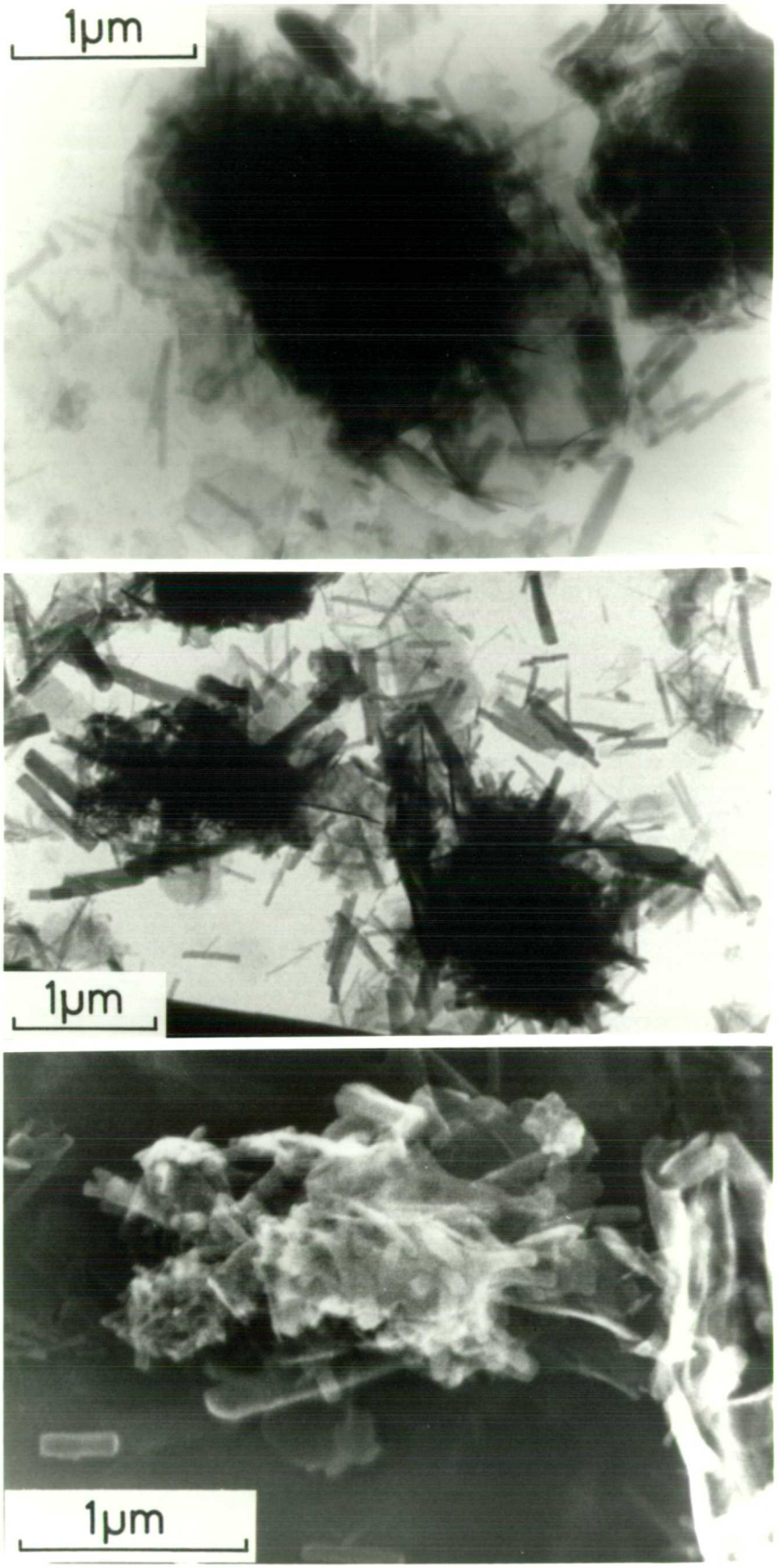

Plate 4C.5 C_3A(NBS) Hydrated with Gypsum for 10 minutes
(a) 'wet' in HVEM, (b) dried, STEM, (c) dried, SEM

morphology. Crystals of gypsum can still be observed. After 4 days no gypsum could be seen in the sample but there is no evidence of any formation of monosulphate plates. The ettringite type rods cover the surface of the grains in a dense tangled mass.

4C.II.3 Discussion

Hydration without sulphate

Soon after the addition of water an amorphous layer is observed around the C_3A grains. From the work of Marinho and Glasser (1984) and the earlier work of Jones and Roberts (1962) and D'Ans and Eick (1953a) it is likely that this amorphous product is a hydrous alumina gel possibly incorporating some adsorbed calcium ions. This layer is very uneven, peeling off the surface in places and is unlikely to significantly inhibit further reaction of the underlying grain. In this work at $^{w}/s = 0.5$ both cubic and hexagonal hydrates were observed in the low sodium C_3A after 2 hours hydration, whereas only hexagonal hydrates were observed in the high sodium C_3A. The reverse was found for these same C_3A solid solutions hydrated in suspensions ($^{w}/s > 100$) by Marinho and Glasser (1984). The concentration of Na^{+} in solution is likely to be different in the two cases which will affect the rate of conversion of hexagonal to cubic hydrates as shown by Spierings and Stein (1976). Apart from this there were no obvious differences in the microstructural development of the two C_3A solid solutions.

Hydration with sulphate

There is clear evidence from this work of the presence of an amorphous layer around the C_3A grains during hydration with calcium sulphate. By extension from the hydration of C_3A without sulphate

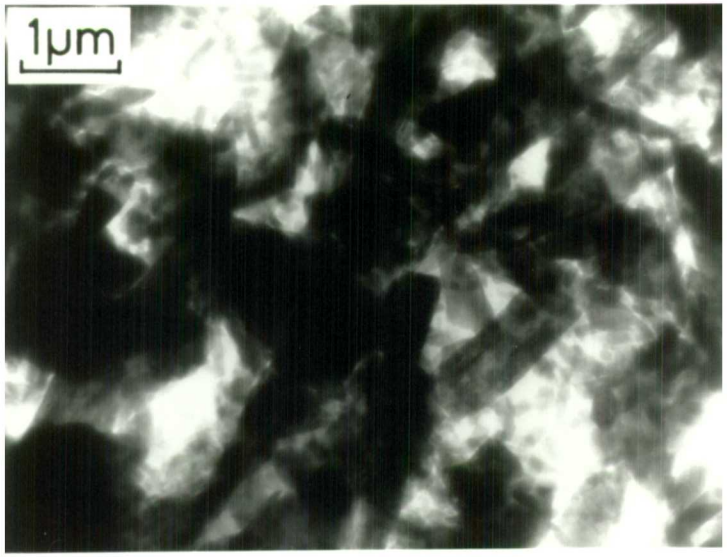

Plate 4C.6 Hydration of C_3A (NBS) with hemihydrate,

(a) 5 minutes
(b) 30 minutes
(c) 1 day
(d) 4 days

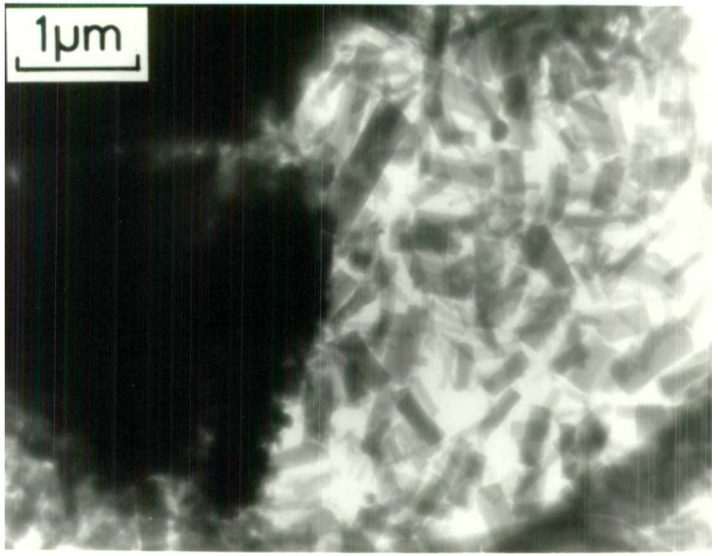

(a) (b)

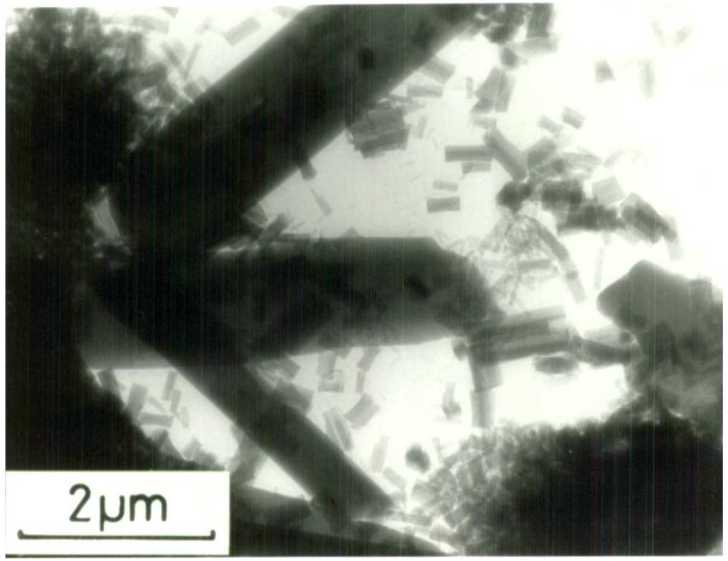

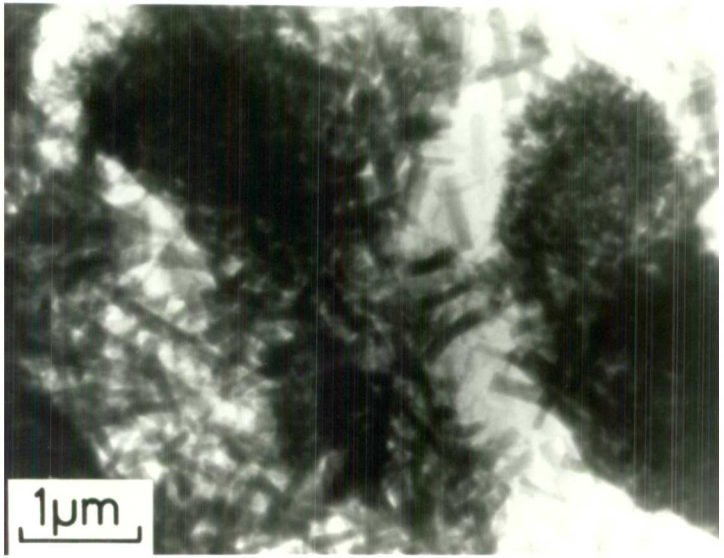

(c) (d)

and from the work of Jones (1939, 1944) and D'Ans and Eick (1953b) this is likely to be an amorphous AH_3 gel, as suggested by Stein and co-workers (Constanje et al, 1973, 1974; Holten and Stein, 1977; Stein, 1980), possibly incorporating some adsorbed calcium and sulphate ions. When this amorphous gel is observed unobscured by other hydrates a distinct boundary between the grain surface and the gel layer can be seen; this indicates that it is formed by solution and reprecipitation, rather than incongruent dissolution with the leaching of calcium ions as proposed by Skalny and Tadros (1977) or a disturbed surface layer suggested by Stein (1980). This amorphous layer is much more dense and homogeneous than that observed in C_3A pastes without calcium sulphate. This change in morphology can probably be attributed to the uptake of calcium and sulphate ions modifying the colloidal product. Similar changes in the appearance of amorphous AH_3 gel were noted by Jones (1939). It is possible that the ettringite rods do provide some screening effect, maintaining a different concentration of calcium and sulphate ions near to the surface of the grains from that in the bulk solution.

Jones (1939, 1944) and D'Ans and Eick (1953b) found that amorphous AH_3 gel is precipitated in the presence of significant concentrations of calcium and sulphate in solution; thus any concentration gradient need not be large and may occur in unstirred pastes even if the screening effect of the ettringite rods is negligible. If such a concentration gradient exists the presence of some C_4AH_{19} as hexagonal plates, observed in this work (plate 4C.3(a)) and by X-ray (Gupta et al, 1973; Schwiete et al, 1966; Collepardi et al, 1978, 1979) is not inconsistent with the phase equilibria determined by Jones (1939, 1944) and by D'Ans and Eick (1953b). Any C_4AH_{19} may contribute to any screening effect, but is not a prerequisite for the formation of a gel layer.

From the present work and the study of the kinetics of the C_3A-$CaSO_4$-H_2O reaction by Brown and LaCroix (1984) and Stein (1962) the rate controlling step in the hydration of C_3A appears to be diffusion through a complex product layer composed of amorphous AH_3 gel and ettringite. This layer may also contain C_4AH_{19}, $C_3A\bar{C}SH_{12}$ ('monosulphate') and/or their solid solutions.

The presence of sodium in solid solution with the C_3A does not appear to affect the qualitative development of microstructure during hydration with calcium sulphate (plates 4C.3 and 4C.4). The larger amount of ettringite observed in the high sodium C_3A might be due to the selectivity of the sample preparation technique, but could be attributed to the absence, or lower permeability of the AH_3 gel layer owing to the increased solubility of aluminium in the presence of Na^+ ions in solution.

In this work ettringite rods are observed at the edge of an amorphous layer and in solution some distance from the surface of the C_3A grains. This plainly indicates that they form by a through solution mechanism. When pastes are dried the rods 'fall back' onto the surface of the C_3A grains (plate 4C.5(b) and (c)). This phenomenon probably led to the erroneous conclusion of Schwiete et al (1966) that ettringite formed by a topochemical mechanism.

There is a marked difference in the morphology of the ettringite phase observed in pastes containing gypsum and that observed in pastes containing hemihydrate. The dissolution of hemihydrate produces solutions which are supersaturated in $(SO_4)^{2-}$ ions with respect to gypsum, whilst dissolution of gypsum does not produce supersaturated solutions (Bombled, 1980). The high $(SO_4)^{2-}$ concentration in pastes containing hemihydrate caused ettringite to precipitate as short, squat rods, (aspect ratio $\sim$ 3) as opposed to long thin rods (aspect ratio > 10) precipitated at lower $(SO_4)^{2-}$ concentrations. This

observation is consistent with that of Mehta (1976) who found that long slender needles of ettringite were formed when a high water to solids ratio was used and that short, prismatic crystals formed at lower water to solid ratios, although he concluded that the amount of space available caused this difference.

4D Hydration of the Ferrite Phase

The ferrite phase is responsible for the grey colour of cement. The hydration of the ferrite phase has probably received the least attention of any of the principle clinker minerals. Its importance in cements, however, cannot be ignored. In ordinary portland cements the interstitial phase is an intimate mixture of C_3A and the ferrite phase so they cannot hydrate independently of one another. Sulphate resistant cements contain little or no C_3A so the effect of the ferrite phase on their hydration cannot be ignored.

4D.I Review of previous work

4D.I.1 Structure and solid solution

The ferrite phase is a solid solution between C_2F and hypothetical 'C_2A' up to $C_2A_{0.7}F_{0.3}$ (Ghosh, 1983). It is commonly referred to as C_4AF which is the average composition of the ferrite phase in cements.

C_4AF contains octahedral and tetrahedral lattice sites which are normally randomly occupied by the iron and aluminium atoms. With carefully controlled preparation, however, it is possible to concentrate the iron atoms in the octahedral sites and aluminium ions in the tetrahedral sites (Pobell and Wittman, 1965).

Many elements can form solid solutions with the ferrite phase such as Mg, Si, Ti, Mn and Cr. MgO and SiO_2 can substitute up to 10% (molar) for $(Al,Fe)_2O_3$ (Regourd and Guinier, 1974).

4D.I.2 Hydration of the ferrite phase

It is generally accepted that the ferrite phase hydrates in an analogous manner to C_3A but at a slower rate; its reactivity increasing with the A/F ratio. Hexagonal and cubic hydrates

isomorphous with C_4AH_{19} and C_3AH_6 are formed in the absence of sulphates. When calcium sulphate is present a 'high' sulphoaluminoferrite hydrate analogous to ettringite (referred to as AFt), and a 'low' sulphoaluminoferrite hydrate analogous to monosulphate (referred to as AFm), can be formed.

The major questions regarding the hydration of the ferrite phase are:

1) How much iron substitutes in the aluminate hydrates.
2) Does any excess iron remain as an amorphous iron hydroxide.

As the C/(A,F) ratio is lower for the ferrite phase than for C_3A some iron or aluminium must be in excess when hydration occurs in the absence of lime.

Jones (1960) has reviewed the early work on attempts to synthesise the 100% iron substituted analogues of the aluminate hydrates. C_4FH_{19} (usually as its dehydrated form C_4FH_{13}), $C_3F(C\bar{S})_3{}^{32}H_2O$ (ettringite analogue) and $C_3FC\bar{S}12H_2O$ (monosulphate analogue) could be precipitated from solution fairly readily. Synthesis of C_3FH_6 (free from contamination by hydrous iron oxide) was only possible when Si contamination occurred from glass ware, the compound C_2FH_8 could not be synthesised.

Hydration of C_2F

Jones (1960) reported that C_2F could be hydrated in stirred suspensions but hydration in paste form (studied by Bogue and Lerch, 1934) was negligible. Jones attributed this low reactivity to the leaching of lime from the surface leaving an iron rich layer which inhibited further reaction. De Keyser and Tenoutasse (1968) and Rogers and Aldridge (1977) also reported the low reactivity of this phase, but in both cases the presence of lime increased the hydration rate.

Hydration of C_4AF and other ferrite solid solutions containing aluminium

Jones (1960) reviewed several investigations of the hydration of C_4AF. In all the studies reported an amorphous reddish brown phase was reported in addition to crystals isomorphous with C_4AH_{19} or C_3AH_6. Jones (1960) considered the dissolution of C_4AF to be incongruent with calcium and aluminium passing into solution, with partial replacement by H_2O, leaving a structureless gel on the surface.

Carlson (1964, 1966) reported that amorphous hydrous Fe_2O_3 was always formed during the hydration of ferrite solid solutions (Fss) in the absence of lime. Even when lime was in excess the hydrated phases were always poorer in iron than the original Fss. In contrast Schwiete and Iwai (1964) reported crystalline products with the same iron to aluminium ratio as the anhydrous material when lime was present.

Using Mössbauer spectroscopy, Tamás and Vértes (1973) concluded that all the iron in C_4AF hydrated to C_3FH_6 leaving amorphous AH_3. Rogers and Aldridge (1977), however, point out that the Mössbauer spectra from C_4FH_{19}, C_3FH_6 and poorly crystalline hydrous ferric oxide are all very similar. Rogers and Aldridge reported the appearance of amorphous hydrous ferric oxides in all their hydration studies. They report the similarity between the Mössbauer patterns of this amorphous phase and that of γ-FeO(OH) and refer to the amorphous phase as F-H. Jones (1960) also points out that there is no known crystalline form of FH_3, only hydrates with the composition $Fe_2O_3.H_2O$ (or FH).

Studies on the heat evolution during the hydration of C_4AF, alone, with lime, with gypsum, and with lime and gypsum (Jawed et al,

1976; De Keyser and Tenoutasse, 1968; Collepardi et al, 1979; Fukahara et al, 1981) show that in all cases the rate of heat evolution is lower than in C_3A. Addition of lime is reported to accelerate the reaction. The addition of gypsum, however, reduces the initial rate of heat evolution, as does the addition of gypsum and lime. As with C_3A a distinct second maximum in the rate of heat evolution is seen corresponding to the reaction of the AFt phase with more anhydrous material to give the AFm phase (De Keyser and Tenoutasse, 1968; Jawed et al, 1976). This peak occurs later in C_4AF pastes than in C_3A pastes, with the same gypsum addition, and is considerably retarded when lime is also present.

No direct evidence for the degree of substitution of iron oxide in the sulphoaluminate hydrates formed during the hydration of C_4AF with calcium sulphate has been reported. By assuming a value for the free energy of formation of iron substituted ettringite, Fukuhara et al (1981) deduced that the AFt formed from C_4AF had the formula:

$$C_3(A_{0.75}F_{0.25}).3C\bar{S}.31H$$

Work at the National Bureau of Standards on the X-ray diffraction patterns from iron substituted AFts formed from solutions and the pattern of AFt formed during C_4AF hydration (L. Struble, unpublished work) indicates that the F/(A+F) ratio in the AFt from C_4AF is between 0 and 0.3.

There is good evidence for the formation of amorphous hydrous ferric oxide (FH) during the hydration of ferrite solid solutions even when there is sufficient lime present for all the iron to enter the calcium alumino ferrite hydrates. In the case of hydration with calcium sulphates there is little evidence: of amorphous FH, of the

A/F ratio in the AFt or of the effect lime has on the A/F ratio.

4D.II Present Work

4D.II.1 Materials and techniques used

Two samples of the ferrite phase were studied, both with the composition C_4AF. One (NBS) was supplied by Dr P. W. Brown of the National Bureau of Standards, Washington, USA; the other (BJD) was supplied by Dr L. Parrott of the Cement and Concrete Association. The two samples had specific surface areas of 3300 cm^2/g and 4000 cm^2/g respectively. The sample BJD had been stored in a desiccator for over two years before investigation which may have affected its behaviour.

Specimens were prepared for examination in the environmental cell as described for alite (4A.II.1). The hydration of the NBS sample was studied with the addition of gypsum and with the addition of hemihydrate. The hydration of the BJD sample was studied with the addition of gypsum. All mixes were made with $^w/_s = 0.5$. Details of the mixes investigated are given in Table 4D.1.

Table 4D.1

Sample	Sulphate Addition	Hydration times
NBS	50% gypsum	10 min, 1 hour, 1 day, 4 days
NBS	50% hemihydrate	10 min, 1 hour
BJD	50% gypsum	1 day, 4 days

4D.II.2 E.M. observations of hydrated C_4AF

The microstructure of the NBS sample hydrated with added gypsum is shown in plate 4D.1. After 10 minutes (plate 4D.1(a)) a large

amount of product with an AFt type morphology is observed. The rods are much longer and thinner than those formed during the hydration of C_3A with gypsum (plates 4C.3(a), 4C.4(a) and 4C.5(a)). The surface of the grains does not look smooth and could be covered with an amorphous layer. After 1 hour's hydration (plate 4D.1(b)) the microstructure is dominated by well formed rods with an AFt morphology. These are larger and considerably thicker than those seen after 10 minutes and frequently exhibit diffraction bend contours. Due to the density of rods it is difficult to determine the nature of the C_4AF surface. Small rounded 'lumps' can be seen amongst the rods; these could be particles of amorphous FH (as observed by Rogers and Aldridge, 1977).

Plate 4D.2 shows the microstructure of the same C_4AF (NBS) hydrated with added hemihydrate. After 10 minutes (plate 4D.2(a)) the microstructure is dominated by gypsum (from the hydration of the hemihydrate), as with C_3A hydrated with hemihydrate (plate 4C.6). It is impossible to distinguish any product from the hydration of C_4AF. After 1 hour (plate 4D.2(b)), however, the microstructure appears similar to that observed with added gypsum (plate 4D.1(b)).

Plates 4D.3 and 4D.4 compare the microstructure of the two samples of C_4AF (NBS and BJD) hydrated with gypsum for 1 and 4 days. At both ages (plate 4D.3) the grains of the NBS sample are densely covered by AFt rods. Even after 4 days (plate 4D.3(b)) there is little evidence of any AFm product: one hexagonal plate can be seen to the right of centre, amongst a region of 'bubbled up' AFt.

Examination of the BJD pastes (plate 4D.4) reveals little product from C_4AF hydration, even after 4 days hydration. There is a lot of gypsum present with some filmy product and the occasional AFt type rod.

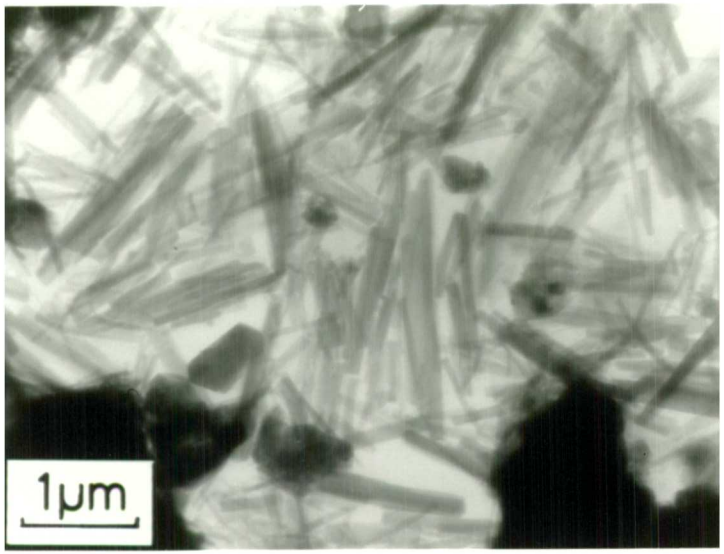

Plate 4D.1
Hydration of C_4AF (NBS) with gypsum in the HVEM,

(a) 10 minutes
(b) 1 hour

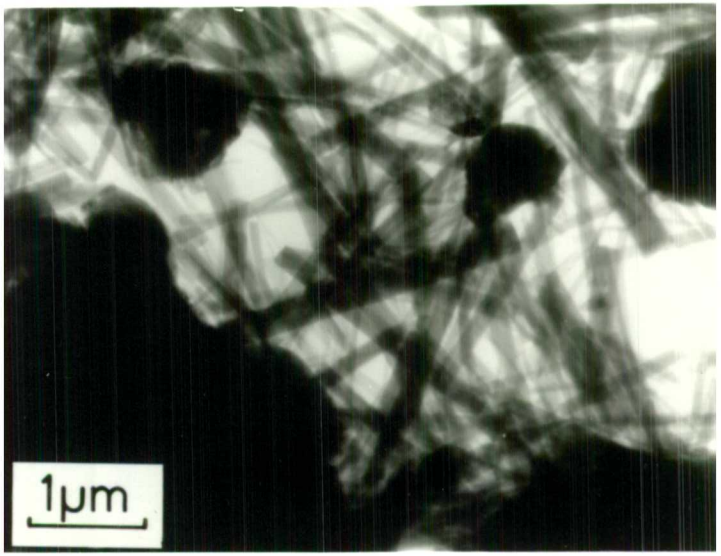

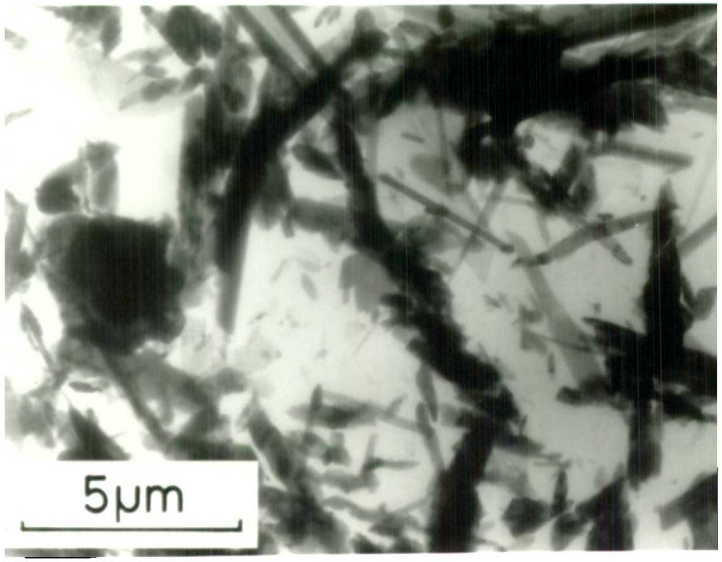

Plate 4D.2
Hydration of C_4AF (NBS) with hemi-hydrate in the HVEM,

(a) 10 minutes
(b) 1 hour

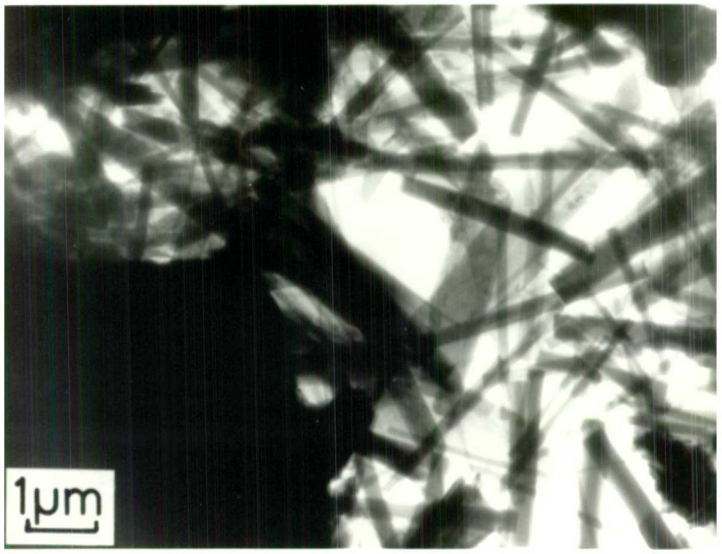

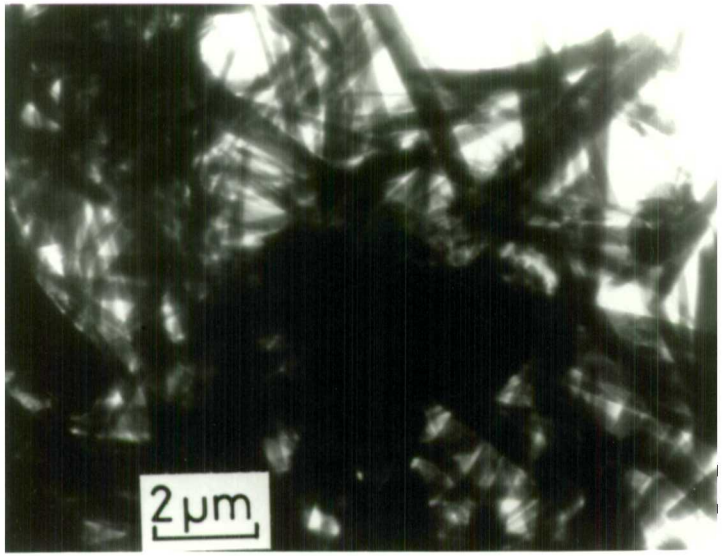

Plate 4D.3
Microstructure of
C_4AF(NBS) in the HVEM
(a) 1 day
(b) 4 days

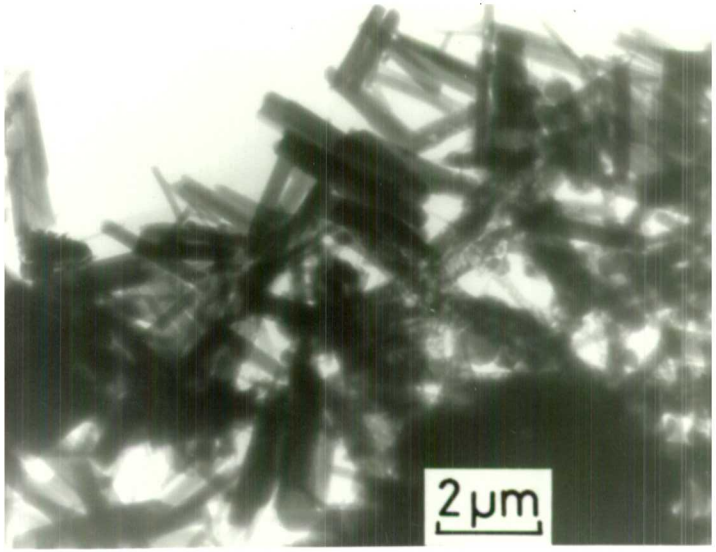

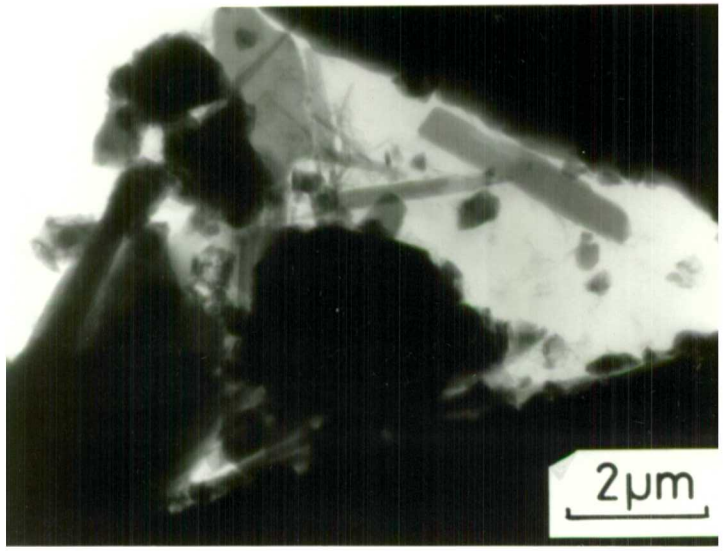

Plate 4D.4
Microstructure of
C_4AF(BJD) in the HVEM
(a) 1 day
(b) 4 days

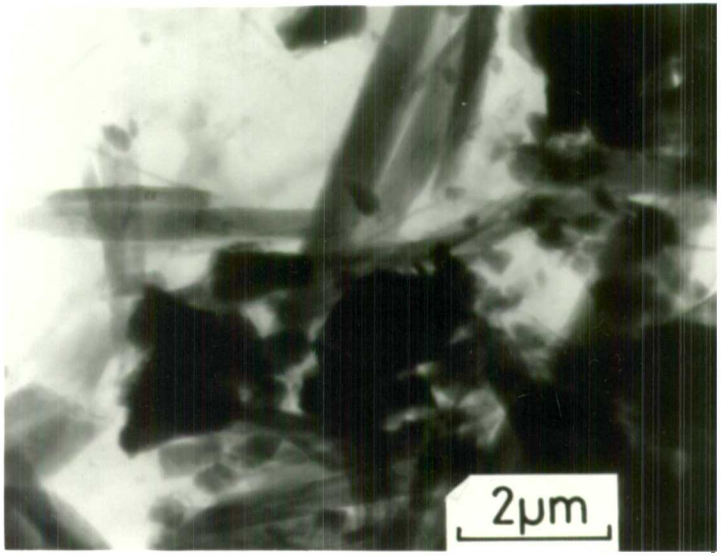

4D.II.3 Discussion

The NBS C_4AF appeared to be much more reactive than the C_3A samples examined (4C.II), in contrast to the low reactivity for C_4AF reported by other workers. The BJD C_4AF, on the other hand, appeared unreactive; this is probably due to the prolonged storage of this sample. M. B. Marinho (private communication) has found similar vast variations in the reactivity of ferrite solid solutions with the composition C_4AF.

The AFt formed in the early stages of hydration, in the NBS sample, has a markedly different morphology to that formed during the hydration of C_3A. This suggests that there is some iron oxide substituted in this AFt or that the presence of iron affects the morphology in some other way. Lumps of amorphous material are observed in hydrated C_4AF which could be amorphous hydrous ferric oxide.

4E Hydration of Mixtures of Cement Phases

In cement pastes the individual phases do not hydrate in isolation. Comparatively little is known about the interactions that can occur. However, a few studies have been made on mixtures of synthetic phases. These mixtures are physical combinations of one ground phase with another, i.e. all grains in the mixture are monomineralic. Cement grains are seldom monomineralic so there are significant differences between mixtures of phases and real cements.

4E.I Review of previous work

4E.I.1 Combined hydration of C_3S and β-C_2S

Tong and Young (1977) found that small additions of C_3S to β-C_2S controlled the concentrations of Ca^{2+} and OH^- in solution during early hydration. They predicted that this would accelerate the hydration of β-C_2S by promoting the earlier precipitation of CH. Berger et al (1979) reported a decrease in the rate of C_3S hydration in 50/50, C_3S/β-C_2S blends. Odler and Schüppstuhl (1982) studied a range of C_3S/β-C_2S blends. They found an increase in the induction period in the 25% C_3S, 75% C_2S blend over blends richer in C_3S, indicating a retardation of C_3S hydration in the presence of β-C_2S. The rate of reaction of β-C_2S was accelerated in all blends over that of pure β-C_2S.

It is apparent that C_3S can accelerate the rate of hydration of β-C_2S and β-C_2S retard that of C_3S, possibly by changing the composition of the liquid phase.

4E.I.2 Combined hydration of C_3A and C_4AF

Jawed et al (1976) found that small quantities of C_3A accelerated the rate of reaction of C_4AF + calcium sulphate pastes.

This was attributed to the faster depletion of calcium sulphate by reaction with the C_3A. In some C_3A + C_4AF + calcium sulphate mixtures two separate heat evolution peaks were found after the initial peak; one corresponding to the reaction C_3A + AFt $\longrightarrow$ AFm and the other to C_4AF + AFt $\longrightarrow$ AFm.

4E.I.3 Combined hydration of C_3S and C_3A

The combined hydration of C_3S and C_3A has been studied by Stein and co-workers (de Jong et al, 1968; Corstanje et al, 1973, 1974). In pastes containing no calcium sulphate it was found that the presence of C_3A retarded the hydration of C_3S. This was attributed to the incorporation of aluminate ions into a first, barrier layer, hydrate and to the changes in the Ca^{2+} and OH^- concentrations. Very small amounts of C_3S accelerated the conversion of C_4AH_{19} to C_3AH_6, whilst increasing C_3S additions significantly retarded this conversion. A wide range of C_3A + C_3S + gypsum mixtures were investigated with C_3A:C_3S ratios varying from 1:1 to 7:1. Many complex interactions were proposed to explain the heat evolution curves produced by hydration of these mixtures. In all cases, however, the ratio of gypsum to C_3A was less than 0.1, much lower than that found in cements.

Regourd et al (1976) studied the hydration of a 76% C_3S + 19% C_3A + 5% gypsum mixture. They found that calcium silico aluminate hydrates analogous to ettringite and monosulphate could be formed, but that these phases were unstable in the presence of SO_4^{2-} ions, converting to the calcium sulphoaluminates.

It is apparent that the silicate and aluminate phases can interact, but to what extent and by what mechanism is unclear.

4E.II Present Work on a C_3S:C_3A:$C\bar{S}\frac{1}{2}H$ Mixture

4E.II.1 Details of mixture and calorimetry

Resin impregnated and polished specimens of a hydrated C_3S:C_3A:$C\bar{S}\frac{1}{2}H$ mixture were supplied by Dr L. Parrott of the Cement and Concrete Association. This mixture was made up of 3 parts alite and 1 part C_3A with an addition of hemihydrate equivalent to 5 wt % of gypsum. The alite was the same synthetic product as that used in section 4A.II.

The rate of heat evolution from this mixture, obtained by Mr D. Killoh of the C&CA, is shown in Fig 4E.1. The second peak is much larger than that for a pure alite, indicating that the hydration of C_3A (presumably to form ettringite) contributes significantly to this peak. There is also a third peak after 48 hours similar to that observed in the hydration of C_3A + calcium sulphate for the reaction of C_3A with ettringite to produce monosulphate.

4E.II.2 BEI of C_3S:C_3A:$C\bar{S}\frac{1}{2}H$ mixture

As the specimens were received already resin impregnated and polished, this mixture was only studied in the SEM using backscattered electron imaging (BEI). An example of the microstructure observed in the paste hydrated for 1 day is shown in plate 4E.1. Plate 4E.1(a) is a BEI, plates 4E.1(c) and (d) are silicon and aluminium X-ray dot maps respectively and the compositions of the areas (as confirmed by EDXA) are shown diagrammatically in plate 4E.1(b). The C_3A grains have a significant gap between the anhydrous core and the hydration shell, whilst the hydration products around the C_3S grains remain in contact with the underlying grain. The shell around the C_3A grains is much thinner than that around the C_3S grains. Areas of calcium hydroxide have engulfed some of the C_3S grains.

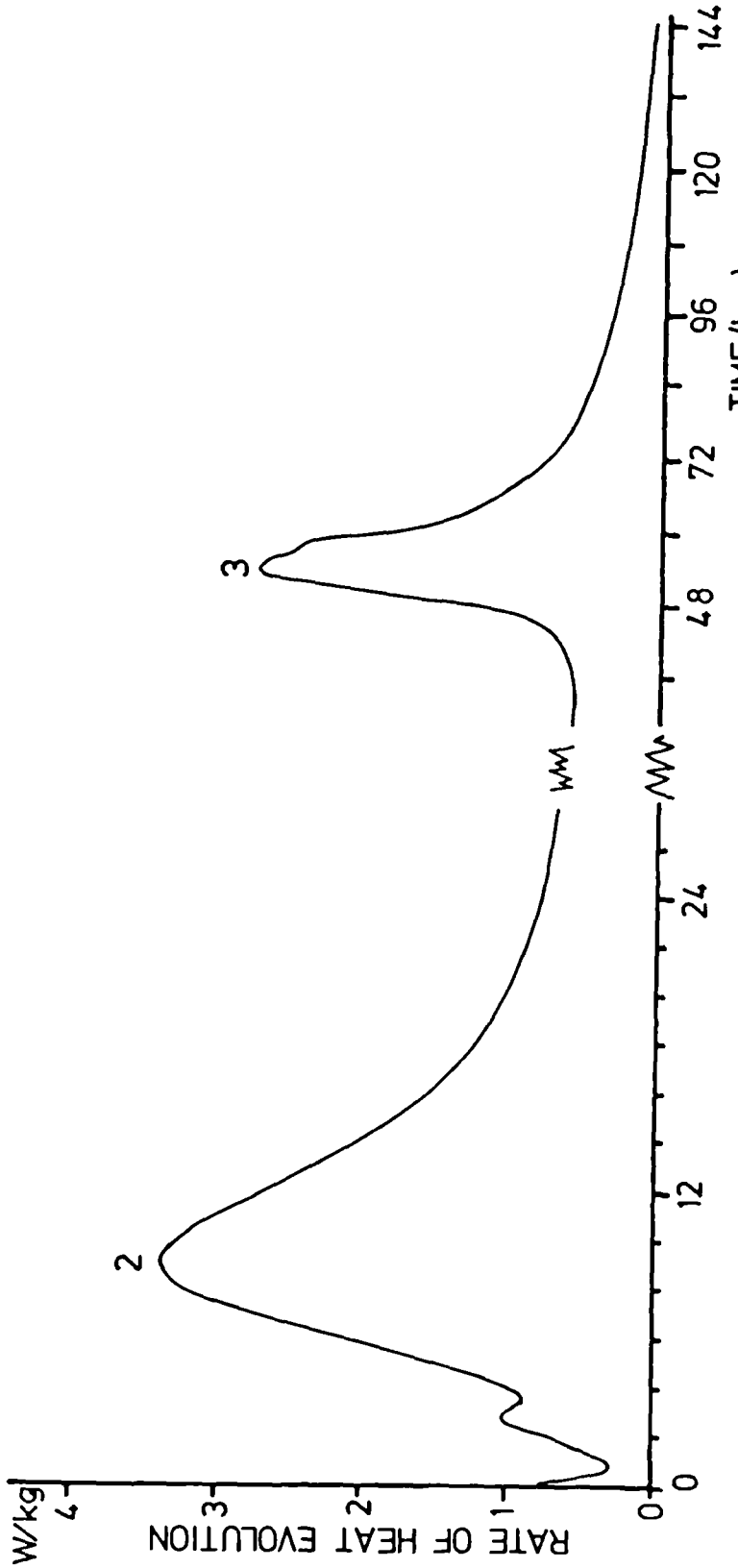

FIG 4E1 Rate of Heat Evolution during the Hydration of an Alite+C3A+hemihydrate Mixture (=5%gypsum)

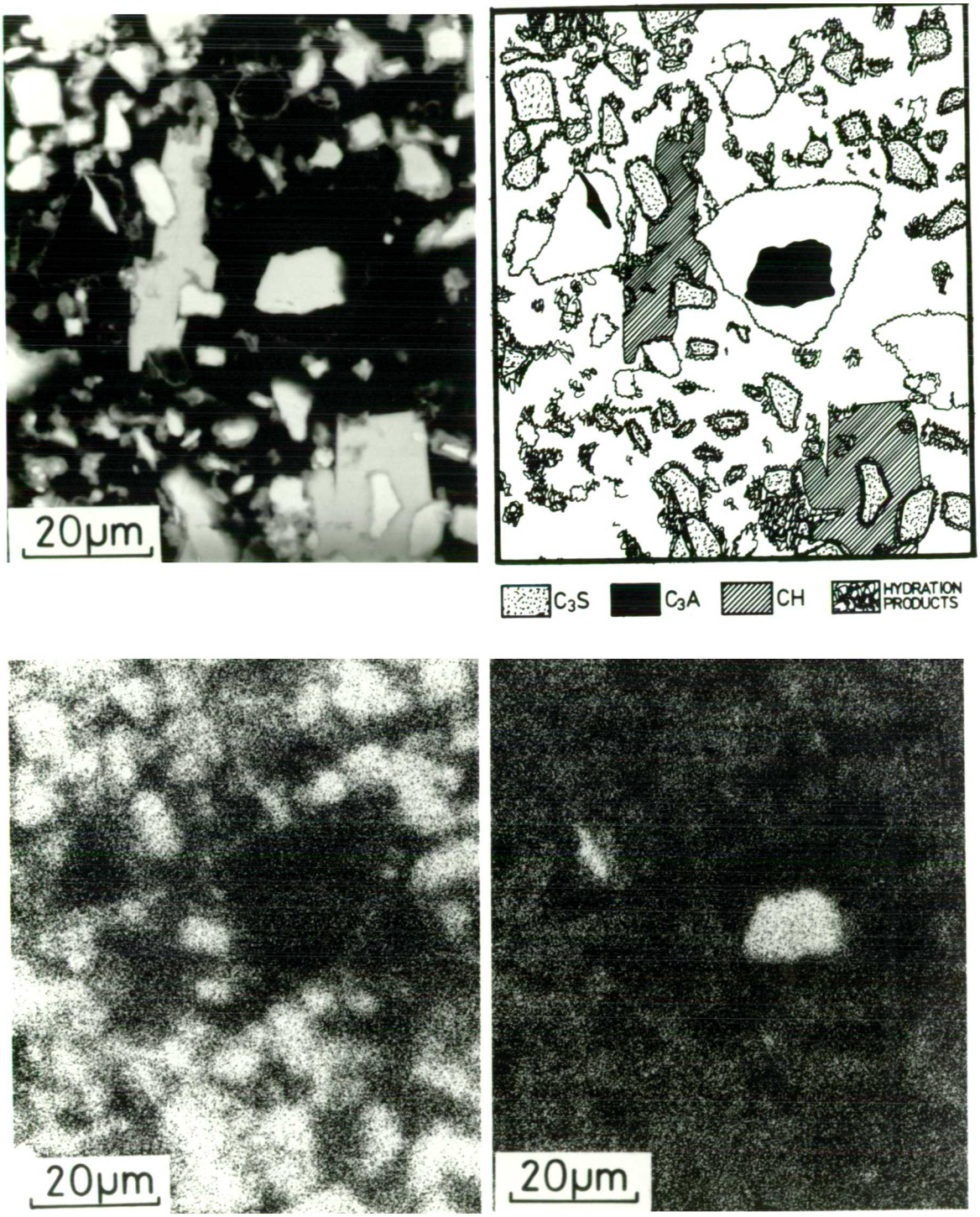

Plate 4E.1 Mixture of 3 parts C_3S:1 part C_3A with 5% gypsum addition. Hydrated for 1 day, resin impregnated and polished.

(a) BEI

(b) diagrammatic representation of phases present

(c) Si, X-ray dot map

(d) Al, X-ray dot map

After 3 days large thin edgewise plates around 10 μm across can be seen in the polished sections. No remaining anhydrous C_3A could be found so it is difficult to determine the spatial relationship of these plates to the distribution of C_3A and C_3S grains. From the calorimeter evidence, however, it might be inferred that these plates form by reaction of the remaining C_3A with ettringite to give monosulphate.

4E.II.3 Discussion

In the presence of C_3A hydrated shells are formed around C_3S grains. The C_3A appears to dissolve beneath these shells and any product is precipitatedon or outside the shell so that a separation between the shell and anhydrous core of up to 10 μm is produced. It is probable that this space is filled with concentrated solution or hydrous amorphous product before drying, perhaps AH_3 gel as in the case of C_3A hydrated with gypsum in the absence of C_3S.

The studies of hydration of C_3S alone and of C_3A just with gypsum (4A.II and 4C.II) in the environmental cell did not show the formation of any separated, hydrated shell. This separated shell phenomenon indicates that the interaction between C_3A and C_3S during hydration can produce substantial changes in the microstructure.

Chapter Five

HYDRATION OF PORTLAND CEMENT

This chapter deals with the hydration of cement as a whole. The first section (A) reviews the literature on the hydration of cement, emphasising the similarities and differences between the hydration of cement and that of its major component alite.

Section B describes the cements used in the present work.

The microstructural development of cement during hydration, as observed by a combination of electron optical techniques, is presented in section C. Section D describes the present work on the rate of heat evolution from the various cements studied and the effects of mixing and particle size on the rate of heat evolution.

5A Review of Previous Work

The hydration of portland cement is determined by the hydration of its constituent phases. The hydration of these phases will be modified relative to their hydration in isolation (Chapter 4), by interactions between them and the presence of impurities.

C_3S or alite, being the major component, is often taken as a model for portland cement. A comparison of changes in the rate of heat evolution, rheology and strength development indicates that the hydration reactions are broadly similar in each case, but there are important differences. Some of these differences which have been

reported in the literature are outlined here and will be discussed more extensively in Chapter 6.

Microstructure of hardened cement paste

Like alite, the microstructure of hardened cement paste is dominated by C-S-H and CH. Based on observations of fracture surfaces, Diamond (1976) described mature cement paste as consisting of about 70% C-S-H gel, 20% CH and small percentages of ettringite, monosulphate and several other minor substances.

Lachowski et al (1980) analysed many particles of hydrated products from portland cement and showed that most phases contained impurities. The C-S-H gel contained significant amounts of Al, Fe and S. The AFm phase contained a mixture of sulphate, hydroxide, Al- and Si- bearing ions in its interlayer sites, and Si was found as an impurity in the AFt phase. It was estimated that about a third of the Al and nearly all the S was present in C-S-H in mature pastes. This indicates that the hydration of the interstitial material and calcium sulphate may affect the properties of the hydration products from the silicate phases as well as forming hydration products other than C-S-H and CH.

Taylor (1984) has described the distribution of elements in a 23 year old cement paste as determined by X-ray analysis in the EPMA. He concludes that the distance ions migrate during hydration is generally small, as is probably the case in pastes of C_3S and β-C_2S. He also reports the appearance of large iron rich regions, similar in form to that of the interstitial phase in the clinker microstructure, which are obviously not seen in hydrated calcium silicate pastes.

Perhaps the most striking difference between cement and alite pastes is the occurrence, in cement pastes, of empty or partially

empty hydration shells. These shells were first reported by Barnes et al (1978a, b, 1979), who called them 'Hadley grains'. Observations of these grains have been reported by several other workers, including Dalgleish et al (1982a and b) and Pratt and Ghose (1983).

Development of microstructure in cement pastes

Several workers (Double et al, 1978; Jennings and Pratt, 1980 ; Groves, 1981) have reported the appearance of a gelatinous layer on the surface of cement soon after mixing with water. This has been described as a semi-permeable membrane, whose rupture under osmotic pressure brings the induction period to an end (Double et al, 1978; Double, 1983). However, no such layer has been observed, during the hydration of C_3S or alite alone (Jennings and Pratt, 1980), so this mechanism would not explain the similarities between the early hydration of cement and C_3S. Dalgleish et al (1982b) observed some etch pitting on the surface of cement grains after 30 minutes, whilst other areas appeared smooth with no hydration products visible in the dried state.

After a few hours' hydration, Dalgleish et al (1982a and b) reported the appearance of small AFt rods on the surface of the cement grains. Similar rods were observed by Locher et al (1980), who associated their formation during hydration with normal setting behaviour. It was observed that if the cement contained too little calcium sulphate, large hexagonal plates of C_4AH_{19} formed causing flash set. In the presence of excess hemihydrate, large lathlike crystals of gypsum formed, leading to false setting. The small AFt rods, however, did not adversely affect the rheology of the cement.

As with alite, the end of the induction period in cement hydration marks the onset of rapid growth of C-S-H and CH, causing

the cement to set and harden (Dalgleish et al, 1982b; Bensted, 1982; Casson et al, 1982). After 12-18 hours the bonding between the hydration shells is sufficient for 'Hadley grains' to be exposed on fracture surfaces (Dalgleish et al, 1982a and b).

After about 16 hours' hydration long AFt rods are observed to have grown through the C-S-H layer (Dalgleish et al, 1982a and b; Pratt and Ghose, 1983).

The age at which AFm phase is detected in cement pastes is generally reported to be between 1 and 7 days, both by XRD (Mather, 1976; Lachowski et al, 1980) and by examination of fracture surfaces in the SEM (Pratt and Ghose, 1983).

Rate of heat evolution during cement hydration

As can be seen from the heat evolution curve shown in Chapter 3 (Fig 3.2), the initial peak in the rate of heat evolution is followed (after the induction period) by several further peaks, in contrast to the single subsequent peak seen during the hydration of alite (Fig 4A.5). The reactions responsible for these further peaks are the subject of much controversy.

The work of Lerch (1946) showed that if a cement contained insufficient gypsum, the second heat peak was closely followed by a higher, sharp, third peak, which was attributed to the formation of monosulphate. With higher additions of gypsum this peak moved to later times and was reduced in intensity (e.g. for a cement containing 14.3% C_3A and 3.5% SO_3 the third peak did not occur until 50 hours hydration). The appearance of this third peak was affected by the alkali content and fineness of the cement as well as by the C_3A content. From this work Lerch defined a 'properly retarded' cement as one in which no third peak occured during the first 30 hours hydration. It should be noted that the cements investigated

by Lerch (1946) contained a much lower proportion of C_3S ($\sim$45% by Bogue) than is found in modern cements ($\sim$55% by Bogue) and correspondingly higher proportions of the interstitial phase. Some of Lerch's results are shown in Fig 5.1(a).

The cements investigated by Stein (1961), showed a third heat evolution maximum after about 50 hours hydration, which was attributed to the formation of monosulphate. However, the reported heat evolution curves show a pronounced shoulder on the second peak at about 16 hours, which is not commented on. Similar shoulders have been found by Pratt and co-workers (Dalgleish et al, 1982a and b; Pratt and Ghose, 1983) to correspond to the appearance of long AFt rods in the microstructure of the cement.

Theisen (1983) has shown that the degree to which the added gypsum is dehydrated can also affect the shape and position of the heat peaks (Fig 5.1(b)). Forrester (1980) has shown that high shear mixing can also affect the heat evolution curve. It is apparent that several variables may affect the heat evolution from cement as well as its phase composition.

There are strong similarities between the 'third peak', reported by Lerch (1946) and Stein (1961), and the 'monosulphate peak', corresponding to the reaction of C_3A and ettringite to form monosulphate, in the rate of heat evolution from C_3A + gypsum. The shapes of these peaks and the effect of gypsum on the time at which they occur are both similar. The shoulder sometimes seen on the second peak does not show this similarity to the 'monosulphate peak' and could be related to a secondary formation of AFt.

If the heat evolution from each phase varies linearly with the amount of that phase present, it should be possible in theory to

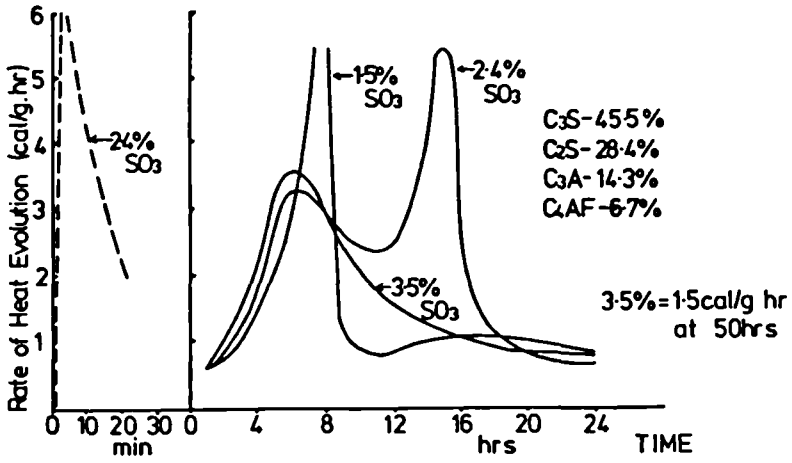

FIG. 5.1 (a) [above, from Lerch, 1946] (b) [below, from Theisen 1983] Effect of Quantity and Degree of Dehydration of Gypsum on the Rate of Heat Evolution of Cement

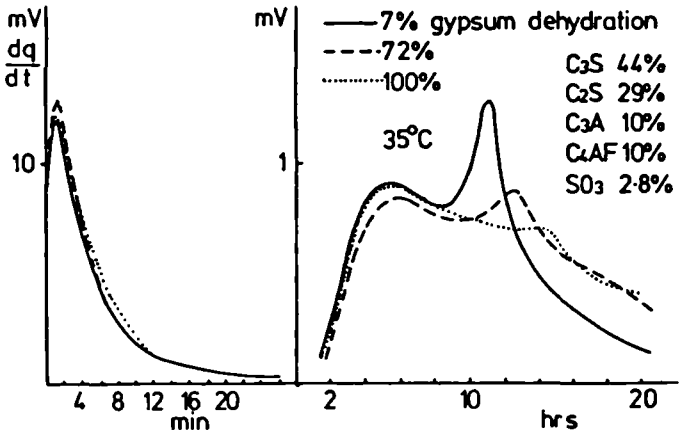

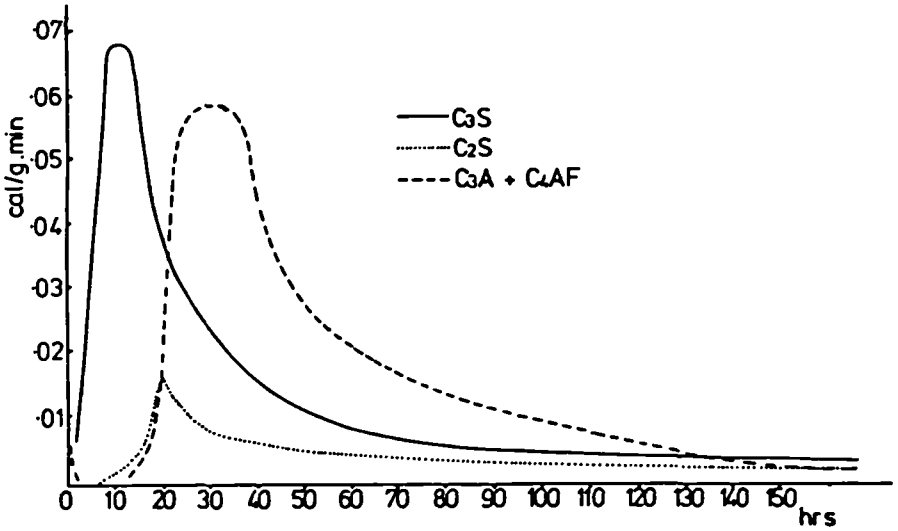

FIG. 5.1 (c) Rate of Heat Evolution from Constituent Phases from Deconvolution of the Heat Evolution Curves of a series of Closely Related Cements (from Kaminski & Zielenkiewicz 1982)

separate the total heat evolution curves from a series of cements, into contributions from each of the phases using a least squares regression analysis. Although it is unlikely that the contribution of any phase will vary linearly over a wide range of phase compositions, it is possible that this relationship may hold over the narrow phase composition range found in portland cements if other factors such as gypsum content and dehydration and mixing are kept constant. Such a deconvolution of calorimetry curves has been reported by Kaminski and Zielenkiewicz (1982) for a narrow range of cements prepared in the laboratory from different mixtures of the same minerals. Their results are shown in Fig 5.1(c) and clearly demonstrate that the second peak corresponds to the hydration of C_3S and the third to the hydration of C_3A.

5B Data on Cements Used in the Present Work

5B.I Commercial cements for calorimetry and microstructure

In total eight commercial cements were studied in the present work: 2 British OPCs; 5 American OPCs and 1 British White Cement.

The cements BT and White (OPC and White Cement respectively) were supplied by Blue Circle Industries, Technical Research Division, who also supplied the chemical analyses and Bogue compositions and other data for these cements. The cement D44 and its chemical analyses, Bogue composition and other data, was supplied by the Cement and Concrete Association.

All the remaining cements (NBS 61-64, NBS 34) were supplied by the National Bureau of Standards. These cements constitute part of the Cement and Concrete Reference Laboratory, Reference Sample Program. Chemical analyses and physical data for these cements were provided by about 100 laboratories; the quoted values

Table 5B.1 Chemical analyses of the cements (wt %)

CEMENT	BT	D44	NBS 34	NBS 61	NBS 62	NBS 63	NBS 64	WHITE
SiO_2	20.3	21.5	19.6	20.5	19.4	20.8	20.7	22.6
Al_2O_3	5.2	4.8	6.9	5.2	6.2	5.9	4.6	4.0
Fe_2O_3	3.1	2.0	2.5	2.1	2.3	2.4	2.7	0.3
CaO	64.7	64.6	62.2	63.1	62.7	63.6	62.7	68.5
MgO	1.1	1.9	2.9	3.9	3.2	2.2	4.1	0.3
SO_3	2.8	2.7	3.2	2.6	3.1	2.5	2.6	2.2
K_2O	0.34	0.7	0.96	0.96	0.78	0.95	0.63	0.16
Na_2O	0.19	0.2	0.37	0.22	0.29	0.21	0.75	0.10
Loss on ignition	1.0	N/A	1.4	1.3	2.0	1.4	2.0	1.5
Free lime	0.7	1.1	0.9	1.3	1.4	1.2	0.5	2.2
Insoluble Residue	0.35	N/A	0.43	0.19	0.29	0.20	0.30	0.06

Table 5B.2 Phase composition (wt %) of the cements by Bogue and QXDA

CEMENT	C_3S		C_2S		C_3A		C_4AF		Calcium sulphate	
	BOGUE	QXDA	BOGUE	QXDA	BOGUE	QXDA	BOGUE	QXDA	BOGUE	QXDA[1]
BT	59.0	67	13.7	15[2]	8.5	5	9.4	6	4.6	HA
D44	54	69	20	22	7	5	6	3	4.5	H
NBS 34	44.2	59	22.2	18	13.7	7[3]	7.5	7	5.5	HA
NBS 61	55.9	66	14.8	19[4]	10.0	6	6.4	4[5]	4.4	GH
NBS 62	51.1	74	16.5	11[6]	12.1	7[7]	7.0	7	5.2	HA
NBS 63	52.1	64	19.9	23	9.5	5	7.4	5[8]	4.3	GH
NBS 64	55.9	68	16.5	15	7.3	2	8.2	9	4.5	HA
WHITE	64.4	63	16.3	27	10.1	5	0.9	0	4.7	GH

Notes

[1] Phases detected qualitatively G = gypsum, H = hemihyrate, A = anhydrite

[2] 13% β, 2% α

[3] 6% cubic, 1% orthorhombic

[4] 16% β, 3% α

[5] A/F = 46/54

[6] 11% β, 3% α

[7] 4% cubic, 3% orthorhombic

[8] A/F = 58/42

Table 5B.3 Other data on the cements

CEMENT	BT	D44	NBS 34	NBS 61	NBS 62	NBS 63	NBS 64	WHITE
Surface area m^2kg^{-1}	340	N/A	376	370	420	395	404	373
Initial set (min)	135	N/A	124	135	105	127	122	125
Final set (min)	180	N/A	243	236	202	222	236	150
Manufacturing process	Dry	Dry	Wet	Wet	Dry	Wet	Dry	Wet

are averages. The Bogue compositions for these cements were calculated at the Cement and Concrete Association (modified version of Appendix I).

All the X-ray analyses were carried out with the assistance of Mr W. A. Gutteridge at the Cement and Concrete Association by the method described in Chapter 2B and Appendix II.

The chemical analyses of the cements are given in Table 5B.1; the Bogue and QXDA phase compositions in Table 5B.2; and the surface areas, initial and final sets and the manufacturing process in Table 5B.3.

The major difference between the British and American OPCs is in the magnesium contents; one of the American cements (NBS 64) would not have passed the British Standard for cement compositions. The alkali contents of the American cements also tend to be higher than those of the British cements.

5B.II Clinker for particle size work

A sample of unground clinker was supplied by the Cement and Concrete Association for the work on the effect of particle size on the rate of heat evolution. The chemical analysis of this clinker is given in Table 5B.4 along with the composition by the simple Bogue calculation (Appendix I).

The clinker was ground in an end-runner mill at the Cement and Concrete Association to pass a 75 μm sieve. The ground clinker was separated in an air classifier by Alpine Process Technology into five size fractions with the nominal ranges shown in Table 5B.5. The actual particle size range was measured using a Malvern Laser Diffraction Particle Sizer. From these measurements the approximate range (containing about 90% by wt of the particles) and the modal size were estimated; these values are also given in Table 5B.5.

Table 5B.4 Analysis of clinker

CHEMICAL ANALYSIS		BOGUE COMPOSITION	
	Wt %		Wt %
SiO_2	23.0	C_3S	52.2
Al_2O_3	5.0	C_2S	26.5
Fe_2O_3	3.3	C_3A	7.5
CaO	65.9	C_4AF	10.2
MgO	1.2		
SO_3	0.45		
K_2O	0.33		
Na_2O	0.18		
Free lime	0.8		

Table 5B.5 Fractionation of ground clinker

FRACTION	NOMINAL SIZE RANGE μm	APPROXIMATE ACTUAL RANGE μm	APPROXIMATE MODAL SIZE μm
F1	75-35	80-30	45
F2	35-16	35-12	20
F3	16-7	25-8	15
F4	7-3	15-4	9
F5	<3	8-2	3.5

An amount of hemihydrate was added to each fraction in proportion to its approximate surface area (calculated on the basis of spherical particles all with the mean size). The addition to the 35-16 μm size fraction was 5 wt %.

5C The Development of Microstructure: Electron Optical Observations

5C.I Techniques used

The development of microstructure in several portland cements was studied using a variety of electron optical techniques (Chapter 3D). SEM of fracture surfaces was used to study several cements (BT, D44, NBS 34, NBS 64, White). Specimen preparation for SEM is relatively simple, although the specimen must be dried and only the fracture path is revealed. Due to the roughness of the fracture surface EXDA is of dubious value.

Using the environmental cell in the HVEM the cement microstructure can be observed without drying. This is especially useful in determining the 'wet' morphology of C-S-H, as in the study of alite and belite (4A.II.2 and 4B.II.2). However, as specimen preparation is difficult and the availability of the microscope limited, only a few cement pastes could be studied using this technique. Specimens are prepared by tearing carbon coated grids out of the hydrating cement (as described in Chapter 4, section AII) hopefully leaving a thin covering of cement which is electron transparent in some areas; thus only a 'fracture surface', through weaker, more porous regions, is observable in profile, which need not necessarily be typical of the bulk.

Preparation of ion beam thinned sections of cement allows the microstructure to be viewed in cross section and at high resolution by TEM and STEM. Unfortunately specimen preparation is extremely difficult, owing to the brittleness of cement and its weakness at early ages. So far it has only been possible to produce thin sections of cement older than 2 months, where the cement has sufficient strength, and at ages less than 1 day, where the cement is sufficiently

porous to allow good resin impregnation, which supports the structure. In addition, only small areas can be thinned sufficiently to allow electron transmission, so the technique is still selective.

Backscattered electron imaging of polished surfaces also allows the microstructure to be examined in cross section although with much lower resolution than STEM of thin sections. This technique, however, is not selective and so can confirm the generality of observations made of thin sections.

Specimen preparation for electron microscopy

The cements were mixed in batches of around 100g or more, usually at a water/cement ratio of 0.5 although one batch of D44 was made at w/c = 0.3 for comparison. In each case the cement was hand mixed with a metal spatula in a plastic beaker for 3 minutes using a shearing action. The cement was then cast into several cylindrical polypropylene moulds around 2cm diameter and 2 cm in height, which were then sealed. At the required time after mixing the moulds were placed into a freezing mixture of methanol and solid carbon dioxide to stop the hydration reaction. In a few cases hydration was stopped by demoulding the cement and placing it in a large volume of methanol for comparison. Samples which were to be hydrated for more than one day were unsealed after one day, by removing the lid of the mould, and placed in water, saturated with calcium hydroxide to prevent leaching of the calcium hydroxide in the cement. Frozen specimens were then transferred to a freeze drier in which the drying chamber was cooled to -35°C and left for 4-7 days. The temperature of the freeze drying chamber was then increased to room temperature over several days so that water vapour would not condense on the specimens when they were removed. The

dried specimens were stored in vacuum desiccators until examination. This method of freeze drying was preferred to drying by methanol as the hydration reaction was stopped more quickly ($\sim$1 min). At very early ages (< 7 hours) careful freeze drying of the specimens without demoulding, and resin impregnation allowed the spatial arrangement of the hydrating cement grains to be preserved. These specimens would have collapsed to a powder on demoulding, necessary for methanol drying.

Small pieces of the cement blocks were fractured off using a hammer; these were mounted on aluminium stubs using colloidal silver ('silverdag') and sputter coated with gold for examination in the SEM. By using 'silverdag' as an adhesive, painting copious amounts of 'silverdag' around the cement-stub junction and selecting thin slices of cement, charging of the fracture surfaces in the SEM was minimised. This was still, occasionally, a problem in very young pastes, where a fairly thick coating of gold was sometimes necessary.

The very young cement specimens collapsed to a powder on demoulding or impact. In these cases the SEM stubs were coated with a thin layer of 'silverdag' and immediately placed in the powder. Excess powder was blown off the stubs with an aerosol, when the 'silverdag' was dry.

The remainders of the cement specimens were vacuum impregnated with epoxy resin (Araldite AY18, HY18 system). Penetration of the cement samples younger than 1 day was very good, deteriorating for older samples such that in specimens older than 1 week only a thin surface layer was impregnated.

Several 1mm slices were cut from each impregnated cement block using a diamond slitting wheel with a non aqueous lubricant (to prevent further hydration).

These slices were polished on one side using graded diamond pastes. The polishing sequence involved lapping the slices for about ½ hour on a copper wheel with 14 μm paste and subsequently polishing for about 3 hours each with 6 μm, 3 μm, 1 μm and 1/4 μm pastes using pelon coated wheels. Between each grade the specimens were cleaned in methanol using an ultrasonic bath. Part of the polished slice was then mounted on an SEM stub and coated with carbon for examination using backscattered electrons in the SEM. The remaining slices were glued, polished side down, on a glass microscope slide, using 'durofix' adhesive, and ground down on the 14 μm wheel until they were optically translucent in places (~100 μm thick). These thin sections were then polished for a short time using 6 μm, 3 μm and 1 μm pastes to give sections about 40 μm thick.

Discs, 3mm in diameter, were cut from the thin sections, whilst they were still mounted on a glass slide using an ultrasonic drill and a carborundum/oil mixture. The discs were then floated off the glass slide in acetone and placed on the specimen stage of a Gatan dual ion beam miller. In this ion beam mill the specimen just rests on the stage and does not need to be clamped between two plates as in most other models. Consequently there is less risk of breaking the fragile cement disc. The cement discs were thinned by argon beams at an angle of 7°. Although this low angle makes thinning slow, a fairly large electron transparent area can be achieved. The thinned discs were then coated with carbon and examined in a JEOL 100CX TEMSCAN, transmission/scanning transmission electron microscope. In many cases the thinned cement was so fragile that it had to be supported on a copper grid in the microscope stage which effectively precluded using EDXA to determine the

chemical composition of regions. Generally STEM was used in preference to TEM to avoid beam damage to the microstructure.

Specimens examined in the wet cell were prepared as described for alite (Chapter 4A.II.1).

So far, it has only been possible to examine the BT cement using the full range of electron optical techniques. All ion beam thinned foils and BEIs of polished surfaces in the subsequent section relate to this cement. Most of the micrographs of fracture surfaces are of D44 pastes; any qualitative differences between these and the other pastes studied by fractography are described in the text.

5C.II Microstructure of unhydrated cement and clinker

Plate 5.1 shows a BEI of a flat polished clinker nodule (Blue Circle Northfleet). Light grey grains of alite and rounded grains of belite (dark grey) can be seen in a fine matrix of C_4AF (light) and C_3A (grey). Fine porosity (black) can be seen in the interstitial phase and coarser porosity ($\sim$100 μm) could be seen throughout the nodule. Several alite grains contain small belite particles. This small area of clinker closely resembles the ideal clinker microstructure described in Chapter 2 (Fig 2.5), but an extensive, non selective study of this clinker was not made. Many cracks can be seen running through the clinker. These run straight through the different phase and not along the grain boundaries, suggesting that the grains formed on grinding would tend to be polymineralic.

Plate 5.2 shows a BEI of a clinker, ground without gypsum in the laboratory, which has been dispersed in epoxy resin and polished. Most of the grains visible contain more than one phase.

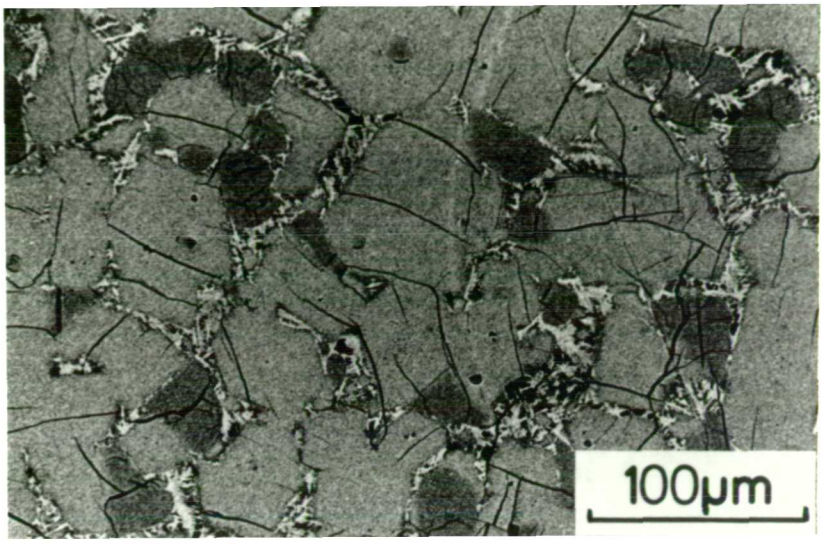

Plate 5.1 Example of the microstructure of unground clinker, BEI in SEM

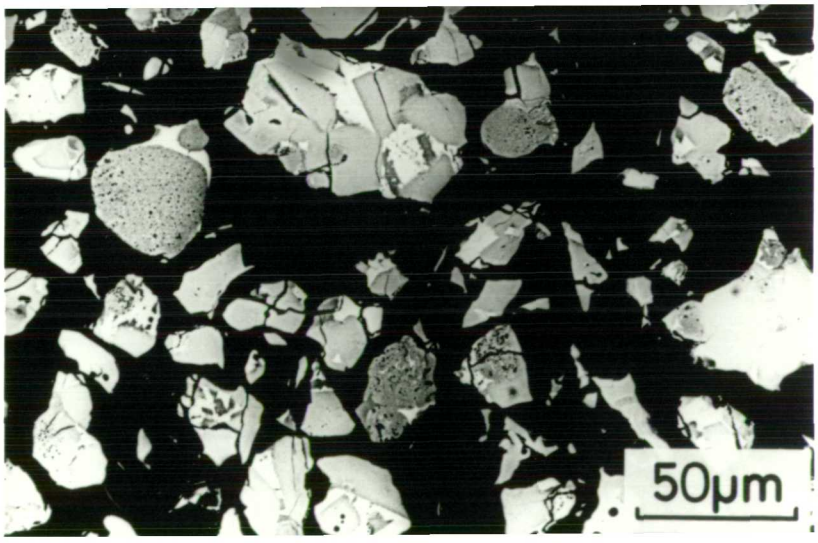

Plate 5.2 BEI of ground clinker dispersed in resin and polished, showing the polymineralic nature of the grains

Plate 5.3 shows an SEM of unhydrated commercial cement (D44) dispersed on silverdag. The wide range of particle sizes can be seen. The grains have sharp edges and smooth faces containing the occasional dent; many of the smaller particles have agglomerated on the surface of the larger particles. Many small lath like particles of calcium sulphate ($\sim$2 μm by $^1/_4$ μm) can be seen on the particle surfaces. The micrograph shown in plate 5.4 is of a cement which has been mixed with water, cast and frozen immediately, then resin impregnated, cut and polished. The distribution of cement grains in a freshly mixed cement paste can be seen. The percentage area occupied by cement was calculated as 42% using an image analyser, which is close to the theoretical level of 40% for a w/c ratio of 0.5 and an average cement density of 3.2 g/cm^3.

5C.III Microstructural development during the first 3 hours of hydration

After hydration for one hour the fracture surface of the cement is covered with small hexagonal rods of AFt (plate 5.5). These are similar in morphology to the ettringite seen during the hydration of C_3A plus hemihydrate (plate 4C.5), indicating that the concentration of $(SO_4)^{2-}$ in solution is high.

In the wet cell after 3 hours hydration (plate 5.6) these rods can be seen dispersed on the carbon support film at some distance from the surface of the hydrating grain, as was also observed during the hydration of C_3A and C_4AF (4C.II.2 and 4D.II.2), suggesting formation by a through solution mechanism. During the drying process any rods in the water filled pore space will fall back onto the surface of the cement grains. It is probable that an amorphous layer associated with the hydration of C_3A (plate 4C.3(a)) and early hydration products from C_3S is present in the 'wet' state,

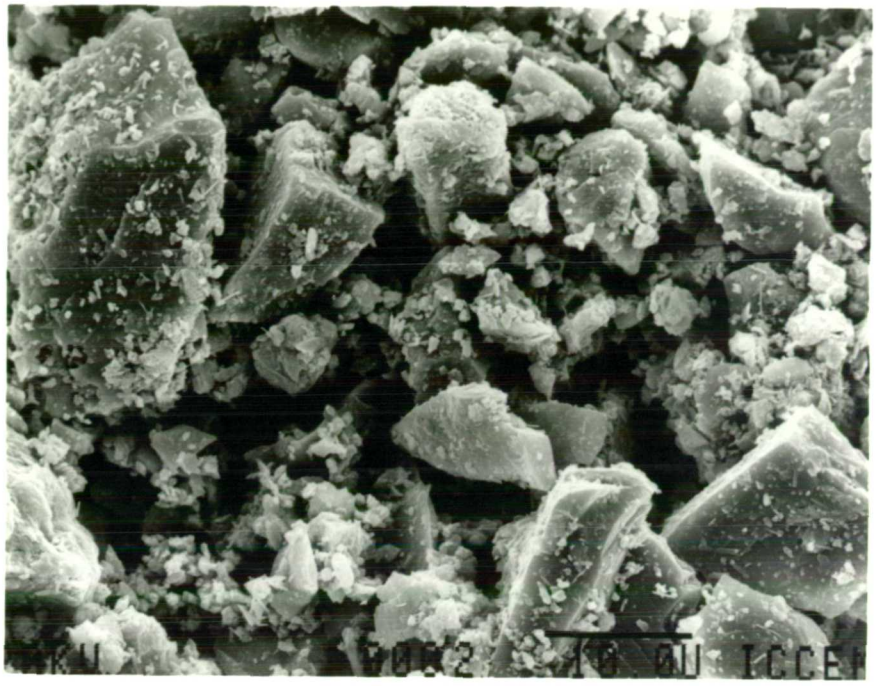

Plate 5.3 Unhydrated cement (D44) in the SEM

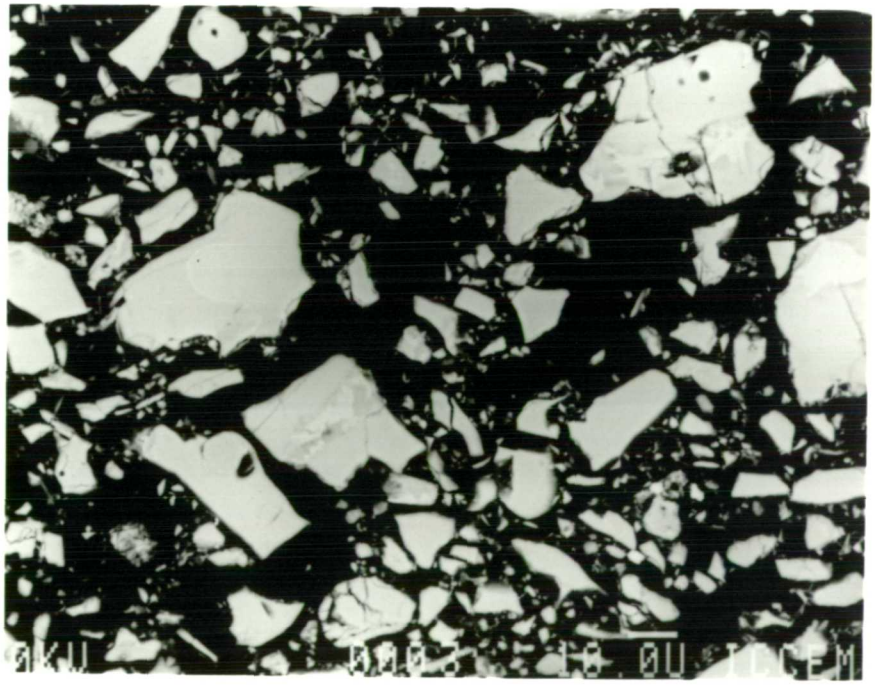

Plate 5.4 BEI of cement paste freeze dried immediately after mixing, resin impregnated and polished

although none was observed clearly in the limited environmental cell work done on cement.

An ion thinned section of a 2 hour old cement paste (plate 5.7) shows AFt rods embedded in an amorphous looking product which could be amorphous aluminium hydroxide or C-S-H. This micrograph also shows that the AFt and gel layer have formed a layer slightly separated from the cement surface. This gap has not been impregnated with resin, indicating that it is fairly isolated from the outer porosity. In the wet state this 'gap' is probably filled with highly concentrated solution or a colloidal product, such as amorphous aluminium hydroxide, which contracts onto the grain surface or hydrate layer on drying.

The density of AFt rods varies widely from region to region and from grain to grain. The denser areas probably correspond to regions of underlying C_3A and the less dense ones to underlying C_3S, although this simplistic view does not take into account the presence of rods in the pore fluid which will fall back on drying in a more random manner.

Variations in the early microstructure between different cements were generally less than variations between different areas in any one cement. However, there does appear to be some difference in the size and aspect ratio of the AFt rods; those seen in pastes of D44 shown here (plate 5.5) are shorter ($\sim$.2 μm) than those seen in other cements ($\sim$.5 μm). This difference could be due to more hemihydrate being present in the cement due to dehydration of the gypsum during grinding.

Crystals of gypsum (such as in the left corner of plate 5.5) could be seen in all the cement pastes, although more were observed in the D44 paste. This supports the supposition that this cement contains a high proportion of hemihydrate which rehydrates to gypsum on the addition of water.

Plate 5.5 Dried fracture surface of cement (D44) hydrated for 1 hour

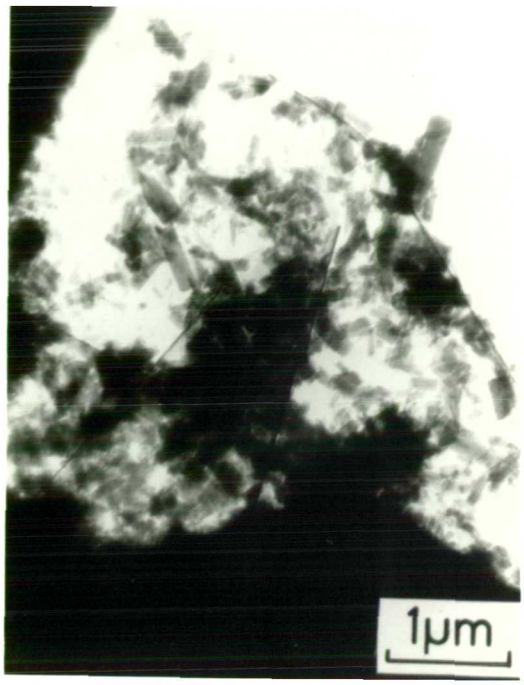

Plate 5.6 'Wet' cement paste (BT) in the HVEM after 3 hours hydration

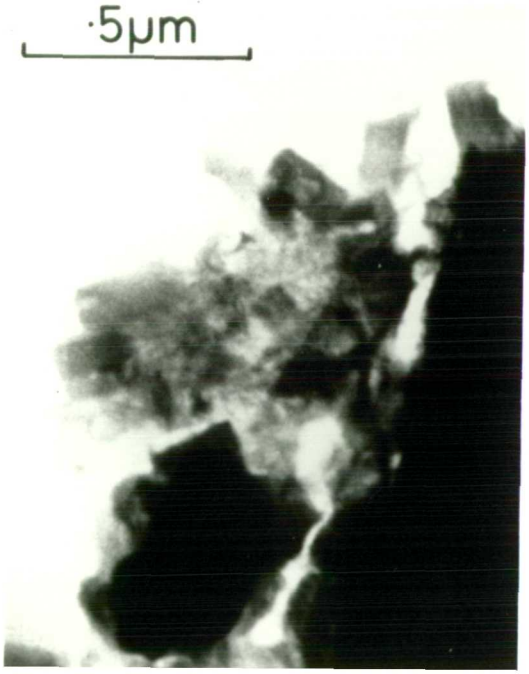

Plate 5.7 STEM of ion-thinned 2 hours old cement paste (BT)

Plate 5.8 Dried fracture surface of 3 hours old cement (D44)

After 3 hours hydration spikey clusters of C-S-H can be seen on fracture surfaces (plate 5.8) amongst the AFt rods. From the environmental cell work on alite (4A.II.2) it is likely that these spikes were foils in the 'wet' state which have crumpled up on drying.

5C.IV Microstructural development from 3 hours to 24 hours

The growth of C-S-H on the outer hydration surface during the acceleratory period can be seen on fracture surfaces (plate 5.9). After 6 hours (plate 5.9(a)) the fibrillar clumps of C-S-H have grown in size and number to cover the AFt rods formed during the first hour of hydration. The C-S-H often appears as sea anemone like rosettes (e.g. top centre plate 5.9(a)), which probably result from the hydration of small (<1 μm) cement particles which were originally agglomerated on the surface of the larger cement grains (cf plate 5.3). (To prevent charging a layer of gold must be evaporated onto the surface; this produces the fine stippled effect).

The C-S-H continues to grow, drying to a fibrillar morphology, (Diamond Type I) where there is plenty of space (plate 5.9(b)), and in a honeycomb morphology (Diamond Type II), where space is more restricted (plate 5.9(c)). In the 'wet' state the C-S-H would have a filmy, foil like morphology.

After 24 hours (plate 5.9(c)) a regrowth of long hexagonal AFt rods has taken place. This probably occurs as the calcium hydroxide concentration falls (due to the precipitation of CH associated with the hydration of C_3S), which allows more gypsum to dissolve. This renewed formation of AFt occured in all the cements studied, although slight variations were seen in the time at which this second growth occured and the rate of growth of the

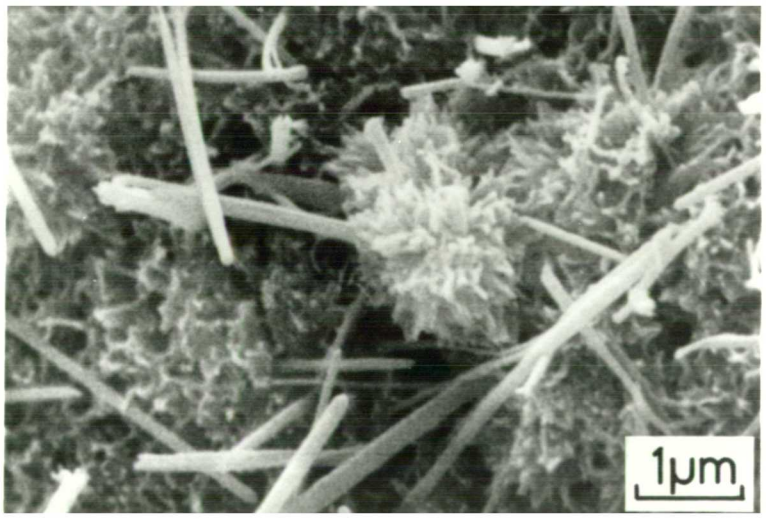

Plate 5.9 Development of microstructure on the surface of cement grains. Fracture surfaces in the SEM

(a) 6 hours (D44)
(b) 10 hours (NBS64)
(c) 24 hours (D44)

AFt rods. Notably in cement NBS 64, this secondary formation of AFt was later (~ 18 hours) than in the other cements and the rods formed were shorter, only just protruding from the C-S-H layer. In the other cements examined in the SEM, regrowth occured after about 13 hours and the rods were several microns long after one day.

During this period calcium hydroxide (CH) is precipitated in the pore space as well defined plate like hexagonal crystals. The crystal facets are cleanly exposed on fracture surfaces, although they appear to have engulfed some regions of C-S-H. There seems to be little or no tendency for calcium hydroxide to nucleate in close proximity to the C-S-H.

When the microstructure is observed in cross-section, as in ion beam thinned cement pastes, the thickening of the hydrated layer over this period can be seen. Plates 5.10(a) and 5.10(b) show ion beam thinned sections of pastes hydrated for 5 hours and 12 hours respectively. It is also apparent that the hydrated layer is detached from the underlying anhydrous grain; in some cases the original grain has completely reacted after 12 hours, leaving a hollow rim of hydration products. Of grains with a remnant core, the smaller grains have dissolved unevenly leaving a gap of variable thickness, whilst this gap is more uniform for the larger grains. As mentioned previously, this gap is probably filled with a concentrated solution or colloidal amorphous product with a high water content before drying, indeed in some areas dried product can be seen in this gap. Similar features have been observed in the environmental cell, indicating that the separated shells are not purely an artifact of drying. Plate 5.10(c) shows a 24 hour old cement paste in the environmental cell; this is not a sliced, cross section but an area where the grains are sufficiently well separated

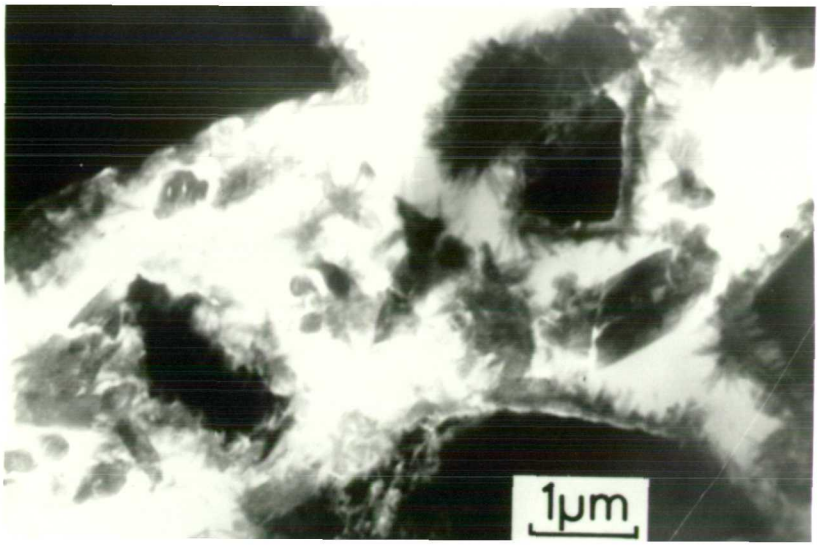

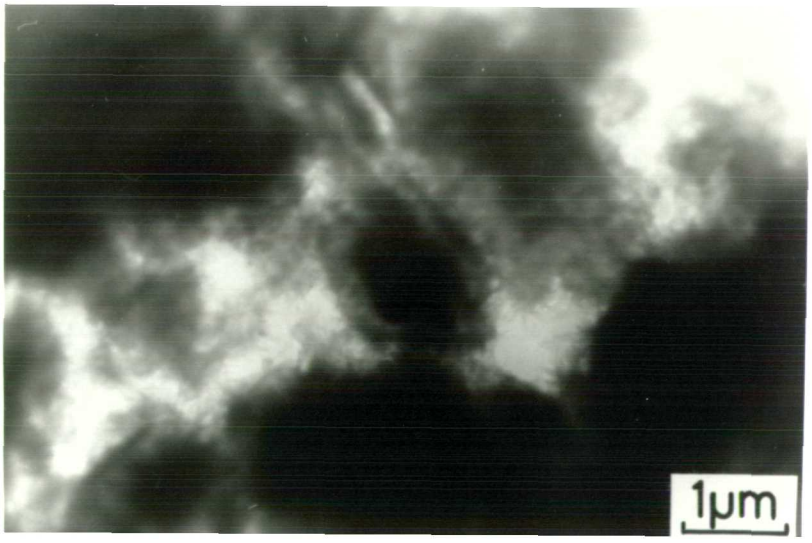

Plate 5.10 Development of separated hydration shells in cement hydration

(a) ion-thinned 5hr paste (BT). STEM
(b) ion-thinned 12hr paste (BT). STEM
(c) 'wet' 24hr paste (BT). HVEM

for electrons to be transmitted. The small grain in the centre has a thick, dark central region corresponding to the anhydrous core surrounded by a less dense region and then a darker 'shell'.

Backscattered electron images (BEI) of polished cement surfaces show the spatial distribution of the hydration products over an extensive area. Electrons are backscattered more strongly from regions of high atomic number (which appear brighter), than regions of low atomic number (which appear darker). Hence, in BEI micrographs the anhydrous cement grains appear bright, areas of calcium hydroxide slightly darker, other hydration products darker still and porosity black. Plate 5.11(a) shows a BEI of the polished surface of an 18 hour old cement paste. It can be seen that large areas of massive calcium hydroxide have formed, engulfing some of the smaller cement grains. Close examination of this polished surface revealed that the vast majority (>90%) of the cement grains have separated hydration shells. Plate 5.11(b) shows an inverse BEI of the same surface, at higher magnification. This inverse image is analogous to an STEM of an ion-beam thinned foil (plate 5.10). In transmission the degree of electron absorption is proportional to the atomic number and thickness of the specimen, thus contrast is the inverse of that produced by electrons back-scattered from a surface. Whilst of lower resolution than in STEM, the filmy spikey nature of the C-S-H in the hydrated shells can be seen. Around some grains the separation of the hydrated shell from the anhydrous core is fairly uniform (e.g. grains to lower right and upper right of centre plate 5.11(b)), these proved to be alite grains by EDXA. In the large uneven shell in the centre the small rounded anhydrous particles are belite, probably originally included in alite which has hydrated. The large dark area just to the left of centre associated with the large uneven shell had a high iron

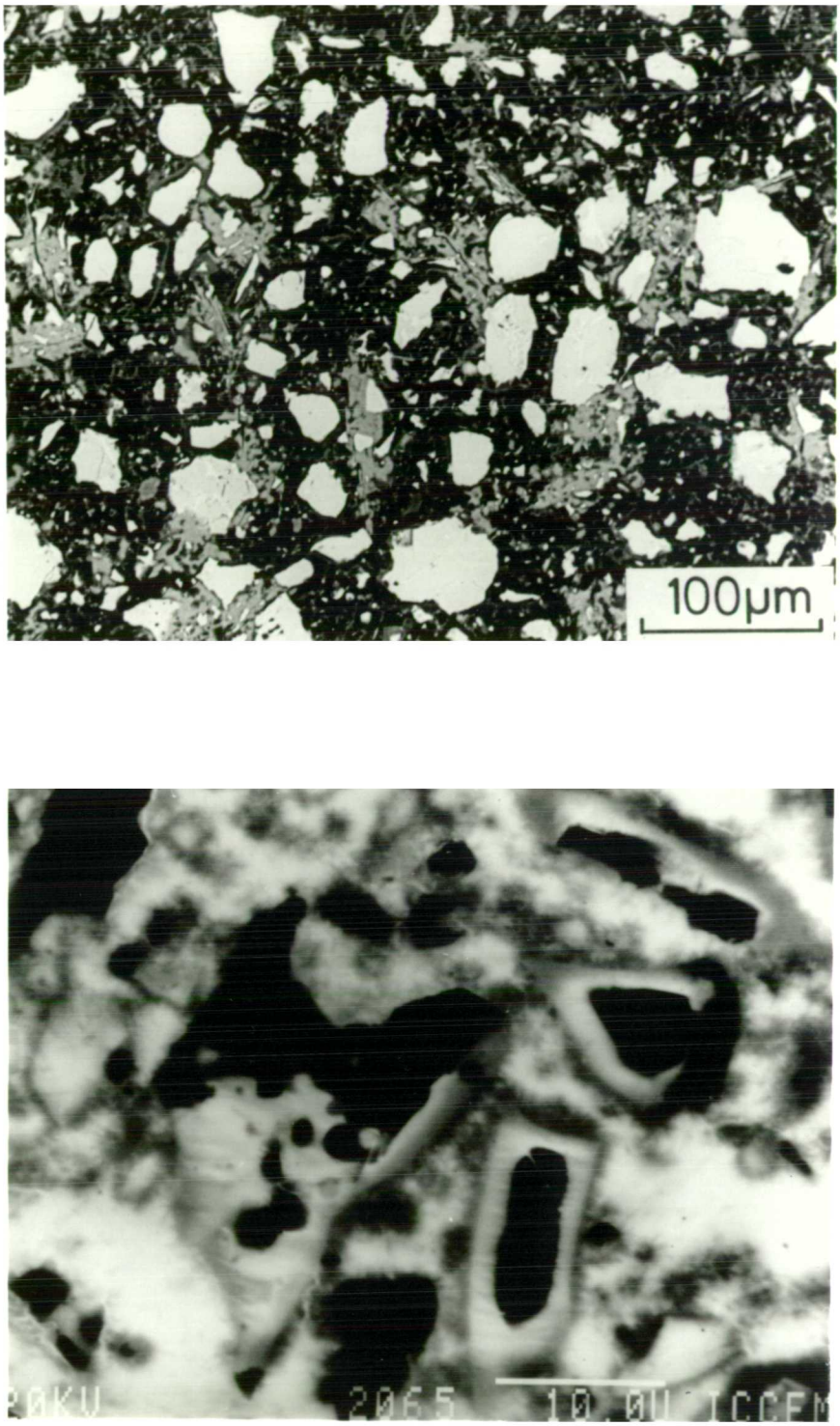

Plate 5.11 BEIs of 18hr resin impregnated and polished cement paste (BT)

(a) low magnification, showing anhydrous grains light, calcium hydroxide light grey, hydration products darker grey and porosity black

(b) high magnification, negative image, showing hydration shells around cement grains

content as did the dark area on the right edge of the small grain to the upper right of centre. Most anhydrous areas not associated with a separated hydrate shell proved to be high iron regions of the interstitial phase.

As mentioned previously (5A), shells of hydration products were originally noted by Barnes et al (1978a and b, 1979), who referred to them as 'Hadley' grains. Their observations were made on fracture surfaces where anhydrous cores often fall out, leaving hollow shells, and so the term 'Hadley' grain has come to refer to a completely empty shell. The present work illustrates that the separation of the shell from its core is always small (<1 μm) when polished surfaces on ion beam thinned sections are examined, hence the term 'separated shell' will be used in preference to the ill defined term 'Hadley grain'.

Whilst separated shells can be seen in thin sections as early as 5 hours, they are not seen on fracture surfaces much before 18 hours when the bonding between the shells is strong enough.

5C.V Development of microstructure after the first day

From examination of fracture surfaces, the most obvious change in microstructure after the first day is the infilling of the structure by CH (plates 5.12 and 5.13). In many cases the alignment of cleavage steps shows that the same crystallographic orientation extends over large areas, engulfing the hydrating grains; this suggests that crystal growth occurs from only a few nuclei. These massive formations of calcium hydroxide can also be seen as light grey regions in BEIs (plate 5.14).

As the outer hydration products interlock more unhydrated cores with separated shells are exposed on fracture surfaces. Generally

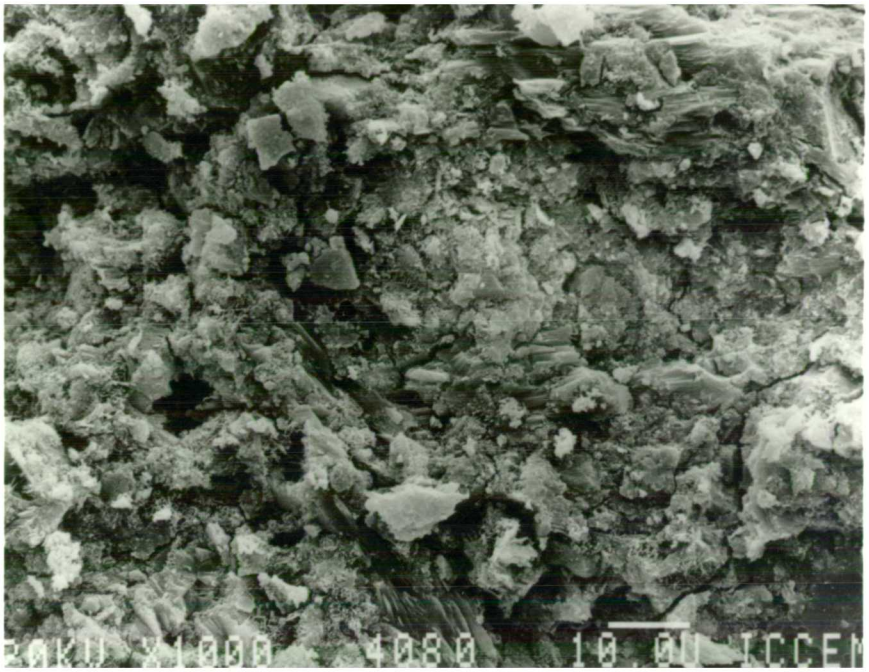

Plate 5.12 Fracture surface of cement hydrated for 1 week (D44)

Plate 5.13 Fracture surface of cement hydrated for 69 days (D44)

the thickness of the hydrated shells increases with age. In more porous regions the C-S-H has a spikey morphology (Diamond Type I), adopting other denser morphologies in more enclosed regions.

Examination of fracture surfaces, however, becomes very selective in this period; large areas reveal little information and areas of interest may not be typical of the bulk. For this reason the overall development of microstructure on a 10-. 1,000 μm level can be studied better by BEIs of polished surfaces.

BEIs of polished cement pastes after 7 days, 30 days and 69 days are shown in Fig 5.14. Even at this low magnification, differences between the areas covered by adjacent micrographs may still be significant. For the quantitative work described subsequently (5C.VIII)much larger areas were considered, than shown here.

After 7 days hydration most grains originally less than 15 μm in size have fully reacted. A large proportion of the anhydrous grains seen on polished surfaces are belite, partly due to its low reactivity and partly to its low grindability which means that a large proportion of the large grains are belite. Where grains have reacted unevenly it is found that the regions apparently unreacted have a microstructure similar to that of the interstitial phase and have a very high iron content.

Massive areas of calcium hydroxide can be seen extending over tens of microns, engulfing smaller grains. These small grains have not reacted to the same extent as similar grains in CH free areas, suggesting that CH restricts the diffusion of water to, and calcium and silicate ions away from, the hydrating grain.

Qualitatively little change in the microstructure can be observed between 7 and 69 days, although quantitative image analysis (5C.VIII) shows that hydration is continuing.

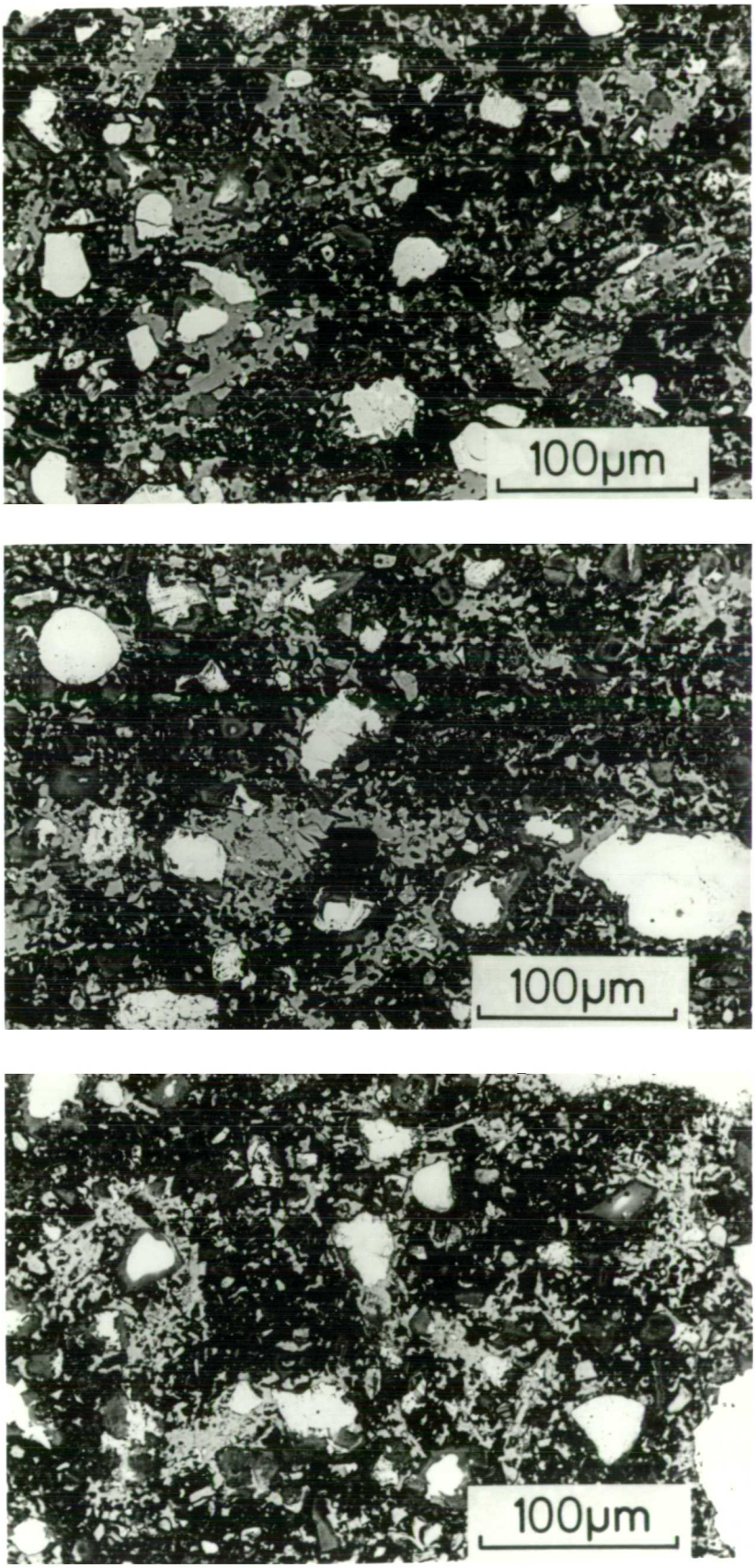

Plate 5.14 BEIs of polished cement surfaces after hydration for

(a) 7 days
(b) 30 days
(c) 69 days

5C.V.I Changes in the morphology of C-S-H

Plate 5.15(a) shows an STEM of a 12 hour paste which has been ion beam thinned. On the outside of the shell there is a layer of C-S-H about a micron thick. At the outer edge of this layer the C-S-H has a fibrillar morphology (partially attributable to drying), whilst beneath this layer the C-S-H gel appears fairly homogeneous. On the inside of the shell more amorphous gel is starting to form in the space between the shell and the anhydrous core.

In an ion-thinned 2 month old paste the microstructure appears as shown in plate 5.15(b). The original 'shell' boundary can be seen running vertically about $^{1}/3$ of the way from the left hand edge of the micrograph. Outside this boundary a layer of C-S-H about 1 micron thick can be seen similar to that in plate 5.15(a). However, after 2 months, the C-S-H gel has a pronounced directionality to it similar to the fibrillar morphology seen in more open regions, but much denser. Inside the shell a fairly homogeneous amorphous gel can be seen. The stippled contrast ($\sim$ 100 Å) that can be seen may be related to colloidal particles in the gel, but could equally well be an artifact of drying and ion beam thinning; any amorphous material gives a random stippled contrast in transmission electron microscopy which is not necessarily related to the presence of discrete particles or microcrystalline regions (e.g. Weaire, 1969).

On the fracture surface of a 2 month paste the pronounced fibrillar morphology of the C-S-H in the open pore space can be seen (e.g. to the upper left of centre in plate 5.15(c)). Hexagonal rods of AFt can also be seen in this region. The region to the right in plate 5.15(c) is the inside of a separated shell, on this inner surface the C-S-H has a dimpled appearance (Diamond Type IV); the dimpling being about 10 times coarser than that seen in the ion thinned section (plate 5.15(b)). The gel drying at the

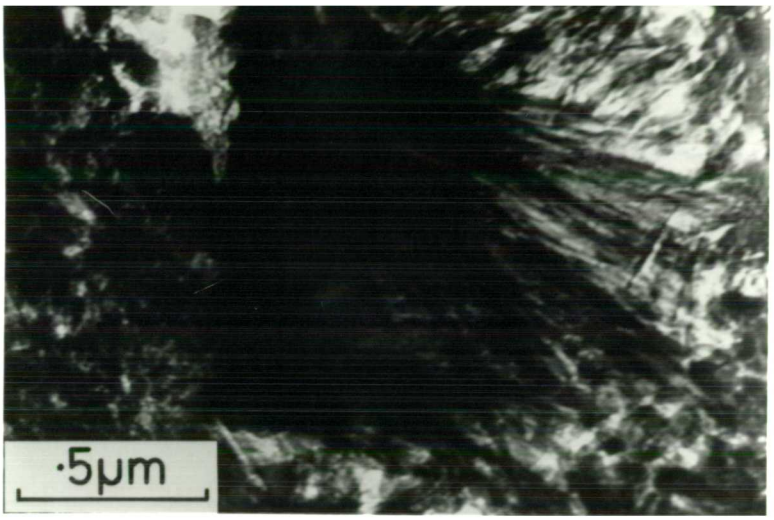

Plate 5.15 Ageing of outer C-S-H product,

(a) ion-thinned 12hr paste (BT), STEM
(b) ion-thinned 2mnth paste (BT), TEM
(c) fracture surface of 2mnth paste, SEM

edge of this inner product is less constrained than that within the layer; this probably causes the difference in scale of the dimpling or stippling seen. Through the thickness of the shell the product appears dense and homogeneous and the original shell boundary cannot be distinguished. It can be seen from plate 5.15(b), however, that differences between the inner and outer product are only present at the 100 Å level and will not be distinguishable on fracture surfaces.

5C.V.2 Hydration of individual cement grains

Plates 5.16 and 5.17 show individual cement grains in detail at various stages of hydration to illustrate some of the features of hydration at the 0.1 to 10 μm level. Many variations can be seen between cement grains, but these can be related to the microstructure of the original grains. The phases referred to in this section were identified by typical morphology, or in the case of polished surfaces, by EDXA.

As stated earlier almost all the grains form a separated hydrate shell; plate 5.16 shows how some of these shells are revealed on fracture surfaces. Plate 5.16(a) shows a separated shell in a 13 hour paste, earlier than when these shells are generally seen on fracture surfaces. The original grain was only about 4 μm in diameter and has completely hydrated except for a small rounded particle of belite that can be seen right at the top of the shell. A similar rounded particle of belite can be seen on the shell fragment in plate 5.16(b), from a one day old paste. These particles of belite were probably originally surrounded by alite as can be seen in clinker microstructures (plate 5.1 and Fig 2.5). On the inner surface of this shell rods of AFt and a few plates of AFm can be seen indicating that the original grain also contained

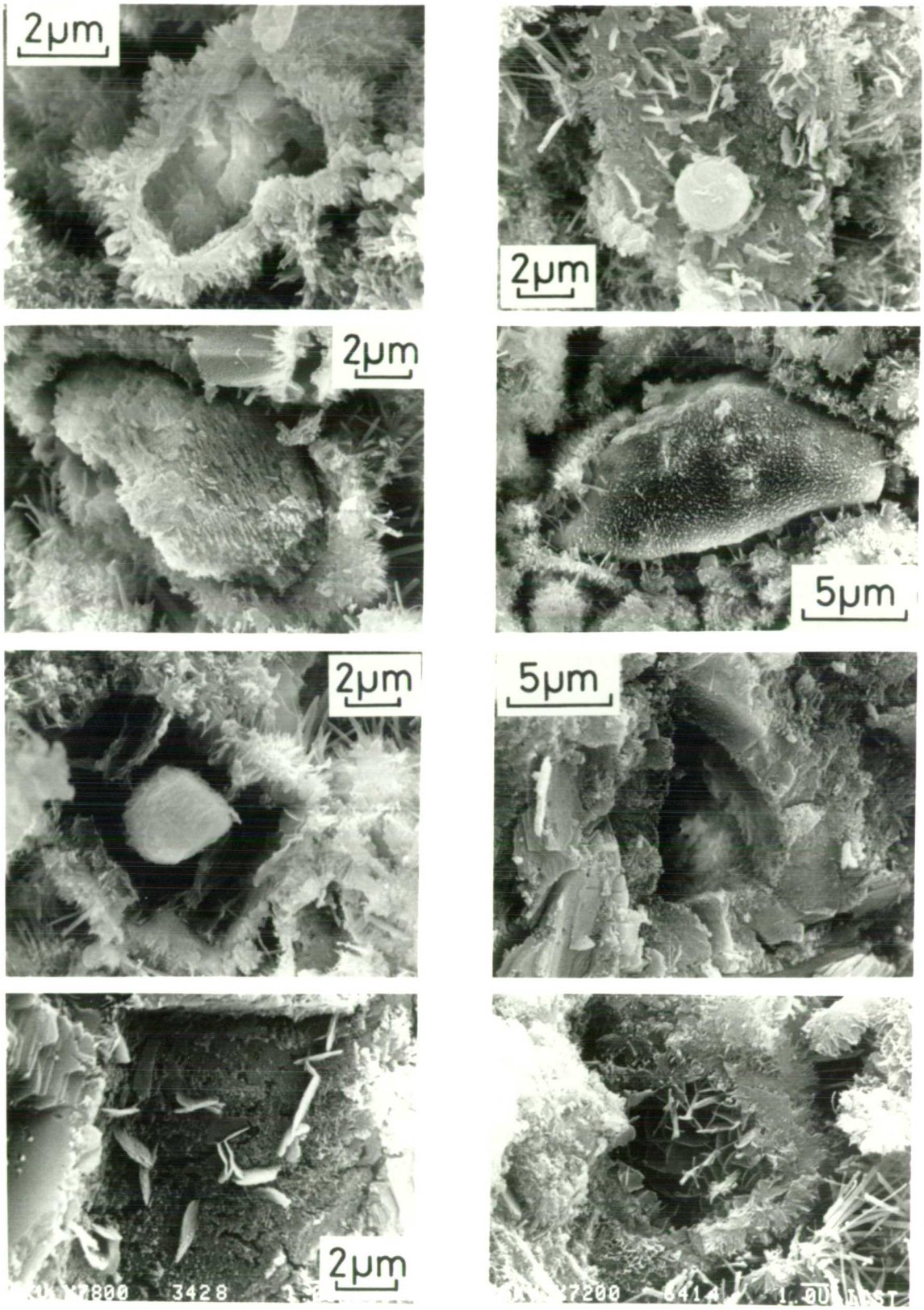

Plate 5.16 Individual cement grains at various stages of hydration,

(a) 13 hours(D44),SEM
(b) 1 day(D44),SEM
(c) 1 day(NBS34),SEM
(d) 1 day(NBS62),SEM
(e) 1 day(NBS34),SEM
(f) 7 days(NBS34),SEM
(g) 7 days(NBS34)
(h) 7 days(NBS64),SEM

some C_3A. Outside the shell only AFt and C-S-H can be seen, in fact AFm was never observed outside the hydrated shells in any of the OPCs studied. This suggests that the environment inside the shell is isolated from the outside by the hydrates. Inside the shell calcium sulphate in solution is quickly consumed in the formation of AFt. This AFt can then react with more C_3A or ferrite phase to give AFm.

Plates 5.16(c) and (d) show separated shells with alite cores after 1 day's hdyration. The grain in 5.16(c), which appears monomineralic, is only slightly separated from its hydrate shell; whilst the shell and anhydrous core in 5.16(d) are separated by about 1 μm, in which space AFt rods and AFm plates can be seen. In plate 5.16(e) the separation between alite core and shell is over two microns but another remnant structure can be seen in this space; this structure is also seen in plate 5.17(a) and will be discussed subsequently. The alite cores in plates 5.16(c), (d) and (e) all have etched surfaces indicating uneven dissolution of the grain, with deposition of product on the inner surface of the hydrated shell. This internal hydration mechanism might be expected to lead to a reduction in the separation of the hydrated shell and its unhydrated core. For the larger grains this appears to be the case, but smaller grains may hydrate completely leaving small hollow shells. Hollow shells are not observed greater than 5 μm in size, but these are still seen even in 3 year old cement pastes.

Plate 5.16(f) shows a shell in a 1 week old paste. The shell is considerably thicker than at one day, and the outer hydrate surface has been engulfed by calcium hydroxide.

Plates 5.16(g) and (h) show AFm plates on the inner surface of hydrate shells; the density of AFm plates seen on these inner surfaces varies widely. This variation is probably related to the amount of

C_3A in the original grain, i.e. the original grain which has hydrated in plate 5.16(g) was mostly alite with a small amount of C_3A, whilst that which has hydrated in plate 5.16(h) was mostly C_3A. In plate 5.16(h) a dense mass of AFt rods can be seen outside the shell, whilst inside the shell there are mostly AFm plates with only a few AFt rods.

Plate 5.17(a) shows a complex hydrated grain. A small remnant core, which is probably mostly belite,remains at the left hand edge of the shell. The shell itself is thin and broken in places, but can be distinguished. On the inside of the shell typical AFm plates can be seen with smooth surfaces. The structure in the centre of the grain is covered with fine, amorphous looking particles. The shape of this structure, as with that in plate 5.16(e), is very like that of the ferrite phase seen in clinker microstructures. This is probably an amorphous hydrous ferric oxide relict formed on hydration of a region of interstitial phase, the C_3A having hydrated from amongst the finely divided ferrite phase. A similar feature can be seen in plate 5.17(b), which is a BEI of a flat polished surface of a 1 week old paste. The bright, fine dendritic phase has a high iron content and is probably a relict of the ferrite phase. This relict is fairly porous where areas of C_3A have hydrated, other regions of C_3A remain amongst the iron rich regions. It is unlikely that the ferrite phase has completely hydrated to leave just hydrous iron oxide (FH), the formation of this amorphous product on the surface will probably inhibit further hydration of the ferrite phase and included C_3A. It is impossible to deduce the extent to which the ferrite phase has reacted as the beam spread for energy dispersive X-ray analysis on this sample is at least 2 or 3 μm, which is much more than the thickness of most of the iron rich regions. Relicts of the ferrite phase are not peculiar to any one cement, plates 5.17(a) and (b) come from different cements and similar features have been seen in several others.

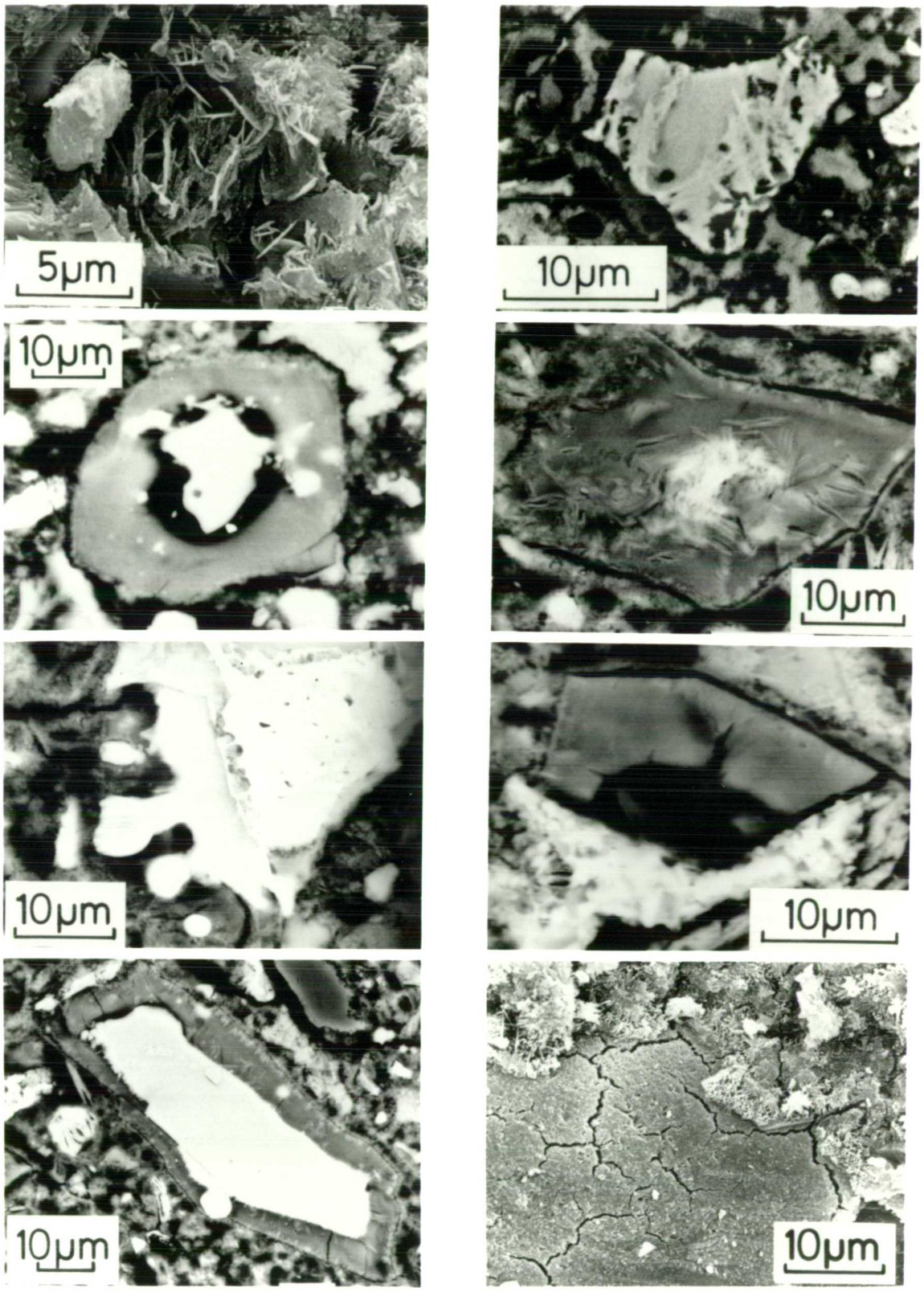

Plate 5.17 Individual cement grains at various stages of hydration,

(a) 7 days(NBS34),SEM
(b) 7 days(BT),BEI
(c) 7 days(BT),BEI
(d) 60 days(BT),BEI
(e) 60 days(BT),BEI
(f) 60 days(BT),BEI
(g) 60 days(BT),BEI
(h) 28 days(NBS_{64}),SEM

Plate 5.17(c) shows the flat polished surface of a 1 week old paste; here the shell thickness is about 8 μm. The hydrate shell has a fairly homogeneous appearance, but the outer edge has a spikey appearance, similar to the outer C-S-H morphology seen in fracture surfaces. After 60 days hydration the grain shown in plate 5.17(d) has almost completely reacted. The inhomogeneities seen in the hydrate layer are probably AFm plates, edge on, which have been engulfed by the C-S-H. A thin boundary between the inner hydrate layer and the outer, spikey, hydrate can be seen; this is probably accentuated by drying, but is frequently observed.

It should be pointed out that the cross-section exposed on flat polished surfaces does not always run through the centre of the grain; for example plate 5.17(d) may be a slice off the bottom of a grain and a section higher up would have shown a larger remnant core. This sectioning effect is particularly evident in the areas surrounding the central grain in each of these backscattered electron micrographs; the uneven distribution of hydration products results from sectioning through many small grains.

Plate 5.17(e) shows an anhydrous grain where the alite (on the left) has substantially hydrated leaving rounded belite grains comparatively unreacted. The original grain which has hydrated in plate 5.17(f) was probably polymineralic. The top part (originally alite) has completely hydrated, leaving a thick hydrate shell; the bottom half (originally interstitial phase) appears virtually unreacted although the extent to which amorphous FH has formed is unknown.

Plate 5.17(g) shows a large alite grain in 60 day old paste surrounded by a hydrate layer about 6-8 μm thick. At this age there is no longer a gap between the anhydrous core and much of the hydrated layer. Enough hydration has occured so that the extra volume of the C-S-H, over that of the alite from which it formed, has filled in the

original space between the shell and the anhydrous core. AFm plates as observed in plate 5.17(d) and unreacted belite grains can also be seen in the hydrated layer. The boundary between inner and outer hydrates can be seen clearly. The appearance of fracture surfaces, such as that of a 28 day old paste shown in plate 5.17(h), probably results from fracture along this boundary. In the upper part of plate 5.17(h) spikey outer C-S-H can be seen, in the lower part the inner hydrate has been exposed. The cracks visible can be attributed to drying shrinkage of the C-S-H gel.

The range of microstructures described in this section can all be explained by the hydration mechanism described in the next chapter (6).

5C.VI Effect of water/cement ratio on the development of microstructure

The effect of water/cement ratio on the development of microstructure was studied on one cement (D44). At early ages (<7 hours) no differences were observed. At later ages the infilling of the microstructure occured earlier at the lower w/c ratio.

Plate 5.18 shows the microstructures of a paste with w/c = 0.5 (plate 5.18(a)) and one with w/c = 0.3 (plate 5.18(b)) both after 18 hours' hydration. At w/c = 0.5 fracture around the outer hydrate layer and through the water filled space, still predominates at this age (plate 5.18(a)). At w/c = 0.3, the cement grains are originally more densely packed, so more bonding between the hydrated shells has occured, and a higher proportion of the water filled space has been filled with calcium hydroxide, after 18 hours' hydration. Consequently, the fracture path runs through the hydrate shells and more separated hydrate shells can be seen on the fracture surface (plate 5.18(b)). In addition, areas of calcium hydroxide cleavage start to predominate on fracture surfaces at earlier ages.

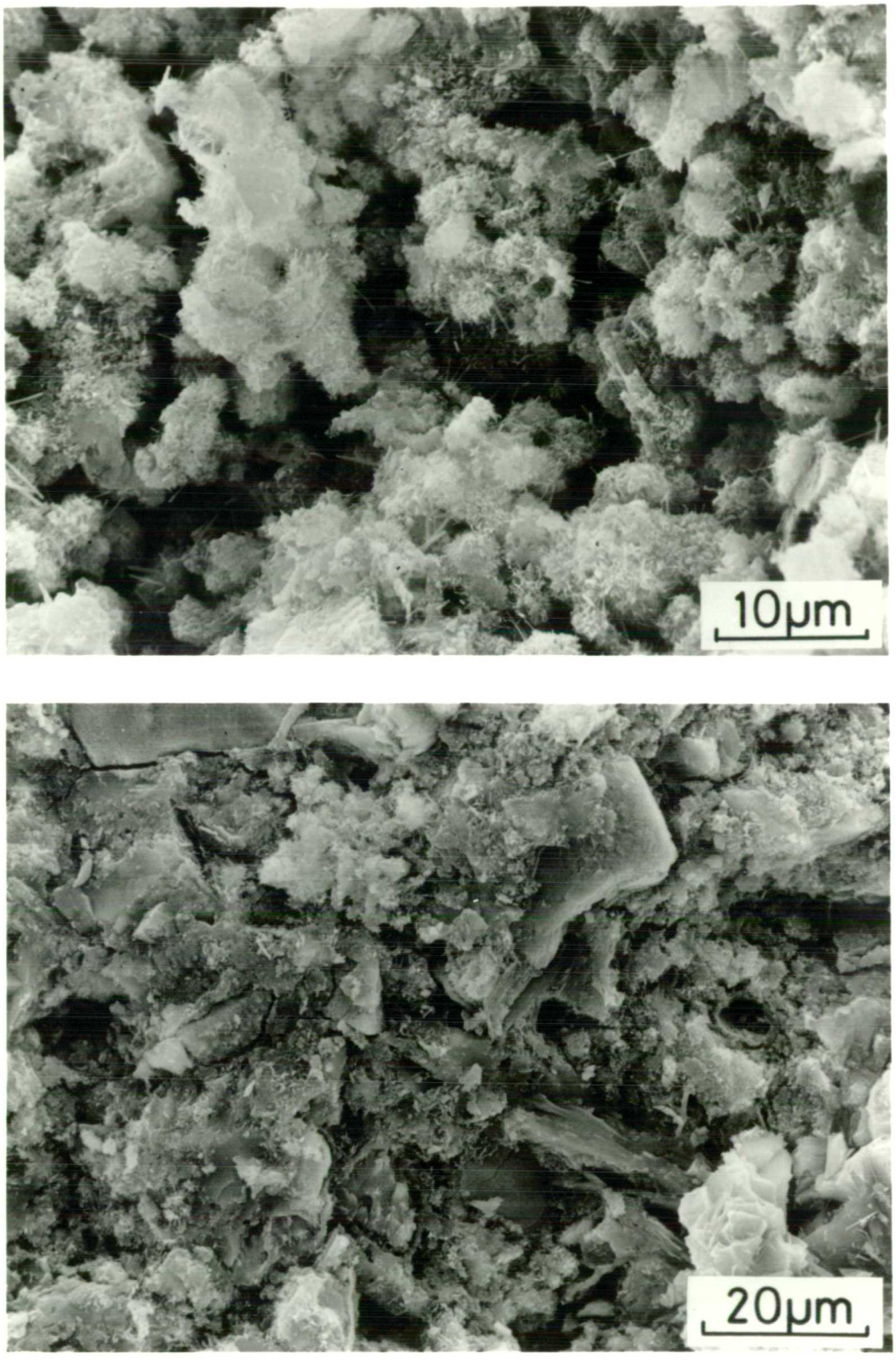

Plate 5.18 Effect of water:cement ratio on early microstructure,

(a) $^{w}/c$ = 0.5 fracture surface of 18hr paste

(b) $^{w}/c$ = 0.3 fracture surface of 18hr paste

As fracture surfaces at later ages are dominated by areas of calcium hydroxide at both water/cement ratios, it is impossible to discern any further differences by this technique. More quantitative differences could be assessed using image analysis on polished surfaces, but this has not been possible in the present work.

It should be noted that separated hydrated shells are observed at w/c = 0.3, similar to those at w/c = 0.5. This indicates that their occurence is not critically dependant on the amount of space available.

5C.VII Development of microstructure in white cement

Plate 5.19 shows fracture surfaces of white cement pastes after various hydration times. For the first 17 hours the microstructure appears qualitatively similar to that of OPC. The secondary growth of AFt starts at about 13 hours; after 17 hours (plate 5.19(a)) there appears to be more AFt present than in OPCs, but this is difficult to assess by examination of fracture surfaces. Separated hydrated shells can also be seen after 17 hours.

Between 17 hours and 1 day a drastic change takes place in the microstructure (plate 5.19(b)), with the appearance of large, thin hexagonal plates in radiating clusters. These plates are about $^1/_4$ μm thick and 10 μm in diameter. Locally, in the region of these clusters, AFt seems to have disappeared. Plenty of AFt rods can be seen in other areas, but these are generally shorter than at 17 hours.

At later ages (plates 5.19(c) and (d)) infilling of the microstructure with calcium hydroxide occurs.

The composition of the thin plates is not known, as satisfactory analysis cannot be made on fracture surfaces. Their morphology resembles that of CH in scale, but the plates are much thinner than in OPCs, and AFm in shape, but the AFm in OPCs is much smaller. The

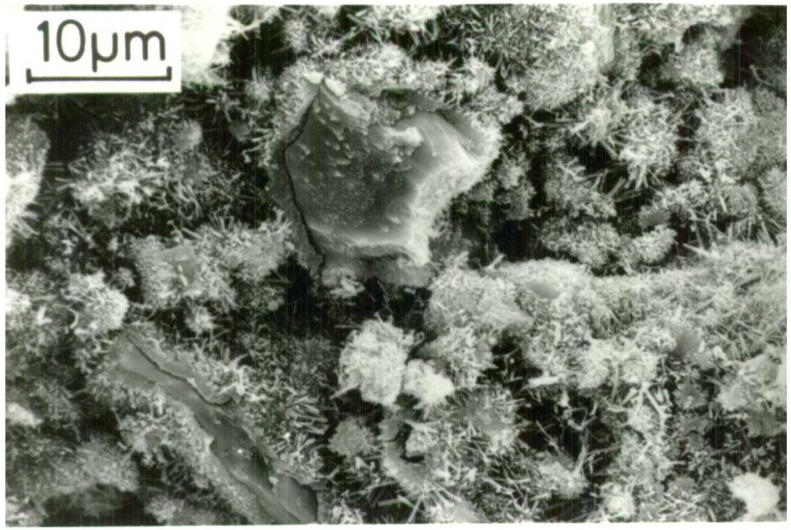

Plate 5.19
Microstructure of white cement. Fracture surfaces at:

(a) 17 hours
(b) 24 hours
(c) 7 days
(d) 69 days

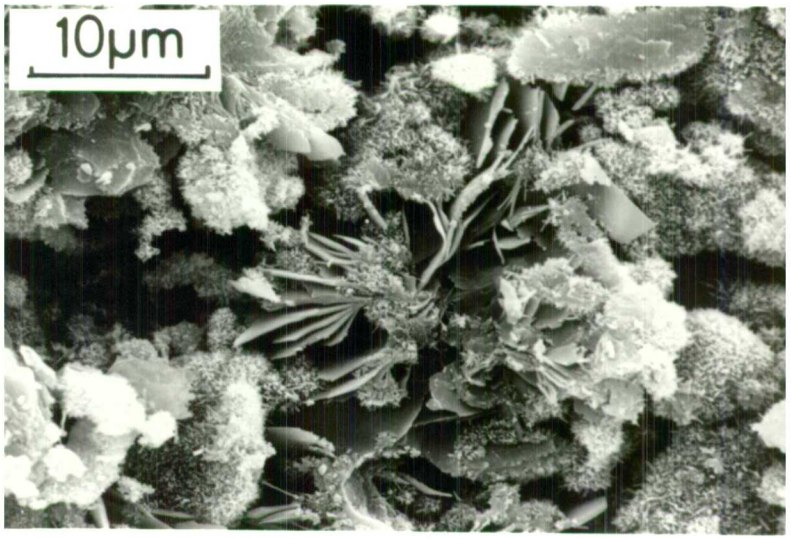

(a) (b)

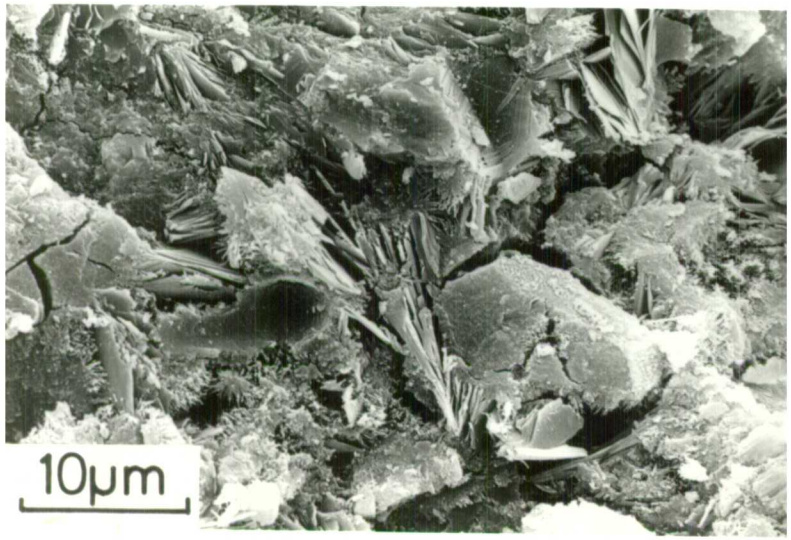

(c) (d)

disappearance of AFt would seem to indicate AFm or a hexagonal calciumaluminate hydrate (i.e. C_4AH_{19}); a solid solution of these two phases might be another possibility. Allowing for differences in the observation technique, these plates appear similar to those formed after 3 days in the C_3S:C_3A:$C\bar{S}\frac{1}{2}H$ mixture (4E.II). This further supports the view that they are AFm plates, although markedly different in morphology to AFm plates seen in the hydration of OPC. More work, using different electron optical techniques, is needed to elucidate the hydration mechanism of white cement.

5C.VIII Quantitative image analysis

There is a large difference in the mean atomic number of the unhydrated cement minerals and those of the reaction products (Table 5C.1). This difference results in good contrast between the unreacted cement grains and their surroundings in backscattered electron images (BEI), so various parameters, such as the total area (and hence volume) of anhydrous material and the size distribution of the grains, can be calculated using an image analyser. The image analyser used in the present work was a Bausch and Lomb, Omnicon 3000.

Table 5C.1 Mean atomic numbers of phases found in hydrated cement

COMPOUND	ABBREVIATED FORMULA	MEAN ATOMIC NUMBER
$3CaO.SiO_2$	C_3S	12.67
$2CaO.SiO_2$	C_2S	12.29
$3CaO.Al_2O_3$	C_3A	12.18
$4CaO.Al_2O_3.Fe_2O_3$	C_4AF	13.22
$Ca(OH)_2$	CH	7.6
$3CaO.Al_2O_3.3CaSO_4.32H_2O$ (ettringite)	$C_3A(C\bar{S})_3 32H$	5.26
$3CaO.Al_2O_3.CaSO_4.12H_2O$ (monosulphate)	$C_3AC\bar{S}12H$	6.08
Calcium silicate hydrate	C-S-H	8.5 (depending on assumed C/S, adsorbed water and micro-porosity)

Results on the degree of hydration determined by BEI of one cement are shown in Fig 5.2. Ten to twenty micrographs were taken of each polished specimen at x300 magnification. The particle size distribution of the anhydrous grains in each set of micrographs was then calculated at two enlargements, using the image analyser. The lower enlargement measured particles in the 100-3 μm range accurately, whilst the higher one gave greater accuracy in the 12-0.5 μm particle size range. The distributions of particle areas from the two enlargements were then combined; greatest weight was given to the higher enlargement for particle areas below 16 μm^2 and to the lower enlargement for areas above 512 μm^2; between these limits the results from the two enlargements were averaged. This combined distribution was then used to derive the mean particle area (and hence volume and diameter) and the % area occupied by anhydrous material.

The graph (Fig 5.2) shows the values of A% v. hydration time for the specimens which have been analysed by this method. The values of A% at 10 min and 2 hours were very close to the theoretical initial A% of 40% (with $^{w}/c$ = 0.5, cement density $\sim 3 g/cm^3$); the latter value was taken as the 0% hydration level.

For comparison several other measures of hydration are plotted on the same graph. The quantitative X-ray diffraction (QXDA) data from Jons and Osbaeck (1980, 1982) are for a different, although similar cement and are some 10% lower than those from BEI. However, their values for overall cement hydration were calculated from the fraction of each phase which had hydrated and the nominal Bogue composition of the cement. The actual proportion of C_3S (the most rapidly hydrating phase) is invariably significantly higher than that estimated by Bogue and hence the real % hydration would also be expected to be higher. Limited X-ray results for the same

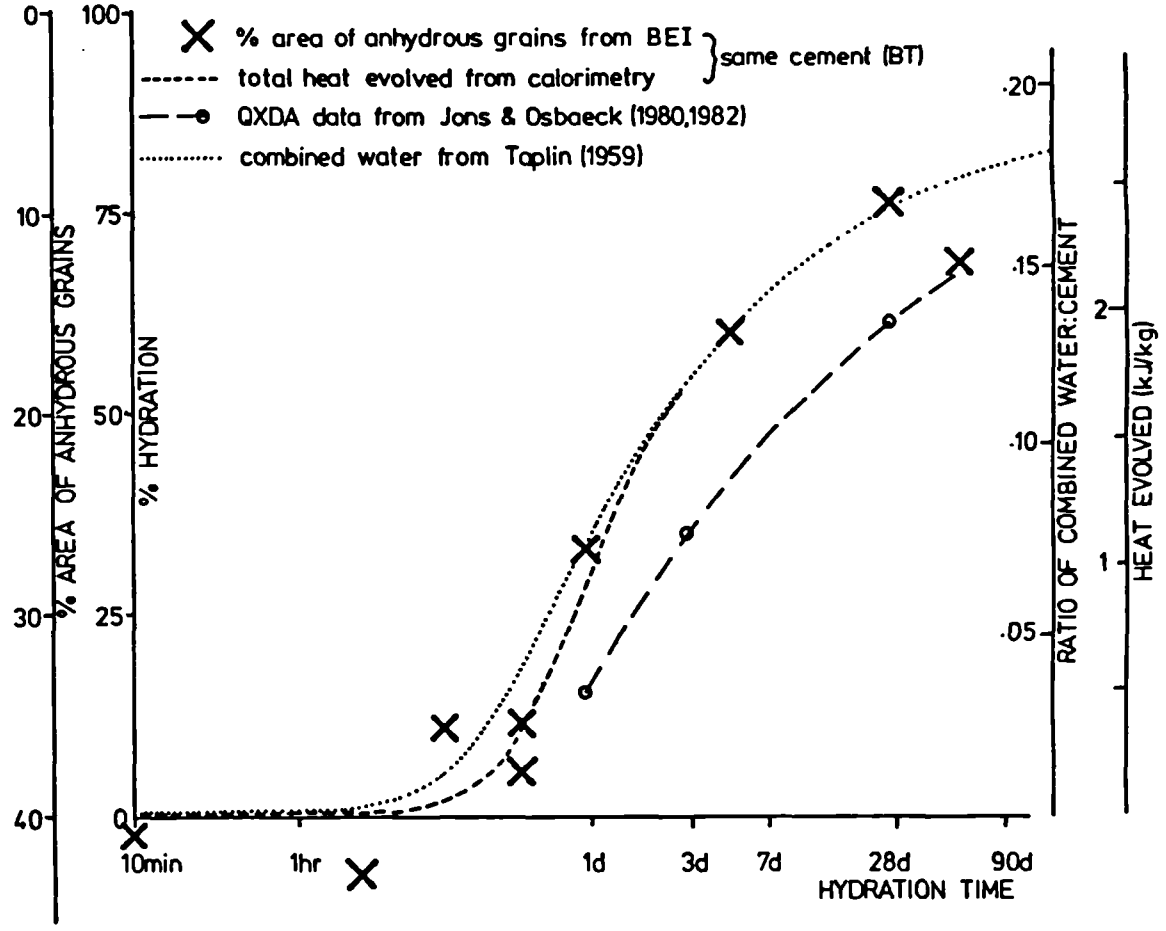

FIG. 5.2 Degree of Hydration from BEI of Polished Cement Sections Compared with other measures of Hydration

cement (BT) lie close to the BEI results. A fair fit is seen with the integrated calorimetry curve from this cement even though the total heat output is not strictly analogous to the % hydration. The combined water content of cement calculated by Taplin (1959) shows remarkably good agreement with the BEI data.

Quantitative image analysis can also be used to calculate the change in grain size distribution with time, the amount of massive calcium hydroxide formed and the pore size distribution. Knowledge of the above is essential in assessing the validity of any mathematical model of hydration. This is an area where considerable further work could be done.

5D Rate of Heat Evolution of the Cements

5D.I Experimental details

The hydration of all the cements described in section 5B was followed using a conduction calorimeter from Wexham Developments designed by Forrester (1970) (see Fig 3.1 and Appendix III). All the cements were hydrated at 20°C with a water to cement ratio of 0.5. The effect of different mixing times was studied on one cement and that of particle size on a fractionated, ground clinker (5B.II).

All the cements were hand mixed, outside the calorimeter in small plastic bags (approximately 5cm x 15cm). Except in the case where the effect of mixing was studied, all cements were mixed for 3 minutes. The plastic bags containing the mixed cements were then sealed and immediately placed in the calorimeter cell (Fig 3.1). The cell took about 30 minutes to regain equilibrium so readings before this time were ignored.

5D.II Comparison of the Calorimetry Curves from the Different Cements

The heat evolution curves of the eight cements studied are shown in Figs 5.3 and 5.4. The curve shown for BT was taken about 2 years after the specimens for microstructural observations were made. Earlier calorimeter curves obtained by Dr A. Ghose on this cement had a higher second peak in the rate of heat evolution.

The initial heat peak (not shown here) is followed by several subsequent peaks. The second peak corresponds to the rapid growth of C-S-H and CH at the end of the induction period, from the hydration of C_3S, observed in the examination of the microstructure.

This second peak is followed by a third peak in most of the cements, which corresponds to the appearance of long AFt rods in the microstructure, in agreement with the findings of Dalgleish et al (1982a and b) and Pratt and Ghose (1983). As discussed in section A, this peak is totally dissimilar to the 'monosulphate' peak seen during the hydration of C_3A + calcium sulphate. As the microstructural development of cements NBS 61 and NBS 63 has not been studied, and as it is difficult to assess relative quantities of phases on fracture surfaces, it is difficult to correlate the height of this third peak with the amount of AFt seen during the secondary hydration of C_3A. However, the weak third peak in NBS 64 did correspond to the appearance of notably less AFt than in the other cements examined.

Despite the association of this third peak with the renewed hydration of C_3A (and/or ferrite phase) there does not appear to be any simple correlation between the amount of C_3A or interstitial phase in the cement and the height of the third peak.

There are some general correlations between the height of this peak and the C_3A:ferrite phase ratio. In cements D44 and NBS 61 the C_3A:ferrite phase ratio is much greater than 1 and these cements

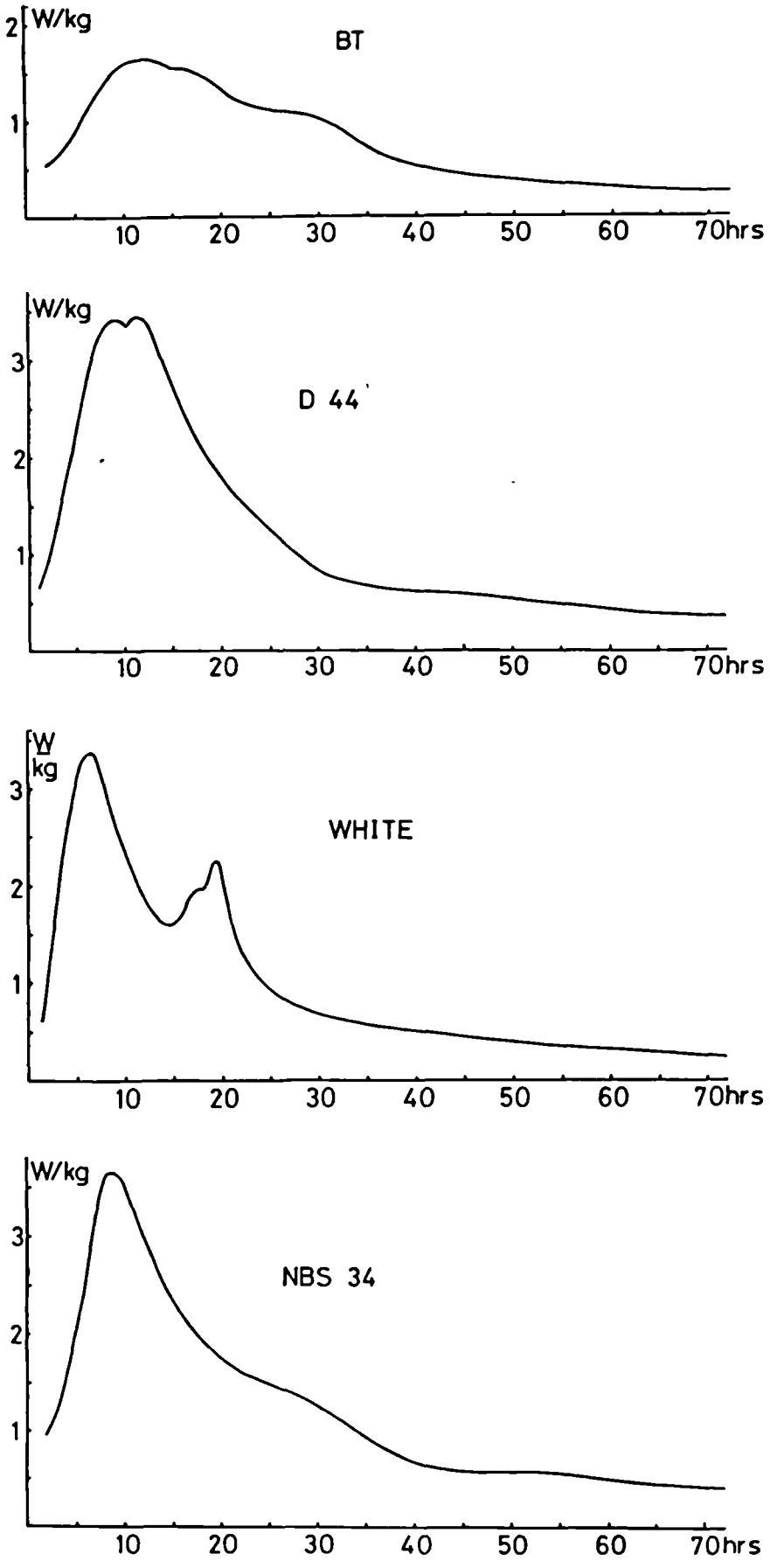

FIG. 5.3 Rate of Heat Evolution for Various Cements

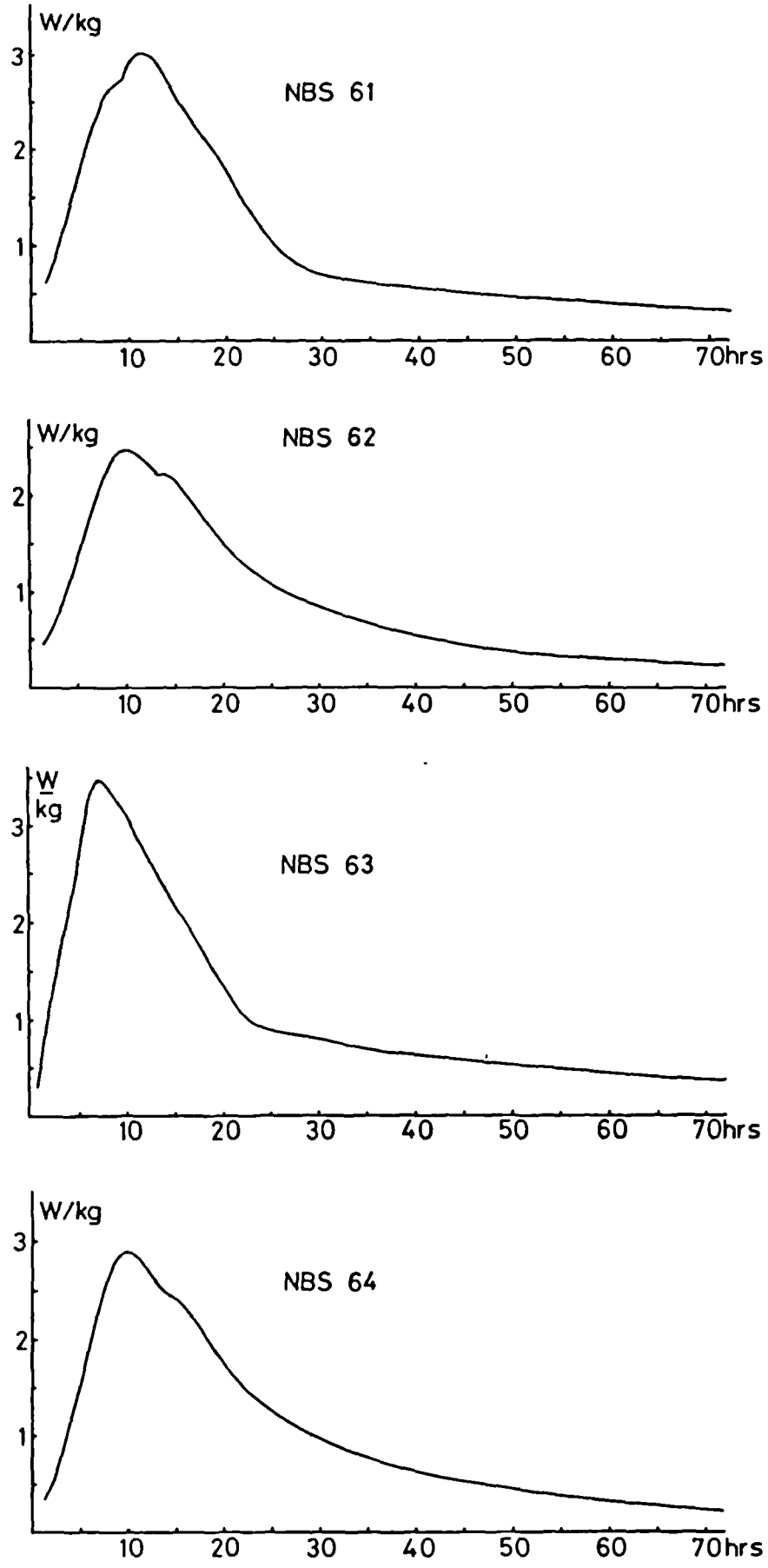

FIG. 5.4 Rate of Heat Evolution for Various Cements

have a strong third peak. In all the other OPCs the C_3A ferrite phase is less than 1 and these all have weaker third peaks. The white cement has a very pronounced third peak (closely followed by a fourth) and this cement contains no ferrite phase.

This relationship, while not rigorous, suggests that the distribution of C_3A and ferrite phase in the interstitial phase is related to the intensity of the third peak. This could be related to the observations of amorphous FH relicts of the ferrite phase which could inhibit the hydration of enclosed C_3A. Further study of the clinker microstructure is needed to confirm this supposition.

In the heat evolution curves from some of the OPCs a weak fourth peak can be seen, corresponding in time to the appearance of monosulphate inside the hydrated shells. The white cement shows a strong fourth peak corresponding to the appearance of large, thin hexagonal plates in the microstructure (section C.VII). This is similar to the typical 'monosulphate' peak seen in the hydration of C_3A + calcium sulphate (Chapter 4, section C) and in the hydration of the C_3S:C_3A:calcium sulphate mixture (Chapter 4, section E.II), which suggests that the platey phase might be monosulphate.

As described in section A, if the heat evolved by each phase in cement was linearly proportional to the amount of that phase in the cement, it should be possible to separate the calorimeter curves into the contributions from the different phases as done by Kaminski and Zielenkiewicz (1982). All attempts to deconvolute the calorimeter curves from this wide range of commercial cements gave meaningless results . The amount and degree of dehydration of gypsum could be partly responsible, but differences in the microstructure of the cement clinker and the consequent distribution of phases in the cements may also contribute.

5D.III Effect of Mixing on Rate of Heat Evolution

The rate of heat evolution of cement D44 was studied with mixing times of 0 minutes, 2 minutes, 6 minutes and 10 minutes. In all cases, except for the 10 minute mix, water was added to the cement in a plastic bag, the cement was mixed for a given time between the fingers and then placed directly into the calorimeter cell. The manipulation of the bag containing the cement meant that even the cement with a nominal mixing time of 0 minutes received some agitation. The cement mixed for 10 minutes was mixed with a metal spatula in a plastic beaker using a shearing action.

The region of the calorimeter curve near the top of the second and third peaks in the rate of heat evolution, for the various mixing times, are shown in Fig 5.5. With no mixing the third peak only appears as a slight shoulder on the second peak. With two minutes mixing the third peak is more pronounced but still lower than the second peak. With 6 minutes mixing the peaks are almost the same height, whilst the third peak is higher than the second with 10 minutes mixing.

The time at which the peaks occur is not significantly affected by mixing except in the sample mixed for 10 minutes, where the position of the second peak (attributed to C_3S) is slightly later in time. A more pronounced retardation of the C_3S peak was found by Lerch (1946) when flash set occured in cements with insufficient gypsum. deJong et al (1968) found a similar retardation of C_3S in pastes of C_3S and C_3A without calcium sulphate.

Mixing might affect the early hydration, by homogenising the solution, removing any concentration gradients, or by disrupting any layer of product on the surface of the grains. Both these effects would be likely to increase the initial rate of dissolution

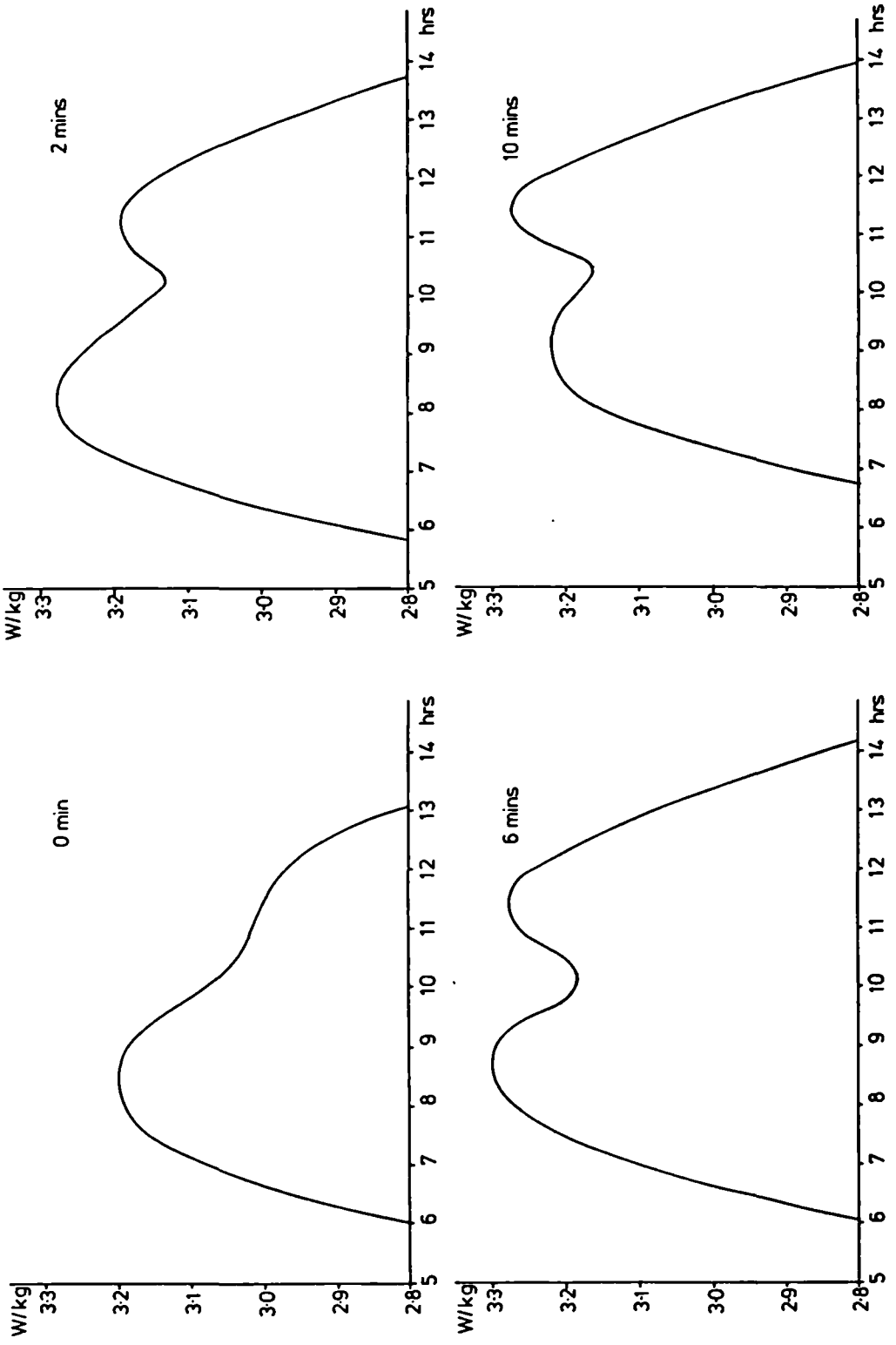

FIG. 5.5 Effect of Mixing Time on Rate of Heat Evolution

of the anhydrous phases. The retardation of the C_3S peak with 10 minutes mixing suggests that more aluminium is present in solution than at shorter mixing times. Details of the mechanism by which the relative peak heights are altered are unclear.

5D.IV Effect of Particle Size on Rate of Heat Evolution

The rate of heat evolution curves for the various size fractions of ground clinker, described in section B, are shown in Fig 5.6. There is very little difference in the position of the second peak in the rate of heat evolution which suggests that the hydration kinetics of C_3S are independent of particle size. This is consistent with the theory that the deceleratory period begins as the diffusion of ions through the product layer becomes rate controlling, the depth of product being independent of particle size at any time.

The second heat evolution peak does occur earlier for the smallest size fraction, but the rate of heat evolution drops very sharply after this peak. This suggests that virtually all the cement is hydrated at the top of this peak. In this case it appears that the cement grains have reacted to a depth of about 1-1.5 μm in the first 15 hours of hydration.

The rate of heat evolution also falls sharply for the 3-7 μm fraction and is near zero after 40 hours' hydration. This suggests that the cement grains react to a depth of about 3 μm within the first 40 or so hours of hydration.

The three larger size fractions all showed a third peak in the rate of heat evolution (not distinguishable for the two largest fractions on the scale of Fig 5.6). It appears that the hydration of the interstitial phase is more affected by particle size than that of C_3S. This is probably due to the relative proportions of this phase exposed on the surface of the grains at different particle sizes.

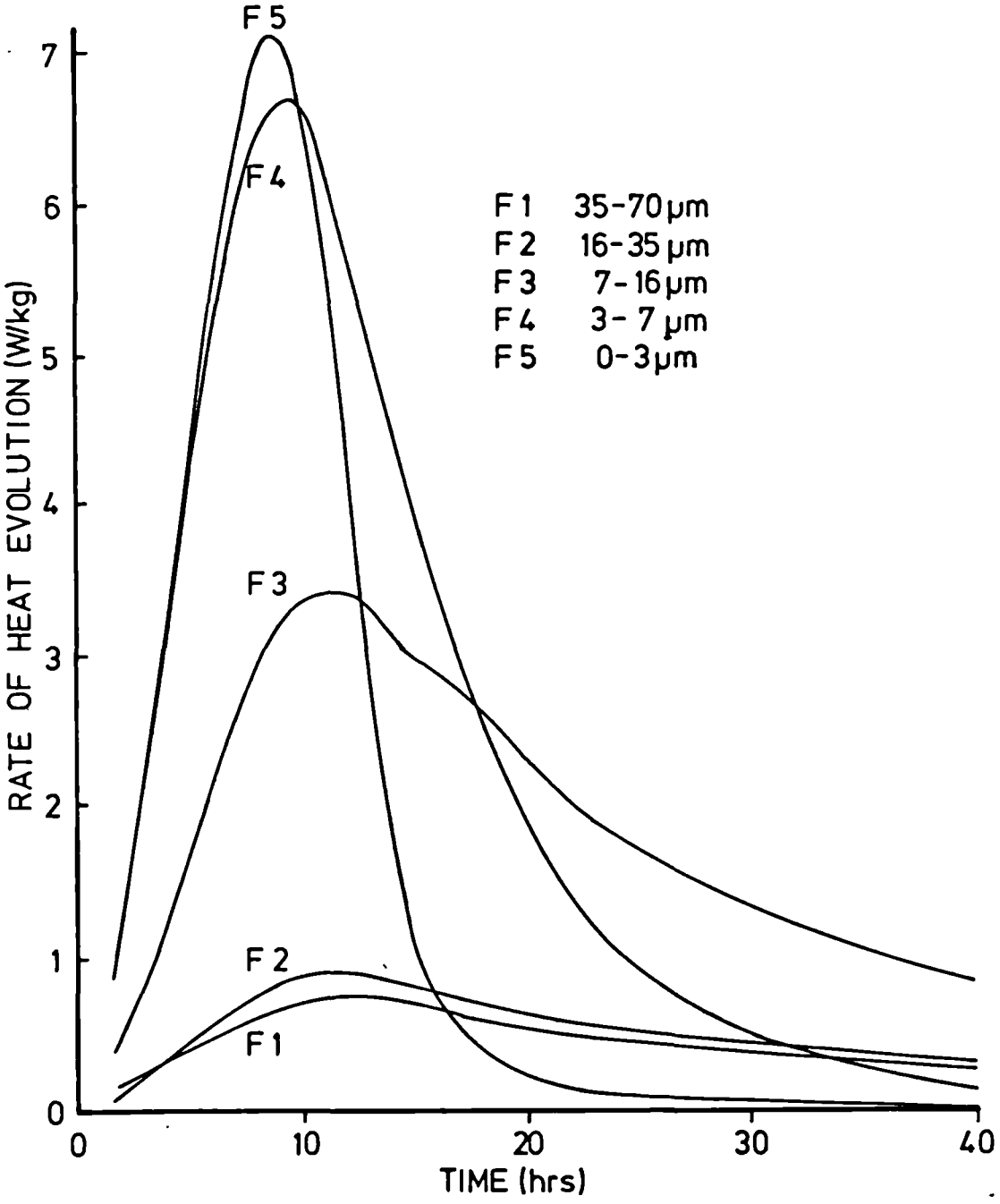

FIG. 5.6 Effect of Particle Size on Rate of Heat Evolution

Chapter Six

DISCUSSION, SUGGESTIONS FOR FURTHER WORK AND CONCLUSIONS

6A Discussion

The hydration of the individual cement phases has been discussed in Chapter 4. In this section the way in which the hydration of these phases is modified in cement is discussed, in terms of the development of microstructure and rate of heat evolution described in Chapter 5.

6A.I Development of Microstructure

Fig 6.1 summarises the development of microstructure of cement in several stages, which form the basis for this discussion of the development of microstructure and possible hydration mechanisms. Belite is usually seen as isolated grains which hydrate very slowly or as small inclusions in other grains which appear unreactive, so this phase is not considered in the discussion.

6A.I.1 Unhydrated cement microstructure (Fig 6.1(a))

In cement clinker the interstitial phase forms the matrix in which alite and belite grains are distributed (Fig 2.5, plate 5.1). Alite is the most brittle phase so fracture through this phase predominates, whilst interphase boundary fracture is uncommon. Consequently most of the resulting cement grains are polymineralic. In the larger grains (~ 40 μm) the grain surfaces are predominantly alite, with only a small fraction of the interstitial phase being exposed. In the smaller grains some fracture through the interstitial

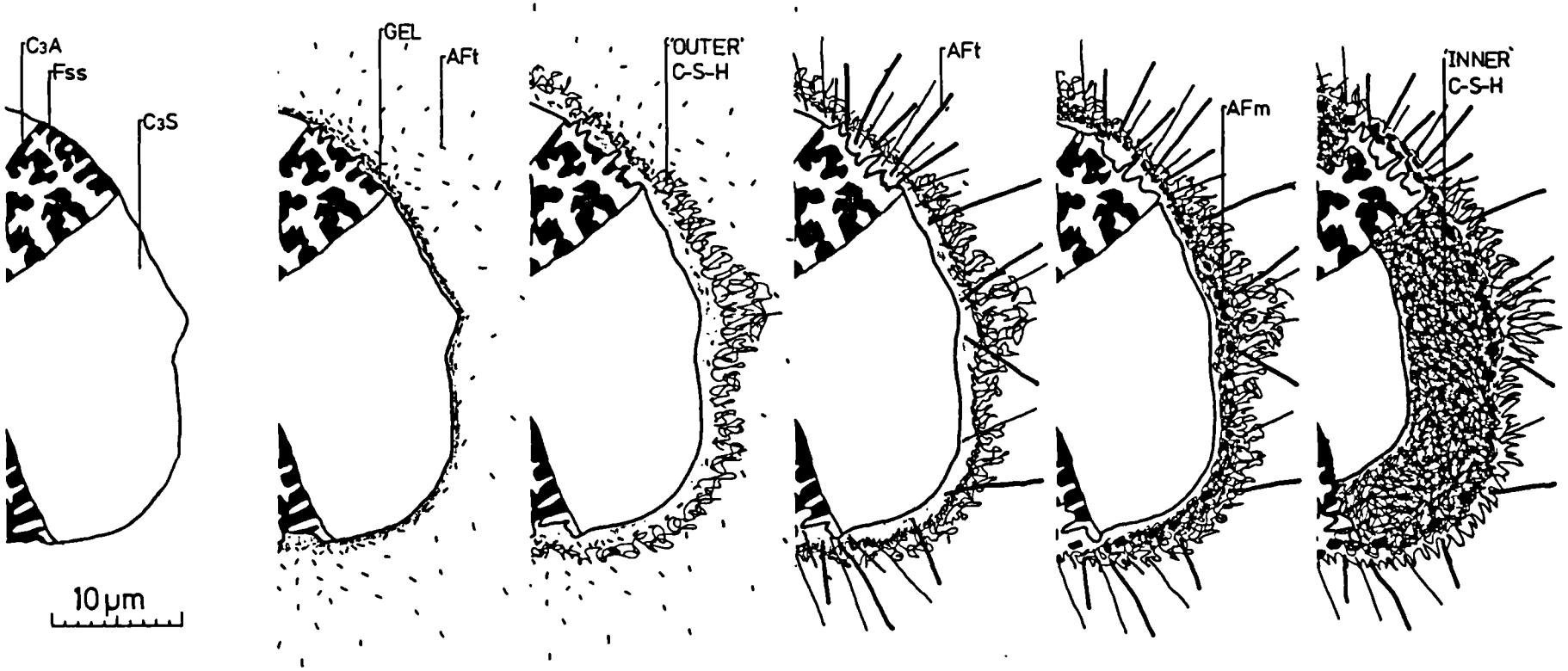

a) Unhydrated
Section of poly-mineralic grain. (scale of interstitial phase is slightly exaggerated)

b) ~10min
Some C_3A (&/or Fss) reacts with calcium sulphate in solution. Amorphous, aluminate rich gel forms on the surface and short AFt rods nucleate at edge of gel and in solution.

c) ~10hrs
Reaction of C_3S to produce 'outer' product C-S-H on AFt rod network leaving ~1µm between grain surface and hydrated shell.

d) ~18hrs
Secondary hydration of C_3A (&/or Fss) producing long rods of AFt. C-S-H 'inner' product starts to form on inside of shell from continuing hydration of C_3S.

e) 1-3days
C_3A reacts with any AFt inside shell forming hexagonal plates of AFm. Continuing formation of 'inner' product reduces separation of anhydrous grain and hydrated shell.

f) ~14days
Sufficient 'inner' C-S-H has formed to fill in the space between grain and shell. The 'outer' C-S-H has become more fibrous.

FIG. 6.1 Microstructural Development during the Hydration of Portland Cement

matrix leaves a higher proportion of this phase exposed on the grain surfaces.

The interstitial phase is ideally a finely divided mixture of C_3A and C_4AF. The actual microstructure of this phase will affect the relative amounts of C_3A and C_4AF exposed on the surface of the cement grains. In a white cement, for example, all the exposed interstitial phase will be C_3A.

Fig 6.1(a) shows a stylised section of a cement grain containing alite and some interstitial phase. The grain is larger than average so that all the stages of hydration can be depicted.

6A.I.2 First heat evolution peak and the induction period (Fig 6.1(b))

During the first few minutes of reaction the anhydrous cement phases start to dissolve and heat is evolved. The concentration of ions in solution rises rapidly. Although the dissolution may be congruent initially, the concentrations of silicon and aluminium are very low after the first few minutes, and the composition of the solution is dominated by Ca^{2+}, OH^- and SO_4^{2-} ions. There are no reports of iron in solution even at very early times so the dissolution of C_4AF may never be congruent. The relative amounts of Ca^{2+} and SO_4^{2-} in the first few minutes have not been extensively investigated, but it may be supposed that any hemihydrate present will dissolve rapidly to give a high concentration of SO_4^{2-} ions, such that the solution is supersaturated with respect to gypsum. As secondary gypsum is precipitated the concentration of SO_4^{2-} will fall, and the simultaneous dissolution of C_3S to give Ca^{2+} and OH^- will further lower the SO_4^{2-} concentration by suppressing the solubility of gypsum. Some of the results of Lawrence (1966) do show a drop in the SO_4^{2-} concentration as the Ca^{2+} concentration rises.

The deficiency of aluminium and silicon in solution, with respect to that expected from congruent dissolution, indicates either the precipitation of some product rich in aluminium or silicon, or the formation of a nonstoichiometric layer on the surface of the cement grains. During the hydration of C_3A + gypsum an amorphous layer, probably AH_3 gel containing calcium and sulphate, was observed on the surface of the C_3A (plate 4C.3(a)). During the hydration of C_3S foils of C-S-H were observed on the surface of the grains (plate 4A.1(a)). The early gel coating observed on cement by other workers (Double et al, 1978; Jennings and Pratt, 1980 ; Groves, 1981) appears similar to the impure AH_3 gel seen during the hydration of C_3A rather than the foils seen during the hydration of C_3S. However, as pointed out by Jennings (1983), the presence of aluminium drastically reduces the solubility of silica in alkaline solutions and the presence of silica would be expected to affect the solubility of aluminium; so any gel layer formed around the polymineralic cement grains will be different from the gelatinous products formed when the phases are hydrated separately. The gelatinous layer observed in the hydration of cement is probably an amorphous, colloidal, product rich in alumina and silica but also containing significant amounts of calcium and sulphate, the exact composition varying with the composition of the underlying grain surface.

Small AFt rods have been observed on dried fracture surfaces after 1 hour's hydration (plate 5.5). These rods probably form at the edge of any gelatinous product, as in the hydration of C_3A + gypsum (plate 4C.3(a)); as indicated by the microstructure of the 2 hour old ion-thinned paste where there is a gap between the grain surface and the product layer of gel and AFt rods (plate 5.7). The morphology of the rods is similar to those seen when C_3A is hydrated

with hemihydrate, indicating a high initial SO_4^{2-} concentration.

During the hydration of C_3A the surface of the grains soon becomes covered with a mass of AFt rods, whose number and density increases with time. Even though a large proportion of the cement grain surface is C_3S, it is still only sparsely covered with AFt rods after 1 hour and the number of rods does not noticeably increase between 1 hour and 3 hours (plates 5.5 and 5.8). It was found by Locher et al (1980) that the amount of anhydrous C_3A decreased sharply for a short time after water was added to the cement and then stopped decreasing, remaining constant for several hours. If the rising concentration of Ca^{2+} in solution suppresses the solubility of gypsum and/or C_3A, this would reduce the rate of formation of AFt and the rate of C_3A hydration.

Locher et al (1980) found that the initial decrease in the amount of C_3A varied from 0.4 to 1.6% and was not simply related to the proportion of C_3A in the cement. The amount of C_3A reacting is probably related to the amount of C_3A exposed on the surface which is dependent on the microstructure of the cement clinker and the fineness of the cement, as described earlier.

Fig 6.1(b) shows the microstructure of the cement grain after about 10 minutes. A gelatinous layer has formed with a thickness of 0.5 μm or less. AFt rods form at the edge of this layer and in the solution, by a through solution mechanism. It is possible that foils of C-S-H also start to form during the induction period, which are not seen in the dried microstructure.

6A.I.3 Acceleratory period (Fig 6.1(c))

At the end of the induction period rapid growth of C-S-H and CH occurs (possible reasons for the ending of the induction period will be discussed subsequently). From ion-thinned sections and wet

cell observations (plate 5.10) it appears that the C-S-H forms on the framework of AFt rods at the edge of the gelatinous layer, so the C-S-H 'shell' and the grain surface are separated. Observations of the outer surface of the hydrated layer on fracture surfaces (plate 5.9) show that the C-S-H foils (or fibres after drying) grow out into the solution, indicating that the shell is very open and porous at this stage, allowing the migration of ions through it. The dissolution of the C_3S surface and the formation of the C-S-H on the outer surface of the shell increases the separation between grain and shell. The formation of the 1-2 μm thick layer of foils probably corresponds to the reaction of a 0.5-1 μm layer of C_3S. The dissolution of this amount of C_3S and the thickness of the original gelatinous layer give the observed separation between grain and shell of up to 1 μm after 12 hours hydration.

When the rapid growth of C-S-H starts, at around 3-4 hours, the foils bond the cement grains together so the cement 'sets', but at this stage the bonding is weak and the cement still fractures around the shells. After about 12-18 hours the bonding between the shells is strong enough to cause fracture through them, exposing the separated shells on fracture surfaces.

Fig 6.1(c) shows the formation of the 'outer' C-S-H as a separated shell. The space between the shell and the grain is probably filled with a colloidal product of high water content in the 'wet' state. The presence of aluminium in this amorphous product probably leads to the incorporation of some aluminium in the C-S-H gel as found by Lachowski et al (1980).

During this period CH forms as well crystallised hexagonal plates in the water filled space. Some small grains start to become engulfed by the growth of CH, while other small grains originally agglomerated on the surface of larger grains hydrate completely and merge into the 'shells' of the larger grains.

6A.I.4 Secondary growth of AFt (Fig 6.1(d))

After about 16 hours a secondary formation of AFt starts to occur, corresponding to the shoulder on the main, second, heat evolution peak. It is not clear exactly what changes in the paste initiate this renewed reaction. The fact that this secondary reaction of C_3A occurs after the rapid growth of C-S-H and CH indicates that the necessary changes are produced by the reaction of the C_3S. It is possible that the drop in Ca^{2+} concentration, as CH starts to precipitate, increases the rate of dissolution of gypsum and of aluminium from the C_3A, so promoting the formation of AFt. Alternatively the reaction of the C_3S could make the gelatinous layer unstable so increasing the rate of C_3A dissolution.

In this renewed reaction the AFt forms as long rods indicating that the concentration of SO_4^{2-} in solution is lower than that earlier when the short AFt rods were formed.

Interestingly a similar rapid growth of long AFt rods was observed by Jennings and Pratt (1979b) when cement which had been hydrated for 1-2 hours as paste was placed in a large volume of distilled water. This phenomenon could also be ascribed to a reduction in the concentration of Ca^{2+} ions in solution by the addition of water, leading to the rapid growth of AFt.

The reaction of C_3A in some polymineralic grains produces locally , large separations between the shell and the anhydrous core, which appear as missing 'corners' in ion-thinned sections. The ferrite phase does not appear to react substantially during this period as relicts are seen on fracture surfaces. Thus the amount of C_3A which can react, and the height of the third calorimeter peak, is determined by the microstructure of the interstitial material itself as well as by the amount exposed on the surface of the grains.

Fig 6.1(d) shows the microstructure of a cement grain after the secondary reaction of AFt (~ 18 hours). Much of the exposed C_3A has dissolved to produce long AFt rods which pass through the C-S-H layer. As the C_3S continues to react 'inner' C-S-H starts to form on the inside of the shell. This thickening of the shell reduces its permeability so that the inside of the shell becomes isolated from the outside after about 1 day's hydration.

6A.I.5 Formation of AFm

Inside the shell the concentration of sulphate in solution drops rapidly as the C_3A reacts. Because of this, but more importantly because C_3A and AFt are both present in this region, AFm forms on the inside of the shell during the next few days. Ignoring the possible substitution of iron and other ions the reaction would be:

$$2C_3A + C_3A.(C\bar{S})_3.32H_2O + 4H_2O \longrightarrow 3C_3A.C\bar{S}.12H_2O$$

The heat produced by this reaction is sometimes visible as a low, broad fourth peak in the rate of heat evolution as noted by Pratt and Ghose (1983), and corresponds to the third peak identified by Lerch (1946) and Stein (1961). From the microstructural observations it does not appear that the direct conversion of AFt to AFm in the absence of C_3A occurs in cement; AFt rods can still be seen outside the shells after several months in most cements.

Fig 6.1(e) shows the formation of small hexagonal plates of AFm on the inside of the shell with the disappearance of AFt in this region. All the exposed C_3A reacts during this stage, but areas enclosed by the ferrite phase may remain unreacted.

The continuing hydration of C_3S thickens the shell with 'inner' C-S-H. The C-S-H occupies a larger volume than the C_3S from which

it forms, so the separation of the shell and the anhydrous core is reduced. As the amount of CH in the originally water filled space continues to increase and C_3S continues to hydrate inside the shell, it must be assumed that Ca^{2+} ions and water can permeate the shell.

6A.I.6 'Internal' hydration of C_3S

The continued hydration of C_3S inside the shell eventually reduces the separation between shell and core to nothing. The separation between shell and core is no longer seen after 2 weeks' hydration and little further hydration is observed in the next 2 months. The thickness of the hydrated layer at this stage is about 8 μm.

Taking the density of saturated C-S-H as around 2.05 g/cm³ (Taylor 1984) and the C/S ratio of C-S-H as 1.7, the reaction of a 7.7 μm layer of C_3S produces a 8.7 μm layer of product; which would fill a 1 μm gap between the grain surface and shell. This calculation is for a flat, 2-dimensional surface of C_3S which is not strictly comparable to a rounded cement grain. However, the close agreement between the observed thickness of the hydrated layer and the thickness calculated to fill the initial separation of grain and shell, indicates that hydration does proceed by an 'internal' mechanism of dissolution of the C_3S surface and formation of C-S-H on the inside of the shell. This internal mechanism is also consistent with limited migration of most atoms during hydration, as suggested by Taylor (1984). This rough calculation also supports the view that all CH is precipitated outside the shell with little if any microcrystalline CH being formed in cement pastes at normal w/c ratios.

Fig 6.1(f) shows the microstructure of a cement grain where the separation between shell and core has been filled in with 'inner'

C-S-H. The interstitial phase appears unreacted in BEIs of polished sections. However, some C_3A at the edge of the interstitial region will probably dissolve and be incorporated in the C-S-H gel. During this period the 'outer' C-S-H becomes more fibrous, but the reasons for this change are unclear.

This stage in the hydration reaction, where the separation between shell and core disappears, will only be reached if the grain is large enough (i.e. $\sim$ 20 μm). Smaller grains will hydrate completely leaving an empty shell. Grains smaller than about 3 μm hydrate almost completely during the acceleratory period, as found in the calorimetry of different particle size fractions, so the C-S-H formed from these small grains will be mostly 'outer' product.

6A.II Some aspects and implications of the microstructural development of cement

6A.II.1 Ending of the induction period

The induction period in cement hydration ends at much the same time as it does in the hydration of C_3S, which suggests that a similar mechanism initiates the acceleratory period in both cases. It has been suggested that the induction period in C_3S ends when a first hydrate of low permeability transforms to a more porous second hydrate. However, the surface of cement during the induction period is covered with a gelatinous product which is quite different from the foil like product observed on the surface of C_3S. These different product layers would not be expected to undergo a similar transformation at a similar time; so microstructural observations appear not to support this mechanism.

Alternatively, as discussed in the context of C_3S hydration (Chapter 4, section A.II.3), although a definite hydrate phase may be present this need not be the cause of the slow dissolution of the

C_3S or cement during the induction period; the dissolution of the C_3S or cement may be reduced by a disrupted or amorphous surface layer. The continued slow dissolution of the C_3S or cement with the precipitation of a C-S-H hydrate phase of lower C/S ratio will eventually produce a solution saturated with respect to both C-S-H and CH. When C-S-H and CH start to precipitate simultaneously from this solution the rate of dissolution of the C_3S or cement can again increase. Although the presence of aluminium, iron and other ions in cement may affect the dissolution of C_3S and the activities of calcium and silica in solution, such a mechanism would be expected to give an induction period of similar length in C_3S cement.

This mechanism would also predict that the composition of the solution during the induction period is in equilibrium with C-S-H. Whilst there is evidence (Brown et al, 1984) that such a phase equilibrium approach is valid in the case of C_3S hydration, the validity of such an approach to the hydration of cement has not been demonstrated and would be difficult to demonstrate in the multicomponent, multiphase, cement system. It is apparent that the rate of dissolution of C_3S must depend on factors other than merely the concentration of Ca^{2+} ions in solution, but what these factors are is unclear.

6A.II.2 Role of interstitial phases

Contrasting the microstructural development of cement and C_3S, it is apparent that C_3A (and/or the ferrite phase) must be present for separated hydrated shells to form. From the work on the C_3S:C_3A:$C\bar{S}$ mixture it is also apparent that separated shells only form around grains containing C_3A. This indicates that most cement grains are polymineralic (as confirmed by examination of unhydrated cement and clinker), as most cement grains (>90%) form separated

shells. It appears that the interstitial phase leads to the formation of a gelatinous layer around the cement grains outside which a shell of C-S-H and AFt forms.

The presence of the interstitial phase also produces several extra peaks in the rate of heat evolution during hydration of cement compared with the hydration of C_3S. The most significant of these is the third heat evolution peak, corresponding to a secondary reaction of C_3A to produce AFt rods. This peak is usually observed as a shoulder on the second heat evolution peak, which is attributable to the hydration of C_3S, sometimes merging with it. When C_3A (and C_4AF) are hydrated in isolation with calcium sulphate this two stage reaction to produce AFt is not seen. It must be concluded that the simultaneous hydration of C_3S in cement causes the hydration of C_3A to stop and then start again, probably due to the influence of the hydration of C_3S on the Ca^{2+} concentration.

Several factors appear to affect the height and position of this third peak. The height probably corresponds to the amount of C_3A exposed on the surface of the cement grains, which depends on the proportion of interstitial phase in the cement, the microstructure of the interstitial phase itself and the fineness of the cement. More work on the microstructure of the clinker and cement before hydration is needed to confirm this supposition.

The extent to which the cement is mixed also affects the third heat evolution peak and suggests that the formation of the early gelatinous product influences the subsequent hydration, but here again, more work is needed.

The hydration of the interstitial phase may also produce a fourth heat evolution peak in cement after about 60 hours. This peak corresponds to the reaction of the interstitial phase with AFt

to give AFm. In most cements this peak is low and broad, as the shell formed by the hydration of C_3S isolates the remaining interstitial phase from AFt formed outside the shell and AFm is only formed on the inside of the shell. In the white cement examined this reaction occured earlier, before the shell isolated the grains from the pore solution, so large AFm plates could be formed. Similarly in the C_3S:C_3A:$C\bar{S}$ mixture the shells formed around the C_3A grains are very thin and extensive reaction of C_3A with AFt can take place to give a strong heat evolution peak and large AFm plates.

The amount and degree of dehydration of the calcium sulphate has a major influence on the heat evolution peaks from hydration of the interstitial phase and on the morphology of the AFt formed. High concentrations of SO_4^{2-} in solution, due to the presence of hemihydrate, favour the precipitation of AFt as short, squat rods, whilst more dilute solutions favour long, thin rods. However, more work is needed to quantify the effect of calcium sulphate on the hydration of cement.

The ferrite phase appears to hydrate very little in cement. The work of Taylor and Newbury (1984) showed that iron rich regions, apparently relicts of the ferrite phase, remain even after 23 years hydration. Whether the formation of an amorphous surface layer of hydrous ferric oxide prevents further hydration of the ferrite phase, or whether all the calcium and aluminium can be leached out leaving only the iron is unclear.

Overall it is clear that the interstitial phase does play a major role in the development of microstructure in cement. How this influence on the microstructure is reflected in the properties of the cement, such as strength and durability, is unclear. Plate 6.1 shows an area of a fracture surface which is dominated by four large grains which have fractured along the interface between hydrated shell

Plate 6.1 Fracture surface of 1 day old cement paste

and anhydrous core; it would seem that the influence of separated shells, at least on the early strength of cement, cannot be ignored.

6A.II.3 Implications for understanding the strength and durability of cement and for modelling cement hydration

The electron optical techniques described in the present work provide a means for characterising the microstructure of cement. Perhaps of greatest importance, in this context, is the image analysis of backscattered electron images of polished cement surfaces. This technique is non selective and can be used to quantify many aspects of the microstructure and microstructural development. The results presented in Chapter 4.C.VIII illustrate how the amount of anhydrous material remaining at any time can be calculated, but preliminary work indicates that the grain size distribution of the anhydrous material, the relative proportions of the different anhydrous phases, the quantity and distribution of calcium hydroxide and the amount and size distribution of porosity in cement pastes can all be calculated using this technique.

Potentially it should be possible to relate the microstructural characteristics of the cement to its strength and durability. For example calcium hydroxide is often considered as a 'weak link' in the cement microstructure and it is well known that stronger, more durable cements can be made by adding fly ash and silica fume, which react with the calcium hydroxide to give C-S-H. Image analysis of BEIs could be used to quantify the way in which these additives modify the microstructure.

Another possibility is to examine changes in the microstructure which take place in aggressive environments, such as sulphate solutions and sea water. An understanding of the way in which degradation occurs would potentially lead to more durable cements.

An ability to characterise the microstructure of cement numerically is also an essential precursor to establishing the validity of any mathematical (computer) model of cement hydration.

6B Suggestions for Further Work

Many areas for further work have been mentioned in the course of the present work, especially in the previous section of this chapter. Further understanding of the hydration of cement must combine information on the interactions of the various anhydrous phases, from studying the hydration of phase mixtures, with a knowledge of the physical arrangement of those phases in cement, through examination of the clinker microstructure and the way in which the clinker is broken up on grinding.

In the present work four main electron optical techniques have been used. Whilst all these techniques must be used to characterise cement microstructure fully, particular areas in which each of these techniques might be further used are outlined below.

Environmental cell in the HVEM

This technique is of great value in studying 'wet' microstructures. The early hydration of both C_3S and cement are still the subject of much controversy. Further work using the environmental cell, in conjunction with other techniques (e.g. solution chemistry) should make it possible to determine the mechanisms responsible for the induction period and to establish the validity of an equilibrium approach to the hydration of cement and its constituent phases.

In addition the environmental cell could also be used to determine the effect of additives, such as silica fume, on the structure and properties of C-S-H gel.

Fracture surfaces

Whilst the study of fracture surfaces can be misleading in determining the bulk microstructure of cement, used in conjunction with other techniques, fracture surfaces could provide much information on the way in which cement fails. Thus fracture surfaces should not be ignored in the study of the mechanical properties of cement and concrete.

Ion beam thinning

Although specimen preparation is very difficult, examination of ion-beam thinned sections of cement can provide much information. The structure of the C-S-H gel in set and hardened cements can be examined and so, potentially, the long term effects of admixtures and additives determined.

Ion-beam thinning could also be used to study the microstructure of the cement-aggregate interfacial region in concrete and that of the cement-steel interface in reinforced concrete. The role of these interfaces in the behaviour of concrete in real structures is very important and still comparatively poorly understood.

BEI of polished cement

As outlined in the previous section the potential of this technique in understanding the properties of cement and concrete is enormous. In the field of cement very little basic research leads to actual advances in the commercial use of cement and concrete. Ultimately advances in the basic understanding of cement hydration can only be usefully linked to the mechanical properties and durability of cement if the microstructure can be characterised numerically.

6C Conclusions

The present work shows how a combination of electron optical techniques can be used to determine the way in which the microstructure of cement develops during hydration. The ways in which the hydration of the constituent cement phases are modified when they are combined in cement have been investigated, and the mechanism of cement hydration has been discussed in terms of the observed microstructural development and the hydration mechanisms of its constituent phases.

It has been found that almost all cement grains form hydrated shells which are separated from the anhydrous core during hydration. This phenomenon can be attributed to the presence of the interstitial phase in cement. The mechanism by which these shells form and the way in which they affect the subsequent microstructural development has been discussed.

The fact that these separated shells are not seen during the hydration of C_3S, indicates that C_3S cannot be used as a model for cement hydration. Significant differences also exist between the hydration of cement and that of constituent phase mixtures. The hydration of portland cement depends upon the physical arrangement of its constituent phases as well as their relative proportions. Ultimately the behaviour and properties of cement can only be understood by determining the development of microstructure and hydration mechanisms of cement itself, rather than any model system.

Image analysis of backscattered electron images of polished cement pastes provides a technique whereby the microstructure of cement can be characterised numerically and thus provides a basis for the systematic improvement of cement properties.

APPENDIX I

The Bogue Calculation

Specimen calculation (from Taylor, 1964)

(i) Chemical analysis of cement or clinker

SiO_2	21.27%	Na_2O	0.34%
Al_2O_3	6.01	K_2O	0.51
Fe_2O_3	2.73	SO_3	1.84
TiO_2	0.21	Loss	1.32
MgO	1.84	Insol.	0.24
CaO*	63.20	Total	99.51

* Total CaO: includes free CaO, 0.46%

(ii) Recalculate the four main oxides, and also SO_3 in the case of a cement, as moles per analysis total. In the case of CaO, first deduct the free CaO.

SiO_2	= 21.27/60.09	= 0.3540
Al_2O_3	= 6.01/101.96	= 0.0589
Fe_2O_3	= 2.73/159.69	= 0.0171
CaO	= 62.74/56.08	= 1.1188
SO_3	= 1.84/80.06	= 0.0230

(iii) Calculate SO_3 as gypsum (in the case of a cement).

Gypsum = 0.0230 x 172.17 = 3.96%

(iv) Calculate Fe_2O_3 as C_4AF.

C_4AF = 0.0171 x 485.97 = 8.31%

(v) Calculate remaining Al_2O_3 as C_3A.

C_3A = (0.0589 - 0.0171) x 270.20 = 0.0418 x 270.20 = 11.29%

(vi) Add up the amounts (in moles) of CaO present as gypsum, as C_4AF, and as C_3A. Deduct the total from the amount of CaO given in paragraph (ii). Let C be the amount of residual CaO thus obtained, and let S be the amount of SiO_2, which is also given in paragraph (ii).

CaO as gypsum, etc = 0.0230 + (4 x 0.0171) + (3 x 0.0418) = 0.2168

whence

C = 1.1188 - 0.2168

= 0.9020

S = 0.3540

(vii) Calculate C_3S and C_2S. If there are x moles of C_3S and y moles of C_2S, then

$3x + 2y = C$ and $x + y = S$

whence

$x = C - 2S$ and $y = 3S - C$

Thus

$$x = 0.9020 - (2 \times 0.3540)$$

$$= 0.9020 - 0.7080$$

$$= 0.1940$$

$$C_3S = 0.1940 \times 228.33 = \underline{44.30\%}$$

$$y = (3 \times 0.3540) - 0.9020$$

$$= 1.0620 - 0.9020$$

$$= 0.1600$$

$$C_2S = 0.1600 \times 172.25 = \underline{27.56\%}$$

(viii) Minor phases: results. Include also MgO (periclase) and free CaO.

C_3S	44.30	CaO	0.46
C_2S	27.56	MgO	1.84
C_3A	11.29	Gypsum	3.96
C_4AF	8.31	Total	97.72

(ix) Check. The total so obtained should be lower than the analysis total by the amounts of the minor oxides not included in the calculation (Na_2O, K_2O, TiO_2), together with the insoluble residue and that part of the loss which is not present in the gypsum.

Alkalis, etc = 0.34 + 0.51 + 0.21 + 0.24 + 1.32 - (0.0230 x 36)%

= 1.79%

97.72 + 1.79 = 99.51% = analysis total in paragraph (i)

APPENDIX II

Experimental and Theoretical Details of QXDA

The method used here was developed by Mr W. A. Gutteridge of the Cement and Concrete Association (Gutteridge, 1984).

10g of cement and 2g of rutile are milled together to a size of less than 5 μm in an agate ball mill with cyclohexane as a grinding aid. Three sub-samples are taken from this mixture; one is used for QXDA whilst the remaining two are each subjected to a selective dissolution procedure KOSH and SAM.

The interstitial phase is dissolved by the KOSH procedure. 3g of cement is stirred for 2 minutes in 100 ml of boiling KOH (10%), sugar (10%) aqueous solution. The residue is removed by filtration, washed in turn by a KOH-sugar solution and acetone, and dried.

The silicate phases are removed by the SAM procedure. 5g of cement is treated with a 1:5 salicylic acid and dry methanol mixture for 1 hour. The residue is filtered, washed and dried.

Qualitative analyses obtained from the residues of the sub-samples determine which of the primary standard data sets are to be used in the QXDA.

The untreated cement sample is prepared for the diffractometer by loading a sample holder from the back to minimise the effects of preferred orientation. Intensity data is collected over the range 25 to 38 degrees with a count time of 20 seconds at each interval of 0.05° 2-theta.

Each set of primary standard data contains 261 values (collected with a count time of 100 seconds at each interval of 0.05 degrees). The first value in the set is the normalised intensity N_1 at 25° two theta; the second value is the normalised intensity N_2 at 25.05 degrees and so on. Likewise the cement data set contains exactly the same number of corresponding values. Thus 261 linear equations could be established using the selected M primary standards:

$$(Np)\ \text{cement} = \sum_{x=1}^{x=M} (Np)_x . W_x + B_p$$

where Bp represents the background contribution to the cement data at [25 + (p-1).0.05] degrees two theta, W_x is the weight fraction of the x-th primary standard. By introducing a broadening factor the data of a primary standard can be broadened to simulate a decrease in crystallite size. Some lateral shifts can also be introduced so as to enhance the fit of the data. Values for W_x are obtained from the 261 equations by the method of least squares. A reliability factor R is calculated using the following relation which gives an assessment of the fit of the QXDA with the experimental data:

$$\sum_{p=1}^{p=261} \left[(Np)\text{cement} - \sum_{x=1}^{x=M} (Np)_x . W_x\right) + Bp\Big]^2 \Bigg/ \sum_{p=1}^{p=261} \left((Np)\text{cement}\right)^2$$

Both R and the sum of the individual weight fractions (expressed as a weight percentage) are used to assess the reliability of the analysis. It has been found that the quantitative analysis of an anhydrous portland cement appears to be reliable when R is less than 0.01 and the total is 100 ± 2%.

APPENDIX III

Wexham Calorimeter - Imperial College Set-Up

Fig AIII shows the system diagramatically.

The hardware consists of:

1 Wexham calorimeters with water temperature control system;

2 Wexham heater and DVM control box. The DVM has been modified here by adding a BCD card (from Amplicon);

3 Dolphin matrix printer;

4 Wexham twin pen y-t recorder;

5 Apple II plus (Europlus) 48K microcomputer including

a) dual floppy drive

b) thunder clock

c) printer interface

d) three home-built interfaces;

6 Home-built relay box for switching DVM between calorimeters.

The computer, through the three home-built interfaces, can switch the DVM between calorimeters, fetch the DVM reading in BCD, drive the chart recorder (in t) and give a y signal to the recorder (with 8 bit resolution, i.e. 1 in 256).

The calorimeter programs

Programs have been written to perform the following functions.

1 Data acquisition, CALPR - controls acquisition of data from calorimeters. The data is filed on floppy disc and may be monitored as a running table and/or graphical display. Three timing options are available:

1) Single time series of regular intervals;

2) Two sequential time series, each of regular intervals;

3) Logarithmic time intervals.

2 Calibration, CALIB - called by CALPR at end of run and consists of solving the first order differential heat equation of the system:

$$W = \frac{dQ}{dt} = K_1 E + K_2 \frac{dE}{dt}$$

where E is the thermal EMF measured, W the power production, Q the total heat generated and K_1 and K_2 constants. During calibration the power is $W_H + W_S$, where W_H is the known heater power and W_S the residual specimen power (assumed constant over the calibration period).

$$E = \frac{W_H + W_S}{K_1} + Ae^{-\frac{K_1 t}{K_2}}$$

Using appropriate boundary conditions K_1 and K_2 can be calculated from the steady state EMF (E_p) attained during calibration and the time ($t_{1/e}$) taken to reach 0.632 Ep.

The system automatically collects thermocouple data during calibration and writes the calculated K_1 and K_2 to the data file.

3 Processing, POWER - converts thermocouple voltages to power values using the first order differential heat equation and K_1 and K_2. This program also has options for:

editing of voltage files to remove spikes;

smoothing of power tables;

plotting and tabulating voltages, power values and integrated power values.

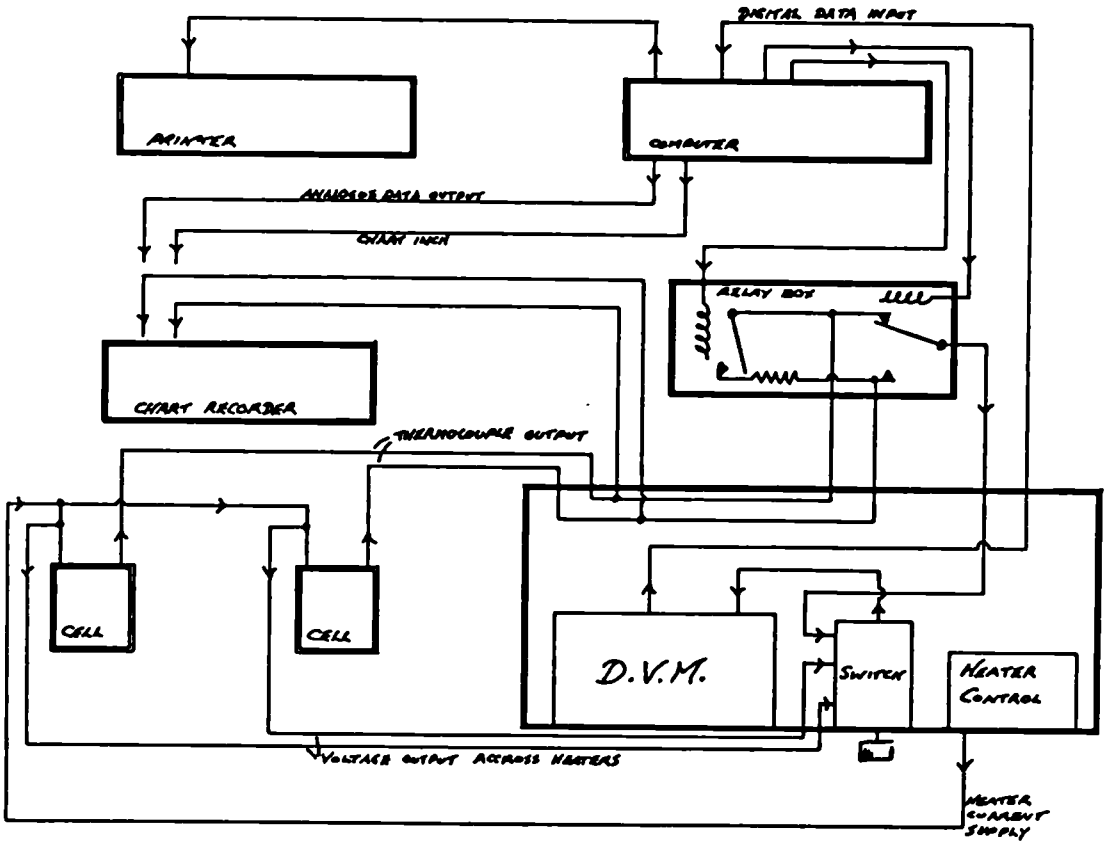

FIG. AIII Diagram of Wexham Calorimeter –
Imperial College set up

References

ALDRIDGE, L. P. (1982) 'Accuracy and Precision of an X-Ray Diffraction Method for Analysing Portland Cement', Cem. Concr. Res. 12, 437-446

ALLEN, T. (1981) 'Particle size measurement', 3rd ed, (Chapman and Hall, London)

ALLINSON, D. L. (1970) 'Environmental cell for use in a high voltage electron microscope', Proc. 7th Int. Cong. Electron Microsc. 1, 169

ALLINSON, D. L., GOSNOLD, A. W. O. and LOVEDAY, M. S. (1972) 'Modified environmental cell for use in a high voltage electron microscope', Proc. 5th Europ. Cong. Electron Microsc., 336

ALLINSON, D. L., LOVEDAY., M. S., GOSNOLD, A. W. O. and HALE, K. F. (1973) 'Applications of the NPL environmental cell', J. Microsc. 97, 209

ANDREEVA, E. P. and KESHELAUA, B. F. (1976) 'Study of the kinetics of dissolution and crystallisation in suspensions of di- and tricalcium silicates', Usp. Kolloidn. Khim. 230; Chem. Abstr. 88: 11041 (quoted in Skalny and Young 1980)

BAILEY, J. E. and HAMPSON, C. S. (1982) 'The Chemistry of the aqueous phase of portland cement', Cem. Concr. Res. 12, 227-236

BAILEY, J. E. and STEWART, H. R. (1984), 'Relationships between microstructural development and the physicochemical nature of OPC. pastes', Proc. Brit. Ceram. Soc. 'Chemistry and Chemically-Related Properties of Cement' (London, 12-13 April, to be published)

BALEK, V. and DOHNÁLEK, J. (1983) 'A new method for investigating cement hydration by radioactive indicators', Cem. Concr. Res. 13, 1-6

BARNES, B. D., DIAMOND, S. and DOLCH, W. L. (1978a) 'The contact zone between Portland cement pastes and glass "aggregate" surfaces', Cem. Concr. Res. 8, 233-243

BARNES, B. D., DIAMOND, S. and DOLCH, W. L. (1978b) 'Hollow shell hydration of cement particles in bulk cement pastes', Cem. Concr. Res. 8, 263-272

BARNES, B. D., DIAMOND, S. and DOLCH, W. L. (1979) 'Micromorphology of the interfacial zone around aggregates in portland cement mortar', J. Am. Ceram. Soc. 62, 21-24

BARNEYBACK, R. S. Jr. and DIAMOND, S. (1981) 'Expression and analysis of pore fluids from hardened cement pastes and mortars', Cem. Concr. Res. 11, 279-286

BARRET, P., BERTRANDIE, D. and MÉNÉTRIER, D. (1980b), 'Etude comparée de la formation de C-S-H à partir de solutions sursaturées et de mélanges C_3S solution'. Proc. 7th Int. Congr. Chem. Cem., Paris 4, II.261-II.266

BARRET, P., MÉNÉTRIER, D., BERTRANDIE, D. and REGOURD., M (1980a) 'Thermodynamic and kinetic aspects of the dissolution of C_3S and formation of C-S-H', Proc. 7th Int. Congr. Chem. Cem., Paris II, II-279-II-284

BEKE, B. and OPOCZKY, L. (1969) 'Feinstmahlung von Zementklinker', Zem. Kalk. Gips. 12, 541-546

BEN-DOR, L. (1983) 'Thermal Methods', in 'Advances in cement technology', ed S. N. Ghosh (Pergamon Press), 673-711

BENSTED, J. (1978) 'γ-dicalcium silicate and its hydraulicity', Cem. Concr. Res. 8, 73-76

BENSTED, J. (1982) 'Chemical Aspects of Normal Setting of Portland Cement' in "Characterisation and Performance Prediction of Cement and Concrete" (Engineering Foundation)

BENSTED, J. (1983) 'Hydration of portland cement', in 'Advances in Cement Technology' ed S. N. Ghosh (Pergamon Press), 307-347

BENSTED, J. and VARMA, S. P. (1974) 'Some applications of infra-red and Raman spectroscopy in cement chemistry - Part I: Examination of dicalcium silicate', Cem. Tech. 5, 256-261

BERGER, R. L., FROHNSDORFF, G. J. C., HARRIS, P. H. and JOHNSON, P. D., (1966) 'Application of X-ray diffraction to routine mineralogical analysis of portland cement', in Highways Research Board SR90, 'Structure of Portland Cement Paste and Concrete', 234-253

BERGER, R. L., BENTUR, A., MILESTONE, N. B. and KUNG, J. H. (1979) 'Structural Properties of Calcium Silicate Pastes: I, Effect of the Hydrating Compound', J. Am. Ceram. Soc. 62 358-362

BIKBAU, M. Y. (1974) 'On Hydration activity of silicates', Proc. 6th Int. Congr. Chem. Cem., Moscow, Supp. paper Section II, 1-6, II-1

BIRCHALL, J. D. and THOMAS, N. L. (1984) 'The mechanism of retardation of OPC. setting by sugars', Proc. Brit. Ceram. Soc. "Chemistry and Chemically-Related Properties of Cement",(London, 12-13 April). To be published

BIRCHALL, J. D., HOWARD, A. J., BAILEY, J. E. (1978) 'On the hydration of portland cement', Proc. Roy. Soc. Lond. A, 360, 445-453

BOGUE, R. H. (1929) 'Ind. Eng. Chem. analyt. Edn 1 (4), 192

BOGUE, R. H. and LERCH, W. (1934) 'Hydration of portland cement compounds' Ind. Eng. Chem. 26, 837-847

BOIKOVA, A. (1980) 'Cement minerals of complicated composition', Proc. 7th Int. Congr. Chem. Cem., Paris II, I.6-I.11

BOIKOVA, A., DOMANSKY, A. I., PARNYONOVA, V. A., STAVITSKAJA, G. P., NIKUSHCHENKO, V. M. (1977) 'The influence of Na_2O on the structure and properties of $3CaO.Al_2O_3$', Cem. Concr. Res. 7, 483-492

BOMBLED, J. P. (1980) 'Influence de sulfates sur les comportements rhéologiques des pâtes de ciment et sur leur évolution', Proc. 7th Int. Congr. Chem. Cem., Paris III, VI.165-VI.169

BREVAL, E. (1976) 'C_3A hydration', Cem. Concr. Res. 6, 129-138

BROWN, P. W., FRANZ, E., FROHNSDORFF, G. and TAYLOR, H. F. W. (1984) 'Analyses of the aqueous phase during early C_3S hydration', Cem. Concr. Res. 14, 257-262

BROWN, P. W. and LACROIX, P. (1984) 'Kinetics of C_3A-$CaSO_4$ Reaction', paper given at 86th annual meeting of the Am. Ceram. Soc, Ceramic Bull. 63, 469

BROWN, P. W. (1984a) to be published

BROWN, P. W. (1984b) Unpublished observation

BUDNIKOV, P. P. and STRELKOV, M. I. (1966) 'Some recent concepts on portland cement hydration', in Highways Research Board Special Report 90, 'Structure of Portland Cement Paste and Concrete', 447-464

BYE, G. (1983) 'Portland Cement Composition, Production and Properties' (Institute of Ceramics, Pergamon Press, Oxford)

CARLSON, E. T. (1964) 'Action of Water on Calcium Aluminoferrites', J. Res. NBS A. Phys. Chem. 68A, 453-463

CARLSON, E. T. (1966) 'Some properties of the calcium aluminoferrite hydrates', Building Science Series 6, National Bureau of Standards, (United States Department of Commerce)

CARLSON, R. W. (1934) 'The vane calorimeter', Proc. ASTM 46, 1252-1292

CASSON, R. B. J., DOMONE, P. L., SCRIVENER, K., JENNINGS, H. M., GILHAM, C. J. and PRATT, P. L. (1982) 'The Use of Ultrasonic Pulse Velocity, Penetration Resistance and Electron Microscopy to Study the Rheology of Fresh Concrete', in "Concrete Rheology", Proceedings, Symposium 'M', Ann. Meet. MRS November, ed J. Skalny

CERVANTES LEE, F. R. and GLASSER, F. P. (1979) J. Applied Cryst. 12, 407-410

CHATTERJI, S. (1980), 'Mechanisms of retardation of C_3A: a critical evaluation', Proc. 7th Int. Congr. Chem. Cem., Paris, IV, 465-470

CHATTERJI, S. and JEFFREY, J. W. (1966) 'The Three Dimensional Arrangement of Hydration Products in Set Cement Paste' Nature 209, 1233-1234

CIACH, T. D. and SVENSON, E. G. (1971) 'Morphology and Microstructure of Hydrating Portland Cement and its Constituents. II. Changes in hydration of calcium silicates alone and in the presence of triethamolamine and calcium lignosulphate', Cem. Concr. Res. 1, 159-176

COLLEPARDI, M., BALDINI, G., PAURI, M. and CORRADI, M. (1978) 'Tricalcium aluminate hydrate hydration in the presence of lime, gypsum or sodium sulphate', Cem. Concr. Res. 8, 571-580

COLLEPARDI, M., BALDINI, G., PAURI, M., and CORRADI, M. (1979) 'Retardation of tricalcium aluminate hydration by calcium sulphate', J. Am. Ceram. Soc. 69, 33-35

COLLEPARDI, M., MONOSI, S., MORICONI, G. and CORRADI, M. (1979) 'Tetracalcium Aluminoferrite Hydration in the Presence of Lime and Gypsum', Cem. Concr. Res. 9, 431-438

COPELAND, L. E. and SCHULTZ, E. G. (1960), discussion of paper by Grudemo, Proc. 4th Int. Sym. Chem. Cem, Washington, I, 648-655

COPELAND, L. E. and SCHULTZ, E. G. (1962) Journal of the PCA 4, 2-12

CORSTANJE, W. A., STEIN, H. N. and STEVELS, J M (1973, 1974) 'Hydration Reactions in Pastes C_3S + C_3A + $CaSO_4.2aq$ + water at 25°C', pt I, Cem. and Concr. Res. 3, 791-806, pt II, Cem. Concr. Res 4, 193-202, pt III, Cem. Concr. Res. 4, 417-431

DALGLEISH, B. J., PRATT, P. L. and MOSS, R. I. (1980) 'Preparation Techniques and the Microscopical Examination of Portland Cement Paste and C_3S', Cem. Concr. Res. 10, 665-676

DALGLEISH, B. J., PRATT, P. L. and TOULSON, E. (1982a) 'Fractographic studies of early hydration products in cement paste', J. Mat. Sci. 17, 2199-2207

DALGLEISH, B. J., GHOSE, A., JENNINGS, H. M. and PRATT, P. L. (1982b) 'The correlation of microstructure with setting and hardening in cement paste', Int. Conf. Concr. at Early Ages, Paris 1, 137-143

DALGLEISH, B. J. and IBE, K. (1981) 'Thin Foil Studies of Hydrated Portland Cement', Cem. Concr. Res. 11, 729-739

D'ANS, J. and EICK, H. (1953a) 'The system $CaO-Al_2O_3-H_2O$ at a temperature of 20°C and the hardening of aluminous cements', Zem. Kalk. Gips. 6, 197-210

D'ANS, J and EICK, H (1953b) 'Das System $CaO-Al_2O_3-CaSO_4-H_2O$ bei 20°C', Zem. Kalk. Gips 6, 302-311

DE KEYSER, W. L. and TENOUTASSE, N. (1968) 'The Hydration of the Ferrite Phase of Cements', Proc. 5th Int. Symp. Chem. Cem., Tokyo, supplementary paper II-120, II, 379-386

DIAMOND, S. (1976) 'Cement paste microstructure - an overview at several levels', in "Hydraulic Cement Pastes: their Structure and Properties" (Cement and Concrete Association) 2-30

DIAMOND, S. and LOPES-FLOREZ, F. (1981) 'Fate of Calcium Chloride Dissolved in Concrete Mix Water', J. Am. Ceram. Soc. 64, C162-C164

DOUBLE, D. D. (1973) 'Some Studies of the Hydration of Portland Cement Using High Voltage (1 MeV) Electron Microscopy', Mater. Sci. and Eng. 12, 29-34

DOUBLE, D. D. (1983) 'New developments in understanding the chemistry of cement hydration', Phil. Trans. R. Soc. London A 310, 52-56

DOUBLE, D. D., HELLAWELL, A. and PERRY, S. J. (1978) 'The hydration of portland cement', Proc. R. Soc. Lond. A 359, 435-451

EITEL, W. (1957) 'Recent investigations of the system lime-alumina-calcium sulphate-water and its importance in building research problems', J. Amer. Concr. Inst. 28, 679-698

FELDMAN, R. F. and RAMACHANDRAN, V. S. (1966) 'The influence of $CaSO_4.2H_2O$ upon the hydration character of $3CaO.Al_2O_3$', Mag. Concr. Res. 18, 185-196

FIERENS, P. and VERHAEGEN, J. P. (1976a) 'Properties nucleophile de surfaces de C_3S', Cem. Concr. Res. 6, 103-111

FIERENS, P. and VERHAEGEN, J. P. (1976b) 'Induction Period of Hydration of C_3S', Cem. Concr. Res. 6 287-296

FIERENS, P. and VERHAEGEN, J. P. (1976c) 'Hydration of tricalcium silicate in paste - kinetics of calcium ion dissolution in the aqueous phase', Cem. Concr. Res. 6, 337-342

FIERENS, P. and TIRLOCQ, J. (1983), 'Nature and Concentration Effect of Stabilising Elements of Beta-Dicalcium Silicate on its Hydration Rate', Cem. Concr. Res. 13, 267-276

FLOWER, H. M. (1973) 'High voltage electron microscopy of environmental reactions', Microscopy 97, 171-190

FORRESTER, J. A. (1970) 'A conduction calorimeter for the study of cement hydration', Cem. Tech. 1 95-99

FORRESTER, J. A. (1980) 'Shear mixed cement pastes', Poster, 7th Int. Congr. Chem. Cem., Paris

FUJII, K. and KONDO, W. (1974), 'Kinetics of the Hydration of Tricalcium Silicate', J. Am. Ceram. Soc. 57 492-497

FUJII, K. and KONDO, W. (1979) 'Rate and Mechanism of Hydration of β-Dicalcium Silicate', J. Am. Ceram. Soc. 62, 161-167

FUKUHARA, M., GOTO, S., ASAGA, K., DAIMON, M and KONDO, R, 'Mechanisms and kinetics of C_4AF hydration with gypsum', Cem. Concr. Res. 11, 407-414

FUNDAL, E., 'Optical Microscopy of Cement Clinker and Raw Mixes', FLS Review No. 25 (F L Smidth, Copenhagen)

FUNK, H. (1960), 'Two Different Ways of Hydration in the Reaction of β-Ca_2SiO_4 with Water at 25-120°C', Proc. 4th Int. Symp. Chem. Cem. paper III-S7, I, 291-295

GHOSE, A. (1980), Ph.D thesis, University of London

GHOSH, S. N. (1983) 'Portland Cement Phases: Polymorphism, Solid Solution, Defect Structure and Hydraulicity', in "Advances in Cement Technology", ed S. N. Ghosh (Pergamon Press), 289-305

GHORAB, H.Y., HEINZ, D., LUDWIG, U., MESKENDAHL, T., and WOLTER, A. (1981) 'On the Stability of Calcium Aluminate Hydrates in Pure Systems and in Cements', Proc. 7th Int. Cong. Chem. Cem., Paris, IV, 496-503

GHOSH, S.N., RAO, P.Q., PAUL, A.K. and RAINA, K. (1979) 'Review: The Chemistry of Dicalcium Silicate Mineral', J. Mat. Sci. 14, 1554-1566

GREENE, K.T. (1960), 'Early hydration reactions of portland cement', Proc. 4th Int. Sym. Chem. Cem., Washington, I, paper IV-1, 359-385

GROVES, G.W. (1981), 'Portland cement clinker viewed by transmission electron microscopy', J. Mat. Sci. 16 1063-1070

GROVES, G.W. (1982) 'Twinning in β-Dicalcium Silicate', Cem. Concr. Res. 12, 619-625

GRUDEMO, A. (1960) 'The Microstructure of Hardened Cement Paste', Proc. 4th Int. Symp. Chem. Cem., Washington, paper V-2, I, 615-647

GRUDEMO, A. (1964) 'Electron Microscopy of Portland Cement Pastes', in "The Chemistry of Cements', ed H.F.W. Taylor (Academic Press) I, 371-389

GUPTA, P., CHATTERJI, S. and JEFFERY, J.W. (1973) 'Studies of the effects of various additives on the hydration reactions of tricalcium aluminate. Part 5'. Cem. Tech. 4, 146-149

GUTT, W. and OSBORNE, G.J. (1970) 'The effect of potassium on the hydraulicity of dicalcium silicate'. Cem. Tech. 1, 121-125

GUTTERIDGE, W.A. (1984), 'Quantitative X-Ray Powder Diffraction in the Study of Some Cementive Materials', Proc. Brit. Ceram. Soc. "Chemistry and Chemically-Related Properties of Cement", (London, 12-13 April), to be published

GUTTERIDGE, W.A. and POMEROY, C.D. (1983), 'Cement in its conventional uses: problems and possibilities', Phil. Trans. R. Soc. Lond. A 310, 7-15

HANSEN, W.C. (1952) discussion of paper by Steinour, Proc. 3rd Int. Sym. Chem. Cem., London, 318-321

HARADA, T., OHTA, M. and TAKAGI, S. (1978) 'Effect of polymorphism of tricalcium silicate on hydration and structural characteristics of hardened pastes', Yogo. Kyokai Shi 86, 7 (quoted in Skalny and Young, 1980)

HOFMANNER, F. (1975) 'Microstructure of Portland Cement Clinker', ("Wolderbank" Management and Consulting Ltd, May)

HOLTEN, C.L.M. and STEIN, H.N. (1977) 'Influence of quartz surfaces on the reaction C_3A + $CaSO_4.2H_2O$ + water', Cem. Concr. Res. 7, 291-296

INGS, J.B., BROWN, P.W., FROHNSDORFF, G. (1983) 'Early hydration of large single crystals of tricalcium silicate', Cem. Concr. Res. 13, 843-848

JAVELAS, R., MASO, J.C., OLLIVIER, J.P., THENOZ, B, (1975) 'Observation directe au microscope électronique par transmission de la liason de ciment-granulats dans des mortiers de calcite et de quartz', Cem. and Concr. Res. 5, 285-294

JAWED, I., GOTO, S. and KONDO, R. (1976) 'Hydration of Tetracalcium Aluminoferrite in the Presence of Lime and Sulphates', Cem. Concr. Res. 6 441-454

JEFFERY, J. W. (1952) Acta. Cryst. 5, 26

JELENIC, I., BEZJAK, A. and BUJAN, M. (1978) 'Hydration of B_2O_3-Stabilised α' and β modifications of C_2S', Cem. Concr. Res. 8, 173-180

JENNINGS, H. M. (1983) 'The Developing Microstructure in Portland Cement', in "Advances in Cement Technology", ed S. N. Ghosh (Pergamon Press), 349-396

JENNINGS, H. M. (1984) to be published

JENNINGS, H. M. and PRATT, P. L. (1979a) 'On the hydration of portland cement', Proc. Brit. Ceram. Soc. 'Mineralogy of Ceramics' 28, 179-193

JENNINGS, H. M. and PRATT, P. L. (1979b) 'An experimental argument for the existence of a protective membrane surrounding portland cement during the induction period', Cem. Concr. Res. 9, 501-506

JENNINGS, H. M. and PRATT, P. L. (1980) 'On the Reactions Leading to Calcium Silicate Hydrate, Calcium Hydroxide and Ettringite during the Hydration of Cement', Proc. 7th Int. Congr. Chem. Cem., Paris, II: II. 141-II.146

JENNINGS, H. M., DALGLEISH, B. J. and PRATT, P. L. (1981) 'Morphological development of hydrating tricalcium silicate as examined by electron microscopy techniques', J. Am. Ceram. Soc. 64, 567-572

JONES, F. E. (1939) 'The Quaternary System $CaO-Al_2O_3-CaSO_4-H_2O$ at 25°C', Trans. Faraday Soc., 35, 1484-1510

JONES, F. E. (1944) 'Quaternary System $CaO-Al_2O_3-CaSO_4-H_2O$ at 25°C; Equilibria with Crystalline $Al_2O_3.3H_2O$, Alumina Gel and Solid Solutions', J. Phys. Chem. 48, 311-356

JONES, F. E. (1944a) 'The Quinary System $CaO-Al_2O_3-CaSO_4-K_2O-H_2O$ (1% KOH) at 25°C', J. Phys. Chem. 48, 356-378

JONES, F. E. (1944b) 'The Quinary System $CaO-Al_2O_3-CaSO_4-Na_2O-H_2O$ (1% NaOH at 25°C), J. Phys. Chem. 48, 379-394

JONES, F. E. (1960) 'Hydration of Calcium Aluminates and Ferrites', Proc. 4th Int. Symp. Chem. Cem, Washington, I, 204-246

JONES, F. E. and ROBERTS, M. H. (1962) 'The System $CaO-Al_2O_3-H_2O$ at 25°C' Building Research Current Papers, Research Series June 1962

de JONG, J. G. M., STEIN, H. N. and STEVELS, J. (1967) 'Hydration of tricalcium silicate', J. Appl. Chem. 17, 246-250

de JONG, J. G. M., STEIN, H. N., and STEVELS, J. (1968) 'The influence of aluminium hydroxide and lime on the hydration of C_3S', J. Appl. Chem. 18, 9-17

de JONG, J. G. M., STEIN, H. N. and STEVELS, J. M. (1968) 'Mutual interaction of C_3A and C_3S during hydration', Proc. 5th Int. Symp. Chem. Cem., Tokyo, Supplementary paper II-35, II, 311-320

JONS, E. S. and OSBAECK, B. (1980), 'The influence of the content and distribution of Al_2O_3 on the hydration properties of portland cement', Proc. 7th Int. Cong. Chem. Cem., Paris, IV, 514-519

JONS, E. S. and OSBAECK, B. (1982) 'The Effect of Cement Composition on Strength Described by a Strength-Porosity Model', Cem. Concr. Res. 12, 167-178

KALOUSEK, G. L. (1976), 'Differential Thermal Analysis Tests of Hydrated Cements and Individual Hydrates', in Transportation Research Circular no. 176, June, "Evaluation of Methods of Identifying Phases of Cement Paste", 30-41

KALOUSEK, G. L. and ROY, R. (1957) 'Crystal Chemistry of Hydrous Calcium Silicates: II, Characterisation of Interlayer Water', J. Am. Ceram. Soc. 40, 236-239

KALOUSEK, G. L., JUMPER, C. H. and TREGONING, J. J. (1943) 'Composition and physical properties of aqueous extracts from portland cement clinker pastes containing added material', J. Res. NBS 30, 215-253

KAMINSKI, M. and ZIELENKIEWICZ, W. (1982) 'The Heats of Hydration of Cement Constituents', Cem. Concr. Res. 12, 549-558

KANTRO, D. L., BRUNAUER, S. and WEISE, C. H. (1962) 'Development of surface in the hydration of calcium silicates: II Extension of earlier investigations to earlier and later stages of hydration', J. Phys. Chem. 66, 1804

KAUSHUNSKII, V. E. and TIMASHEV, V. V. (1978) 'Lattice defects in a solid solution of Al_2O_3 in tricalcium silicate', Inorg. Mater. 14, 854-856

KONDO, R. and DAIMON, M. (1969) 'Early hydration of C_3S: A solid reaction with induction and acceleration periods', J. Am. Ceram. Soc. 52, 503-508

KONDO, R. and UEDA, S. (1968) 'Kinetics of Mechanisms of the Hydration of Cements', Proc. 5th Int. Symp. Chem. Cem., Tokyo, Principal paper II-4, II, 203-255

KNUDSEN, T. (1980) 'On the particle size distribution in cement hydration', Proc. 7th Int. Congr. Chem. Cem, Paris, II, I-170-I-175

KNUDSEN, T. (1982) 'Modelling hydration of portland cement', in "Characterisation and Performance Prediction of Cement and Concrete' (Engineering Foundation), 125-149

KRISTMANN, K. (1978) 'Portland cement clinker mineralogical and chemical investigations, Pt II Electron Microprobe Analysis', Cem. Concr. Res. 8 93

KURCZYK, H. G. and SCHWIETE, H. E. (1960) 'Concerning the hydration products of C_3S and β-C_2S', Proc. 4th Int. Symp. Chem. Cem., Washington, paper III-S13, I 349-358

LACHOWSKI, E. E., MOHAN, K., TAYLOR, H. F. W. and MOORE, A. E. (1980) 'Analytical Electron Microscopy of Cement Pastes, Pt II Pastes of Portland Cements and Clinkers', J. Am. Ceram. Soc., 63, 447-452

LACHOWSKI, E. E. and DIAMOND, S. (1983a) 'Investigations of the composition and morphology of individual particles of portland cement paste: 1. C-S-H gel and calcium hydroxide particles', Cem. Concr. Res. 13, 177-185

LACHOWSKI, E. E. and DIAMOND, S. (1983b) 'Investigations of the composition and morphology of individual particles of portland cement paste: 2. Calcium sulphoaluminates', Cem. Concr. Res. 13, 335-340

LAWRENCE, C. D. (1966) 'Changes in the composition on the aqueous phase during hydration of cement pastes and suspensions', in Highways Research Board SR90, "Structure of Portland Cement Paste and Concrete', 378-391

LAWRENCE, F. V. Jr., REID, D. A. and De CARUACHO, A. A. (1974) 'Transmission Electron Microscopy of Hydrated Dicalcium Silicate Thin Films', J. Am. Ceram. Soc. 57, 144-148

LEA, F. M. (1970) 'The Chemistry of Cement and Concrete', 3rd ed, (Edward Arnold Ltd)

LERCH, W. (1946) 'The influence of gypsum on the hydration reactions of portland cement', Proc. ASTM 46, 1252

LOCHER, F. W., RICHARTZ, W. and SPRUNG, S. (1980) 'Setting of cement', Zem. Kalk. Gips 33, pt 6, 271-277, English translation Zem. Kalk. Gips 33, pt 8, 150-153

LONGUET, P., BURGLEN, L. and ZELWAR A. (1973) 'The liquid phase of hydrated cement' (in French), Rev. Mater. Constr. 676, 35-41

MAKI, I. and CHROMY, S. (1978) Il Cemento, 3, 247

MARINHO, M. B. and GLASSER, F. P. (1984) 'The Early Stages of the Hydration of Tricalcium Aluminate and its Sodium-containing Solid Solutions', Proc. Brit. Ceram. Soc. 'Chemistry and Chemically-Related Properties of Cement' (London, 12-13 April), to be published

MASCOLO, G., MARCHESE, B., FRIGIONE, G. and SERSALE, R. (1973), 'Influence of polymorphism and stabilising ions on the strength of alite', J. Am. Ceram. Soc., 56, 222-223

MATHER, K. (1976) 'Examination of Cement Pastes, Hydrated Phases, and Synthetic Products by X-Ray Diffraction', in Transportation Research Circular No 176, June, "Evaluation of Methods of Identifying Phases of Cement Paste", 9-30

MAYCOCK, J. N., SKALNY, J. and KALYONCU, R. (1974) 'Crystal Defects and Hydration, I. Influence of Lattice Defects', Cem. Concr. Res. 4, 835-847

MEHTA, P. K. (1969) 'Morphology of calcium sulphoaluminate hydrates', J. Am. Ceram. Soc. 52, 521-522

MEHTA, P. K. (1976) 'Scanning Electron Micrographic Studies of Ettringite Formation', Cem. Concr. Res. 6, 169-182

MÉNÉTRIER, D., JAWED, I., SUN, T. S. and SKALNY, S. (1979) 'ESCA and SEM studies on early C_3S hydration', Cem. Concr. Res. 9, 473-482

MÉNÉTRIER, D., McNAMARA, D. K., JAWED, I. and SKALNY, J. (1980) 'Early hydration of β-C_2S: Surface Morphology', Cem. Concr. Res. 10, 107-110

MIDGLEY, H. G. (1974) 6th Int. Congr. Chem. Cem., Moscow, Suppl. paper Section I

MOORE, A. E. (1964) 'Comparison of the results obtained for the compound composition of portland cements by X-ray diffraction, microscopy and wet chemical methods', in "Analysis of Calcareous Materials', Monograph 18 (Soc. Chem.Ind.), 372-386

NURSE, R. W. (1952) 'The dicalcium silicate phase', Proc. 3rd Int. Symp. Chem. Cem., London, 56-77

NURSE, R. W., MIDGLEY, H. G., GUTT, W. and FLETCHER, K. (1960), 'Effect of polymorphism of tricalcium silicate on its reactivity', in Highways Research Board SR90, "Structure of Cement and Concrete", 258-268

ODLER, I. and DÖRR, H. (1979) 'Early Hydration of Tricalcium Silicate. II. The Induction Period', Cem. Concr. Res. 9, 277-284

ODLER, I. and SCHÜPPSTUHL, J. (1981) 'Early Hydration of Tricalcium Silicate. III Control of the Induction Period', Cem. Concr. Res. 11, 765-774

ODLER, I. and SCHÜPPSTUHL, J. (1982) 'Combined Hydration of Tricalcium Silicate and β-Dicalcium Silicate', Cem. Concr. Res. 12, 13-20

ONO, Y., KAWAMURA, S. and SODA, Y. (1968) 'Microscopic Observations of Alite and Belite and Hydraulic Strength of Cement', Proc. 5th Int. Symp. Chem. Cem., Tokyo, I, 275-284

PARROTT, L. J. (1983) 'Novel methods of processing cement gel to examine and control microstructure and properties', Phil. Trans. R. Soc. Lond., A 310, 155-166

PEARSON, P., ALLEN, A. and DOUBLE, D. D. (1982) 'An investigation on the nature of porosity in hardened cement paste using small angle neutron scattering', paper given at 4th Seminar on Cement and Concrete Science, Oxford, 16-17 September

PETERSEN, I. F. (1980) 'The pore structure and grindability of clinkers', Proc. 7th Int. Cong. Chem. Cem, Paris, II, I.73-I.78

POBELL, F. and WITTMAN, F. (1965) Phys. Letts. 19, 175

POWERS, T. C. (1961) 'Some physical aspects of the hydration of portland cement' J. Res. Dev. Labs. PCA 3, 47-56

POWERS, T.C. and BROWNYARD, T.L. (1948) 'Studies of the physical properties of hardened portland cement pastes', Bull PCA 22, March

PRATT, P.L. (1982) 'Mechanisms of Hydration of Portland Cement', in "Characterisation and Performance Prediction of Cement and Concrete", (Engineering Foundation), 51-68

PRATT, P.L. and GHOSE, A. (1983) 'Electron microscope studies of portland cement microstructures during setting and hardening', Phil. Trans. R. Soc. Lond, A310, 93-103

PRATT, P.L. and JENNINGS, H.M. (1981) 'The microchemistry and microstructure of portland cement', Ann. Rev. Mater. Sci. 11, 123-149

PRITTS, J.M. and DAUGHERTY, K.E. (1976) 'The effect of stabilising agents on the hydration of β-C_2S', Cem. Concr. Res. 6, 783-796

RAMACHANDRAN, V.S., FELDMAN, R.F. and BEAUDOIN, J.J. (1981) 'Concrete Science, Treatise on Current Research', (Heyden and Son Philadelphia), 54-88

RAYMENT, D.L. and MAJUMDAR, A.J. (1980) 'The composition of CSH phases in hydrated C_3S paste' Proc. 7th Int. Cong. Chem. Cem., Paris, II, II-64

RECHENBERG, W. and SPRUNG, S. (1983) 'Composition of the Solution in the Hydration of Cement', Cem. Concr. Res. 13, 119-126

REGOURD, M. (1979a) 'Fundamentals of cement production: The crystal chemistry of portland cement minerals. New data', in "Cement Production and Use", (Engineering Foundation)

REGOURD, M. (1979b) 'Il Cemento', 75, 323

REGOURD, M. and GUINIER, A. (1974) Principal Paper, Proc. 6th Int. Congr. Chem. Cem., Moscow

REGOURD, M., HORNAIN, H., and MORTUREUX, B. (1976), 'Evidence of calcium silicoaluminates in hydrated mixtures of tricalcium silicate and tricalcium aluminates', Cem. Concr. Res. 6, 733-740

RODGERS, S.A., CLAYDEN, N.J. and DOBSON, C.M. (1984) 'Solid State NMR Studies of Cement Hydration', Proc. Brit. Ceram. Soc, "Chemistry and Chemically-Related Properties of Cement", (London, 12-13 April), to be published

ROGERS, D.E. and ALDRIDGE, L.P. (1977) 'Hydrates of calcium ferrites and calcium aluminoferrites', Cem. Concr. Res. 7, 399-410

ROY, D.M., O'HOLLERAN, T.P. and NEURGAOUKAR, R.R. (1978) 'Il Cemento', 3, 337

ROY, D.M. (1981) 'Portland cement: Constitution and Processing, pt 1 - Cement Manufacture', J.E.M.M.S.E. 3, 625-647

SCHWIETE, H.E. and IWAI, T. (1964) 'Uber das Verhalten der ferritischen Phase im Zement vaahrend de Hydratation', Zem. Kalk. Gips 17, 379-386

SCHWIETE, H. E., LUDWIG , U. and JAGER, P. (1966) 'Investigations in the System $3CaO.Al_2O_3$-$CaSO_4$-CaO-H_2O', in Highways Research Board, SR90, "Structure of Portland Cement Paste and Concrete", 353-367

SCRIVENER, K. L. and PRATT, P. L. (1983) 'Characterisation of Portland Cement Hydration by Electron Optical Techniques', in "Electron Microscopy of Materials", Symp. 'N', Ann. Meet. MRS, November, in press

SCRIVENER, K. L. and PRATT, P. L. (1984a) 'Backscattered Electron Images of Polished Cement Sections in the Scanning Electron Microscope', Proc. 6th Int. Conf. Microscopy of Cements, 26-29 March, in press

SHIN, G. Y. and GLASSER, F. P. (1983) 'Chemistry of Cement Pore Fluids: I Suspension Reactions of $Ca_{3-x}Na_{2x}Al_2O_6$ Solid Solutions with and without Gypsum Additions', Cem. Concr. Res. 13, 366-376

SIERRA, R. (1974) 'Contribution to the kinetic study of hydration of tricalcium silicate', Proc. 6th Int. Congr. Chem. Cem., Moscow, 2, pt 1, 138-143

SINCLAIR, W. J. and GROVES, G. W. (1984a) 'The Structure of Alites', Proc. Brit. Ceram. Soc "Chemistry and Chemically-Related Properties of Cement" (London, 12-13 April,) to be published

SINCLAIR, W. J. and GROVES, G. W. (1984b) 'Transmission Electron Microscopy and X-Ray Diffraction of Doped Tricalcium Silicates', J. Am. Ceram. Soc., 67, 325-330

SKALNY, J. and TADROS, M. E. (1977) 'Retardation of tricalcium aluminate hydrate by sulphates', J. Am. Ceram. Soc. 60, 174

SKALNY, J. and YOUNG, J. F. (1980) 'Mechanisms of Portland Cement Hydration', Proc. 7th Int. Congr. Chem. Cem., Paris, II, II-113-II-1145

SPIERINGS, G. A. C. M. and STEIN, H. N. (1976) 'The influence of Na_2O on the hydration of C_3A', I. Paste hydration, Cem. Concr. Res. 6, 265-272, II. Suspension hydration, Cem. Concr. Res. 6, 487-497

STEIN, H. N. (1961) J. Appl. Chem., 11, 474

STEIN, H. N. (1963) 'Some Characteristics of the Hydration of $3CaO.Al_2O_3$ in the Presence of $CaSO_4.2H_2O$', Silic. Ind. 28, 141-145

STEIN, H. N. (1980) 'The colloid chemistry of calcium aluminate hydrates' Proc. 7th Int. Congr. Chem. Cem, Paris, IV, 449-454

STEINHERZ, A. R. and WELCHMAN, N. (1958) 'The reaction of portland cement with water' (in French), Rev. Mater. Constr. (ed. C), 517, 265-271

ŠTEVULA, L. and PETROVIČ, J. (1981) 'Hydration of polymorphic modifications of C_3S', Cem. Concr. Res. 11, 183-190

STEWART, H. R. and BAILEY, J. E. (1983) 'Microstructural studies of the hydration products of three tricalcium silicate polymorphs', J. Mat. Sci. 18, 3686-3694

STRUBLE, L. (1982) 'A Review of Clinker Analysis by QXRD', in "Characterisation and Performance of Cement and Concrete' (Engineering Foundation, 1983)

STUCKE, M. S. and MAJUMDAR, A. J. (1976) 'The Composition of the Gel Phase in Portland Cement Paste', in "Hydraulic Cement Pastes: their Structures and Properties" (Cement and Concrete Association)

SUZUKI, K., SHIBATA, S. and ITO, S (1978) 'The Hydration and the Strengths of High Temperature Phases of $2CaO.SiO_2$', Review of 32nd Gen. Meeting - Technical Session, Tokyo, May (Cement Association of Japan)

SUZUKI, K., ITO, S., SHIBATA, S. and FUGII, N. (1980) 'Hydration and strength of α-, α'- and β-dicalcium silicate stabilised with Na-Al, K-Al, Na-Fe and K-Fe', Proc. 7th Int. Cong. Chem. Cem., Paris, II, II.47-II.51

SUZUKI, K., NICHIKAWA, T., KATO, K., HAVASHI, H. and ITO, S. (1981) 'Approach by zeta potential measurement on the surface change of hydrating C_3S', Cem. Chem. Res., 11, 759-764

SWANN, P. R. (1972), 'High voltage microscope studies of environmental reactions', in "Electron Microscopy and Structure of Metals", (University of California Press), 878

SWANN, P. R. and TIGHE, N. J. (1972) 'Performance of a differentially pumped environmental cell in the AE1 EM7', Proc. 5th Europ. Cong. Electron Microsc, 360

TADROS, M. E., SKALNY, J. and KALYONCU, R. S. (1976) 'Early hydration of tricalcium silicate', J. Am. Ceram. Soc. 59, 344-347

TAKEMOTO, K., SAIKI, Y. and YAMAGUCHI, T. (1976) 'Infrared Absorption tests on partially hydrated cement pastes and pure phases', in Transportation Research Circular no. 176, June, "Evaluation of Methods of Identifying Phases of Cement Paste", 41-47

TAMÁS, F. D. (1982), 'Electrical Conductivity of Cement Pastes', Cem. Concr. Res. 12, 115-120

TAMÁS, F. D. and VÉRTES, A. (1973), 'A Mossbauer Study on the Hydration of Brownmillerite ($4CaO.Al_2O_3.Fe_2O_3$)', Cem. Concr. Res., 3, 575-581

TAPLIN, J. H. (1959) Australian J. Appl. Sci., 10, 329

TARTE, P. (1968) 'Recherches Structurales sur les Constituents des Ciments II. les Phénomènes de replacement isomorph dans l'aluminate tricalcique', Silic. Ind. 33, 333-339

TAYLOR, H. F. W. (1964) 'The Chemistry of Cements' (Academic Press, London)

TAYLOR, H. F. W. (1968) Proc. 5th Int. Symp. Chem. Cem., Tokyo, 2, 1

TAYLOR, H. F. W. (1979) 'Cement Reactions: The Silicate Phases', in "Cement Production and Use" (Engineering Foundation) 107-115

TAYLOR, H.F.W. (1984) 'Studies on the Chemistry and Microstructure of Cement Pastes', Proc. Brit. Ceram. Soc. "Chemistry and Chemically-Related Properties of Cement', (London, 12-13 April) to be published

TAYLOR, H.F.W. and ROY, D.M. (1980) 'Structure and composition of hydrates', Proc. 7th Int. Cong. Chem. Cem., Paris, I, II-2/1 - II-2/13

TAYLOR, H.F.W. and NEWBURY, D.E. (1984a) 'Calcium Hydroxide Distribution and Calcium Silicate Hydrate Compositions in Tricalcium Silicate and β-Dicalcium Silicate Pastes', Cem. Concr. Res. 14, 93-98

TAYLOR, H.F.W. et al (1984) Report of Rilem committee 68-MMH Task Group 3, Chairman H.F.W. Taylor

THOMPSON, R.A., KILLOH, D.C., FORRESTER, J.A. (1975) 'Crystal chemistry and reactivity of the MgO-stabilised alites', J. Am. Ceram. Soc., 58, 54

TIAN, A. (1923) 'Utilisation de la méthode calorimetrique dynamique chimique (Use of the dynamic chemical calorimetric method), Bulletin Societe Chimique de France 33, 427-429

TIEGS, T.N. (1975) 'Investigation of ion-thinned tricalcium silicate pastes by transmission electron microscopy', M.Sc thesis, University of Illinois, Urbana-Champaigne, Illinois

THEISEN, K. (1983) 'Relationship between gypsum dehydration and strength development in Portland cement', Zem. Kalk. Gips, 36, 571-577

THOMAS, N.L., JAMESON, D.A. and DOUBLE, D.D. (1981) 'The Effect of Lead Nitrate on the Early Hydration of Portland Cement', Cem. Concr. Res. 11, 143-154

THOMAS, N.L. and BIRCHALL, J.D. (1983) 'The retarding action of sugars on cement hydration', Cem. Concr. Res. 13, 830-842

TONG, H.S. and YOUNG, J.F. (1977) 'Composition of solutions in contact with hydrating β-dicalcium silicate', J. Am. Ceram. 60, 321-328

VALENTI, G.L., SABALELLI, V. and MARCHESE, B. (1978) 'Hydration kinetics of tricalcium silicate solid solutions at early ages', Cem. Concr. Res. 8, 61-72

VARMA, S.P., HENDERSON, E. and WALL, C.D. (1981) 'The Application of Low Temperature Infra-red Spectroscopy to Studies of Iron Substitution in Tricalcium Aluminate', Cem. Concr. Res. 11, 205-210

WEAIRE, D. (1969), 'The Structure of Amorphous Solids', Contemp. Phys. 17, 173-191

WELCH, J.H., and GUTT, W. (1960) 'The effect of minor components on the hydraulicity of the calcium silicates', Proc. 4th Int. Symp. Chem. Cem., Washington, I, 59-68

WILLIAMSON, R.B. (1972) 'Solidification of Portland Cement', Prog. Mater. Sci. 15, 189-286

WINSLOW, D. N. (1982) 'The Pore Structure and Surface Area of Hydrated Portland Cement Paste' in "Characterisation and Performance Prediction of Cement and Concrete' (Engineering Foundation), 105-119

WINSLOW, D. N. and DIAMOND, S. (1974), 'Specific Surface of Hardened Portland Cement Paste as Determined by Small Angle X-Ray Scattering', J. Am. Ceram. Soc. 57, 193-197

YAMAGUCHI, G., TAKEMOTO, K., UCHIKAWA, H. and TAKAGI, S. (1960) 'The rate of hydration of cement compounds and portland cement estimated by X-ray diffraction analysis', Proc. 4th Int. Symp. Chem. Cem., Washington, Paper IV-S4 I, 495-500

YOUNG, J. F. (1972) 'A review of the mechanisms of set-retardation in portland cement pastes containing organic admixtures', Cem. Concr. Res. 2, 415-433

YOUNG, J. F., TONG, H. S. and BERGER, R. L. (1977) 'Compositions of solutions in contact with hydrating tricalcium silicate pastes', J. Am. Ceram. Soc. 60, 193-198

YOUNG, J. F. and TONG, H. S. (1977) 'Microstructure and strength development of beta-dicalcium silicate pastes with and without admixtures', Cem. Concr. Res. 7, 627-636